Multi-scale modeling of sediment and nutrient flow dynamics in the Ouémé catchment (Benin)– towards an assessment of global change effects on soil degradation and water quality

Dissertation

zur

Erlangung des Doktorgrades (Dr. rer. nat.)

der

Mathematisch-Naturwissenschaftlichen Fakultät

der

Rheinischen Friedrich-Wilhelms-Universität Bonn

vorgelegt von

Yaovi Aymar Bossa

aus

Kpinnou, Benin

Bonn, Juni 2012

Angefertigt mit Genehmigung der Mathematisch-Naturwissenschaftlichen Fakultät der
Rheinischen Friedrich-Wilhelms-Universität Bonn

1. Gutachter: Prof. Dr. B. Diekkrüger

2. Gutachter: Prof. Dr. Ir. E. K. Agbossou

Tag der mündlichen Prüfung: 07.09.2012

Erscheinungsjahr: 2012

Dedication

To all my family, first to my wife Hélyette Arielle Bossa, who supported me with faith and love. My Children, Heysenam and Helynam Bossa for whom I did not often have enough time, but who gave me courage and motivation. To my parents, Antoine, Josephine, Reine, Valerie, Odile, Constance, Ines, Brigitte, Benoît, Bernard, my parents and brothers in-laws (Théophile, Clotilde, Harsys and Théo-wyls), and my nephews (Rosine, Octave, Rose,..) this is my most emotional way of saying thank you for giving me support and tenderness.

Acknowledgements

This work has been supported by the Federal German Ministry of Education and Research (BMBF, Grant No. 01 LW 06001B) as well as the Ministry of Innovation, Science, Research and Technology (MIWFT) of the federal state of Northrhine-Westfalia (Grant No. 313-21200200) for the funding of the IMPETUS project in the framework of the GLOWA program. The German Academic Exchange Service has supported this work through a three year scholarship.

I am very grateful to Mr. Bernd Diekkrüger, Professor at the Department of Geography of the University of Bonn, responsible of the Hydrology Research Group and supervisor of this work, who has really spent time for me, giving me daily advises, and has early gave me unconditional support in my orientation. He also gave me many opportunities to visit international conferences. His patience to listen to my questions sometimes not clear enough and his commitment to a well done work were my main motivation. I am really so proud for having belonged to his working group.

I express my gratitude to all belonging to the Hydrology Research Group, especially Dr Simone Giertz, Gero Steup, Dr Luc Sintondji, Dr Claudia Hiepe, Dr Anna Klose, Henning Busche, Britta Höllermann, Jakob Sorge, Guido Scuito, Mareike, Asfaw Kebede Kassa, Derib Sisay, Daniela Dowersteg, Dr Oliver Schulz, Ambros Waidosch, Aurelien Tossa, Andreas Enders, Thomas Cornelissen, Dr. Constanze Leemhuis, whose contributions in various forms were very valuable. Scientific rigor, commitment, passion and intellectual generosity made the exchanges with them interesting and enjoyable.

I express my gratitude to Dr Igué and Dr Gaiser, who took an active part in all related to soil investigation, leading to the publication of the sixth chapter of this thesis in the Geoderma Journal.

Many thanks to IMPETUS in all its hierarchy and its participants at the both sides Germany and Benin, since they have taken an active part in my background construction, through series of integrated trainings in soil hydrodynamics, hydrological process modeling coupled with Geographic Information Systems and Remote Sensing, within the capacity building rubric of the IMPETUS project. As for the administrative side, I cannot forget Prof. Dr Reichert, Dr Michael Christoph, Andreas Preu, and all of you whose names are not mentioned here.

I am grateful to Mr. Euloge Agbossou, Professor at the Faculty of Agricultural Sciences (FSA) at the University of Abomey-Calavi (Bénin). Few months before completing my master degree, he gave me the opportunity to meet Prof. Diekkrüger, Dr Giertz and Mr Steup, who accepted me to join their Research Group just after the defense of the Master degree. He believed soon in my potential, he has forged my personnal confidence face to a completely new professional environment, and seized spontaneously every opportunity that can be relevant to my education and my professional profile. I couldn't forget his closed assistants, Dr Luc Sintondji and Dr Bernard Ahamidé, who have played remarkable roles for achieving the objectives of this work.

Bearing in mind that I was originally compartmentalized to the scientific field of fundamental Physics, thraiting only few aspects of Hydrology Sciences (e.g. continuum mechanics), it is the time to thank Professor Brice Sinsin, currently Rector of the University of Abomey-Calavi, who motivated me and gave me the opportunity (through a master program in Natural Resources Management at the faculty of Agricultural Sciences, co-piloted with Belgium Universities) to glimpse the transdisciplinarity of Environmental Sciences. I am really grateful to him.

I have often resorted to various contributions from Pierre Adisso, Head of the Coordination Service of Integrated Water Resources Management of the Benin General Directorate of Water. He has shown a strong attachment to the success of this work, and has created good working environment for me inside his institution. To Mr. Antoine Gohoungossou, responsible of the Hydrology Service, Dr Arnaud Zannou, responsible of the Ouémé 2025 Project, Dr Félix Azonsi, Director of the Water Service of the General Directorate of Water of Benin, I say thank you for having doing your best to help me. Thanks to Martial Dossou, Farouk, Lamidi, Doussi, Comfort, Florence, Dr. Vincent Orékan from IMPETUS, Maxime Wubda, Afouda Simon, Theodore Ouani-Yossidé from IRD. I do not forget Mr Ahlonssou of DMN, Dr Valens Mulindabigwi, Mr Pofadji of CePEG, and my friends Ulrich Demagbo of CCA.

Abstract

Beyond aspects such as the quantification of soil and water degradation, this work investigated impacts of differences in the input boundary conditions (e.g. soil map, land use) on the performance of the Soil and Water Assessment Tool (SWAT). Effects of different local crop management scenarios (e.g. fertilizer input) on the simulation of plant growth and soil nutrient load to surface water and groundwater systems were also evaluated. The study was carried out in the Ouémé catchment (49,256 km²) at the outlet of Bonou in Bénin, where different sub-catchments were extensively investigated.

Therefore, three different soil maps have been used: two maps of the hierarchical Soil and Terrain digital database approach (SOTER) and the soil mapping at the reconnaissance level, with one dominant soil type per mapping unit approach (ORSTOM); all three were available at the same resolution. The mapping approach's impact on the model results was within the same magnitude of that of maps with different resolutions but developed with the same mapping approach. While the latter aspect is often studied, the first one is usually neglected.

A land use map was refined for the study area, enabling the evaluation of four management scenarios: fertilizer supplied only to cotton, rice and maize, as is common in Benin (Sc0); crop systems without the use of fertilizer (Sc0a); similar fertilizer inputs to all cropping systems (Sc1); and the original land use map without fertilizer inputs (Sc1a). Compared to the first scenario, the latter two scenarios, commonly used in regional scale modeling, exhibited distinct biases in plant growth parameters, crop yields, water yield, sediment yield and nitrogen load.

A regionalization methodology has been developed and applied to derive scale dependent regression-based parameter models, using catchment physical properties depending on spatial scale as explanatory variables for SWAT model parameters obtained from multi-scale investigations, for accurately simulating water-sediment-nutrient fluxes at ungauged and large scale basins. With respect to process representation in the SWAT model, it was found that in the Ouémé catchment, geology appears to be a major driver of hydrological response, correlating significantly with eleven out of fifteen model parameters. Slope appears to be powerful to control the channel conductivity, groundwater threshold for base flow generation and soil evaporation compensation (accounting for capillary, crusting and cracking actions). The soil type lixisol, which is a dominant soil component within the Ouémé catchment, partly explained the surface runoff lag and the maximum retrained sediment. The occurrence of lateritic consolidated soil layer explained the soil susceptibility to erosion and drainage density explained the fraction of aquifer percolation. Parameters such as the curve number, controlling the surface runoff were not consistently explained by the catchment properties, leading to a slightly overestimation of runoff peaks, probably due to the non-uniqueness of the considered calibrated parameter set. These relationships were successfully used to compute daily runoff hydrographs (Model efficiency ranged from 0.61 to 0.67 and coefficient of determination of roughly 0.70) at different catchment scales (from 1179 km² to 23488 km²). By adopting this methodology two difficulties in model setup in the Ouémé catchment were overcome: parameter scale-effects and associated uncertainty issues for large scale model application and the lack and non-accurateness of boundary condition data (e.g. stream water-sediment-nutrient measurements).

Climate and land use change impacts on the ongoing land and water degradation were compared at different spatial scales (Donga-Pont: 586 km²; Ouémé-Bonou: about 49,256 km²). Surface runoff, groundwater flow, sediment and organic nitrogen loads were dominantly affected by land use change of -8 to +50%, while water yield and evapotranspiration were dominantly affected by climate change of -31 to +2%.

It was found that variables such as surface runoff, groundwater flow, sediment and transported nutrients, mainly sensitive to land use change were significantly affected by the increasing scale, while variables such as water yield and evapotranspiration, mainly sensitive to climate change, have changed almost similarly for the both scales.

Zusammenfassung

Neben Aspekten der Quantifizierung der Degradation von Boden und Wasserressourcen, untersucht die vorliegende Arbeit den Einfluss veränderter Eingabedaten (z.B. Bodenkarte, Landnutzung) auf Modellergebnisse des Modellsystems SWAT (Soil and Water Assessment Tool). Weiterhin werden Szenarien der landwirtschaftlichen Nutzung auf der lokalen Skala (z.B. Eintrag von Düngemitteln) auf Pflanzenwachstum und Nährstoffgehalte des Oberflächen- und Grundwassers berechnet. Als Untersuchungsgebiet dient das Einzugsgebiet des Quémé in Benin.

Zur Analyse der Bedeutung der Bodeninformation wurden drei unterschiedliche Bodenkarten verwendet: zwei Datensätze des hierarchischen ‚Soil and Terrain digital database'-Ansatzes (SOTER) sowie der ORSTROM-Ansatz (Bodenkartierung mit einem dominanten Bodentyp pro kartierter Einheit). Es konnte gezeigt werden, dass die Verwendung unterschiedlicher Konzepte zur Erstellung der Bodenkarte Unsicherheiten erzeugt, die in der gleichen Größenordnung liegen wie bei der Verwendung von Bodenkarten unterschiedlichen Maßstabs. Während die Maßstabsabhängigkeit häufig untersucht wurde, wurde die Auswirkung unterschiedlicher Kartierkonzepte bislang nicht betrachtet.

Die vorhandenen, groben Landnutzungsinformationen wurden verfeinert, um die Auswirkung verschiedener Managementmaßnahmen zu untersuchen. Auf Grundlage einer Landnutzungsklassifikation wurden drei Modellszenarien entwickelt: (1) Wie in Benin üblich, wurden nur Baumwolle, Reis und Mais in geringer Höhe Düngemittel zugeführt; (2) die gleiche Menge Düngemittel wurde auf alle Anbausysteme verteilt; (3) es wurden keine Düngemitteln zugeführt. Gegenüber dem ersten Szenario zeigten die Szenarien zwei und drei, die typischerweise für die Modellierungen auf der regionalen Skala genutzt werden, systematische Abweichungen des Pflanzenwachstums (z.B. Wasser- und Stickstoff-Stresstage) sowie von Ernteertrag, Wasserverfügbarkeit, Sedimentaustrag und Stickstofffracht

Eine Regionalisierungsmethode wurde entwickelt, um unter der Verwendung multiskaliger physikalischer Einzugsgebiets-Parameter als erklärender Variablen skalenabhängige regressionsbasierte Parametermodelle für das SWAT-Modell zu erzeugen. Diese Parametermodelle ermöglichen eine genaue Simulation der Wasser-, Sediment- und Nährstoffflüsse unbeobachteter großskaliger Einzugsgebiete. Hinsichtlich der Prozessdarstellung im SWAT Modell konnte gezeigt werden, dass die hydrologische Reaktion im Einzugsgebiet des Ouémé im Wesentlichen von der Geologie beeinflusst wird. Die Hangneigung korreliert in hohem Maße mit der Leitfähigkeit des Gerinnes, dem Schwellenwert des Basisabflusses sowie dem Bodenevaporationsbeiwert (der kapillaren Aufstieg, Verkrustung und Bodenrisse erklärt). Der im Ouémé Einzugsgebiet dominante Bodentyp Lixisol, erklärt zum Teil die Verzögerung des Oberflächenabflusses und den maximalen Sedimentrückhalt. Verfestigte Lateritschichten erklären die Erosionsanfälligkeit während die Gewässernetzdichte den Anteil der Grundwasserneubildung erklärt. Parameter wie die ‚Curve Number', die den Oberflächenabfluss kontrolliert, konnten nicht aus Einzugsgebietseigenschaften abgeleitet werden, was zu einer leichten Überbewertung der Abflussspitzen auf größeren Skalen führt. Dieses ist auf die nicht eindeutige Bestimmbarkeit der Modellparameter bei der automatischen Kalibrierung zurückzuführen, die zu großen Unsicherheiten in den Modellergebnissen führen kann. Die entwickelten Beziehungen konnten erfolgreich für die Berechnung des täglichen Abflusses (Modelleffizienz von 0.61 bis 0.67, Bestimmtheitsmaß von ca. 0.7) auf unterschiedlichen Skalen (von 1179 km² bis 23488 km²) angewendet werden. Der Ansatz erlaubt es, zwei Probleme bei der Modellentwicklung im Ouémé-Einzugsgebiet zu lösen: Skaleneffekte bei der Bestimmung der Modellparameter mit den dazugehörigen Unsicherheiten bei der großskaligen Modellierung sowie fehlende oder fehlerhafte Daten für die Kalibrierung (z.B. Abflüsse und Sedimentausträge).

Auf unterschiedlichen Skalen (Donga-Pont: 586 km²; Ouémé-Bonou: ca. 49,256 km²) konnte darüber hinaus der Einfluss des Klima- und Landnutzungswandels auf die andauernde Degradation der Land und Wasserressourcen quantifiziert werden. Oberflächen- und Grundwasserabfluss, Sediment und organischer Stickstoff sind vor allem durch den Landnutzungswandel beeinträchtigt (-8 bis +50%),

während das Wasserdargebot und die Evapotranspiration hauptsächlich durch den Klimawandel beeinflusst werden (-31 bis +2%).
Darüber hinaus konnte gezeigt werden, dass sich Oberflächen- und Grundwasserabfluss, Sediment und transportierte Nährstoffe, die vor allem auf veränderte Landnutzung reagieren, signifikant von der betrachteten Skala abhängen, wohingegen Wasserdargebot und Evapotranspiration, die vor allem sensitiv auf den Klimawandel reagieren, skaleninvariant sind.

Résumé

Au-delà des aspects tels que la quantification de la dégradation des sols et des eaux, ce travail a examiné également les effets des différences dans les conditions aux limites (cartes des sols et utilisation des terres) sur la performance de l'outil d'évaluation des sols et de l'eau (Soil and Water Assessment Tool- SWAT). Des effets de différents scénarii de gestion locale des cultures (apport d'engrais par exemple) sur la simulation de la croissance des plantes et le transport d'éléments nutritifs du sol vers les eaux de surface et souterraines ont été évalués. L'étude a été menée dans le bassin versant de l'Ouémé à l'exutoire de Bonou au Bénin, couvrant une superficie de 49256 km².

En effet, trois différentes cartes des sols ont été utilisées: deux cartes obtenues par l'approche de base de données numériques et hiérarchiques des sols et des reliefs (SOil and Terrain- SOTER) et l'approche ORSTOM (cartographie des sols à l'échelle de reconnaissance, avec un type de sol dominant par unité de cartographie); tous trois étant disponibles à la même résolution. L'impact de l'approche de cartographie sur les résultats du modèle se trouve dans le même ordre de grandeur que celui des cartes ayant des résolutions différentes, mais développées avec la même méthode de cartographie. Alors que ce dernier aspect est souvent étudié, le premier est généralement négligé. Une carte d'utilisation des terres a été affinée, permettant l'évaluation de trois scénarii de modélisation: systèmes de culture détaillés avec apport d'engrais uniquement au coton, le riz et le maïs, tel que courant au Bénin (Sc0); systèmes de culture détaillés sans apport d'engrais (Sc0a); la carte originale d'utilisation des terres avec apport d'engrais similaire à tous les systèmes de cultures (Sc1); et la carte originale d'utilisation des terres sans apport d'engrais (Sc1a). Par rapport au premier scénario, les deux derniers scénarii, couramment utilisés dans la modélisation à l'échelle régionale, ont montré de distincts biais sur les paramètres de croissance végétale (par exemple nombre de jours de stress hydrique et de stress en azote), le rendement des cultures, la production d'écoulements de surface, le transport de sédiments et d'éléments nutritifs des sols.

Une méthodologie de régionalisation a été développée et appliquée pour dériver des modèles de paramètres, dépendant de l'échelle spatiale et basés sur des modèles de régression, pour simuler avec précision acceptable, les flux d'eau-sédiments-nutriments pour les bassins non jaugés, voire ceux de tailles très grandes. En effet, des propriétés physiques de bassin versant dépendant de l'échelle spatiale ont été utilisées comme variables explicatives des paramètres du modèle SWAT, préalablement obtenus à partir d'investigations multi-échelles. En respect à la représentation des processus dans le modèle SWAT, il est trouvé que dans le bassin versant de l'Ouémé, la géologie est un facteur important de la réponse hydrologique, étant significativement corrélée avec onze des quinze paramètres du modèle considérés. La pente moyenne des bassins semblent puissamment contrôler la conductivité des chenaux des cours d'eau, le seuil d'eau souterraine nécessaire pour enclencher les écoulements de base et la compensation de l'évaporation du sol (comptant pour des effets de capillarité, d'encroûtement et de fissure des sols). La présence de sols ferrugineux tropicaux lessivés à concrétions- lixisol (un type de sol dominant dans le bassin versant de l'Ouémé) explique en partie le décalage du ruissellement de sous-surface et le taux maximum de sédiments remobilisé. La présence de couches de sols consolidées et latéritiques a expliqué la sensibilité des sols à l'érosion et la densité de drainage des bassins a expliqué la fraction d'eau percolée vers les aquifères. Des paramètres tels que les numéros de courbes de ruissellement (curve number), contrôlant le ruissellement de surface n'ont pas été systématiquement et solidement expliqués par les propriétés des bassins, ce a qui conduit à une légère surestimation des pics de ruissellement, peut-être en raison de la non-unicité du groupe de paramètres calibrés considérés, qui certainement comportent encore de mauvaises informations. Ces relations ont été utilisées avec succès pour calculer des hydrogrammes de ruissellement à une résolution temporelle journalière, avec une efficacité du modèle allant de 0,61 à 0,67 et des coefficients de détermination d'environ 0,70, et à des échelles spatiales différentes (bassins de 1179 km² à 23488 km²). En adoptant cette méthode, deux difficultés dans la mise en œuvre du modèle dans le bassin versant de Ouémé pouvait être surmontées: les effets d'échelle qui affectent souvent les paramètres des modèles et les enjeux d'incertitudes associées pour des applications à grande échelle, aussi bien que le manque et la non-

exactitude des données sur les conditions aux limites mesurables (les débits des cours d'eau, la concentration des sédiments en suspension et la concentration en nutriments provenant des sols).
Les impacts du changement climatique et de l'utilisation des terres sur la dégradation des eaux et des terres en cours dans le bassin ont été comparés à différentes échelles spatiales (Donga-Pont: 586 km²; Ouémé-Bonou: 49256 km²). Les ruissellements de surface, les écoulements souterrains, les pertes de sédiments et de nutriments organiques (azote et phosphore organiques) ont été affectées par les changements dans l'utilisation des terres (comme effets dominants) de -8 à +50%, tandis que la production totale d'eau du bassin et l'évapotranspiration ont été affectées par les changements dans le climat (comme des effets dominants) de -31 à + 2%.
Il a été constaté que les variables telles que le ruissellement de surface, les écoulements souterrains, les pertes de sédiments et nutriments, principalement sensibles aux changements d'utilisation des terres ont été significativement affectées par l'augmentation de l'échelle spatiale, alors que les variables telles que la production totale d'eau du bassin et l'évapotranspiration, principalement sensibles aux changements climatiques, ont changé presque similairement pour les différents échelles spatiales investiguées.

Table of contents

List of figures

List of tables

Abbreviations

ALPHA_BF	Base flow recession factor [d]
BMBF	Federal Ministry of Education and Research, Germany
BS	Base Saturation [%]
CATCH	Coupling of the Tropical Atmosphere and Hydrological Cycle (Couplage de l'Atmosphère Tropicale et du Cycle Hydrologique) : Research Project
CEC	Cation Exchange Capacity [cmol/kg]
CEC_clay	Cation Exchange Capacity of the clay fraction [cmol/kg]
CEC_soil	Cation Exchange Capacity of the soil [cmol/kg]
CeRPA	Regional Center of Agricultural Promotion (Centre Régional pour la Promotion Agricole)
Ch_K2	Effective channel hydraulic conductivity [mm/hr]
CLUE-S	Conversion of Land Use and its Effects at Small regional extent
CN2	Curve Number [-]
CPCS	Commission of Pedology and Soil Mapping (Comission de Pédologie et de Cartographie des Sols)
CSTV	Catchment Spatial Threshold Value
CV	Coefficient of variation
DANIDA	Danish International Development Agency
DEM	Digital elevation model
DG-Eau	General Directorate of Water (Direction Nationale de l'Eau)
DMN	National Directorate of Meteorology, Benin (Direction Météorologique Nationale du Benin)
ESCO	Soil evaporation compensation factor [-]
ET_{pot}	Potential evapotranspiration
FAO	Food and Agriculture Organisation of the United Nations
GCM	General Circulation Model
GIS	Geographic Information System
GLOWA	Global change of the water cycle, BMBF programme
GW	Groundwater
GW_DELAY	Ground water delay [d]
GWQMN	Threshold depth for ground water flow to occur [mm]
HRU	Hydrologic Response Unit
HVO	Upper Ouémé Catchment (Haute Vallée de L'Ouémé)
IA	Index of agreement according to WILLMOTT (1981)
IGN	National Institute of Geography, Benin (Institut Géographique National du Bénin)
IMPETUS	Integrative management project for an efficient and sustainable use of freshwater resources in West Africa
INRAB	National Institute of Agricultural Research, Benin (Institut National des Recherches Agricoles du Bénin)
INSAE	National Institute of Statistics and for Economical Analysis, Benin (Institut National de la Statistique et de l'Analyse Economique du Bénin)
IPCC SRES	Intergovrnmental Panel on Climate Change Special Report on Emissions Scenarios
IRD	Research Institute for Development (Institut de Recherche pour le Développement)

ITCZ	Inter Tropical Convergence Zone
LAI	Leaf area index [m^2/m^2]
MAEP	Ministry of Agriculture, Livestock and Fisheries (Ministère de l'Agriculture, de l'élevage et de la pêche)
MCL	Maximum Concentration Level [g/l]
ME	Model efficiency according to NASH & SUTCLIFFE (1970)
MOS	Model Output Statistics
MPI-OM	Max Planck Institute Ocean Model
NPERCO	Nitrate percolation coefficient [-]
NPK	Nitrogen Phosphorus and Potassium
NPKSB	Nitrogen Phosphorus Potassium Sulfur Bore
NTU	Nephelometric Unit as a measure of turbidity
OBEMINES	Beninese Office of Mines (Office BEninoise des MINES)
OM_RP	ORSTOM soil Map with Reference soil Profiles
PHU	Potential Heat Unit [°C]
PTF	Pedotransfer function
Q_{base}	Base flow [mm]
Q_{surf}	Surface runoff [mm]
Q_{tot}	Total streamflow [mm]
RCHRG_DP	Fraction of deep aquifer percolation [-]
REMO	REgional climate MOdel
REVAPMN	Threshold water level in shallow aquifer for revap [mm]
RIVERTWIN	Integrated River basin Management in Contrasting Climate Zones: EU Research Project
SM_RP	Soter Map with Reference soil Profiles
SM_VP	Soter Map with Virtual soil Profiles
Sol_K	Saturated hydraulic conductivity [mm/hr]
SOL_Z	Soil depth [mm]
SOTER	SOil and TERrain
SPEXP	Exponent for calculating max sediment retrained [-]
SRTM	Shuttle Radar Topography Mission
SS	Sum of Square errors
SSC	Suspended Sediment Concentration
SURLAG	Surface runoff lag coefficient [-]
SWAT	Soil and Water Assessment Tool
SWCP	Stream Water Chemical Parameters
UN	United Nations
UNDP	United Nations Development Programme
UNESCO	United Nations Educational, Scientific and Cultural Organization
USDA-ARS	United States Department of Agriculture – Agricultural Research Service
USEPA	United States Environmental Protection Agency
USLE_K	Soil erodibility factor [0.013 t $m^2h/(m^3$ t cm)]
USLE_P	Practice factor [-]
VIF	Variable Inflation Factor

WASCAL	West African Science Service Center on Climate and Adapted Land Use: Research Project
WEGE	Weather Generator
WHO	World Health Organization
WTRYLD	WaTeR YieLD
95PPU	95 percent prediction uncertainties

1. General introduction

1.2. Framework of the study

Conscious of the global environmental degradation and its multiple impacts on the human well-being, the German Ministry of Education and Research launched the GLOWA programme (GLOWA = GLObal change of the WAter cycle) in 2000, including the multidisciplinary IMPETUS project ("Integratives Management-Projekt für einen Effizienten und Tragfähigen Umgang mit Süsswasser in West Afrika" or in English: Integrated management project for an efficient and sustainable use of freshwater resources in West Africa). It was a joint venture of the Universities of Bonn and Cologne and the project aim was to develop strategies for sustainable future water management at regional levels while taking into account global environmental changes and socio-economic framework conditions, in the Wadi Drâa in Morocco, and the Ouémé catchment in Benin. The IMPETUS project was run from 2000 to 2011 and was successively dedicated to: (1) the identification and analysis of factors influencing the water cycle; (2) the modeling of future scenario impacts on the water cycle; and (3) management options for decision making based on scenario analysis and decision support systems for different problem clusters. More details about the IMPETUS-Project are provided in Speth et al. (2010).
The current study is a part of the IMPETUS project, although run beyond the official running time of the project. As that, it is connected to earlier investigations addressing hydrological, hydrogeological, and pedological processes (e.g. Junge, 2004; Giertz, 2004; Sintondji, 2005; El Fahem, 2007; Hiepe, 2008), socioeconomic aspects related to land degradation, resource management, and climate change (Paeth et al., 2008; Doevenspeck, 2005).

1.3. Problem statment

The appearance and persistence in recent decades of several degradation indices of natural resources quality worldwide (UNDP, 2003; Speth et al., 2010) mobilizes more and more attention. It is comprehensible that the Millennium Goals for Development (UN, 2005) recommended among others, to ensure an environmental sustainability by integrating sustainable development principles into country policies for reversing the loosing trend of environmental resources face to increasing population and their multiple needs.
Together, natural harsh conditions (e.g. harsh tropical climate conditions) and anthropogenic impacts cause the loss of soil particles and nutrients (nitrogen (N) and phosphorus (P)) into water systems. This has many serious consequences, including the decline of crop yield (Igué, 2000) (related to soil depth reduction and soil nutrient depletion), acidification and loss of biodiversity in stream and lake systems, and habitat degradation in downstream water systems (MAEP, 2007).
Climate changes affect the hydrological cycle, thus modifying the transformation and transport characteristics of nutrients (Bouraoui et al., 2002). A specific case of study of potential impact of climate change on surface water quality in North America has shown among the effects to be expected, an increase in diffuse source pollutant loads in nutrient cycling (Murdoch et al., 2000). Previously, Novotny and Olem (1994) indicated that diffuse losses of nutrients, especially those from agricultural origins, are among the major contributors to the total nutrient load to the water systems.
Several works worldwide (Abbott et al., 1986; Sivapalan and Viney, 1994a, 1994b; Diekkrüger and Arning, 1995; Arnold et al., 1998; Andersen et al., 2003; Blöschl and Sivapalan, 1995) provided process understanding frameworks (e.g. model development) ranging from the complexity of hydrological processes (i.e. discontinuity, periodicity, randomness) to the local and regional nutrient cycling, transport and other related problems, estimates of future trends, and assessments of possible solutions (i.e. through management scenarios). This allowed several modeling tasks since the last decades, using nowadays complex process based models with multiple specific limitations

(Andersen et al., 2003; Blöschl and Sivapalan, 1995). Among the major weaknesses are: (1) the non-explored uncertainties on the model performance, which may be caused by alternative mapping concepts if used to derive soil maps; (2) the non-explored uncertainties on the simulation of plant growth, yield, soil particle and nutrient transport, which may be caused by crop system aggregation at regional scale; (3) the use of inappropriate modeling scales (which increase the scale-effects on the model parameters due to the model internal aggregation) that complicates the model parameter issues and problems related to data availability and accessibility.

1.4. Objectives

The overall objective of the study is to contribute to the sustainable management of Benin's natural resources in indicating often neglected uncertainties which should be considered in the scenario elaborations for supporting well-balanced management decisions. It is also expected to provide information on stream water chemical quality and the depletion rate of soil nutrients, both aspects which were not investigated during the official running time of the IMPETUS project (Speth et al., 2010).
Specifically, the study objectives are: (1) establishment of suitable soil data base as input for hydrological and erosion process modeling as well as nitrogen and phosphorus load evaluation for the whole Ouémé basin (roughly 49,256 km^2); (2) assessment of impacts of crop and fertilizer pattern on the modeling issues in the well investigated Donga-Pont catchment level; (3) assessment of the physical and chemical contamination of surface-groundwater, linked to agricultural diffuse sources; (4) development of an approach to understand the scale dependent impact of spatial heterogeneity on the simulation of hydrological processes; and (5) evaluation of global change on soil degradation and water quality from meso to regional scale.
In this study, various research questions arising from the problems stated above have been explored such as: (1) how the output of the physically based model SWAT depends on the soil mapping approach; (2) how within-aggregative mapping unit variability and soil layer/soil property aggregation, affect the SWAT model output; (3) how valid is a given soil map obtained with a given mapping approach for hydrological evaluations; (4) how different small-scale processes may efficiently contribute to a large-scale assessment; and (5) how and with which uncertainties parameters are transferable to ungauged sub-catchments.

1.6. Structure of the thesis

This thesis is organized in 10 chapters, starting with a short introduction of the study framework and objectives. Chapter 2 describes the research area in providing details on the spatial information data (e.g. land use) used. Chapter 3 provides concept definitions (state of the art) such as hydrological cycle, water balance, erosion and model typology. Chapter 4 describes the methods used such as the model components, while chapter 5 describes the laboratory methods, the modeling procedures, and the algorithms used for the calibration, sensitivity and uncertainty analysis. Chapter 6, analyses the effects of different soil databases (via mapping/aggregation concepts) on modeling of hydrological processes and sediment yield in Benin. Chapter 7 discusses the effects of changing crop patterns and management practices on the simulation of N and P loads to surface and groundwater in a semi-humid and meso scale catchment in Benin. In the chapter 8 are presented the scale effects of catchment properties on modeling soil and water degradation in Benin, and chapter 9 compares simulation results of land and water degradation under land use and climate change scenarios from meso (586 km^2) to regional scale (49,256 km^2). Finally, a general conclusion is given in the chapter 10.

2. Research area

2.1. Location

The Ouémé catchment at the Bonou outlet extends to 49, 256 km^2 of surface area and makes up of roughly 43% of the Benin country (Barthel et al., 2009) between 6.8 and 10.2 °N of latitude. About 89% of the catchment is located in Benin, about 10% in Nigeria and about 1% in Togo (Fig. 2.1).

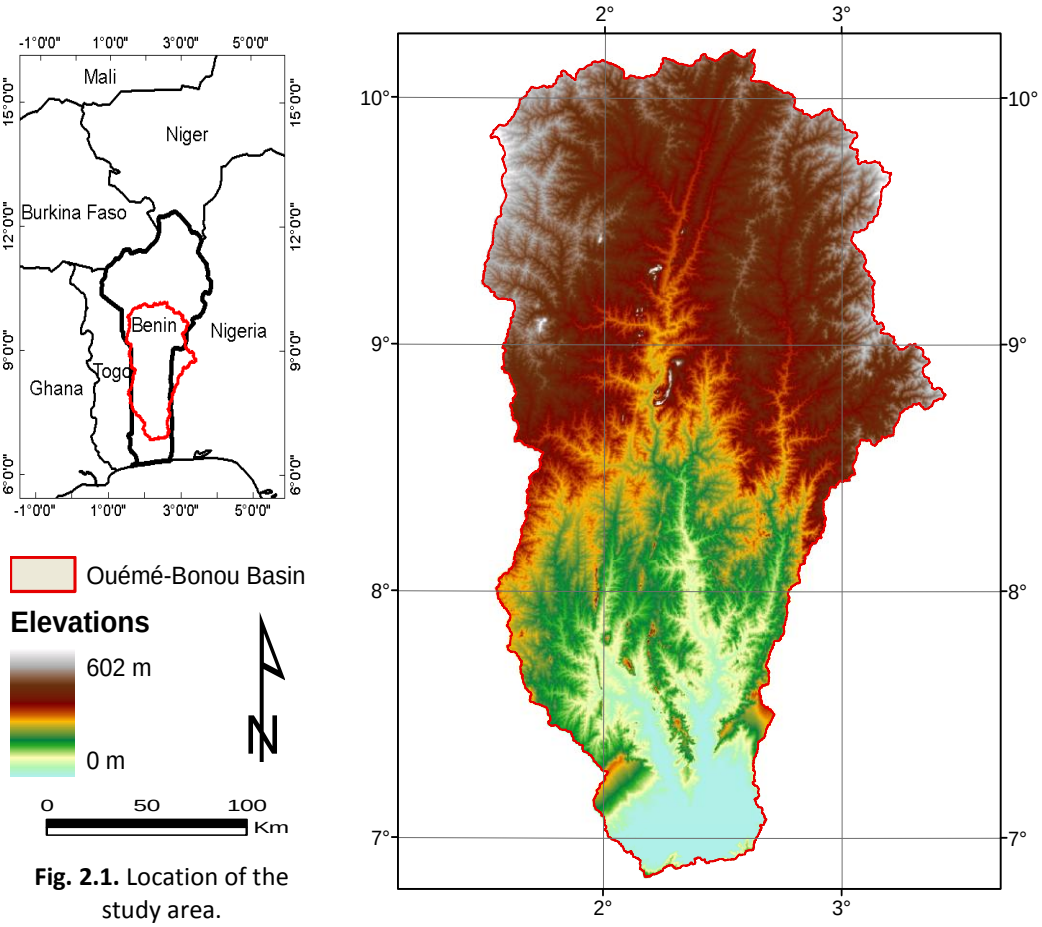

Fig. 2.1. Location of the study area.

On a global view, Benin extends from the Niger River to the Atlantic Ocean, with a relatively flat terrain. Benin lies entirely in the tropical sub-saharan region with a wet and dry climate. A semi-arid environment is met northwards, made up of savannahs and small mountains (about 600 m), while the south of the country consists of a low coastal plain with marshlands, lakes and lagoons.

2.2. Geology and geomorphology

The geology of Benin consists of two main rock types (metamorphic/crystalline rocks and sedimentary rocks) as summarized by Faure and Volkoff (1998):

(1) metamorphic/crystalline rocks (Precambrian/Dahomeyan basement), consisted predominantly of complex migmatites granulites, with granitic/gneissic intrusion, divided into two differentiated units: (i) a *granite gneissic unit* in the east, composed of rocks corresponding to a medium metamorphic gradient: amphibole-gneiss, biotite-gneiss and some basic rocks as amphibolites embedded in folded granite gneiss–syntectonic granites that form the main lithologic component; and (ii) a *granulitic and aluminous gneissic unit* westward, composed of several Late- or Post-Panafrican granitic intrusions.

(2) sedimentary rocks distributed in three basins: (i) the *coastal basin* formed by Cretaceous-Tertiary series made up of clays, sands, gravel, ferruginous sandstone overlain by clayey sands and fluviatile deposits_Continental Terminal.in which the 'Terre de Barre' is differentiated; (ii) the *Kandi Basin* in the north-east, comprises a Cambrian base-conglomerate, Paleozoic sandstones and clays, Cretaceous sandstones and a Continental Terminal cover with ferruginous sand-stones; and (iii) part of the *Volta Basin* (in the north-west), composed of siltstones and sandstones with interlayered limestones, tillites, limestones and silexites, phosphates of the Buem unit and quartzite sandstones that are gradually metamorphosed toward the east. The metamorphic equivalents of these sandstones constitute the *Atacora unit* that forms the highest relief line of the area.

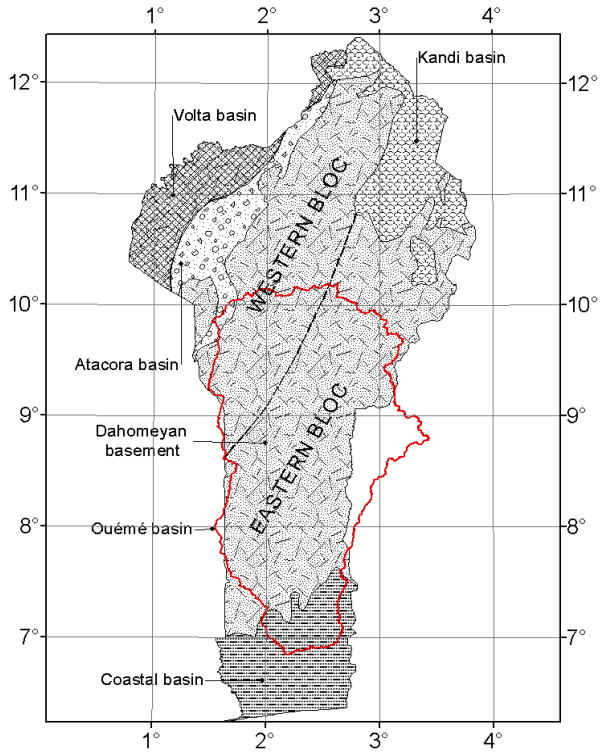

Fig. 2.2. Benin geological basins (modified from Faure and Volkoff, 1998)

The Ouémé catchment is mainly characterized by the Precambrian basement, consists predominantly of complex migmatites granulites and gneisses, including less abundant mica shists, quarzites and amphibolites (Reichert et al., 2010). Syn – and post – tectonic intruisions of mainly granites, diorites, gabbros and volcanic rocks are present (Wright and Burgess, 1992; Reichert et al., 2010).

With a topographic relief generally low (highest elevation point of 658 meter) the land surface may be slightly ondulating (granitic – gneissic plateau), strongly fractured (granitic peneplain) with typical seasonally waterlogged linear depressions (inland valleys) (Menz, 2010). The terrain of the lower basin, consisting of soft sedimentary bedrock, is monotone, less accentuated and formed by anastomosing rivers, erosion and siltation.

2.3. Climate

According to Faure and Volkoff (1998), Benin is divided into four bioclimatic zones: (i) a littoral humid tropical zone (1200 to 1400 mm of annual rainfall); (ii) a littoral and inland sub-humid zone (900 to 1200 mm of annual rainfall) with wooded savannas in the low basin of the Ouémé river and the low basin of the Mono river near the Togo border; (iii) a wetter inland zone (1200 to 1400 mm of annual rainfall) with woodlands and savannas corresponding to the central dorsal of Nikki–Djougou; and (iv) a continental dry northern zone (900 to 1200 mm of annual rainfall) with dry bushes and savannahs.

Situated in the wet (Guinean coast) and dry (Guinean Soudanian zone) tropical climate, the Ouémé catchment records annual mean temperature of 26 to 30°, annual mean rainfall of 1,280 mm (from 1950 to 1969) and 1150 mm (from 1970 to 2004) at the climatic station of Parakou (cf. Fig. 2.3) (Fink et al., 2010a). The Guinean Soudanian zone (north of the catchment) has a unimodal rainfall season (from April to September) that peaks in August whereas the Guinean coast zone (south of the catchment) exhibits a bimodal rainfall season (from March to July and from August to October) that peaks in June and September (cf. Fig. 2.3).

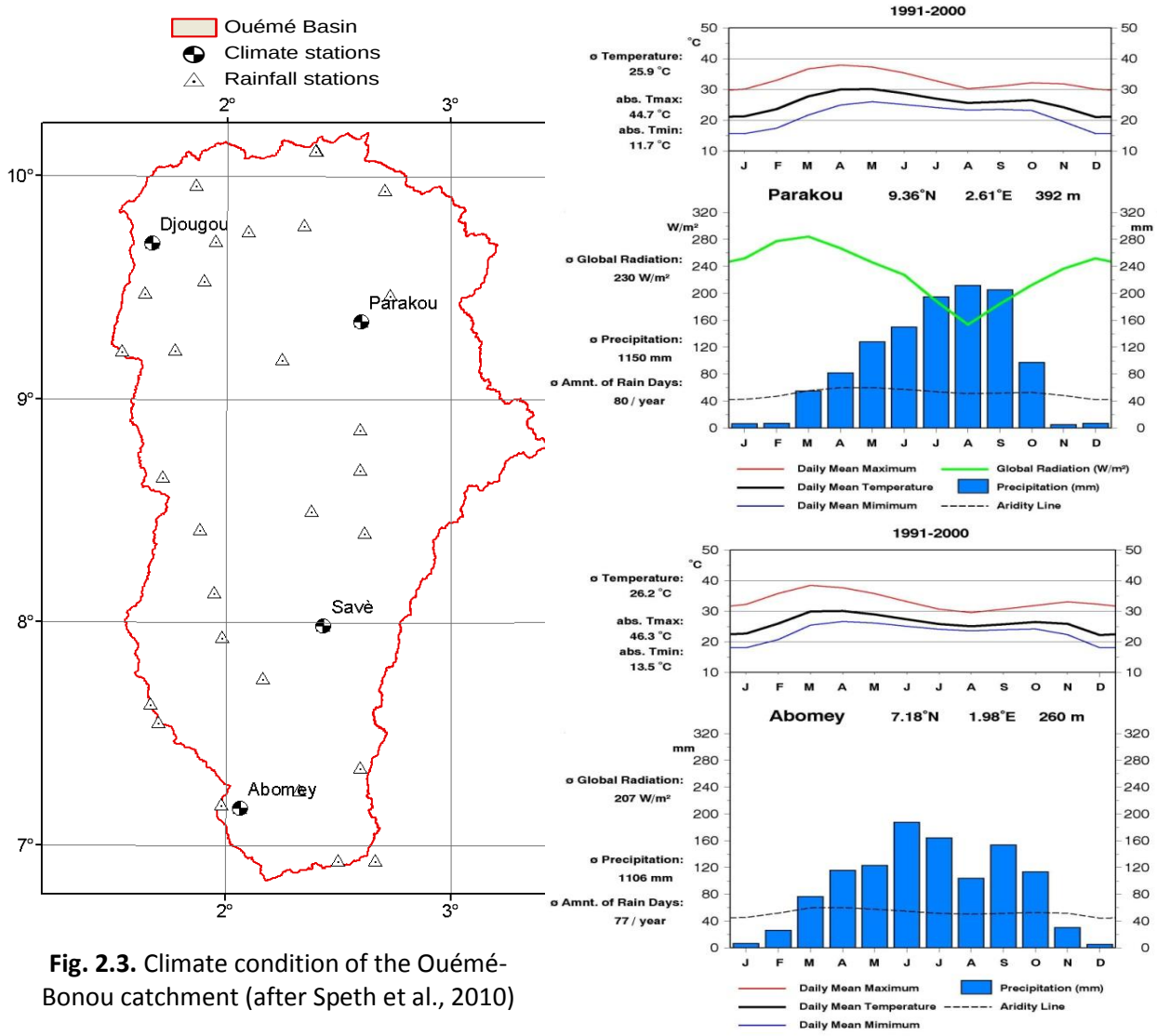

Fig. 2.3. Climate condition of the Ouémé-Bonou catchment (after Speth et al., 2010)

Rainfall variability analysis revealed a multi-decadal dry episode (rainfall anomalies) commenced around 1970 with remarkable drought periods in the early 1970s and early to mid-1980s in the Sahelian region, and higher year-to-year variability with sequences of dry years in the coastal Guinean regions (Fink et al., 2010a).

When compared with the standardized rainfall time series for the central Sahel and the Guinean coast (Fig. 2.4), it is appeared that the Ouémé regions exhibit a similar rainfall variability than the Guinea coast rainfall index, but the northern Ouémé region exhibits a strong coherence with rainfall anomalies of the Sahel on decadal time scales (Fink et al., 2010b).

It should be highlighted that these variations in the West African climate (rainfall) are generally attributed to the irregular movement of the Inter Tropical Convergence Zone (ITCZ) (Cochémé and Franquin, 1967). However, local factors, such as surface conditions, orography phenomena and atmospheric disturbances are important too (Shelton, 2009). The Inter Tropical Convergence Zone (ITCZ) is the zone of discontinuity between two air masses with distinctly different moisture characteristics (Le Barbé et al., 2002): (i) the maritime (humid) air mass originating from the Atlantic Ocean and associated with the south-western winds, commonly referred to the southwest monsoon (Fink et al., 2010b); and (ii) the continental (dry) air mass originating from the African continent and associated with the north-eastern Harmattan winds. The ITCZ has its most northerly position in August and its southern most position in January (Weischet & Endlicher, 2000). It is evident that increasing atmospheric disturbance (e.g. gas emission) and changes in landscape surfaces may

strongly affect the air mass characteristics, and thus may increase climate variability and climate change.

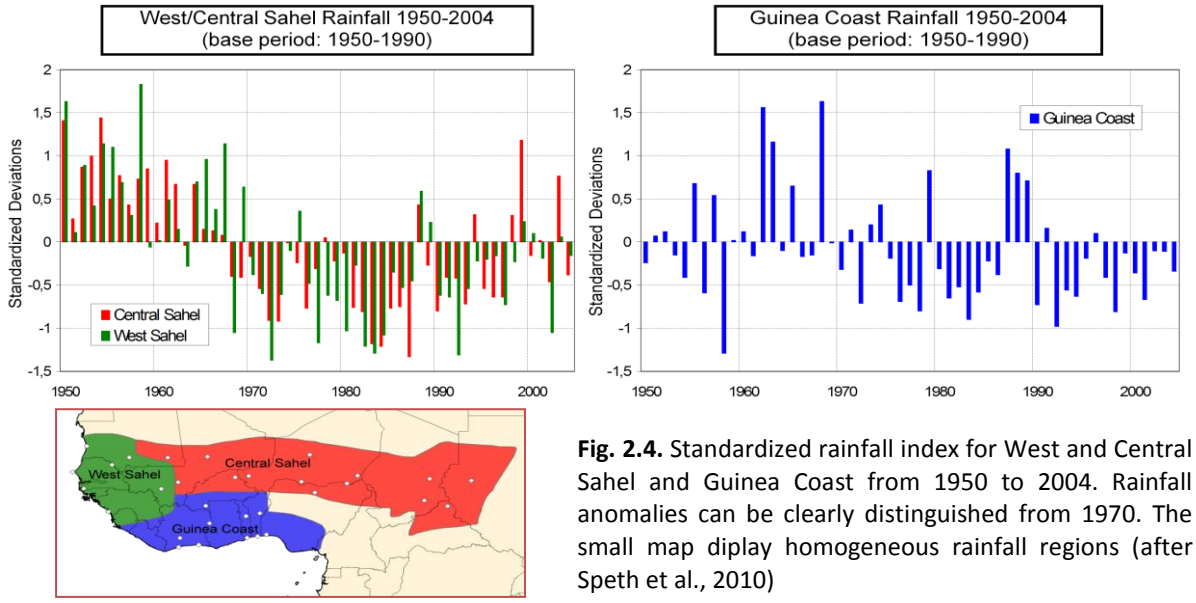

Fig. 2.4. Standardized rainfall index for West and Central Sahel and Guinea Coast from 1950 to 2004. Rainfall anomalies can be clearly distinguished from 1970. The small map diplay homogeneous rainfall regions (after Speth et al., 2010)

2.6. Hydrology

With a length of about 510 km and with two most important tributaries, Zou (150 km) and Okpara (200 km), the Ouémé river drains into Lake Nokoué (150 km^2) and flows through the coastal lagoon system into the sea (Diekkrüger et al., 2010). While Fig. 2.5 shows only the investigated sub-catchments in this study, Tab. 2.1 presents an exhaustive list of the gauged sub-catchments.

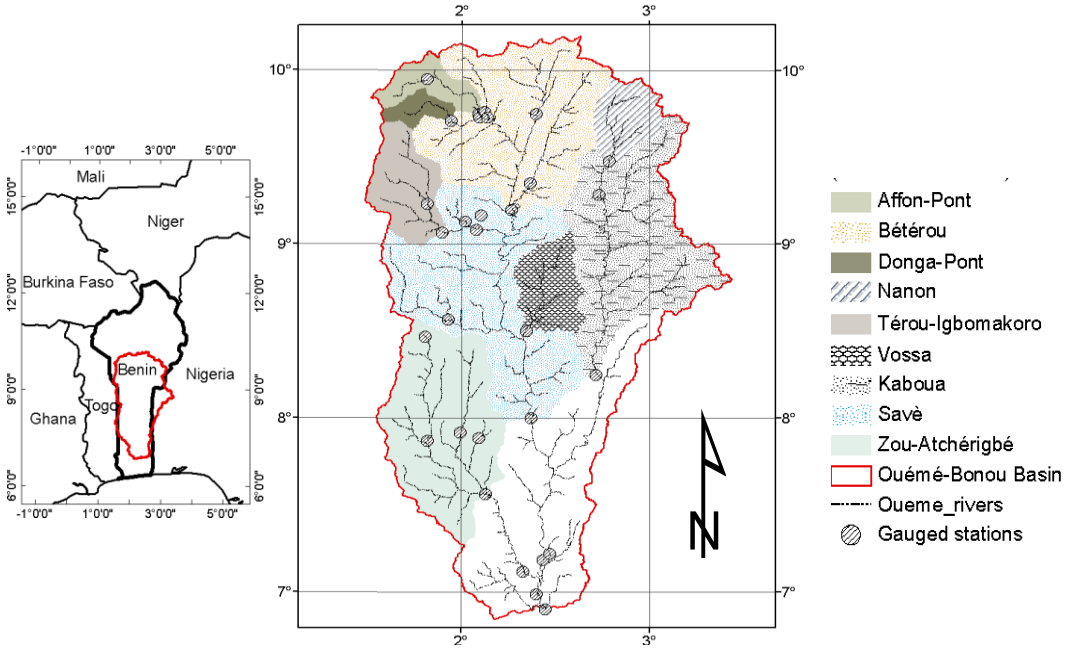

Fig. 2.5. Investigated gauged sub-catchments and hydrometric network of Ouémé-Bonou catchment.

Tab. 2.1. Ouémé river sub-catchments and sizes.

Catchment	River	Longitude	Latitude	Organization	Catchment size [km²]
Affon	Ouémé	2.10	9.75	DG-Eau	1165
Aguimo	Aguimo	2.02	9.13	IRD	402
Ara	Donga	1.61	9.75	IRD	13
Atchérigbé	Zou	2.13	7.56	DG-Eau	6980
Aval-Sani	Ouémé	2.15	9.72	IRD	3283
Barérou	Yérou-Maro	2.38	9.36	DG-Eau	2162
Bétérou	Ouémé	2.27	9.20	DG-Eau	10050
Bonou	Ouémé	2.45	6.91	DG-Eau	49256
Donga affon	Donga	2.10	9.73	IRD	1330
Dome	Zou	2.32	7.10	DG-Eau	8303
Donga-Kolo	Donga	1.69	9.75	IRD	105
Donga-Pont	Donga	1.95	9.71	IRD	586
Gourou-Bori	Ouémé	2.40	9.76	IRD	1607
Igbomakoro	Térou	1.88	9.08	IRD	2334
Kaboua	Okpara	2.72	8.25	DG-Eau	9477
Nanon-Binessi	Okpara	2.79	9.48	IMPETUS	1557
Sagon	Ouémé	2.44	7.19	DG-Eau	12
Sani	Sani	2.12	9.76	IRD	745
Sarmanga	Térou	1.82	9.23	IRD	1378
Savè	Ouémé	2.38	8.01	DG-Eau	23485
Tébou	Ouémé	1.87	9.95	IRD	515
Vossa	Beffa	2.34	8.49	DG-Eau	1935
Wanou-Cote	Térou	2.09	9.09	DG-Eau	3133
Wé-Wé	Wé-Wé	2.12	9.39	DG-Eau	293
Zagnanado	Ouémé	2.47	7.21	DG-Eau	38141
Zoundji	Zou	1.83	7.87	DG-Eau	1552
Bori-Gourou	Alpouro	2.40	9.76	DG-Eau	1607

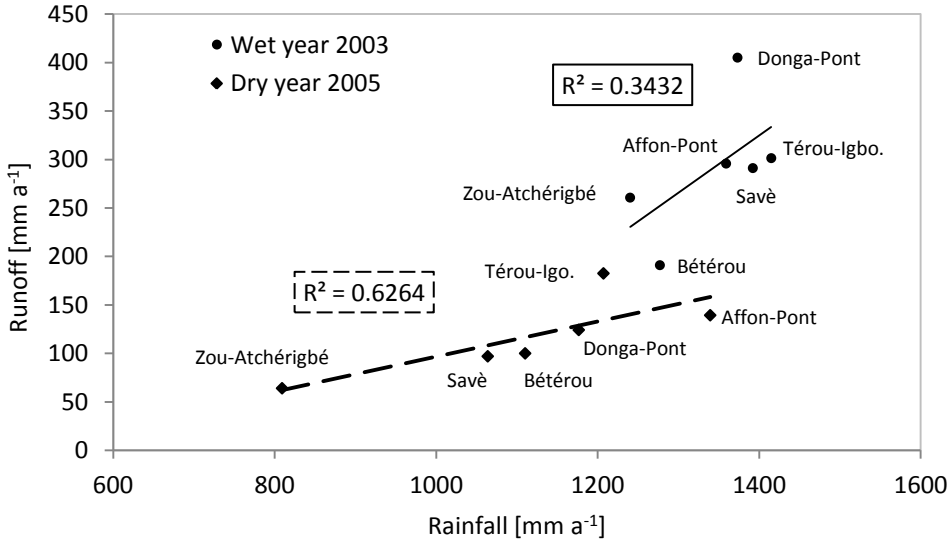

Fig. 2.6. Rainfall - runoff relationships for the main Ouémé sub-catchments for the wet year 2003 and the dry year 2005 (Donga-Pont: 586 km²; Affon-Pont: 1179 km²; Térou-Igbo.: 2344 km²; Atchérigbé: 6978 km²; Bétérou: 10072 km²; Savè: 23488 km²).

Rainfall-runoff variability is high in the catchment (Fig. 2.6), leading to runoff coefficients varying from 0.10 to 0.26 (of the total annual rainfall), with the lowest values for the savannahs and forest landscapes (Diekkrüger et al., 2010). Given the importance of the inland-valley areas within the Ouémé catchment (Speth et al., 2010), high impacts on the processes may be expected, but not invested in detail neither in any previous works nor in this work. Beyond this aspect, a general framework of process understanding is provided in the chapter 3. The rainfall anomalies observed

since 70's in the Sahelian and Guinean West African regions (cf. section 2.3) are reflected in the Ouémé catchment water balance, mainly the total water discharge (IMPETUS, 2002). As it can be seen in the Fig. 2.7 a persistent decrease of the annual total discharge at the Bétérou gauging station (cf. Fig. 2.5) is detected since the 70's to 2000.

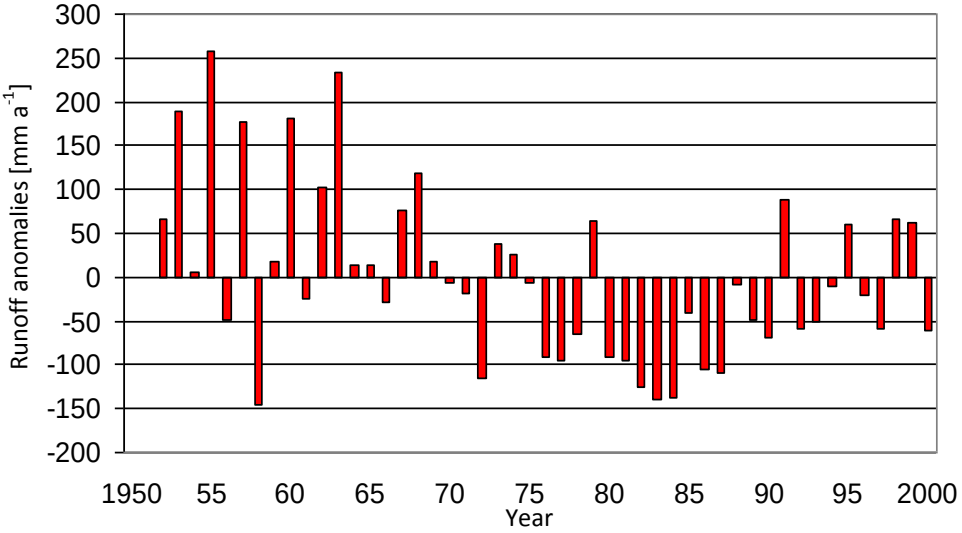

Fig. 2.7. Deviation from the average yearly discharge of the Ouémé at the Bétérou station from 1950 to 2000 (IMPETUS, 2002)

2.4. Soils

In the Ouémé catchment the main landscape elements are the crest and the upper, middle and lower slopes (together referred to high peneplains), following by the valley fringe and colluvial footslopes, and the valley bottoms and terraces (low peneplains and floodplains) (Igué 1996; Igué, 2000). As the most widespread landscape element within the Ouémé catchment, the high peneplains is consisted of three major soil types (Igué, 2000): deep to very deep red soils, moderately deep, shallower and gravelly soils that overlie some time the rock (basic basement Dubroeucq 1967) or petroferric horizon (gneiss/migmatite basement) (Dubroeucq 1967, Windmeijer and Andriesse 1993).

At regional scale, predominant soil are fersialitic soils (ferruginous tropical soils), characterized by clay translocation and iron segregation (ferruginous tropical soils with concretions), which lead to a clear horizon differentiation (Faure and Volkhoff, 1998; Gaiser et al., 2010).

A local scale description (Fig. 2.8) has shown a typical catena with soils formed on the slopes, leached ferruginous tropical soils (Orthidystri-Epi- or Endoskeletic Acrisols/Haplic Lixisols or Typic Kandi-ustults/Typic Kandiustalfs) (Busche et al., 2005; Junge, 2004; Sintondji, 2005, Hiepe, 2008; Gaiser et al., 2010). Leached and indurated ferruginous tropical soils (Hyperalbi-Petric Plinthosols/Plinthic Petraquepts) are developed at lower parts of the slopes. Hydromorphic soils (Humic Gleysols/Typic Epiaquepts) are found in the inland valleys. In the riverbeds, poorly evolved soils are distributed (Arenic Fluvisols/Typic Ustifluvents) (Junge, 2004; Sintondji, 2005, Hiepe, 2008; Gaiser et al., 2010). Examples of physical and chemical contain for Gleysol and Acrisol are provided in Fig. 2.9.

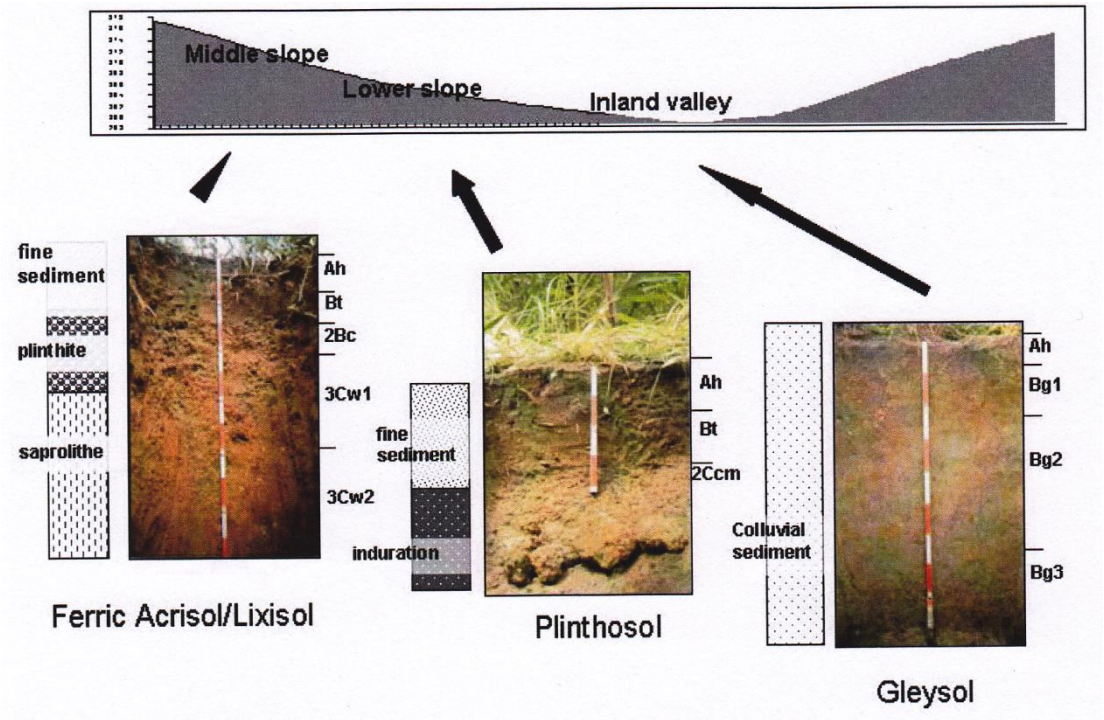

Fig. 2.8. Main soil distribution of a typical soil catena in the Térou-Igbomakoro sub-catchment (Junge, 2004).

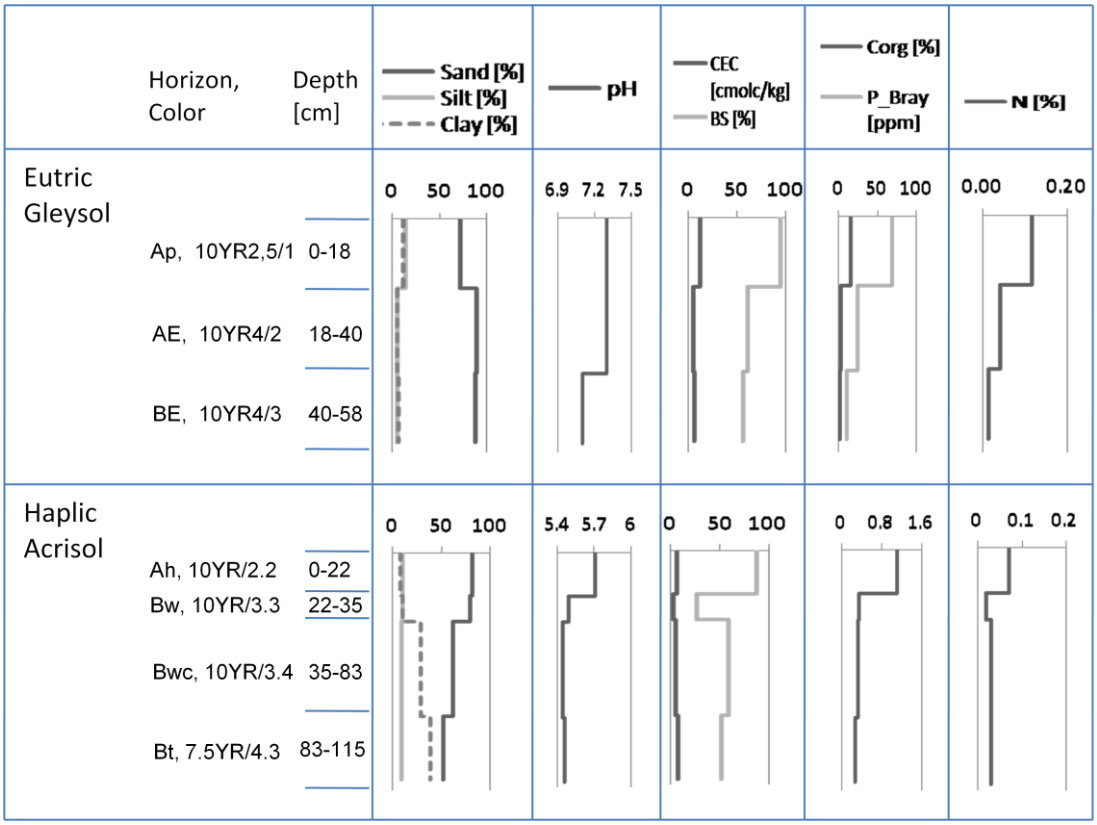

Fig. 2.9. Example of physical and chemical contain for Gleysol and Acrisol as investigated.

2.5. Vegetation

The Ouémé catchment landscape is characterized by forest islands, gallery forest, savannah, woodlands, agricultural lands, pastures and mosaics of cropland and bush fallow, plantation with Parkia, Cashew and palm trees (Bossa, 2007). Agriculture and other human activities have led to large scale deforestation and fragmentations leaving only small blocks of natural vegetation types within a matrix of degraded secondary habitats (Porembski et al, 2010). Woodland and savannah are the main types of natural vegetation found in the upper basin, while the southern part is characterized mainly by gallery forests. The vegetation density is higher in the north than the south, due to a lower population density. Bush fires occurring regularly during the dry season enhance runoff and erosion due to clearing of the vegetation which results in a rapid degradation of the soils. From the base to top of the hills, the vegetation physiognomy varies (Bossa, 2007):

(1) the vegetation of thalwegs is consisted of wood savannahs and gallery forests with species such as *Anogeissus leiocarpus, Daniellia oliveri, Lophira lanceolata;*

(2) on hydromorphic soils are found species such as *Anogeissus leiocarpus, Pterocarpus santalinoïdes, Terminalia macroptera, Acacia caffra*, and plantation species such as *Mangifera indica, Carica papaya, Psidium quayaya, Tectona grandis* (teck), *Dolonix regia*, *Anacardium occidentale* ;

(3) the vegetation of plains are savannah trees consist of species such as *Daniellia oliveri, Isoberlinia doka, Parkia biglobosa, Pteleopsis laxiflous, Pterocarpus erinacens, Vitellaria paradoxa, Bridelia ferruginen, Chlorophora excelsa, Detarium microcarpus*, Poaceae such as *Imperata cylindrica*, *Schizachirum pulchellum, Eragrostis namaguensis, Andropogon gayanus* are part of the plain vegetation. In the fractures of migmatite and gneiss blocks are found species such as *adansonia digitata* (baobab), *Ceiba pentandra, Isoberlinia doka, Pterocarpus africana*; and

(4) lichens and mosses are found at the hill summits.

2.7. Ethnic groups and migrations

With roughly 7 million inhabitants and a demographic growth of 3.3% in 2002 (INSAE, 2003), Benin population is characterized by strong spatial disparities: 238 inhabitants/km² in south and 27 inhabitants/km² in central and North Benin (Heldmann et al., 2010). Two major socio-cultural groups are dominant at the national level: (i) the southern-central group with Fon and related groups like Adja and Yoruba/Nagot; and (ii) the northern group with Bariba, Dendi, Bètamaribè, Yoa, Lopka and Fulani (INSAE, 2003).

For example in the Department of Collines (centre of the Ouémé catchment), the ethnic group Yoruba (26.5%) has the majority, followed by the group Mahi (25.7%), Idaasha (14.9%) and Fon (13%), according to INSAE (2003). These peoples are engaged in many activities such as agriculture which is mainly practiced by the ethnic group Ife, Mahi, Fon, Cotocoli, Betamaribé and Adja, who use members of the Kabia group as seasonal agricultural workers. The Yoruba are traders while the Fulani are commonly cattle farmers. It should be noted that the Fon and Adja, who migrated to this area are mainly in search of vast fertile land they cannot find at home. The communes and villages are characterized by high multiculturalism of even more than 40 ethnic groups with more than 75% of migrants (case of Bétérou, commune of Tchaourou in the upper Ouémé catchment).

In addition, job seeking and attractiveness of cities lead the youth to rural exodus towards neighboring countries (before Ghana and nowadays Nigeria). This migration results in a significant reduction of potential workers, something that contributes to the decline in agricultural production.

3. Hydrology, erosion and model definition

3.1. Hydrological cycle and water balance

Modern hydrology is broadly defined as the science that studies the occurrence and movement of water on and under the Earth's surface, water's chemical and physical properties, water's relationship to biotic and abiotic environmental components, and human effects on water (Ward and Robinson, 2000; Shelton, 2009). The hydrosphere is composed of four large reservoirs with permanent exchanges (Fitts, 2002): (i) the seas and oceans, (ii) inland/continental waters (surface water, soil and groundwater), (iii) the atmosphere water, and (iv) the cryosphere. The exchangeable water between these different reservoirs may be temporarily as vapor, clouds and precipitation (under the influence of solar energy and air masses).

According to Shelton (2009), recognizing the full natural range of phenomena included in the hydrologic cycle is aided by conceptualizing the hydrologic cycle as consisting of two branches: (1) a terrestrial branch encompasses continental processes and (2) an atmospheric branch provides an energy and moisture redistribution mechanism. The terrestrial branch of the hydrologic cycle consists of the inflow, outflow, and storage of water in its various forms on the continents. The primary focus of the terrestrial branch is the natural processes at or near the land surface that ultimately produce surface and subsurface runoff and directly influence cycles of other materials that shape the Earth's surface (Stricker et al., 1993; Shelton, 2009).

De Marsily (1995) mentioned in his work that any loss of water by one of both parts (atmospheric and terrestrial) is a gain for the other part, what guarantees a certain stationarity of the water cycle. The continental branch of the cycle (according to De Marsily, 1995) involves at soil level two types of reservoirs (case of tropical regions) housing complex physical processes, conditioning internal trade on one hand and external exchanges with the atmospheric circulation on the other hand: (1) surface water reservoirs that contains all the water stored in surface depressions, from smaller (due to surface roughness) to larger flood plains, rivers, lakes, marshes, ponds, etc.; and (2) soil and subsoil reservoirs in which water is stored as soil moisture and groundwater.

The precipitated water over the catchment is divided into intercepted water, retained water on the soil surface, infiltration and runoff (Beven, 2001). All of the intercepted water and part of the water retained in the soil surface and seeping is lost through evaporation and transpiration (Arnald et al., 1998). The blade surface water runoff becomes direct runoff and is an important part of the flow to the outlet. The other components of the flow at the outlet are the delayed interflow and base flow derived respectively from the infiltrated water in the unsaturated zone and water from groundwater (Beven, 2001). These hydrological processes interact in complex ways over time and space. Taking into account the scales of the process variability in models is one of the major challenges of the modern hydrology. To understand this variability, it is common to investigate over a long period, changes in water balance.

The International Glossary of Hydrology (UNESCO, 1992) defines the water balance as the balance based on the principle that during a certain time interval, the total contributions to a watershed or an aquatic entity must be equal to the total output plus the change, positive or negative, of water volume stored in the watershed or the entity (Fig. 3.1). The water balance is thus defined at the watershed scale and results in the simplified equation:

$$\Delta S = P + Q_{in} + G_{in} - (Q_{out} + G_{out} + ET) \quad \text{(Eq. 3.3)}$$

where, ΔS = change in the storage, P = Precipitation, Q_{in} = Surface surface inflow, Q_{out} = surface outflow, ET = Evapotranspiration, G_{in} = sub-surface inflow and G_{out} = sub-surface outflow.

The determination of the water balance terms may become complex when interactions between neighboring watersheds occur. Indeed, the watershed is not always a closed system as is often

considered, the superposition of topographic watershed and hydrogeologic watershed is not always perfect. As a result, exchanges between neighboring watersheds occur in the ΔS component, which complicates its accurate assessment (Zannou, 2006).
Soil moisture is a key parameter in the hydrological cycle, because on that, depend several exchanges: infiltration, surface runoff, amount of water absorbed by vegetation. The soil moisture dynamic in the tropics is represented by the balance equation (Ngo-duc, 2005):

$$\frac{\partial w}{\partial t} = P - E \pm R \pm Df \qquad \text{(Eq. 3.1)}$$

where, *w* is the soil moisture (in *mm*), *P*, the total precipitation, *E*, total evapotranspiration *R*, surface runoff and *Df*, profile bottom drainage. The total evapotranpiration is the sum of soil evaporation (E_{sol}), the stored water by the canopy (*EI*) and plant transpiration (*Tr*):

$$E = Esol + EI + Tr \qquad \text{(Eq. 3.2)}$$

3.2. Soil hydraulic properties and soil water

Soil is a typical heterogeneous multi-phasic porous system, which, in its general form, contains three phase components: (1) the solid phase of the soil matrix (formed by mineral particles and solid organic materials), (2) the liquid phase, which is often represented by water and which could more properly be called the soil solution; and (3) the gaseous phase, which contains air and other gases (Ali, 2010). According to Musy and Soutter (1991), soil may be defined as the reorganized product from the alteration of the surface layer of the terrestrial crust, mainly under influences of climatic and biological agents.
From a hydrologist's point of view, soils are porous environments consisting of grain, more or less cemented, and forming a skeleton around which remain empty spaces (porosity). These spaces are partially or completely saturated with water. The physical properties of water along with the size and distribution of pore spaces determine how much water is stored in a given volume and how easily water moves through the soil material (Fitts, 2002). Castany (1961) defines as "drainage porosity" the ratio of the volume of free water that may contain a porous environment in a saturation state and then release as a result of a complete drainage. De Marsily (1994) defines rather as "kinematic porosity" the ratio of water volume that can flow to the total void volume.
Several phenomena may limit the drainage or kinematic porosity: the adsorption of a water layer on the solid grain surface (bound water) by molecular attraction and capillary forces, and the existence of non-connected pores (Fitts, 2002). These different properties predispose the soil to a water content rather variable and leading it to the so-called non-saturation or saturation condition (van Genuchten, 1980). The volumetric water content of a soil (θ) varies from a residual value near zero to the maximum value (θ_s) when the soil is saturated.
In addition, water in porous environment is characterized by its energy state, which defines the total potential energy, resulting from the addition of acting forces (Smith and Mullins, 2000). One may define the hydraulic charge (or total potential energy), which often comes down to the sum of the gravitational potential and the matrix potential (consequence of capillary forces and adsorption from solid matrix, which attract and bind to the solid phase in the soil). The matrix potential is defined as positive under the water table surface and negative otherwise. The first case is encountered in the so-called saturated environments, and the second in unsaturated environment. It should be emphasized that the fundamental difference between these two types of environment is the resistance to flow, observed in non-saturated environment, which is significantly absent in saturated environment (Musy and Soutter, 1991).

3.3. Infiltration and Evaporation

Infiltration is the movement of water from soil surface into the soil. According to Musy and Soutter (1991), infiltration can be defined as the movement of water from soil surface to soil layers when the soil receives rain or is exposed to flooding. The opposite movement of water results in evapotranspiration, which represents plant consumption (transpiration) or the climatic demand expressed by the moisture deficit of the air (evaporation). Evaporation from free water surfaces and moist soil surfaces occurs when the ambient air vapor pressure gradient is less than the vapor pressure at the evaporating surface and an external source of energy is present (Shelton, 2009). Transpiration is a more complex process and the transpired water rate differs considerably from one plant species to another, largely in response to the plant rooting depth and the vegetative area (Shelton, 2009).
Many factors can influence the infiltration of water into the soil. Indeed, the soil may have some stratification, a surface crust or an initial moisture profile which is not homogeneous due to successive sequences of infiltration, redistribution and evaporation. Infiltration is influenced by the hydrodynamic properties of successive soil layers and the initial state of the profile. One can also consider two different forms of stratification. The one related to the soil pedogenesis reflecting the vertical succession of soil horizons and those related to the degradation of soil structure on the surface (surface crusts). It may be added the strata resulting from human activities, such as compacted horizons or plow pans.

3.4. Runoff generation

The combination of soil hydraulic properties, topography, anthropogenic impacts and rainfall events may highly control the soil water flow as well as infiltration and evapotranspiration, and different hydrological processes may occur at different length scales. According to Blöschl and Sivapalan (1995), runoff generation may be associated with rainfall intensities exceeding infiltration capacities (which produces infiltration excess/Hortonian overland flow), a ‘point phenomenon’ and can, as such, be defined at a very small length scale. Blöschl and Sivapalan (1995) explained that the saturation excess runoff (i.e. saturation overland flow) is an integrated process and needs a certain minimum catchment area to be operative. This is because, typically, the main mechanism for raising the groundwater table (which in turn produces saturation overland flow) is the lateral percolation above an impending horizon. Also, subsurface storm flow needs a certain minimum catchment area to be operative. Channel flow typically occurs at larger scales above a channel initiation area up to the length scales of the largest river basins (Blöschl and Sivapalan, 1995).
Clearly, surface runoff is affected by both meteorological factors (rainfall intensity, amount, duration; distribution of rainfall over the drainage basin; climatic conditions that affect evapotranspiration, such as temperature, wind, relative humidity, season), geology and topography of the land (land use, vegetation, soil type, basin shape, elevation, slope, ponds, lakes, sinks) and human activities (Sintondji, 2005; Giertz, 2006; Hiepe, 2008; Speth et al., 2010).

3.5. Erosion and soil degradation

Erosion is a natural process that confronts the whole world. Erosion can be seen as any movement of soil particles away from their original location. Susceptibility to erosion and the occurrence proportion depend on land use, geology, geomorphology, climate, soil texture, soil structure and the nature and density of vegetation. Arnold et al. (1989) defined erosion as a form of degradation as severe as compaction, reduction of organic matter rate, soil surface deterioration, insufficient subsurface drainage, salinity and soil acidification. All these forms of serious degradation, in

themselves, accelerate soil erosion. The agents of soil erosion are water (water erosion) and wind (wind erosion).

Rainfall intensity and runoff are very important in the water erosion initiation and evolution. According to Arnold et al. (1998), the impact of raindrops can break aggregates and disperse the soil particles in all directions (splash effect).
Several erosion types have been mentioned among other by Morgan (1979, 1986): sheet erosion, gully and ravine erosion. Indeed, after beating the soil surface and making it virtually impermeable, the water runs off in large sheet, loading the finest elements (clays, organic materials and humus), essential for soil fertility. Gully erosion occurs when sheet runoff (erosion) is gathering little by little at the favor of small slopes. A steepening of the slope may increase the water speeds, so getting more force, resulting in regressive erosion (digging backwards) also called ravine erosion.
Roose et al. (2004), in their appreciation of water erosion processes have highlighted the linear erosion, having major importance on steep slopes, where the water and soil particles flow through channels often blocked by stones or plant tufts.
Sediment yield may be defined as the fraction of the land surface eroded particles leaving a catchment. Topography, soil, geology, land use, climate/rainfall regime and crop system management are among other factors that may influence the loading and delivery rate. Oeurng et al., (2010) analyzed the dynamics of suspended sediment transport and yield in a large agricultural catchment in southwest France, and found that there were significant correlations between total precipitation, discharge peak, total water yield, flood intensity and sediment variables during the flood events, but no relationship with antecedent conditions.

Erosion and soil degradation have evolved in very considerable proportions in Africa, especially in tropical Africa. Moreover, to achieve the Millennium Development Goals (UNDP, 2005), it is crucial to take serious measures against erosion and soil degradation, which are primarily sheet and gully erosion that scours the humus horizon in one generation (Roose et al., 2004).
Many researches have been conducted in parts of Africa to understand the processes as for the determinant and promoting causes, related to the specific climatological, meteorological and soil condition (Giertz et al., 2006, Bormann et al. 2005; Laouina et al., 2004, Roose et al., 2004, Speth et al., 2010). Indeed, an application of the Universal Soil Loss Equation (Roose et al. (2004) have shown that tropical soils are quite vulnerable to tropical rains, despite their very high stability. Many studies in Benin (Gbessemehlan, 1988; Biaou, 1995; Dissou, 1992; Sintondji, 2005; Hiepe, 2008; Speth et al., 2010) showed a fast degradation of natural resources. It is shown that agricultural soils are degrading very quickly. In the upper valley of Ouémé basin (Benin), Bormann et al. (2005) indicated a soil loss of about 40 tons per hectare per year in agricultural land compared to 3.9 tons per hectare per year in the savannahs.
The Ouémé basin is exposed to a low productivity and water resources availability, given the close relationship established between the water balance, the changes in the vegetation and soil degradation (Falkenmark and Widstrand, 1992 and Speth et al., 2010).

3.6. Impacts of global change on water and land resources in the tropics

Vulnerability to change, whether climate-induced or related to changes in land use/land cover, is a major threat, consisting at the same time of a water dimension (lower level of the water table), an agrarian dimension (falling yields) and an environmental dimension (weakening of the soil and increasing erosion) (Laouina et al., 2004). Several investigations on the global change processes and its impact on the hydrological cycle have shown that global climate change has a significant influence on the regional water resources (Bormann et al., 2005; Speth et al., 2010).
Many studies led on hydro-meteorological variability in the world and especially in several West Africa catchments account for the effectiveness of changes taking place. Paturel et al. (2003) has

shown that the rainfall deficit of about 10 to 30% observed in the Niger basin (in the north of Benin) since the 70's led to a decline of more than 40% of the river water.
Leduc et al. (2001), Seguis et al (2004), Mahe et al. (2005) stated that the decrease in flow rate observed in the Sudano-Guinean catchments (including parts of the Ouémé catchment) is probably related to a decrease of groundwater resources, which amplifies the effect of rainfall deficit. They highlighted also that the drying and warming expected in the semi-humid African regions may cause a water deficit in higher grade and reduce infiltration rate (less groundwater recharge).
All investigations indicate that at the local level, the water balance is extremely sensitive to changes in vegetation and soil degradation (Giertz et al., 2006; Speth et al., 2010). According to Bormann et al. (2005), Benin will be exposed to the effects of severe water stress from the year 2025, taking into account the population development.

3.7. Hydrological models and their application in the tropics

A model may be defined as a set of equations reflecting complex phenomena, often used to describe complex systems, including predictions of their future trends. It may be seen in hydrology as a formalization of knowledge of the processes involved in the water cycle. According to Loague and VanderKwaak (2004), the aim of a model is precisely not to reproduce reality in all its complexity, but rather to capture in a vivid, often formal, way what is essential to understanding some aspect of its structure or behavior. In the watershed hydrology, the model is designed primarily to simulate various levels of detail, the physical processes involved in the transfer of moisture flux such as interception, evapotranspiration, changes in soil water content, surface runoff, infiltration, percolation, storage of groundwater and river flow (Le Lay, 2006). Hydrological models are used to associate these processes dynamically to better understand their nature, role and interaction in time and space.
Schematically, modeling can be seen as a simulation of the spatio-temporal evolution of prognostic variables such as watershed runoff in response to the spatiotemporal evolution of forcing variables (e.g. precipitation), taking into account a number of state variables or internal variables such as soil moisture. Characteristic information of the studied system may be generally included in the models (measurable characteristics used directly as input variables) (Le Lay, 2006). Other characteristics of the system may have a more subjective nature, as for the formal description and assumptions that are made of the studied system (model parameters).
From suggested model classifications (Clarke, 1973; Ambrose, 1999; Beven, 2001; Loague and VanderKwaak, 2004, Le Lay, 2006), two main criteria can be distinguished when designing a watershed model: (i) how the hydrological processes will be described and (ii) the spatial representation of the catchments. The process description in the models has led to three different terminologies: (i) statistical models; (ii) conceptual models; and (iii) physical-based models. As for the spatial representation of the catchments, two different terminologies are most used: lumped models and distributed or semi-distributed models.

“Statistical models”, often based on regressions, aim to characterize the rainfall-runoff relationship, without involving the physical nature of the watershed. They are less used in impact studies, since many parameters affecting runoff are non-stationary (e.g. evapotranspiration, vegetation, land use, extraction of groundwater, etc.).
“Conceptual models”, which break down the watershed functioning into sub-processes. In most cases, the watershed is represented as a collection of interconnected reservoirs, described by balance equations and draining laws. If they can simulate comprehensively various water cycle components (evapotranspiration, runoff, recharge and groundwater flow, water storage), they are nevertheless a highly simplified of the watershed functioning. The reservoir interconnexion and the used drainage laws are most often derived from an empirical approach, and the parameters are of little physical significance.

"Physically-based models" aim to represent the physical processes in the watershed dynamic, within a unified theoretical framework. They use conservation relationship (mass, energy, momentum) described by a system of partial differential equations with parameters (in principle measurable), related to system physical properties (Abbott et al., 1986). They are based on a high resolution spatiotemporal discretization, to simulate in any point and at any time the system evolution.
The Soil and Water Assessment Tool (SWAT) model (Arnold et al., 1998), used for simulating water balance and soil degradation in the following chapter of this thesis, may be placed between the conceptual and physically-based models. One should highlights that the model classification is up to now a non-closed discussion, leading often to many contradictions.

It is possible to consider the basin as a single homogeneous entity, represented by mean parameters or equivalents, taking into account spatial heterogeneities indirectly: this is called a global approach, leading to the so-called "lumped models".
The watershed may be spatially discretized, in order to consider fully and explicitly, the spatial variability of processes. The resulting model is called "distributed models". The degree of consideration of spatial heterogeneities distinguishes the "semi-distributed models" from distributed models, although the acceptance of these terms is subject to discussions. Specifically, as for the Soil and Water Assessment Tool (SWAT) model (Arnold et al., 1998), it may be placed between the distributed and semi-distributed models.

In the African sub-Sahara countries, different hydrological model concepts are nowadays used. Most of these models would be able to predict impacts of climate and land use change on the hydrological processes, water availability, and the degradation of natural resources in general (Giertz et al., 2006; Speth et al., 2010). Moreover, closed relationships between water balance and changes in the vegetation have been already highlighted by Speth et al. (2010). Although simple models (often used to bypass the known data gap in the region) may allow the assessment of different hydrological components, it is become essential and crucial to use more complex distributed and physically-based models, to be able to consider climate and land use change effects on hydrological processes. This arises three different problems to be solved: (1) how to bridge the data gap; (2) how to deal with the traditional difficulties to determine groundwater flow component of streamflow (Arnold and Allen, 1999), which still is unclear for the regional hydrologists; and (3) how to deal with the numerous physically-based model parameters (which should be in principle measured, but quite difficult, even in the developed countries), much influenced by modeling scale. It should be simply noted that increasing efforts are in progress for creating various types of databases through cooperation/developing projects such as the IMPETUS project, the WASCAL project (), etc..

4. Modeling approach

4.1. Model description

The Soil and Water Assessment Tool (SWAT) is a hydrological and water quality model developed by the United States Department of Agricultural-Research-Service (USDA-ARS) (Arnold et al., 1998). It is a continuous-time model that operates at a daily time-step. It allows the assessment of various subsurface flows and storages (Fig. 4.1) and related sediment and nutrient loads, takes into account the feedback between plant growth, water, and nutrient cycle, and helps to understand land management practice effects on water, sediment, and nutrient dynamics. It incorporates a kinematic storage model for subsurface flow modeling in two-dimensional cross-chapter along a flow path down a hillslope which is important for an appropriate modelling of subsurface flow processes. It is a catchment scale model which can be applied from small (km^2) to regional and large scale (100,000 km^2). The catchment is subdivided into sub-catchments/sub-basins using a Digital Elevation Model (DEM). Each sub-catchment consists of a number of Hydrological Response Units (HRU) which are homogeneous concerning soil, relief, and vegetation but are not georeferenced within the sub-catchment. SWAT has been successfully applied over the world for hydrological process assessment, water quality studies, and recently for crop yield assessment (Srinivasan et al., 2010). It was successfully applied for several Benin catchments and even the whole West Africa sub-continent (4-million km^2) for modeling water availability (Sintondji, 2005; Busche et al., 2005; Hiepe, 2008; Schuol et al., 2007). The following description is based on Arnold et al (1998) and relevant explanations from Sintondji (2005) and Hiepe (2008).

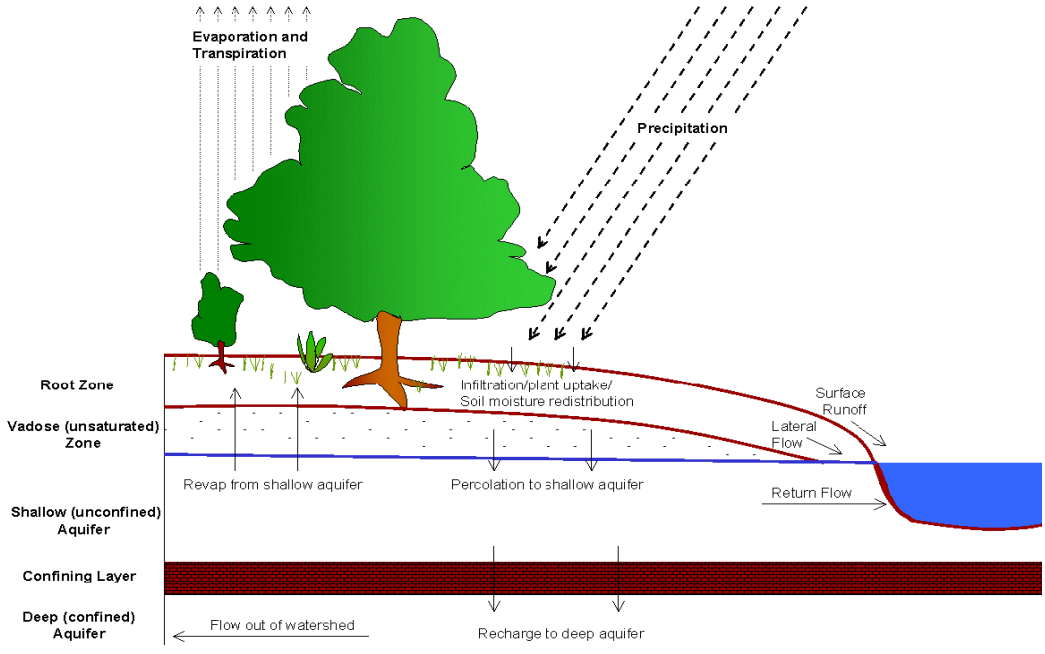

Fig. 4.1. Schematic representation of the hydrologic cycle (after Neitsch et al., 2001)

Water balance

The land phase of the hydrologic cycle as computed in the SWAT model is based on the water balance equation Eq. 4.1). Runoff amounts are predicted for each sub-catchment and then routed to the channel.

$$SW_t = SW_0 + \sum_{i=1}^{t}(R_i - Q_i - ET_{a,i} - W_{seep,i} - Q_{gw,i}) \quad \text{(Eq. 4.1)}$$

Where SW_t is the final soil water content [mm], SW_0 is the initial soil water content on day *i* [mm], *t* is the time (days), R_i is the amount of precipitation on day *i* [mm], Q_i is the amount of surface runoff on day *i* [mm], $ET_{a,i}$ is the amount of evapotranspiration on day *i* [mm], $W_{seep,i}$ is the amount of water entering the vadose zone from the soil profile on day *i* [mm], and $Q_{gw,i}$ is the amount of return flow on day *i* [mm].

Surface runoff

Surface runoff is predicted using a modified version of the SCS CN method (SCS, 1972, 1986). This method involves various types of data related to vegetation, hydrologic soil group, slope, and antecedent moisture condition (Eq. 4.2).

$$Q = \frac{(R-0.2S)^2}{(R+0.8S)} \quad \text{for} \quad R > 0.2S \quad \text{and} \quad Q = 0 \quad \text{for} \quad R \le 0.2S \quad \text{(Eq. 4.2)}$$

$$S = 25.4\left(\frac{1000}{CN} - 10\right) \quad \text{(Eq. 4.3)}$$

where Q is the daily surface runoff [mm], R is the daily rainfall [mm], and S is a retention parameter. S varies within basins under various soil, land use, management, and slope conditions and responds to changes in soil water content over time. The parameter S is related to the curve number (CN) by (Eq. 4.3).
The peak runoff rate is the maximum runoff rate that occurs with in a given rainfall event. The peak runoff rate is an indicator of the erosive power of a storm and is used to predict sediment loss. SWAT calculates the peak runoff rate with a modified rational method as a function of surface runoff, sub-catchment area, time of concentration and the fraction of daily rainfall during time of concentration:

$$q_{peak} = C \cdot i \cdot \frac{Area}{3.6} = \frac{Q_{surf}}{R_{day}} \cdot \frac{R_{tc}}{t_{conc}} \cdot \frac{Area}{3.6} = \frac{\alpha_{tc} \cdot Q_{surf} \cdot Area}{3.6 \cdot t_{conc}} \quad \text{(Eq. 4.4)}$$

Where, q_{peak} is the peak runoff rate [m^3/s], C the runoff coefficient [-] (quotient of Q_{surf} and R_{day}), i the rainfall intensity [mm/h] (quotient of R_{tc} and t_{conc}), $Area$ the sub-catchment area [km^2], *3.6* a conversion coefficient, R_{tc} the rainfall during time of concentration [mm], R_{day} the daily rainfall [mm], t_{conc} the time of concentration for the sub-catchment [h], α_{tc} the fraction of daily rainfall that occurs during the time of concentration [-], and Q_{surf} the surface runoff [mm].
The time of concentration is the amount of time from the beginning of a rainfall event until the entire sub-basin area is contributing to flow at the outlet. In other words, the time of concentration is the time for a drop of water to flow from the remotest point in the sub-basin to the sub-basin outlet. The time of concentration is calculated by summing the overland flow time (the time it takes for flow from the remotest point in the sub-basin to reach the channel) and the channel flow time (the time it takes for flow in the upstream channels to reach the outlet). For large sub-catchments with a time of concentration being greater than one day, SWAT incorporates a surface runoff storage feature to lag a portion of the surface runoff release to the main channel (Eq. 4.5).

$$Q_{surf} = \left(Q'_{surf} + Q_{stor,i-1}\right) \cdot \left(1 - e^{\frac{-surlag}{t_{conc}}}\right) \quad \text{(Eq. 4.5)}$$

Where, Q_{surf} is the surface runoff discharged to the main channel on a day [mm], Q'_{surf} the generated surface runoff in the sub-catchment on a day [mm], $Q_{stor,\,i-1}$ the surface runoff stored or lagged from the previous day [mm], *surlag* the surface runoff lag coefficient [-], t_{conc} the time of concentration for the sub-catchment [h].

Potential and actual evapotranspiration

Evapotranspiration is a collective term that includes all processes by which water at the earth's surface is converted to water vapor. It includes evaporation water intercepted by the plant canopy, transpiration, sublimation and evaporation from the soil and water systems. Potential soil water evaporation is estimated as a function of potential evapotranspiration and leaf area index. Three methods to estimate PET have been incorporated into SWAT: the Penman-Monteith method (Monteith, 1965; Allen et al., 1989), the Priestley-Taylor method (Priestley and Taylor, 1972) and the Hargreaves method (Hargreaves et al., 1985). The Penman-Monteith method as used in this study requires solar radiation, air temperature, relative humidity and wind speed, and combines components that account for energy needed to sustain evaporation, the strength of the mechanism required to remove the water vapor and aerodynamic and surface resistance terms:

$$\lambda E = \frac{\Delta \cdot \left(H_{net} - G\right) + \rho_{air} \cdot c_p \cdot \left|e_z^0 - e_z\right| / r_a}{\Delta + \gamma \cdot \left(1 + r_c / r_a\right)} \quad \text{(Eq. 4.6)}$$

where, λE is the latent heat flux density [MJ/m^2/d] , E the depth rate of evaporation [mm/d], Δ the slope of the saturation vapour pressure-temperature curve (de/dT [kPa/°C]), H_{net} the net radiation [MJ/m^2/d], G the soil heat flux [MJ/m^2/d], ρ_{air} the air density [kg/m^3], C_p the specific heat at constant pressure [MJ/kg/°C], e_z^0 the saturation vapour pressure of air at height z [kPa], e_z the actuel water vapour pressure of air at height z [kPa], γ the psychrometric constant [kPa/°C], r_c the plant canopy resistance [s/m] (function of the leaf area index), and r_a the diffusion resistance of the air layer (aerodynamic resistance) [s/m].
SWAT uses a part of the daily rainfall amount to first fills the canopy storage before any water is allowed to reach the ground. The maximum storage capacity varies as a function of LAI. SWAT first evaporates any rainfall intercepted by the plant canopy with a potential rate. Next, SWAT separately calculates the potential transpiration and potential soil evaporation using a modified approach of Ritchie (1972). The depth distribution used to determine the maximum amount of water allowed to be evaporated is given by Eq. 4.7.

$$\mathrm{E}_{\mathrm{soil},z} = \mathrm{E}_{\mathrm{s}}^{\mathrm{ll}} \cdot \frac{\mathrm{z}}{\mathrm{z} + \exp\left(2.374 - 0.00713 \cdot \mathrm{z}\right)} \quad \text{(Eq. 4.7)}$$

Where, $E_{soil,z}$ is the evaporative demand at depth z [mm], E_s^{ll} the maximum soil water evaporation on a given day [mm], z the depth below the surface [mm].
The coefficients in the exponential term were chosen so that 50% of the evaporative demand is extracted from the top 10 mm of soil and 95% of the evaporative demand from the top 100 mm of the soil. This assumption can be modified by the soil evaporation compensation coefficient (ESCO). Actual soil water evaporation is estimated by using exponential functions of soil depth and water

content. Plant transpiration is simulated as a linear function of potential evapotranspiration and leaf area index. The actual amount of transpiration on a day equals the plant water uptake for the day which depends on the amount of water required by the plant for transpiration and the amount of water available in the soil. The depth distribution used to determine the maximum amount of water uptake from the soil surface to a depth z is by Eq. 4.8.

$$W_{up,z} = \frac{E_t}{[1 - \exp(-\beta_w)]} \cdot \left[1 - \exp\left(-\beta_w \cdot \frac{z}{z_{root}}\right)\right] \quad \text{(Eq. 4.8)}$$

where, $W_{up,z}$ is the potential water uptake from to soil surface to a depth z [mm], E_t the maximum plant transpiration on a given day [mm], z the depth below the surface [mm], Z_{root} the rooting depth [mm], and β_w the water-use distribution parameter [-].

Percolation

Percolation may be defined as the movement of water through the soil profile caused by differences in the soil properties. A soil profile may be defined as a vertical section of soil, showing successive layers from the ground surface to the parental rocks. Soil properties may be understand as measured or inferred parameters such as the void ratio, porosity, specific gravity, dry unit weight, saturated unit weight, liquid limit, etc.. Percolation through the soil layers may be caused by differences in water content. In SWAT percolation occurs when field capacity of a soil layer is exceeded and the layer below is not saturated. The flow rate is governed by the saturated conductivity and leads to groundwater recharge, which is partitioned into two aquifer system: an unconfined (shallow) aquifer allowing base flow generation to streams within the catchment, and a confined (deep) aquifer contributing to the base flow outside the catchment. The amount of water that moves from one layer to the underlying layer is calculated by the storage routing technique (Eq. 4.9).

$$w_{perc,ly} = SW_{ly,excess}\left(1 - e^{\frac{-\Delta t}{TT_{perc}}}\right) = SW_{ly,excess}\left(1 - e^{\frac{-\Delta t \cdot K_{sat}}{SAT_{ly} - FC_{ly}}}\right) \quad \text{(Eq. 4.9)}$$

Where, $W_{perc,ly}$ is the amount of water percolating to the underlying soil layer [mm], $SW_{ly,excess}$ the drainable volume of water in the soil layer [mm], Δt the length of time step [h], TT_{perc} the travel time for percolation [h], SAT_{ly} the amount of water in the soil layer when completely saturated [mm], FC_{ly} the water content of the soil layer at field capacity [mm], and K_{sat} the saturated hydraulic conductivity for the layer [mm/h].

Lateral flow

Lateral flow depends on the hydraulic conductivities in the soil layers, and an impermeable or semi-permeable layer at a shallow depth. SWAT incorporates the kinematic storage model for subsurface flow developed by Sloan and Moore (1984) (Eq. 4.10).

$$Q_{lat} = 0.024 \cdot \left(\frac{2 \cdot SW_{ly,excess} \cdot K_{sat} \cdot slp}{\phi_d \cdot L_{hill}}\right) \quad \text{(Eq. 4.10)}$$

where $SW_{ly,excess}$ is the drainable volume of water stored in the saturated zone of the hillslope per unit area (mm H_2O), K_{sat} is the saturated hydraulic conductivity (mm·h^{-1}), slp is the increase in elevation

per unit distance, Φ_d is the drainable porosity of the soil (mm/mm), L_{hill} is the hillslope length (m), and 0.024 is a factor needed to convert meters to millimeters and hours to days.

Groundwater flow

Groundwater is water in the saturated zone under pressure greater than atmospheric. Water enters groundwater storage primarily by percolation, although recharge by seepage from surface water bodies may occur. Water leaves groundwater storage primarily by discharge into rivers or lakes, but it is also possible for water to move upward from the water table into the capillary fringe (see Fig. 4.1). SWAT simulates an unconfined aquifer that contributes to the flow in the main channel (shallow aquifer) and a confined (deep aquifer). Eq. 4.11 shows the daily water balance for the shallow aquifer. The shallow aquifer storage is recharged by percolation from the unsaturated zone and reduced by baseflow, deep aquifer recharge, upwards flows into the soil zone and with drawal. The baseflow is implemented as a linear storage with a specific recession coefficient (Eq. 4.12).

$$aq_{sh,i} = aq_{sh,i-1} + w_{rchrg} - Q_{gw} - w_{revap} - w_{deep} - wu_{sa} \quad \text{(Eq. 4.11)}$$

$$Q_{gw,i} = Q_{gw,i} \cdot e^{-\alpha \Delta t} + w_{rchrg}\left(1 - e^{-\alpha \Delta t}\right) \quad \text{(Eq. 4.12)}$$

Where, $aq_{sh,i}$ is the shallow aquifer storage on the day i [mm], $aq_{sh,i-1}$ the shallow aquifer storage the day before [mm], W_{rchrg} the recharge entering the aquifer [mm], Q_{gw} the groundwater flow or baseflow into the main channel [mm], W_{revap} the amount of water moving into the soil zone as response to water deficiencies [mm], W_{deep} the amount of water percolating from the shallow aquifer into the deep aquifer [mm], WU_{sa} the water use from the shallow aquifer [mm], α the base flow recession constant [-], describes the lag flow from the aquifer, estimation by baseflow filter techniques. Besides several specific groundwater coefficients SWAT defines minimum thresholds for the shallow aquifer for the occurrence of return flow and the water flow to the unsaturated zone or to the deep aquifer.

Sedimentation component

Erosion involves the detachment, transport and deposition of soil particles and aggregates. Sediment yield is defined as the total amount of eroded material to be delivered from its source to a downstream control point. Thus, sediment yield rates directly depend on both soil loss rates and the transport efficiency of surface runoff and channel flow. Erosion caused by rainfall and runoff is computed with the Modified Universal Soil Loss Equation (MUSLE, Eq. 4.13) (Williams, 1975).

$$SY = 11.8 \cdot \left(Q_{surf} \cdot q_{peak} \cdot area_{hru}\right)^{0.56} \cdot K_{USLE} \cdot C_{USLE} \cdot P_{USLE} \cdot LS_{USLE} \cdot CFRG \quad \text{(Eq. 4.13)}$$

Where SY is the sediment yield [t ha^{-1}], Q_{surf} is the surface runoff [mm], q_{peak} is the peak runoff rate [m^3 s^{-1}], K_{USLE} (or *USLE_K*) is the USLE erodibility factor [0.013 t m^2 h (m^3 t cm)$^{-1}$], C_{USLE} is the USLE crop management factor [-], P_{USLE} is the USLE erosion control factor [-], LS_{USLE} is the USLE slope length factor [-] and *CFRG* is the coarse fragment factor [-].

Nitrate in surface runoff

Nitrate may be transported with surface runoff, lateral flow or percolation. To calculate the amount of nitrate transported with the water, the concentration of nitrate in the mobile water is calculated. This concentration is then multiplied by the volume of water flowing in each pathway to obtain the

mass of nitrate lost from the soil layer. The concentration of nitrate in the mobile water fraction is calculated as:

$$conc_{NO3,mobile} = \frac{NO_{3,ly} \cdot \left(1 - \exp\left[\frac{-w_{mobile}}{(1-\theta_e)\cdot SAT_{ly}}\right]\right)}{w_{mobile}} \quad \text{(Eq. 4.14)}$$

where $conc_{NO3,mobile}$ is the concentration of nitrate in the mobile water for a given layer (kg N/mm H_2O), $NO3_{ly}$ is the amount of nitrate in the layer (kg N/ha), w_{mobile} is the amount of mobile water in the layer (mm H_2O), θ_e is the fraction of porosity from which anions are excluded, and SAT_{ly} is the saturated water content of the soil layer [mm].

Soluble phosphorus in surface runoff

The primary mechanism of phosphorus transport in the soil is by diffusion. Diffusion is the migration of ions over small distances (1-2 mm) in the soil solution in response to a concentration gradient. Due to the low mobility of soluble phosphorus, surface runoff will only partially interact with the soluble P stored in the top 10 mm of soil. The amount of soluble P transported in surface runoff is:

$$P_{surf} = \frac{P_{solution,surf} \cdot Q_{surf}}{\rho_b \cdot depth_{hru} \cdot k_{d,surf}} \quad \text{(Eq. 4.15)}$$

Where P_{surf} is the amount of soluble phosphorus lost in surface runoff (kg P/ha), $P_{solution,surf}$ is the amount of phosphorus in solution in the top 10 mm (kg P/ha), $Q_{,surf}$ is the amount of surface runoff on a given day (mm H_2O), ρ_b is the bulk density of the top 10 mm (Mg/m^3) (assumed to be equivalent to bulk density of the first soil layer), $depth_{surf}$ is the depth of the "surface" layer (10 mm), and $k_{d,surf}$ is the phosphorus soil partitioning coefficient (m^3/Mg).

Organic nutrient in surface runoff

Organic N and organic/mineral P attached to soil particles may be transported by surface runoff to the main channel. These forms of nutrients are associated with the sediment loading from the field and changes in sediment loading will be reflected in their loading amount. Organic N and P transported with the sediment are calculated with a loading function developed by McElroy et al. (1976) and modified by Williams and Hann (1978) to consider each runoff events. The loading function estimates the daily organic N runoff loss based on the concentration of organic N in the top soil layer, the sediment yield, and the enrichment ratio (concentration of organic N in the sediment divided by that in the soil).

$$orgN_{surf} = 0.001 \cdot conc_{orgN} \cdot \frac{sed}{area_{hru}} \cdot \varepsilon_{N:sed} \quad \text{(Eq. 4.16)}$$

where $orgN_{surf}$ is the amount of organic nitrogen transported to the main channel in surface runoff (kg N/ha), $conc_{orgN}$ is the concentration of organic nitrogen in the top 10 mm of soil (g N/ ton), *sed* is the sediment yield on a given day (tons), $area_{hru}$ is the HRU area (ha), and $\varepsilon_{N:sed}$ is the nitrogen enrichment ratio.

The enrichment ratio is defined as the ratio of the concentration of organic nitrogen transported with the sediment to the concentration in the soil surface layer. SWAT calculates an enrichment ratio for each storm event. The concentration of organic nitrogen in the soil surface layer, $conc_{orgN}$, is calculated:

$$conc_{orgN} = 100 \cdot \frac{\left(orgN_{frsh,surf} + orgN_{sta,surf} + orgN_{act,surf}\right)}{\rho_b \cdot depth_{surf}} \quad \text{(Eq. 4.17)}$$

where $orgN_{frsh,surf}$ is nitrogen in the fresh organic pool in the top 10 mm (kg N/ha), $orgN_{sta,surf}$ is nitrogen in the stable organic pool (kg N/ha), $orgN_{act,surf}$ is nitrogen in the active organic pool in the top 10 mm (kg N/ha), ρ_b is the bulk density of the first soil layer (Mg/m^3), and $depth_{surf}$ is the depth of the soil surface layer (10 mm). The amount of phosphorus transported with sediment to the stream is calculated:

$$sedP_{surf} = 0.001 \cdot conc_{sedP} \cdot \frac{sed}{area_{hru}} \cdot \varepsilon_{P:sed} \quad \text{(Eq. 4.18)}$$

where $sedP_{surf}$ is the amount of phosphorus transported with sediment to the main channel in surface runoff (kg P/ha), $conc_{sedP}$ is the concentration of phosphorus attached to sediment in the top 10 mm (g P/ metric ton soil), *sed* is the sediment yield on a given day (metric tons), $area_{hru}$ is the HRU area (ha), and $\varepsilon_{P:sed}$ is the phosphorus enrichment ratio.
The enrichment ratio is defined as the ratio of the concentration of phosphorus transported with the sediment to the concentration of phosphorus in the soil surface layer. SWAT calculates an enrichment ratio for each storm event. The concentration of phosphorus attached to sediment in the soil surface layer, $conc_{sedP}$, is calculated:

$$conc_{sedP} = 100 \cdot \frac{\left(\min P_{act,surf} + \min P_{sta,surf} + orgP_{hum,surf} + orgP_{frsh,surf}\right)}{\rho_b \cdot depth_{surf}} \quad \text{(Eq. 4.19)}$$

Where $minP_{act,surf}$ is the amount of phosphorus in the active mineral pool in the top 10 mm (kg P/ha), $minP_{sta,surf}$ is the amount of phosphorus in the stable mineral pool in the top 10 mm (kg P/ha), $orgP_{hum,surf}$ is the amount of phosphorus in humic organic pool in the top 10 mm (kg P/ha), $orgP_{frsh,surf}$ is the amount of phosphorus in the fresh organic pool in the top 10 mm (kg P/ha), ρ_b is the bulk density of the first soil layer (Mg/m^3), and $depth_{surf}$ is the depth of the soil surface layer (10 mm).

4.2. Calibration, sensitivity and uncertainty

Hydrologic models, no matter how sophisticated and spatially explicit, aggregate at some level of detail complex, spatially distributed vegetation and subsurface properties into much simpler homogeneous storages with transfer functions that describe the flow of water within and between these different compartments (Vrugt et al., 2008).
Many types of uncertainties are pointed out by Pappenberger and Beven (2006): (1) uncertainties in the model drivers (inputs and boundary conditions such as rainfall, land use, soil); (2) uncertainties in the model factors (resolution and scale); (3) dependencies in the model factors (model components, model parameters, structural errors); (4) uncertainties related to uncertainty estimation methodology; and uncertainties in the observations used in the model calibration.
In addition Abbaspour (2008) pointed out conceptual model uncertainties such as: (1) uncertainties due to processes that are included in the model, but their occurrences in the watershed are unknown to the modeler; and (2) uncertainties due to processes unknown to the modeler and not included in the model.

According to Vrugt et al. (2008) a consequence of this process simplification is that most of the parameters in these models cannot be inferred through direct observation in the field, but can only be meaningfully derived by calibration against an input - output record of the catchment response.
Various methodologies are used for analyzing the incertainties in the distributed catchment models: Markov Chain Monte Carlo Simulation- MCMC (Kuczeraa and Parent, 1998; Vrugt at al., 2003, 2008); Sequential Uncertainty Fitting- SUFI2 (Abbaspour, 2008); Parameter solution- Parasol (van Griensven and Meixner, 2007); and Generalized Likelihood Estimation- GLUE (Beven and Binlley, 1992).
In this work, an automatic calibration, sensitivity and uncertainty analysis have been performed using the SWAT-CUP interface (Abbaspour, 2008) with the SUFI-2 procedure with the Sum of Squared Error (SS) set as an objective function (Eq. 4.20).

$$SS = w_1 \sum_{i=1}^{n_1} \left(Q_m - Q_s\right)_i^2 + w_2 \sum_{i=1}^{n_2} \left(S_m - S_s\right)_i^2 + w_3 \sum_{i=1}^{n_3} \left(N_m - N_s\right)_i^2 \qquad \text{(Eq. 4.20)}$$

where, $w_i = 1/n_i\sigma_i^2$, σ_i^2 is the variance of the i[th] measured variable, *Q*, *S* and *N* represent the discharge, the sediment and the nitrate concentration respectively. *m* and *s* are used for measurements and simulated respectively. *n* is the number of observed values.

Discharge, sediment and nitrate were simultaneously calibrated. Table 4.4 shows the calibration and validation periods for the different sub-catchments investigated, considering discharge, sediment concentrations and nitrate concentrations.

Tab. 4.1. Calibration periods for the different sub-catchments investigated. Validation periods are provided in brackets.

	Donga	Vossa	Térou	Atchérigbé	Kaboua	Bétérou
Discharge	2006-2008 (1998- 2005)	1998-2000 (1995)	2002-2005 (1998-2001, 2006)	2007- 2008 (2001-2006, 2009)	2004- 2006 (1995-1998)	2006-2009 (1998-2005)
Sediment	2008 (2005)	- -	2004-2005 (2006)	2008 (2009)	- -	2008-2009 (2004-2005)
Nitrate	2008 (2008-2009)	- -	- -	2008 (2009)	- -	2008-2009 (2008)

Different criteria were used to assess the model performance and the optimal calibrated parameter values as resumed from (1) to (4) below.

(1) Calculation of the model goodness of fit to the measurements, which are the coefficient of determination R^2, the model efficiency of Nash & Sutcliffe ME (1970), and the index of agreement of Willmott (1981). The coefficient of determination R^2 (see Eq. 4.22) describes the linear dependency between measured and simulated values within the range of -1 to 1. A model which systematically over- or underpredicts may still result in good R^2. The ME (Eq. 4.23) describes the degree of accordance between observed and simulated values and varies between - ∞ to 1. The ME coefficient indicates how well observed variable peaks are captured by the simulations. The index of agreement is rather strongly influenced by the mean value (simulated or observed variable). The Index of Agreement evaluates the performance of the temporal characteristics of the discharge curves (see Eq. 4.24). The index covers a range of 0 to 1. A value of 1 indicates a complete agreement between measured and simulated values.

$$r = \frac{n \cdot \left(\sum_{i-1}^{n} x_i \cdot x'_i\right) - \left(\sum_{i-1}^{n} x_i\right) \cdot \left(\sum_{i-1}^{n} x'_i\right)}{\sqrt{n \cdot \Sigma_{i-1}^{n} x_i^2 - \left(\sum_{i-1}^{n} x_i\right)^2} \cdot \sqrt{n \cdot \sum_{i-1}^{n} x'^2_i - \left(\sum_{i-1}^{n} x'_i\right)^2}} \qquad \text{(Eq. 4.22)}$$

where, n is the number of variables, x_i the measured variable, and x'_i the simulated variable.

$$ME = \frac{\sum_{i-1}^{n}\left(x_i - \bar{x}_i\right)^2 - \sum_{i-1}^{n}\left(x'_i - \bar{x}_i\right)^2}{\sum_{i-1}^{n}\left(x_i - \bar{x}_i\right)^2} \quad \text{(Eq. 4.23)}$$

where, *n* is the number of measurements, x_i the measured variable, and $\bar{x}_i$ the arithmetic mean of $x_i\,(i=1,\ldots,n)$.

$$IA = 1 - \frac{\sum_{i-1}^{n}\left(x_i - x'_i\right)^2}{\sum_{i-1}^{n}\left(\left|x_i - \bar{x}\right| + \left|x'_i - \bar{x}'\right|\right)^2} \quad \text{(Eq. 4.24)}$$

where, *n* is the number of compared values, X_i the measured variable, $\bar{x}$ the arithmetic mean of $x_i\,(i=1,\ldots,n)$, x'_i the simulated variable, and $\bar{x}'_i$ the arithmetic mean of $x'_i\,(i=1,\ldots,n)$.

(2) the comparison of the simulated water yield components (direct surface runoff and baseflow) to the observed components, estimated with the baseflow filter program of Arnold et al. (1995) (Eq. 4.25).

$$q_t = \beta * q_{t-1} + \frac{1+\beta}{2} * (Q_t - Q_{t-1}) \quad \text{(Eq. 4.25)}$$

where, q_t is the quick flow component at time *t* from the total flow Q_t and β is the filter parameter.

(3) The degree to which all uncertainties are accounted for is quantified by a measure referred to as P-factor, which is the percentage of measured data bracketed by the 95% prediction uncertainty. Although all processes and model inputs such as rainfall are considered, the model output is subject to a number of sources of uncertainty as stated above and highlighted by Brown & Heuvelink (2005). Therefore, although also uncertain, the percentage of measurements captured (bracketed) by the prediction uncertainty is a good measure to assess the uncertainty issue. It has to be kept in mind that the paradox situation may occur in that the greater the uncertainty, the greater the possibility that experimental data will lie within this uncertainty. This means that the greater the uncertainty, the more difficult it is to show that the model is invalid (Anderson & Bates, 2001). The 95% uncertainty prediction is calculated at the 2.5% and 97.5% levels of cumulative distribution of an output variable obtained through Latin Hypercube sampling, excluding 5% of the very bad simulations (due to very bad parameter combination).

(4) For measuring the strength of the uncertainty analysis, the R-factor, which is the ratio of average distance between 2.5 and 97.5 percentiles of the cumulative distribution of the simulated variable and the standard deviation of the corresponding measured variable, is calculated by Eq. 8. SUFI-2 seeks to bracket most of the measured data with the smallest possible uncertainty band.

$$R - factor = \frac{1}{k\sigma_X}\sum_{l=1}^{k}\left(X_U - X_L\right)_l \quad \text{(Eq. 8)}$$

where k is the number of observed data points, σ_X is the standard deviation of the measured variable *X*, and X_U and X_L are respectively the 2.5th and 97.5th percentiles of the cumulative distribution of every simulated point.

Theoretically, the value for P-factor ranges between 0 and 100%, while that of R-factor ranges between 0 and infinity. A P-factor of one and an R-factor of zero is a simulation that exactly corresponds to the measured data. The degree to which the factors are different from these numbers

can be used to judge the strength of the calibration. A larger P-factor can be achieved at the expense of a larger R-factor.

The sensitivity of each parameter (t-stat) is measured by calculating a multiple regression system, which regresses the Latin Hypercube-generated parameters against objective function values. A t-test is then used to identify the significance of each parameter. The p-values associated with this t-test provide the significance of the sensitivity of each parameter (a value close to zero has a high significance). The sensitivities are estimates of the average changes in the objective function resulting from changes in each parameter, while all other parameters are variable. This gives relative sensitivities based on linear approximations and thus only provides partial information about the sensitivity of the objective function to model parameters.
Sensitivity analysis was also carried out using the "Latin Hypercube One-factor-at-a-Time" (LH-OAT) method, a combined method designed and proposed by Morris (1991). The "Latin hypercube (LH)" is improved compared to the Monte Carlo approach. The simplest Monte Carlo analysis involves random samplings from uniform or normal distributions. It allows an analysis of changes in model predictions due to changes in model input. The "Latin hypercube" (McKay et al., 1979) uses a stratified sampling approach with fewer samples. Each cumulative density function of the model parameters is divided into m classes with an probability equal to 1/m. Random values are generated for the combination of all parameters, while ensuring that each class is sampled once. Thus, the model is executed m times with a random combination of unlimited number of parameters. The "One-factor-at-a-Time" involves a sequential change starting from an initial parameter vector n (x1, ..., Xn). The advantage of this method is that only one parameter is changed for each simulation and changes in results can be attributed to changes in one parameter alone.
Additionally, sensitivity has been performed by the “one factor at-a-time” method (OFAT) using equation 4.26 (de Roo, 1993). Sensitivity indices of the model input parameters have been calculated for the daily mean squared error between simulated and observed discharge. The advantage of the OFAT-method is that sensitivity is clearly attributed to a single parameter while all others are kept constant.

$$SI_{10} = \frac{|O_{P10} - O_{M10}|}{O_o} \qquad \text{(Eq. 4.26)}$$

with O_{p10} = model output with a 10% increase of the parameter value, O_{M10} = model output with a 10% decrease of the parameter value, and O_o = model output with the base simulation.

5. Input and monitoring data

In SWAT, the catchment is discretized into numerous sub-catchments. Sub-catchments are delineated from the Digital Elevation Model using a threshold concept parameter, and are linked to one climate station, providing climate data such as daily precipitation and potential evapotranspiration. Within each sub-catchment, the distribution of soils and vegetation is considered by Hydrological Response Units (HRUs) created by overlaying three types of data layers (topographic map, soil map, and land use map), accordingly to a catchment spatial threshold, which is a key parameter controlling the internal aggregation procedure in the model (Romanowicz et al., 2005). Each HRU is represented by specific parameters, such as the terrain properties, the chemical and physical soil properties, and properties of the vegetation types. Hiepe (2008) reported that the number of sub-catchments strongly affects simulation results due to the spatial linkage between sub-catchments and climate information.
Tab. 5.1 shows the nature and source of the different data layers, their scales and types of parameters and investigations, in the structure as required for applying the SWAT model in the Ouémé catchment.

Tab. 5.1. General model input data used in this study. Soil and land use data are from IMPETUS (Christoph et al., 2008) and INRAB (Institut National de la Recherche Agricole du Bénin; Igue, 2005), Climate data are from IMPETUS, IRD (Institut de Recherche pour le Développement), and DMN (Direction de la Météorologie Nationale), Geology data is from OBEMINES (Office Béninoise des MINES). PHU is defined as Potential Heat Unit, LAI as Leave Area Index, and CN2 as Curve Number 2.

Data (data sources)	Scale	Parameters and types of investigation
Topography (DEM SRTM)	90 m resolution	Elevation, overland, channel lengths, channel slopes, sub-basins delineation, sub-basins slopes, etc.
Soil (SOTER INRAB & IMPETUS)	1 : 200,000	Saturated conductivity, organic carbon, bulk density, Texture, soil erodibility factor, soil available water content, pH, OrgN, etc.
Land use (Classification Satellite data RIVERTWIN)	250 m resolution	Biomass, PHU, LAI, CN2, etc.
Management (CountryStat, MAEP, CeRPA)	HRU scale	Tillages, crop systems, conservation measures, fertlization, etc.
Weather (DMN, IRD, IMPETUS)	33 stations	Daily wind speed, precipitation, temperature, solar radiation, etc.

Hydrological process studies often require large amounts of observed data in time and space, including stream water discharge, suspended sediment concentrations, nutrient concentrations, etc. In the specific case of modeling, they are used to constrain the uncertainties in predicted variables (Pappenberger and Beven, 2006). Access to multiple data types rhymes with more constraints and hence an outcome more accurate modeling issues.
Modelling the water cycle, the sediment and nutrient dynamics at the field scale (HRU scale) requires spatial and temporal representation of management techniques, including crop calendar (planting, harvesting, etc.), tillage operations, fertilization, and various other practices. All this highly influences the nitrogen and phosphorus cycles and may result in degradation of land fertility and pollution of aquifers and surface waters. At the SWAT process scale, two inorganic pools (NH_4^+ and NO_3^-) and three organic pools (fresh organic N associated with crop residue and microbial biomass, the active and the stable organic N associated with the soil humus) are for example considered to simulate the nitrogen cycle.

5.1. Soil data

Three different soil databases are established at the scale 1:200.000 for the whole Ouémé catchment, in corporation with INRAB (Institut National de la Recherche Agricole du Bénin). The theoretical and practical aspects of the more recently developed soil aggregation and mapping

method, SOil and TERrain digital database approach (SOTER, van Engelen & Ting-tiang, 1995) were considered as well as the French Commission of Pedology and Soil Mapping approach (CPCS, 1967) (cf. chapter 6 for more details).

5.2. Land use data

The land use/cover map considered in this study has been established a 250 m resolution from 3 scenes satellite images LANDSAT ETM+ of 2003 (Igué et al., 2006; RIVERTWIN, 2007). After image treatment, imaged maps were established and interpretation keys were defined. For efficacy reasons, the interpretation was carried out at the scale of 1/50.000 in order to get maximum information. Field controls were done. More than 650 observation points were checked during the ground checks. Finally, 17 land use/cover classes were defined (Tab. 5.2 and Fig. 5.1). A subsequent accuracy check shows that the overall accuracy is high (87 %) (Igué et al., 2006). The land use unit "mosaic of cropland and fallow" has been mapped most precisely, whereas the classification of the unit "humid and dry dense forest" has the lowest precision. The most common crops in the basin are among others yams, maize, rice, groundnuts, sorghum and cotton.

Tab. 5.2. Land use/cover categories, their area and percentage of total area (Ouémé-Bonou catchment).

Land use categories	Land use code	Area (km^2)	Percentage of total area
Galery forest	GF	1759	3.98
Humid and dry dense forest	FD	1220	2.76
Swamp formations	FM	17	0.04
Riverain formations	FR	107	0.24
Woodland and woodland savannah	FCSB	6716	15.2
Flooding savannah	SM	222	0.5
Tree and shrub savannah	SA	17231	38.99
Saxicolous savannah	SS	313	0.71
Grassland	PH	14	0.03
Mosaic of cropland and bush fallow	CJ	13713	31.03
Mosaic of cultivation with Parkia and Cashew trees	CJNA	32	0.07
Mosaic of cultivation with palm trees	CJP	1189	2.69
Industrial plantations	PI	127	0.29
Village plantations	PV	1209	2.74
Barren lands/area without vegetation	BAR	5	0.01
Urban and built-up	AG	277	0.63
Water bodies	PE	47	0.11

The land use scenarios considered in this study were computed in the framework of an EU funded project (RIVERTWIN, 2007). As described by Götzinger (2007) the major driver for land use change is population growth and subsequent conversion of the natural savannah vegetation into settlements, roads, and a mosaic of fields by slash and burn clearance. Together with stakeholders, two socio-economic scenarios have been set up: (1) La, stronger economic development, controlled urbanization, 3.2% population growth per year; and (2) Lb, weak national economy, uncontrolled settlement and farmland development, 3.5% population growth per year. These scenarios are also used in the national planning administration of Benin. For each scenario, the population growth has been translated into a specific demand for settlements and agricultural area according to the development of the national framework. This demand has been satisfied according to the proximity to roads and existing villages, new settlements and agricultural areas have been created leading to the land use distribution. Changes in the Ouémé land use according to the scenarios La and Lb are mainly expressed by the conversion of the savannah into croplands and pastures (Fig. 5.2) in a range of 10 to 20% of the agricultural lands for the scenario La and 20 to 40% for the scenario Lb.

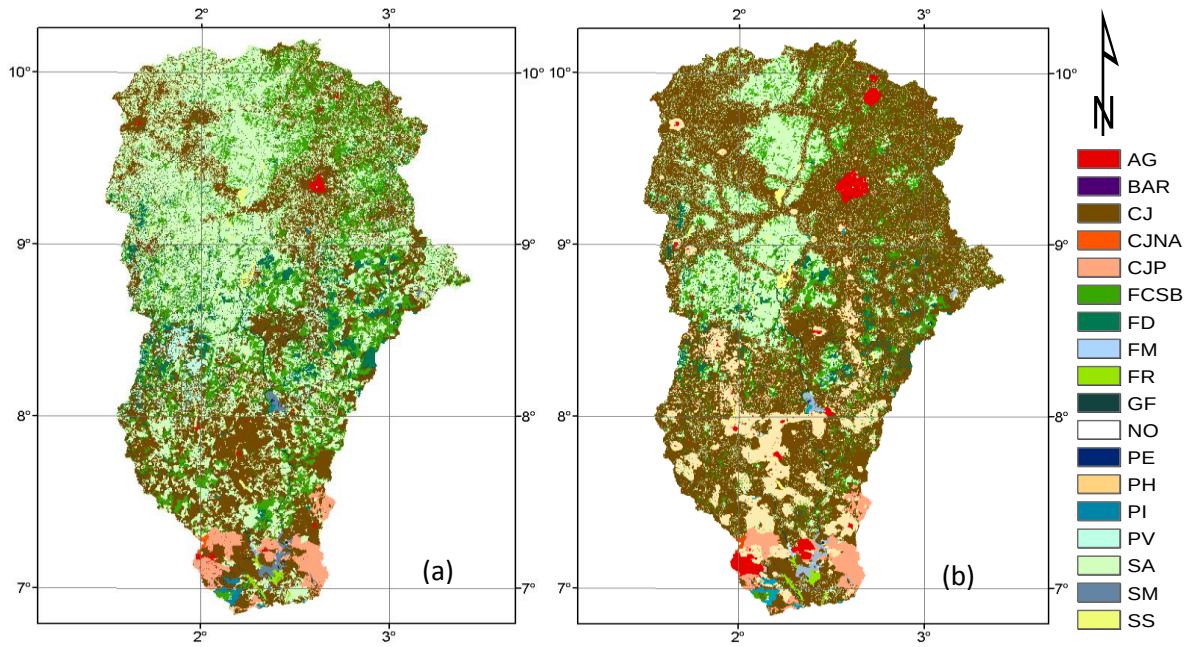

Fig. 5.1. Land use/cover of the Ouémé basin. The legend is fully explained in Tab. 5.2. ((a): reference map (2003); (b): Lb 2025-2029) (After RIVERTWIN, 2007)

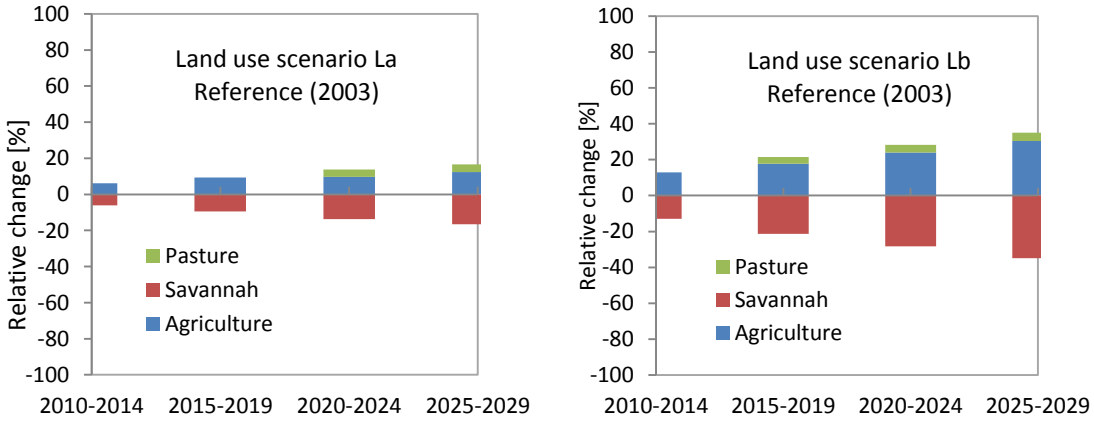

Fig. 5.2. Change in land use in reference to the land use patterns (from satellite image 2003): scenarios La and Lb.

In the framework of the IMPETUS project, Judex (2008) used the CLUE-S land use change model to parameterize the land use/land cover data derived from satellite images and socio-economic data. Thus, several future scenarios of spatial land cover/land use changes were calculated but unfortunately limited to the Upper Ouémé region, and weren't used in the current study.

5.3. Soil and crop management

The agricultural potential within the basin is considerable because of the nature of its much diversified soils and relatively modest hydro-climatic conditions. Indeed, several types of crops are cultivated, ranging from food crops to the cash crops. Activities related to each type of culture are led in well known time intervals (by farmers) as well as related cultural practices. The main food crops cultivated in the basin include: cereals, oilseeds, tubers, legumes and vegetables.

1) Cereals: (1) maize (*Zea mays*), the most widespread crop in the study area; (2) rice (*Oryza sativa*), grown mainly in inland valleys on hydromorphic soils; and (3) sorghum (*Sorghum vulgare*).
2) Oilseeds: groundnut (*Arachis hypogea*) and sesame are the main types of oilseeds grown in the study area.
3) The tubers and roots: (1) yam (*Dioscorea alata*), where the cultivated space in a given season is left the following season, leading to the destruction of the islets of remaining woodlands; (2) cassava (*Manihot esculenta*), requiring little work and accepting associations; and (3) sweet potato (*Ipomea Batala*), including two varieties (white and red) are grown in the basin.
4) Legumes: cowpeas (*Vigna unguiculata*) and groundnuts (*Voandzeia subterranea*).
5) Vegetable crops: okra (*Abelmoschus esculentus*), pepper (*Capsicum annuum*) and tomato (*Lycopersion esculentum*), grown mainly in inland valeys.

The main cash crop cultivated in the basin is cotton, occupying in average three to four hectares per farmer (sometimes in a rotation system where cotton is planted just corn has matured, for example).

Crop calendar

The agricultural calendar strictly depends on dates of first rains of the season, rainfall rhythms and knowledge of growth cycles of crop. Rainfall data of 2004-2007 agricultural campaigns, activity reports for the same periods (CeRPA and MAEP), interviews and observations allowed the shown schedule of Tab. 5.3, used to develop the baseline agricultural practices introduced in SWAT (Soil and Water Assessment Tool) model applied over the study area.

Tab. 5.3. Crop calendar. P=clearing and plowing, S=sowing, M=maintenance: hoeing and fertilization H=harvest (Source: own field investigation and agricultural campaigns 2005-2006 and 2006-2007 (CeRPA and MAEP)

Crop	Jan.	Feb.	Mar.	Apr.	May	Jun	Jul.	Aug.	Sep.	Oct.	Nov.	Dec.
Maize		P		S	M		H					
Sorghum					S	S		M			H	H
Rice			P		S	M				H		
Cassava		P		S	M						H	
Yam	P	S	M				H	H			H	
Cowpeas		P	S	S		H	HS		M		H	H
Groundnut		P		S	M		H	PS			H	H
Sesame			P	P	S	M		H				
Tomato			P	S		H	H					
Okra			P	S		H	H	H				
Pepper						S	S	M	M		H	H
Cotton				P	P	S	S	M	M		H	H

Tillage techniques and crop association/rotation

The most used tools in the study area are the hoe and the machete (Bossa, 2007). Thus field preparation start with cutting shrubs and bushes with machete, calcinating of trees and cleaning up with hoes depending on the season. Yams and sweet potatoes are grown on mounds, while crops such as corn, sorghum, legumes and root crops are grown with or without ridges. A spacing of 0.80 m is generally practiced for the ridges (Bossa, 2007).
From experience, the farmer often choose appropriately according to slopes and local topographic conditions the best ridge orientation in order to significantly reduce losses of soil and nutrients and allow good water drainage of soils (own field observations). Thus, we observed ridges parallel to the slope, contour and staggered ridges.

Moreover, it should be noted that motor tractors are rarely used by the farmers. But a gradual introduction of rice tillers begins.
In summary, we found that the labor tools have remained traditional, and that farmers are looking to improve their yields, what justifies the increasingly used of agricultural inputs (fertilizer NPK, urea, insecticide, etc.) for maize, cotton and rice, with intense demands of drilling and hydro- agricultural dams.
Crop associations met, include yam-maize-okra, maize-cassava or maize-groundnut, maize-sorghum, maize-cowpeas. Crop rotations are not very present in the cultural practices of farmers, since there are relatively enough cultivation spaces (due to low population density in most parts of the Ouémé catchment). Moreover, shifting cultivations are practiced (subsistence farming), consisting to cultivate the fields for one or two years and leave them for fallows (few decades) in order to restore soil fertility.

5.4. Climate data

The climate condition of the Ouémé catchment (as considered in the modeling works) was presented in Fig. 2.3. The whole national rainfall network (under DMN authority, 'Direction Nationale de la Météorologie') counted roughly 100 measurement sites by 2005 (Diederich and Simmer, 2010), against roughly 65 for the upper Ouémé catchment by 2006, which has been equipped by the Germans GLOWA-IMPETUS project and IRD-CATCH/AMMA ("Institut de la Recherche pour le Développement-Couplage de l'Atmosphère Tropicale et du Cycle Hydrologique/African Monsoon Multidisciplinary Analyses") (Pohle et al., 2010). In this study, only 33 rainfall stations have been considered from above-mentioned stations due to severe discontinuities in the data series at some stations and the necessity to cover the years 2008 to 2010, for which water quality and lost soil nutrient data were collected. It is evident that this causes difficulties for analyzing the rainfall-runoff process given the region rainfall characteristics. Indeed, it was shown that the daily rainfall accumulation at one location may surpass 150 mm (corresponding to roughly 10% of mean yearly accumulation), with 80 mm falling within two hours, while slight or no rainfall may occur at a point only 20 km away from that location (e.g. orographic precipitations) (Diederich and Simmer, 2010).

Climate scenarios are often calculated worldwide by the scientific community for impact assessment studies in order to support well-balanced decisions for natural resources and environmental protection. The climate scenarios considered in this work were provided by Paeth et al. (2009) for the Africa continent between -15°S and 45°N latitude (Fig. 5.3), using the regional climate model REMO driven by the IPCC SRES scenarios A1B and B1. REMO is a regional climate model that is nested in the global circulation model ECHAM5/MPI-OM (Paeth et al. 2008). As described by Christoph et al (2008) the IPCC SRES scenario A1B describes a globalized world of rapid economic growth and comparatively low population growth. The SRES scenario B1 also characterizes a future globalized world with a low population growth. However, in this scenario the economic structures change rapidly towards a service and information economy with reduced material intensity and the introduction of clean, sustainable technologies. Consequently, the predicted CO_2 emissions and temperature increases are lower than for the A1B scenario. Considering REMO initial runs, the rainfall amount and variability were systematically underestimated over West Africa with a shift in its pattern towards more weak events and fewer extremes (Paeth and Diederich, 2010). This has lead to the application of MOS (Model Output Statistics) to adjust the rainfall data (monthly bias correction) using other near-surface parameters such as temperature, sea level pressure and wind components from the model. Since the regional-mean (precipitation) strongly differed from the observed spatial patterns of daily rainfall events, a conversion of the MOS-corrected regional-mean from REMO to local rainfall event patterns has been done. As reported by Gaiser et al. (2011), a weather generator (WEGE) was applied, producing virtual station data, matching the rainfall stations in Benin, which was finally adjusted to the statistical characteristics of observed daily precipitation at the rainfall stations by

probability matching (Paeth and Diederich, 2010). Climate changes in the Ouémé catchment have resulted in a decrease of annual rainfall between 9 and 12% for the scenario B1 and for the next 20 years. It increases of up to 4% for the scenario A1B over the period 2010-2014, before decreasing of up to 14% between 2015 and 2029. Maximum and minimum temperatures are expected to vary around ±3% over the next 20 years (Fig. 2.6).

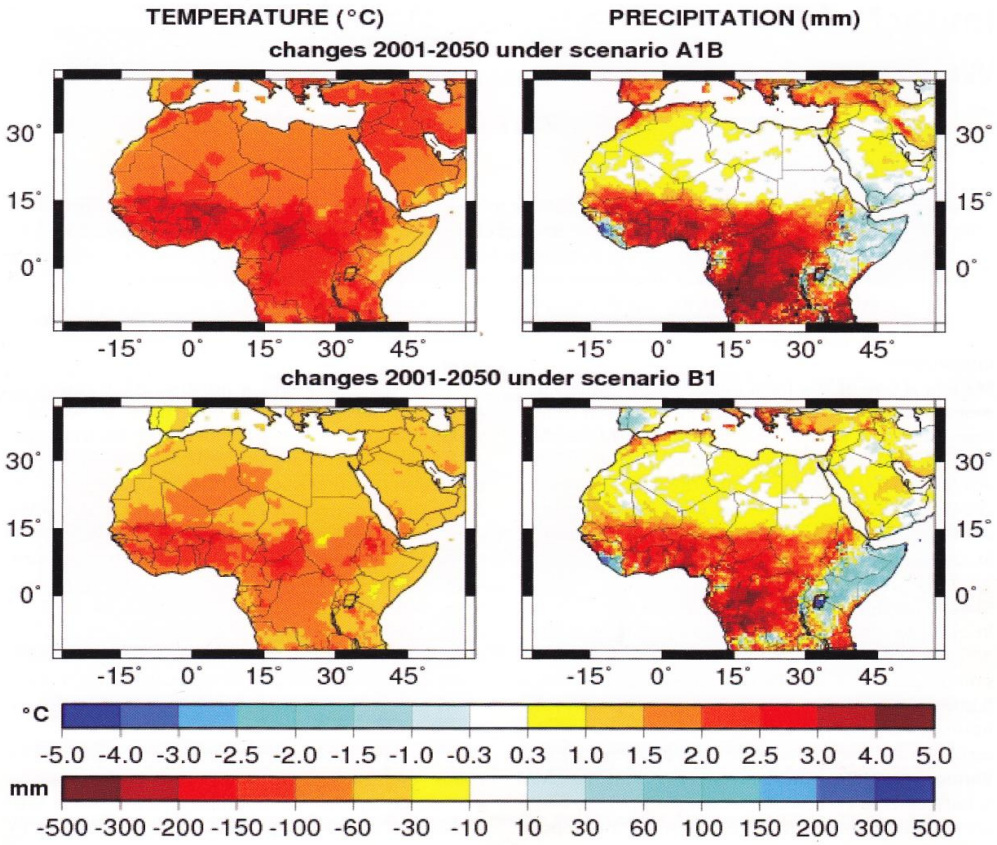

Fig. 5.3. Projected changes in annual precipitation and near-surface temperatures until 2050 over tropical and northern Africa due to increasing greenhouse gas concentrations and man-made land cover changes (Paeth, 2004). The scenario A1B describes a globalized world of rapid economic growth and comparatively low population growth. The scenario B1 also characterizes a future globalized world with a low population growth.

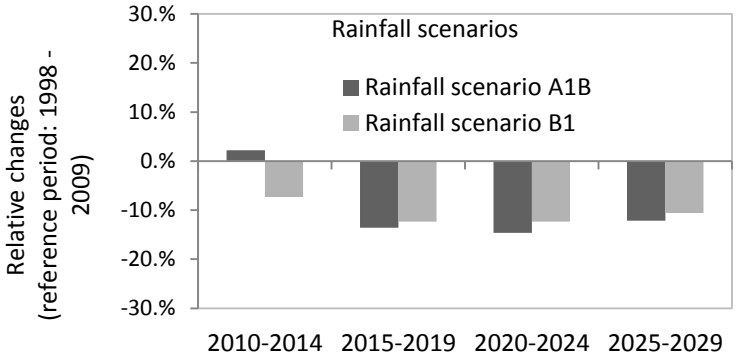

Fig. 5.4. Relative change in future rainfall (reference period: 1998 – 2009) for the Ouémé-Bonou catchment, REMO outputs, adjusted by MOS.

5.5. Discharge data

Due to the high cost of hydrometric equipments, the gauging network in Benin is relatively limited and almost exclusively located at the relatively large basin outlets. The available descriptions of the

hydrological regimes are not sufficient, since it does not allow the resource evaluation wherever it is available. Runoff regionalization is necessary and requires method developments to estimate, from existing rainfall data, runoff characteristics of ungauged sites.
The observation networks in the Ouémé catchment is installed by the National Directorate of Water (DG-Eau) since the 50's and has been recently (from 1998) densified in the upper catchment through cooperation with the Research Institute for Development (IRD), the Danish International Development Agency (DANIDA) and the German IMPETUS project. The catchment network totalizes today roughly 27 gauging stations (cf. Fig. 2.5). Many years of missing data are sometimes observed in the measured series, which may severely limit the simultaneous use of the different stations in hydrological studies. For example in the present study the available data regarding the surface state, are derived from 2003 satellite image (Landsat ETM+), while about only 8 sub-basins present acceptable continuous time-series data around this year. Traditionally, the water level is read manually twice a day, before automatic and continuous-time water-level recorders (Thalimedes) were introduced from 1998. Regular campaigns of discharge measurements are made every year during the rainy periods to establish rating curves used to convert measured water levels in continuous discharge. Due to many problems such as the accessibility of the gauging site, the lack of equipments and technical support, discharge peaks are not often measured, leading to errors in the stage-discharge relationships. Moreover, this is more remarkable in the gauging stations located in the delta area (flat and very large river bed, directly connected to large flood plains, and difficult to access during flooding events) of the lower Ouémé catchment, where measured peaks (e.g. Bonou station (49,256 km²)) are often significantly underestimated.

5.6. Suspended sediment and organic Nitrogen /Phosphorus content

Estimating soil loss from measurements of sediment transport in streams and rivers faces several problems. Taking the measurements is time consuming and expensive; the accuracy of the measurements is likely to be poor; and even if there are good data on the transport in a stream it is not known where the soil came from and when (FAO, 1996).
Suspended sediment is the finer particles which are held in suspension by the eddy currents in the flowing stream, and which only settle out when the stream velocity decreases, such as when the streambed becomes flatter, or the stream discharges into a pond or lake (FAO, 1996). Bed transport (large size particles, rolled along the streambeds) is often difficult to be measured for large river systems and is therefore not investigated in the present study.
In the Ouémé catchment, suspended sediment concentrations are strongly affected by factors such as soil erosion and flow rate, with strong interdependencies with the water turbidity. This complexity may be taken into account if site-specific relationships between turbidity and suspended sediment concentration are derived from filtered water samples, since simple filtering does not allow a high temporal resolution with manageable effort (Hiepe, 2008). In this study, the turbidity is determined by the nephelometric method, using turbidimeters for measuring incident light dispersion and attenuation. Turbidity of water is due to the presence of finely divided suspended solids: clay, silt, silica grains, organic matter, etc.. It gives an idea about the colloidal matter content suspended in water. Water samples (9 liters per day, with an average of up to 90 samples per year per site) were collected in 2004, 2005, 2008, 2009 and 2010 at 4 gauging stations (Donga-Pont, Térou-Igbomakoro, Bétérou, Zou-Atchérigbé, cf. Fig. 5.5). The water has been filtered in order to calculate daily suspended sediment concentration. Multi-parameter probes YSI 600 OMS (including one turbidity-broom sensor YSI 6136) were installed at the same stations to register continuous time series of suspended sediment concentrations to consider the hysteresis effects on the relationship between sediment and discharge (Van Noordwijk et al., 1998). Suspended sediment as well as turbidity data for the years 2004 – 2005 were performed by Hiepe (2008).
After filtration, the sediments were analyzed for organic nitrogen and non soluble/organic Phosphorus content, required for the simulation of nutrient depletion. Weekly scale sample were

generated to ensure the minimum amount of sediment required according to the available laboratory methods. Soluble/organic Phosphorus contents were analyzed in the laboratory of Geography Department of the University of Bonn (using a spectrophotometer), while the Organic Nitrogen contents were analyzed in the laboratory of Plant Nutrition Institute of the University of Bonn, using a CHNS-O Analyzer (Elemental Analyzer EuroEA 3000 Series).

Fig. 5.6 shows the relationships between turbidity and suspended sediment concentration obtained by linear regressions. As mentioned above, these rating curves are used to compute continuous time series of suspended sediment concentrations to correct the hysteresis effects on the relationship between sediment and discharge.

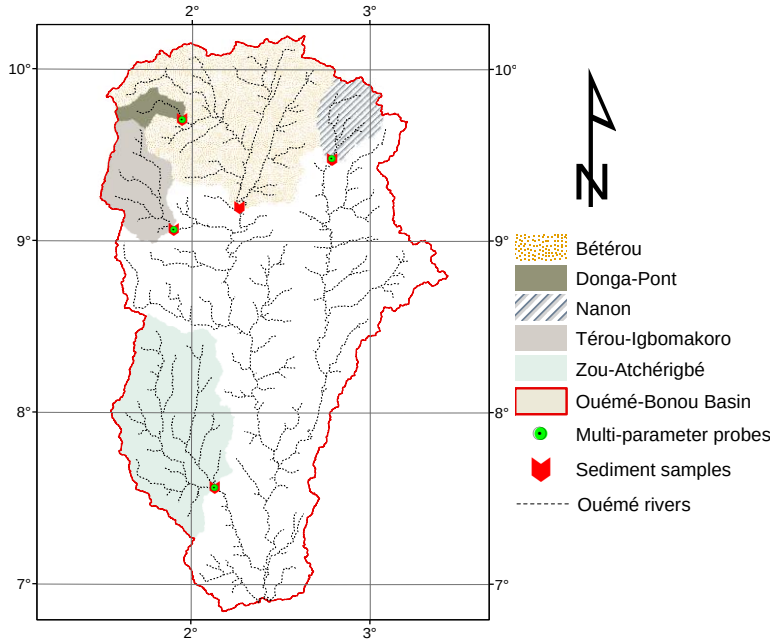

Fig. 5.5. Investigated gauging stations for the suspended sediment measurements and stream water chemical parameters. The Bétérou gauging station was investigated from 2004 to 2006 for the suspended sediment concentration (SSC) and from 2008 to 2010 for SSC and stream water chemical parameters (SWCP); Donga-Pont, from 2004 to 2005 for SSC and in 2008 for SSC and SWCP; Nanon only in 2010 for SSC and SWCP; Térou Igbomakoro investigated from 2004 to 2005 for SSC; and Zou-Atchérigbé investigated from 2008 to 2010 for SSC and SWCP. SSC for the years 2004 to 2005 were performed by Hiepe (2008).

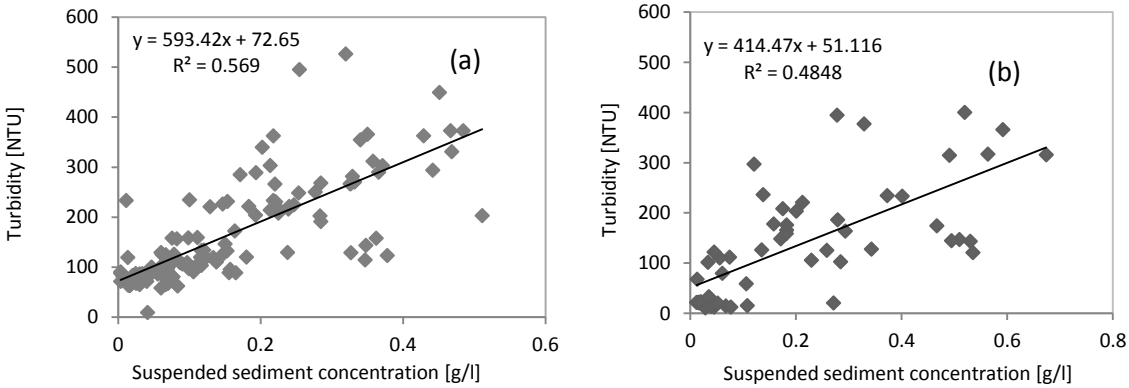

Fig. 5.6. Linear regression (turbidity vs. suspended sediment), (a): Donga-Pont (n = 121); years 2004, 2005 and 2008, (b): Zou-Atchérigbé (n = 56), year 2009.

Figure 5.7 shows the suspended sediment curves performed at daily scale for the Donga-Pont and the Zou-Atchérigbé gauging stations. Important parts of these curves were simply from the daily water

sample collection, because of dysfunction of the turbidity probes. Tab. 5.4 presents the organic C, N, and P content of the suspended sediment at the Donga-Pont and Zou-Atchérigbé gauging stations.

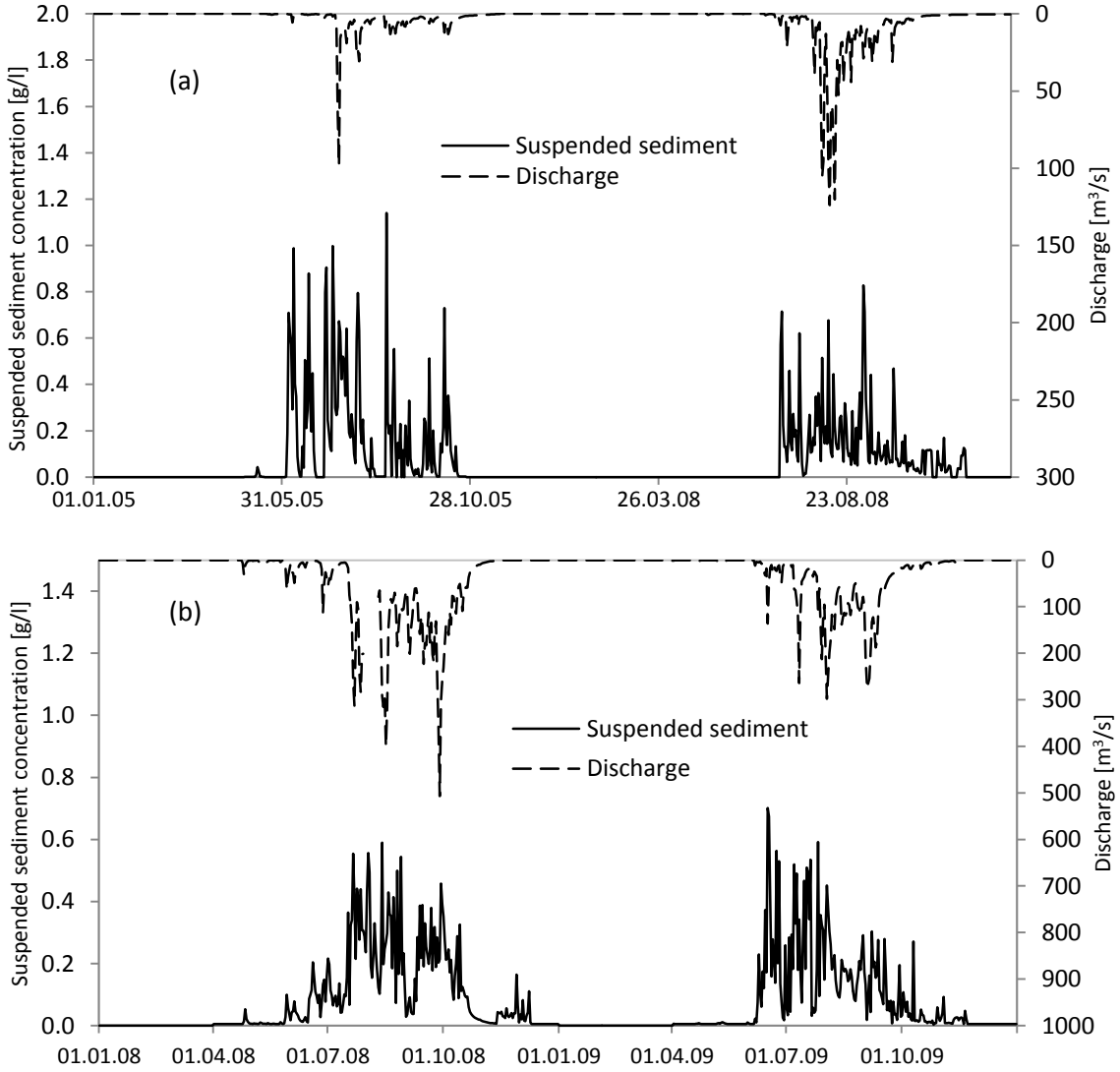

Fig. 5.7. Suspended sediment concentrations, (a): Donga-Pont gauging station, (b) Zou-Atchérigbé gauging station.

Tab. 5.4. Sediment organic C, N, and P content (from daily sediment amount obtained from gravimetric filtration) at the Donga-Pont and Zou-Atchérigbé gauging stations.

Measurement sites (periods)	Statistics	OrgN (%)	OrgP (mg/Kg)	C (%)
Donga-Pont	Mean	0.18	7.38	2.49
(15.06.2008 to 29.11.2008)	Maximum	0.28	13.00	4.02
	Mean Deviation	0.04	1.62	0.72
Atchérigbé	Mean	0.26	37.57	3.34
(15.06.2008 to 29.11.2008)	Maximum	0.36	65.60	4.49
	Mean Deviation	0.05	11.46	0.59
Atchérigbé	Mean	0.20	26.26	2.51
(08.06.2009 to 29.11.2009)	Maximum	0.36	42.04	4.02
	Mean Deviation	0.07	6.84	0.74

5.7. Stream water chemical parameters

Weekly water samples (in total 110 samples) were collected (2008-2010) at four gauging stations (Donga-Pont, Bétérou, Atchérigbé and Nanon, cf. Fig. 5.5) for the determination of chemical parameters such as NH_4+, NO_3^-, NO_2^-, SO_4^{2-} and PO_4^{3-}, required for water quality simulation.
The samples were taken in clean plastic or glass bottles. In order to obtain optimal results, the samples were immediately analyzed after collection (IMPETUS lab Parakou). If it turns out to be impossible to analyze them quickly, the bottles were completely filled and capped carefully avoiding excessive agitation or prolonged contact with air. Samples were sometimes stored up to 24 hours by cooling to 4 ° C, but brought back to room temperature before analysis. The laboratory methods used are in general approved by the United Sates Environmental Agency (USEPA) and described below accordingly to the laboratory manual.
Table 5.5 summarizes analyze results for the Donga-Pont and Zou-Atchérigbé gauging station. Due to road construction around the Donga-Pont gauging station, no samples were collected in 2009 and 2010. In general the concentrations are relatively low. One should notice that the sampling time scale of the stream chemical parameter, mainly the nitrate concentration (one time a week) has significantly affected the extend and the continuity of the data series collected, since many peak events were likely missed. This was particularly critical, due to the use of nitrate test in 2008 and 2009 to check the samples prior to any laboratory determination. In this context, laboratory determinations were only performed for the samples that reveal a nitrate concentration of more than 1 mg/l. A similar procedure has been adopted for the other chemical parameter such as ammonia, phosphate, etc., for which no laboratory determination was finally done.

Tab. 5.5. Water quality condition at the Donga-Pont and Zou-Atchérigbé gauging stations.

Measurement sites (periods)	Statistics	NO_3^-	NO_2^-	NH_4^+	PO_4^{3-}	SO_4^{2-}
Donga-Pont (n=20)	Mean	1.783	<0.05	<0.025	<1.5	<40
(29.06.2008 to 17.11.2008)	Maximum	3.024	<0.05	<0.025	<1.5	<40
	Mean Deviation	0.511	-	-	-	-
Atchérigbé (n=17)	Mean	2.743	<0.05	<0.025	<1.5	<40
(20.05.2008 to 18.11.2008)	Maximum	6.94	<0.05	<0.025	<1.5	<40
	Mean Deviation	0.728	-	-	-	-
Atchérigbé (n=8)	Mean	7.36	<0.05	<0.025	<1.5	<40
(01.09.2009 to 06.10.2009)	Maximum	13.64	<0.05	<0.025	<1.5	<40
	Mean Deviation	1.16	-	-	-	-
Atchérigbé (n=9)	Mean	7.63	0.05	0.66	2.37	-
(21.06.2010 to 06.09.2010)	Maximum	21.56	0.06	1.15	9.88	-
	Mean Deviation	4.74	0.02	0.18	1.86	-

6. Analyzing the effects of different soil databases on modeling of hydrological processes and sediment yield[1]

Abstract

Besides other information, environmental modeling requires data concerning soil properties and their spatial distribution. The quality and the applicability of soil maps not only depend on their scales, but also on the concept of the mapping procedures. To study the effects of different soil mapping approaches on the performance of the Soil and Water Assessment Tool (SWAT), a modeling study was carried out in the Zou-Atchérigbé catchment (6980 km², Fig. 2.5) which is a tributary of the Ouémé catchment (Republic of Benin, West Africa). Two different maps of the hierarchical Soil and Terrain digital database approach (SOTER; old and new) were considered in conjunction with the ORSTOM approach (soil mapping at the reconnaissance level, with one dominant soil type per mapping unit) all at the same scale. The effects of less coarser new SOTER mapping units and soil layer aggregation on the model results were evaluated. Sensitivities regarding the model input parameters with respect to the different soil databases are quantified. Based on daily water discharge measurements at the catchment gauging station, the SWAT model was calibrated (period 2001 to 2004) and validated (period 2005 to 2006) with reasonable results (coefficient of determination, model efficiency, and index of agreement, about 0.70 for weekly discharge) but with a slight underestimation of the total water yield for the coarser old SOTER database. With respect to the annual discharge, the calibration compensates for the differences in the different soil databases. The validation identified the less coarser new SOTER map as the best (with respect to modeling of weekly discharge) used in our study (showing higher model efficiency (0.59), higher coefficient of determination (0.61), and higher index of agreement (0.87)). Combined effects of the coarser old SOTER mapping units vs. aggregated soil layers have a measurable influence on lateral flow and sediment yield within the study area. High spatial variability in surface runoff and sediment yield patterns caused by the different mapping approaches were simulated although calibration of the discharge resulted in similar quality measures. Changes in the model parameters discriminated clearly the effects of soil mapping approaches from those of the mapping unit/parameter aggregation and have shown that SWAT could be calibrated successfully for discharge with the three databases, but differences between the soil mapping approaches with respect to discharge could not be balanced out.

Keywords: hydrological processes, SWAT, SOTER, soil parameterization, soil aggregation, soil mapping

6.1. Introduction

Assessment studies of land and water degradation have developed from mere static descriptions based on monitoring and sampling to the analysis of multiple scenarios using simulation models. At the regional scale, such studies increasingly involve the use of calibrated and validated simulation models to calculate nitrogen and phosphorus fluxes to groundwater and surface water. The nitrogen and phosphorus load models used in many studies were developed at the field scale, which further requires an upscaling step to enable regional scale calculations. For that, soil data, mainly soil maps

[1] Published as: Bossa, A.Y., Diekkrüger, B., Igué, A.M., Gaiser, T., 2012. Analyzing the effects of different soil databases on modeling of hydrological processes and sediment yield. Geoderma 173-174, 61–74.

may be critical. How the soil map has been developed (mapping approach) and the type of information deducible for environmental modeling is an important question. For example, soil maps based on genetic soil types may not have the information required for environmental modeling.

Besides different soil mapping approaches, soil data aggregation is often an important preparative phase in simulation exercises at large-catchment levels. As established in numerous studies (Becker & Braun, 1999; Romanowicz et al., 2005), the aggregation of soil data has a considerable impact on modeling rainfall runoff processes. Therefore, prior to any model calibration, the parameterization of the soil should be analyzed in detail for distributed hydrological modeling at catchment levels (Refsgaard et al., 1996).

Running the simulation models with aggregated data often implies that the models will respond linearly to spatial variations in the model's parameters as the variability within a mapping unit is not considered. This was demonstrated with an acidification model by Kros et al. (1993).

Often, it is assumed that the average of the properties is sufficient to characterize the behavior within an aggregative plot. However, as discussed by Weller (2002) and Diekkrüger (2003), simple averaging cannot be performed for a non-linear relationship. A physically-based model like SWAT (Soil Water Assessment Tool, Arnold et al., 1998), as applied in this study, is based on non-linear relationships.

Three important research questions arise from this finding: (1) whether the output of the physically based model SWAT depends on the soil mapping approach, (2) how within-aggregative mapping unit variability and soil layer/soil property aggregation, affect the SWAT model output, and (3) how valid is a given soil map obtained with a given mapping approach for hydrological evaluations.

As part of the long-term IMPETUS study (Christoph et al., 2008), the current work addresses the effects of different soil databases to obtain suitable inputs for modeling hydrological and erosional processes as well as nitrogen and phosphorus loads at the regional scale. The theoretical and practical aspects of the more recently developed soil aggregation and mapping method, SOil and TERrain digital database approach (SOTER, van Engelen & Ting-tiang, 1995) are considered in comparison to the French Commission of Pedology and Soil Mapping approach (CPCS, 1967). Therefore, the existing SOTER map (Igué, 2005), with its associated virtual soil profiles/aggregative soil parameters (SM_VP defined as SOTER Map with Virtual Profiles), was revised by refining the terrain units. As a result, a new SOTER map with referenced soil profiles (SM_RP defined as SOTER Map with Reference Profiles) was obtained. The ORSTOM aggregative soil maps (Dubrouecq, 1967; Volkoff, 1966, 1969) also consider referenced soil profiles (OM_RP defined as ORSTOM Map with Reference Profiles). The ORSTOM soil map differs from SOTER in that it gives only the most dominant soil type for a mapping unit. Differences in topography do not change these fundamental characteristics (Dubroeucq, 1977).

Special attention should be paid to the way the soil parameter problem is addressed and how the soil databases affect a model's parameters. Specifically, in the Zou (6980 km^2) sub-catchment considered in this study, the sensitivity of the parameters of the distributed hydrological model SWAT is quantified with respect to the different soil databases. Effects of the mapping approach as well as those related to the mapping unit/soil parameter aggregation on the surface runoff patterns, evapotranspiration and sediment yield patterns were quantified.

The SWAT model has already been successfully applied to several Ouémé sub-catchments: (1) the Térou sub-catchment (Sintondji, 2005), (2) the Zou sub-catchment (Sintondji et al., 2009), and (3) the Upper Ouémé (Hiepe, 2008), and have focused on hydrological processes, water balance and rainfall erosion, using the French soil map (ORSTOM/ CPCS). The current study aims at the quantification of effects of different soil mapping approaches on hydrological and sediment yield modeling issue at catchment scale.

6.2. Materials and methods

6.2.1. CPCS approach and the OM_RP database

The French CPCS (Commission de Pédologie et de Cartographie des Sols) system (CPCS, 1967) was developed from 1963 to 1967 by a group of French soil scientists led by Aubert and Duchaufour (Yerima and van Ranst, 2005). It is a morphogenetic system of soil classification and classifies the factors of soil genesis by their morphological characteristics. As such, the morphological characteristics, which are taken into consideration, must translate the evolutionary process in an effective and harmonious manner. This genetic classification system, which uses mostly ecological criteria, is still being used by the French soil cartography service. However, a new French Soil Classification System called the "Referentiel Pedologique Francais (RPF)" under the auspices of INRA and coordinated by D. Baize and M.C Girard is being developed (Duchaufour, 1988).
In successive steps, the French Commission of Pedology and Soil Mapping (CPCS) developed the French soil classification (CPCS, 1967), which is a hierarchical approach consisting of the elements class, subclass, group, subgroup, family, series, and phase. The classification system is based on the following basic principles: (1) the class takes into account the evolution of the profile (presence of certain layers), the intensity of weathering, the type of humus, and some basic factors like hydromorphy (water), or solonetz (salts); (2) the sub-class is essentially defined by the soil and the climate; (3) the group is defined by morphological characteristics that reflect a specific process; (4) the sub-groups distinguish between the intensity of a group process and the action of a secondary process; and (5) the family takes into account the bedrock.
The basic unit used in the legend of the soil maps of the Republic of Benin at 1:200,000 is the soil family, which includes all series of the same sub-group formed on the same rock or parent material (Faure & Volkoff, 1998; Volkoff, 1969). It represents the most common soil type in a given area, but differences in topography do not change its fundamental characteristics (Dubroeucq, 1977). Under these conditions, most of the hydromorphic soils flanking rivers, and soils developed on colluvial materials downstream, as well as outcrops of rocks, are not mapped.
The OM_RP database was created by associating a reference soil profile to each ORSTOM mapping unit taken from the studies of Sintondji (2005), Sintondji et al. (2009), and Hiepe (2008).

6.2.2. SOTER approach implemented in the Ouémé catchment

The SOTER approach is a hierarchical terrain component concept that has several advantages. First it follows the workflow of a land inventory more naturally, as one tends to split up the major landscape elements step-by-step and to refine by adding further details to the rough outline. The opposite task, i.e., the aggregation of defined parts to a larger pattern, is also supported by the new structure. A direct consequence of this new design is the ease of scale changing (facilitating multi-scaled evaluation studies).
The methodology used in this work originated from the idea that land (in which terrain and soil occur) incorporates processes and systems of interrelationships between physical and biological phenomena evolving through time. The idea was developed initially in Russia and Germany (Haase and Schmidt, 1971; Haase et al., 1984). A similar integrated concept was used in a land-system approach developed in Australia and developed further by Cochrane et al. (1981) and Gunn et al. (1990). SOTER has continued this development by defining land as being made up of natural entities consisting of combinations of terrain and soil.
The method and descriptions of the land structures in Benin were followed the SOTER procedures manual (van Engelen & Ting-tiang, 1995). This procedure identifies an area of terrain (land unit) with distinctive, often repetitive, patterns of geomorphologic or geological elements together with a corresponding soil pattern. A separation of units is made if it can be mapped at the given scale, i.e., if the borders can be determined based on the available information and if the resulting areas are big

enough to be shown on the map. If so, these resulting areas can be mapped and digitized. The elements belonging to these units are stored in two different databases: the geometry is stored in the Geographic Information System (GIS) and attribute-information regarding the elements belonging to the units is stored in another database on three main levels:

- Terrain unit, with its pattern of landform such as elevation, major landform and general lithology.
- Terrain components, containing data for slope, surface form, and groundwater, etc. A terrain unit has one or more terrain components (crest, slopes, and valleys) (Igué, 1997). In the case they cannot be mapped at the given scale, the information related to non-mappable terrain components is stored in the attribute database alone, and no entry is made into the geometric database. Moreover, at larger scales (1:50 000, for example), the three terrain components (crest, slopes, and valleys) are mapped (Igué, 1996; Spohrer, 1999).
- Soil components, containing information regarding the soils. The components are described by some general data, such as the position and proportion of the terrain component, surface properties, and by reference profiles. The soil components can be mapped at the given scale. Here, a soil component is not described by a single reference profile but by a set of soil profiles that can contain a free number of soil descriptions. The set is open for further differentiation of data.

In order to correctly study these three levels, toposequences constitutes the best method adapted for studying tropical regions composed of terrain with a distinctive, often repetitive pattern of surface forms (Bocquier, 1971; Boulet, 1974; Igué, 1985; Fritz, 1996; Stahr et al., 1995). A toposequence is defined as a sequence of soil properties which do differ from the top to the base because of topography as a soil-formation factor. The introduction of toposequences permits investigators: (1) to collect an extensive inventory of the soils occurring within the different terrain units and components; (2) to acquire further information about the spatial soil type occurrence; (3) to cut ideal transects across geomorphic units in order to obtain information about the spatial arrangement of soil types; (4) to obtain spatial information about surface features (soil crusting, soil surface color, vegetation, and land use) on smaller and larger scales; (5) to correlate surface characteristics within soil types, and (6) finally to perform a supervised classification of the landscape. Thus, an intensive inventory of the soils and their spatial distribution within a terrain was undertaken for the Ouémé catchment by the National Institute for Agriculture Research of Benin. The terrain components are differentiated into 45 terrain sub-components, according to the petrography, slope gradient, and relief intensity (Fig. 6.1), which are each delineated and described. The terrain components in the study area were formed from Precambrian crystalline basement, usually known as “Basement complex,” largely composed of acid metamorphic rocks of the “Dahomeyen series’’ (gneiss, magmatite, granite, and quartzite). Also present are basalt, gabbro, mylonite, volcano-sedimentary intrusive rhyolite, sandstone, and conglomerate (OBEMINE, 1989).

The first version covering the entire Ouémé catchment (called “old” in the following text) was conducted by Igué (2005). As part of this study, a new version (called “new”) was produced by refining the mapping units and adding more details following the same procedure. Mapping terrain units and even terrain components were made possible using a detailed topographic map covering the study area at a 1:50,000 scale (IGN, 1954-1963).

The identified units were combined with geological maps at a scale of 1:200,000 (OBEMINE, 1989). The main differentiating criteria were the change of landscape morphology (slope gradient), geology, and hydromorphy for valley and plain. The maps were digitized with GIS (ArcMap).

The new soil and terrain database is being established with data from earlier studies (Dubroeucq, 1967; Volkoff, 1966; Youssouf, 1982; Igué, 1991; Fritz, 1995; Sporer, 1999; Igué et al., 2000; Weller, 2002; Maeir, 2004; Sintondji, 2005; Sintondji et al., 2009 and Hiepe, 2008) and new data from intensive ground checks and transect studies.

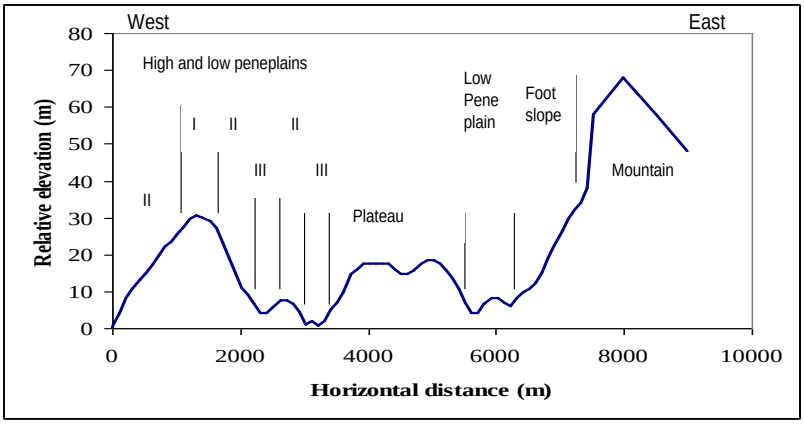

Fig. 6.1. Representative transect of the geomorphic units "high and low peneplain" and "mountain" on gneiss basement at Savalou (I: crest, II: slope, III: valley) (After Igué, 2000).

6.2.3. Description of the SM_VP and SM_RP databases

The SM_VP database is based on the old SOTER map (Igué, 2005) and has been generated by aggregating soil physical properties for virtual soil profiles. Therefore, only one virtual profile has been associated with each terrain component based on all soil profiles occurring within it. Various steps of aggregation are used: (1) at the profile level, through weighting the vertical proportion of soil horizons within two virtual layers (n=1,131 soil profiles have been used); and (2) at the terrain component level, through area-specific weighting factors for soil components (n=480 soil components were explored and used).

The SM_RP database is based on the refined (new) SOTER map and was compiled by associating reference soil profile with each mapping unit. For that purpose, the profile sets for each soil component (found within each terrain component) were used to choose the *dominant* soil component according to the importance of the estimated surface area of all soil components within each terrain component. This means that a reference profile is chosen (including a reference to the most widespread land-use type) for each calculated dominant soil component from the group of all profiles linked to it. In order to maintain and confirm existing data, field surveys were made by the toposequence method. Transects were positioned both along tracks or roads and across the bush. On the surveyed area, more than 2702 observations by auger drillings and 584 profiles were done**.** 2263 soil horizon were sampled for different physical and chemical analysis. In addition to that, 213 profiles have been georeferenced from other studies.

6.2.4. Databases and the soil properties

Soil texture and soil organic carbon are the basic soil properties obtained by laboratory analysis for each soil profile used to create the different databases. They were acquired from very diverse sources, but more than 90% are based on the method of Reeuwijk (1995):

- Texture: After destruction of organic matter (for organic matter content > 1%), the samples were dispersed with $Na_4P_2O_7$ and sieved wet into the fractions. Coarse sand (2 - 0.2 mm), fine sand (200 – 50 µm), coarse silt (50 - 20 µm). Fine silt (20 - 2 µm) and clay (< 2 µm) were determined by sedimentation.
- Organic carbon: Oxidation with potassium dichromate ($K_2Cr_2O_7$), and titration with iron ammonium sulfate ($Fe(NH4)_2(SO_4)_2$).

Considering these properties, many other parameters were derived for the three databases, such as the quotient of organic carbon to organic nitrogen content (C/N-ratio), soil organic matter (Sorg), Cation Exchange Capacity of the clay fraction (CEC_clay), base saturation (BS) (as a percentage of the sum of exchangeable bases of the cation exchange capacity (CEC_soil)), and soil erodibility (USLE_K).

The bulk density (BD), saturated hydraulic conductivity (SOL_K), and the soil- available water capacity (SOL_AWC) used in the OM_RP database were also measured in the laboratory (Sintondji, 2005; Sintondji et al., 2009, and Hiepe, 2008) but are based purely on calculations for the SM_RP and SM_VP databases. For that purpose, Acutis and Donatelli's (2003) Soil Parameter Estimate model (SOILPAR, v.2.00 beta) was used to estimate the saturated hydraulic conductivity (SOL_K), and soil-available water capacity (SOL_AWC) for the SM_RP database. Various methods (pedo-transfer functions) are implemented in this model, including the point pedo-transfer functions of Baumer (1990) and Rawls and Brakensiek (1982 & 1985).
With regard to the SM_VP database, the following references have been used: (1) saturated hydraulic conductivity (SOL_K) was estimated using the approach of Tomasella and Hodnett (1997); (2) Field Capacity and Permanent Wilting Point were estimated using the approaches of Tomasella and Hodnett (1998), Gaiser et al. (2000), and Rawls and Brakensiek (1982); and (3) the Van Genuchten Parameter were taken from Maidment (1992).
Different methods were used for this calculation because it was assumed that the water-retention behavior of soils dominated by high-activity clay (CEC > 24 cmol/kg clay) might differ from those with low-activity clay (CEC <24 cmol/kg clay). Thus, the whole data set was subdivided into groups of low-activity clay (LAC) soils and non-low-activity clay soils (Gaiser et al., 2000).

6.2.5. Model components vs. soil mapping approach

The simulated SWAT processes are controlled by many parameters presented in Fig. 6.2 and described below. In this study the focus is on the model components and parameters affected by the soil mapping approaches and the soil mapping unit/parameter aggregation (cf. Tab.6.1). As shown, the discharge dynamic, the annual hydrological water balance, the annual sediment yield and their patterns within the research area may be affected. Further descriptions are provided in the following paragraphs.

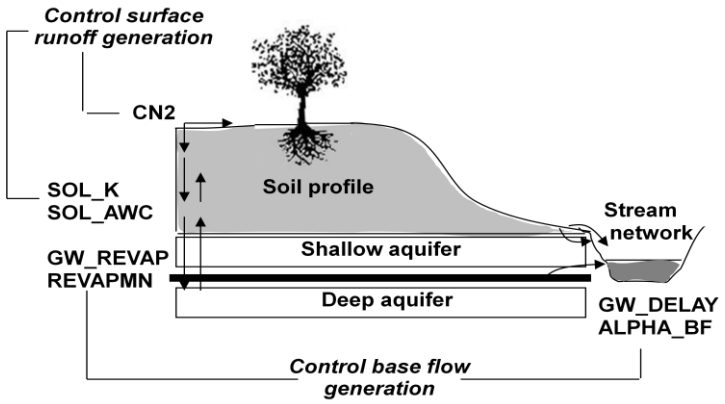

Fig. 6.2. General overview of the processes simulated by SWAT and the parameters that control these processes. CN2: SCS Curve Number [-]; SOL_K: soil hydraulic conductivity [mm h-1]; SOL_AWC: soil available water capacity [vol %]; GW_REVAP [-] and REVAPMN [mm]: rate and threshold for describing the water exchange between root zone and shallow aquifer; ALPHA_BF: groundwater recession constant [d]; and GW_DELAY: groundwater delay time [d]. (Modified from Heuvelmans et al., 2004).

Tab. 6.1. Model components and parameters directly affected by the soil map. HRU: hydrological response unit, ET: actual evapotranspiration [mm]; CN2: SCS Curve Number [-]; SOL_K: soil hydraulic conductivity [mm h-1]; SOL_AWC: soil available water capacity [vol. %]; ESCO: Soil evaporation compensation factor [-].

	Surface runoff	Aquifer recharge	ET	Erosion
soil mapping approach	CN2, HRU (patterns, slope)	-	ESCO	CN2, HRU (patterns, slope)
soil parameter aggregation	SOL_K, SOL_AWC	SOL_K, SOL_AWC	SOL_AWC	-
soil mapping unit aggregation	CN2, HRU (patterns, slope)	-	ESCO	CN2, HRU (patterns, slope)

Surface and sub-surface runoff generation: the runoff curve number (CN2 for medium soil moisture conditions), soil-available water capacity (SOL_AWC), and the soil hydraulic conductivity (SOL_K) are the important parameters that influence surface flow in SWAT. Surface runoff is predicted using a modified version of the SCS CN method (SCS, 1972, 1986) (Eq. 4.2 and 4.3). This method involves various types of data related to vegetation, hydrologic soil group, slope, and antecedent moisture condition of the catchment.
An increase of the curve number implies an increase of surface runoff. Initial values (Tab. 6.2) for calibration are chosen according to land use and the soil hydrologic groups (SCS Engineering Division, 1986). As mentioned above, CN2 values highly depend on the hydrologic soil group, slope, and antecedent moisture condition of the HRU. The slope belongs to the group of HRU physical parameters, derived from a Digital Elevation Map. Any change in the HRU patterns will result in changed slope distribution, as consequence of the mapping approach or the soil mapping unit aggregation. Given the dependence of the CN2 values on HRU slopes (mountain and hill slopes, low and high peneplain slopes) which are important mapping criteria in the SOTER approach but not considered in the traditional French approach. Therefore, it is expected that the different mapping approaches result in significant different patterns of CN2 values within the research area. In consequence, significant changes in the surface runoff patterns within the research area may occur. It should be noticed that changes can be attributed to the soil mapping approach when comparisons are made between the OM_RP and SM_RP databases, while changes can be attributed to mapping unit/soil parameter aggregation when the SM_RP and SM_VP are compared.

Tab. 6.2. Runoff curve numbers for different land cover and soil hydrologic groups (SCS Engineering Division, 1986).

	Hydrologic soil groups			
Cover types	A	B	C	D
Forest evergreen	25	55	70	77
Wood savannah	39	61	74	84
Pasture	49	69	79	84
Fallow	77	86	91	94
Agricultural land	67	77	83	87
Residential	31	59	72	79

The soil-available water capacity (SOL_AWC) is the maximum volume of water that is available to plants when soil moisture is at field capacity. An increase of its values implies a decrease of the surface runoff. It is highly affected by the parameter aggregation.
This is similar for the lateral flow which can be significant in areas with soils having high hydraulic conductivities in the surface layers (SOL_K), and an impermeable or semi-permeable layer at a shallow depth. In such a system, rainfall will percolate vertically until it encounters the impermeable layer; the water then ponds above the impermeable layer, forming a saturated zone, i.e., a perched water table. This saturated zone is the source of water for lateral subsurface flow. SWAT incorporates the kinematic storage model for subsurface flow developed by Sloan and Moore (1984) (Eq. 4.10).

Base flow generation: besides the parameters “revap” (GW_REVAP) and the threshold water level in a shallow aquifer for capillary rise or percolation to deep aquifer (REVAPMN) which are influenced by the soil map, base flow recession constant (ALFA_BF), groundwater delay time (GW_DELAY), threshold water level in a shallow aquifer for base flow (GWQMN), and aquifer percolation coefficient (RCHRG_DP), are the important variables that influence the base flow generation.
The groundwater "revap" coefficient (GW_REVAP) controls the amount of water that moves from a shallow aquifer to the root zone (capillary rise) as a result of soil moisture depletion and the amount of direct groundwater uptake from deep-rooted trees and shrubs.
A water flux from the shallow aquifer to the root zone or to plants is allowed only if the depth of water in the shallow aquifer is equal to or greater than a minimum value (REVAPMN).

Two other parameters that govern catchment response are the base flow recession factor alpha and the groundwater delay. The base flow factor or recession constant (ALPHA_BF) characterizes the groundwater recession curve. This factor approaches zero for flat recessions and approaches one for steep recessions. The groundwater delay (GW_DELAY) is the time required for water leaving the bottom of the root zone to reach the shallow aquifer.
The base flow generation parameters are not significantly affected by soils and will not further analyzed in this study.

Evapotranspiration: actual evapotranspiration is computed using the Penman method (1956). Actual evapotranspiration is highly affected by the soil evaporation compensation factor (ESCO) and soil available water capacity (SOL_AWC), already described in the surface runoff generation chapter.
The soil evaporation compensation factor (ESCO) adjusts the depth distribution for evaporation from the soil to account for the effect of capillary action, crusting, and cracks. This parameter is negatively proportional to the maximum evapotranspiration in a nonlinear fashion. Therefore, larger values result in less evapotranspiration (ET), and thus a larger water yield (WTRYLD). A range of 0.001 ~ 1.0 is recommended. It is highly influenced by the mapping unit aggregation due to the change in the HRU patterns and therefore in the pore, crust and crack patterns.

Erosion: for calculating soil erosion, a modified version of the Universal Soil Loss Equation (Williams, 1975) is implemented in SWAT (Eq. 4.13). The slope length factor (Eq. 4.13) belongs to the group of HRU physical parameters, derived from a Digital Elevation Map. Any change in the HRU patterns will result in new slope length factor distribution, as consequence of the mapping approach or the soil mapping unit aggregation. The erodibility factor (Eq. 4.13) is directly affected by the soil parameter aggregation. Therefore significant changes can be expected in the annual sediment yield and its pattern within the research area.

General input data: Figure 6.3 shows the nature and source of the different data layers, their scales and types of parameters and investigations required for applying the SWAT model in the Ouémé catchment.

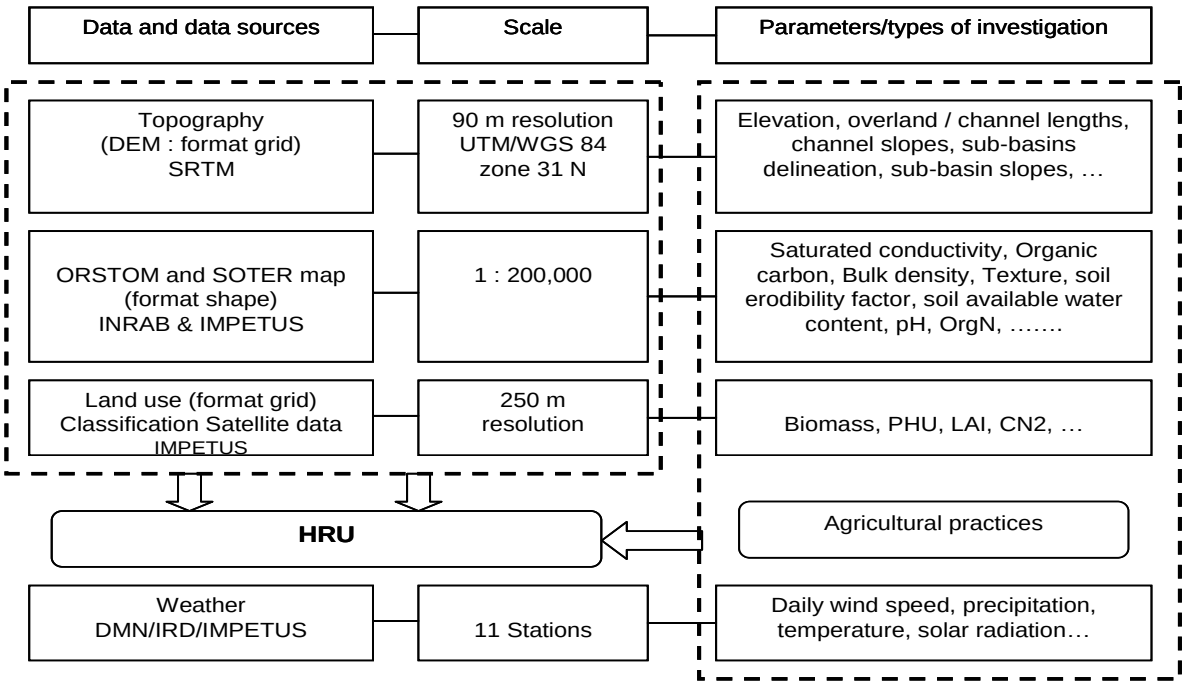

Fig. 6.3. General model input data used in this study. Soil and land use data are from IMPETUS (Christoph et al., 2008) and from INRAB (Institut National de la Recherche Agricole du Bénin; Igué, 2005).

As explained in the chapter 5, in SWAT, the catchment is discretized into numerous sub-catchments. Sub-catchments are delineated from the Digital Elevation Model using a threshold concept parameter (CSTV), and are linked to one climate station, providing climate data such as daily precipitation and potential evapotranspiration. Therefore, the number of subcatchments strongly affects simulation results due to the spatial linkage between sub-catchments and climate information (Hiepe, 2008).
Within each sub-catchment, the distribution of soils and vegetation is considered by Hydrological Response Units (HRUs) created by overlaying three types of data layers (topographic map, CPCS/SOTER soil map, and land use map). Each HRU is represented by specific parameters, such as the terrain properties, the chemical and physical soil properties and properties of the vegetation types. Again, a threshold concept determines the number and size of HRUs per sub-catchment, preventing multiple small HRUs due to fragmented input layers. For the multiple HRUs, the soil mapping approach and aggregation is critical. As the HRUs are non-georeferenced units, the number and properties of HRUs should be balanced, with respect to the underlying database. In this study, CSTV values were maintained constant during SWAT implementation using the different soil maps.
Beyond the general input data presented in Fig. 6.3, daily discharges recorded at the catchment outlet are available from 2001 to 2006 and are used for calibration (2001-2004) and validation (2005-2006). Although daily time steps are simulated by SWAT, comparing simulated and observed discharge is performed on a weekly time scale resolution.

6.3. Results and discussion

6.3.1. Main differences between the soil databases

Figure 6.4 shows the different soil maps used. The ORSTOM map (OM_RP) and the SOTER map (SM_VP) have almost the same density of cartographic units of 0.038 and 0.041 units/km² respectively compared to 0.06 units/km² for the SOTER map (SM_RP). Tab. 6.3 and Fig. 6.4 show the spatial pattern as well as the differences between the three databases for a single mapping unit. Large variations in the magnitudes of the values of saturated hydraulic conductivity and erodibility factor were found. For example, the saturated hydraulic conductivity values increase from the databases OM_RP, SM_RP to SM_VP, while the erodibility factor decreases in the same order. A significant influence on the water balance components, as well as on the total sediment yield, can be expected from this variability. According to Bollini and Rosseau (1978), the classification of erodibility values presented in Tab. 6.4 shows the effect that might be expected with regard to soil erosion. In the soil units described in Fig. 6.5, the erodibility of the topsoil varies between “resistant to erosion” and “sensitive to erosion”.

Tab. 6.3. Example of relationships between overlapping soil map units (cf. Fig. 6.4; SM_VP: SOTER map with virtual profiles, SM_RP: SOTER map with referenced profiles, OM_RP: ORSTOM map with referenced profiles).

SOTER unit (Old) SM_VP	SOTER unit (New) SM_RP	WRB classification	CPCS classification OM_RP	Typical geomorphological unit	Land use
BJ33	BJ33A	Ferric Luvisol (LVf)	Ferruginous tropical soils with concretions	High peneplains on gneiss migmatite	Savannah
	BJ33B	Haplic Luvisol (LVh)	Leached ferruginous tropical soils	High to higher peneplains on gneiss migmatite	Crop/ fallow
	BJ33C	Haplic Lixisol (LXh)	Leached ferruginous tropical soils with concretions	Higher peneplains on gneiss migmatite	Savannah
	BJ33D	Albic Plinthosol (PTa)	Leached and indurated ferruginous tropical soils	Higher to highest peneplains on gneiss migmatite	Savannah
	BJ33E	Ferric Alisol (Alf)	Ferruginous tropical soils with concretions	Higher to highest peneplains on gneiss migmatite	Crop/ fallow

Tab. 6.4. Classification of erodibility (K factor in USLE) according to Bolline & Rosseau (1978).

Erodibility [0.013 t m2 h/(m3 t cm)]	Classification
< 0.1	very resistant to erosion
0.1 - 0.25	resistant to erosion
0.25 - 0.35	medium resistance to erosion
0.35 - 0.45	sensitive to erosion
> 0.45	very sensitive to erosion

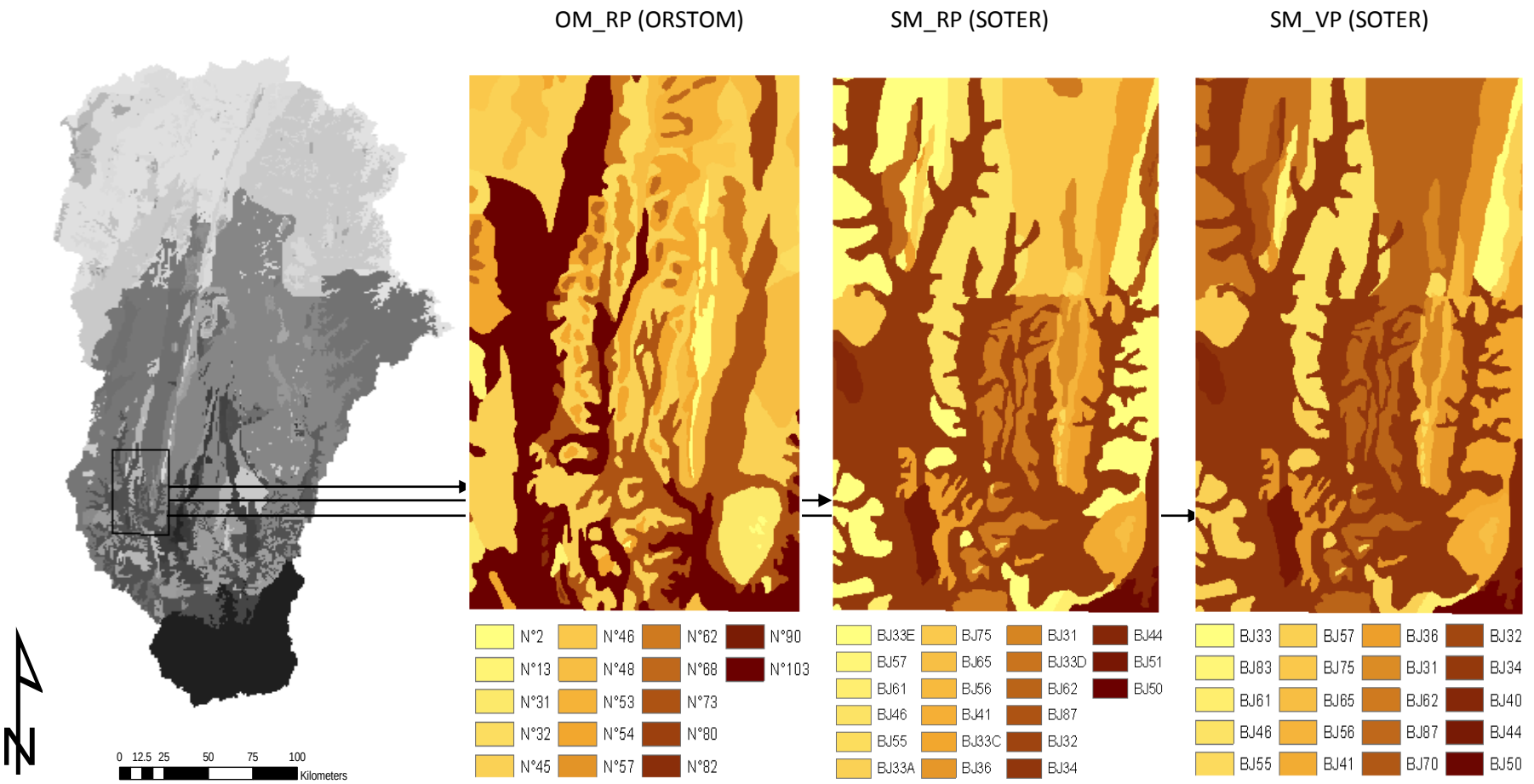

Fig. 6.4. Different soil maps used in the study. On the left hand, the soil map is given for the Ouémé catchment. On the right hand the cuttings show details of the Zou catchment. For the explanation of the representative soil profiles see Tab. 6.3.

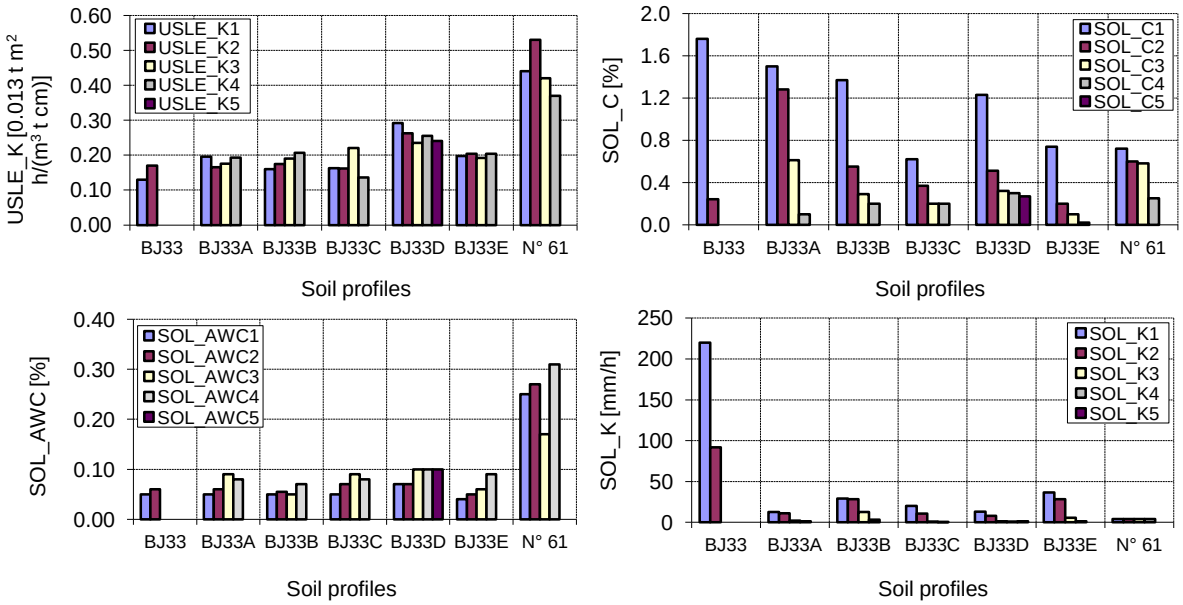

Fig. 6.5. Soil properties for selected reference profiles (cf. Fig. 6.4 and Tab. 6.3) of the different databases for the layers 1 to 5 of the given soil profiles for soil erodibility (USLE_K), soil carbon (SOL_C), soil available water content (SOL_AWC), and soil hydraulic conductivity (SOL_K).

6.3.2. Discharge dynamics (calibration and validation)

SWAT has been calibrated using discharge data for the period 2001-2004. Next, the model was validated using discharge data from the period 2005-2006. The model input parameters were automatically calibrated using the sum of squared errors between simulated and observed discharge as quality measure.

The correlations (scatter plots) between the simulated and the observed discharges over the calibration period are presented in Fig. 6.6 for the different mapping approaches. Fig. 6.7 shows weekly observed and simulated water discharges and the total water yield for the calibration period 2001 – 2004 and for the different soil databases (OM_RP, SM_RP, and SM_VP). For descriptions of the model parameters, see the discussion below. The statistical indicators (coefficient of determination, model efficiency, and index of agreement) are all acceptable (about 0.70 for weekly discharge) with a slight underestimation of the total water yield. These values for goodness-of-fit are highly affected by the quality of the observed values, which exhibit considerable errors at the Zou gauging station. Any clear effects due to differences between the soil databases used have not been discovered at this stage. One can conclude that with respect to the weekly discharge the calibration balanced out the differences in the different databases.

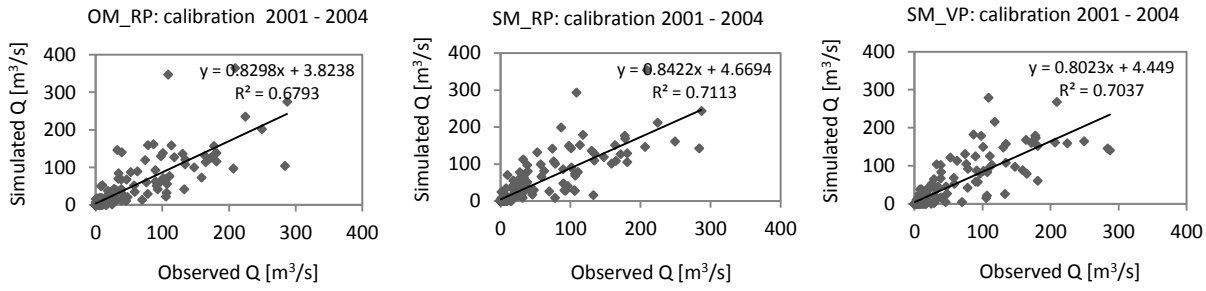

Fig. 6.6. Scatter plot of weekly simulated versus observed discharge for the calibration period 2001-2004 for the investigated three soil data bases.

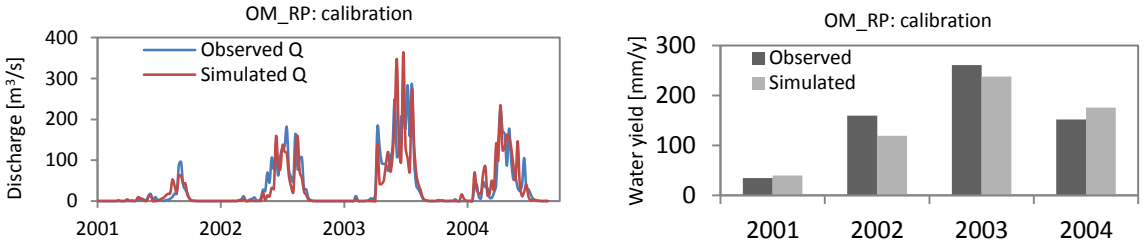

Calibration (OM_RP)	Observed Q	Simulated Q	R^2	ME	IA
Mean discharge (m^3/s)	33	32	0.68	0.64	0.9
Mean water yield (mm/y)	152	146	0.9	0.89	0.97

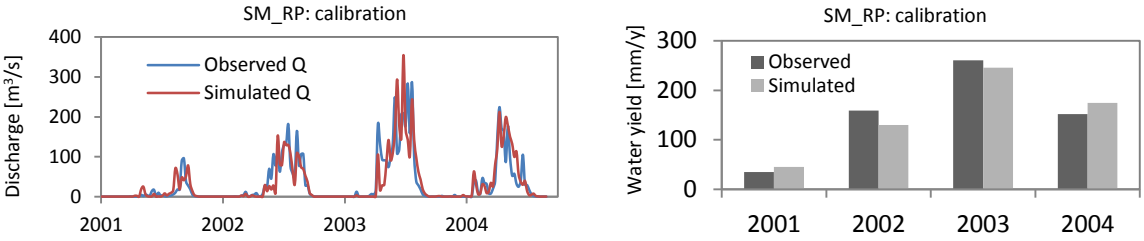

Calibration (SM_RP)	Observed Q	Simulated Q	R^2	ME	IA
Mean discharge (m^3/s)	33	33	0.71	0.69	0.92
Mean water yield (mm/y)	152	151	0.94	0.93	0.98

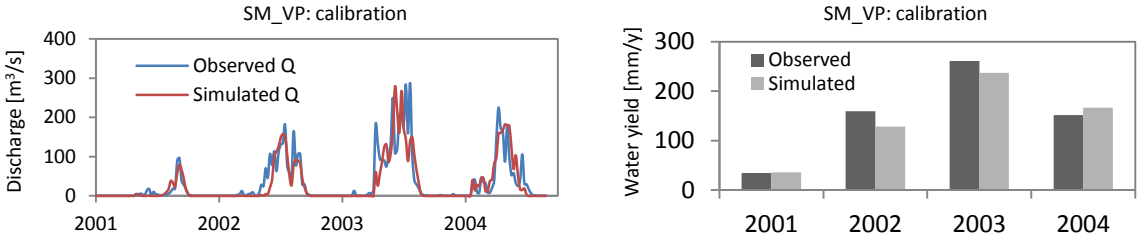

Calibration (SM_VP)	Observed Q	Simulated Q	R^2	ME	IA
Mean discharge (m^3/s)	33	32	0.7	0.69	0.91
Mean water yield (mm/y)	152	145	0.95	0.93	0.98

Fig. 6.7. Weekly observed and simulated discharge and water yield for the calibration period 2001-2004 for the investigated three soil databases. R^2 coefficient of determination, ME model efficiency, IA index of agreement.

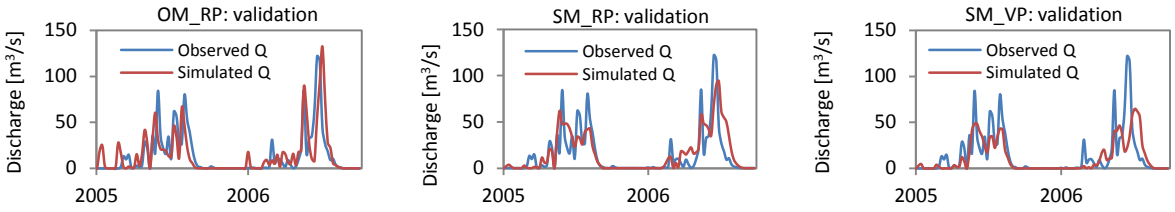

Validation	Observed Q [m^3/s]	Simulated Q [m^3/s]	R^2	ME	IA
OM_RP	13.55	13.6	0.47	0.4	0.82
SM_RP	13.55	14.92	0.61	0.59	0.87
SM_VP	13.55	11.19	0.42	0.4	0.76

Fig. 6.8. Weekly observed and simulated discharge for the validation period 2005-2006 for the investigated three soil databases. R^2 coefficient of determination, ME model efficiency, IA index of agreement.

Figure 6.8 shows weekly observed and simulated water discharges for the validation period (2005 – 2006) and for the different soil databases (OM_RP, SM_RP and SM_VP). Lower goodness-of-fit was found for the soil database SM_VP. The SM_RP showed higher model quality (higher model efficiency (0.59), higher coefficient of determination (0.61), and higher index of agreement (0.87)) and is therefore the best approach for discharge simulation.

6.3.3. Water balance and total sediment yield (calibration)

Water balances, as well as the total sediment yield are given in Tab. 6.5 in which the annual mean over the calibration years is summarized. When analyzing the water balance components, a clear dependency on the underlying soil database differences was found (cf. Tab. 6.5):

(1) A significantly higher lateral subsurface flow for the soil database SM_VP. This trend is entirely consistent with the point made above regarding the differentiation of soils. While the results obtained using OM_RP and SM_RP are similar, the results computed using SM_VP differ significantly. One can conclude that the combined effects of the coarser SOTER map unit and the aggregated soil layers (by aggregating soil properties) have large influences on lateral subsurface flow.

(2) A significant decrease of the actual evapotranspiration computed using soil databases from OM_RP, SM_RP to SM_VP. The amounts computed using soil databases SM_RP and SM_VP are similar but differ significantly from the one computed using the OM_RP database, and

(3) a significant decrease of the total sediment yield computed using soil databases OM_RP, SM_RP to SM_VP, respectively. Here also, the amounts computed using soil databases SM_RP and SM_VP are similar but differ significantly from the one computed using the OM_RP database. It therefore seems problematic to apply the OM_RP database for river water quality evaluation.

The observed differences concerning actual evapotranspiration and total sediment yield can be solely explained by the soil mapping approach.

Tab. 6.5. Mean annual water balance and total sediment yield for the Zou catchment for the calibration period 2001 – 2004.

Water balance components/total sediment yield	OM_RP	SM_RP	SM_VP
Precipitation (mm a^{-1})	1149	1149	1149
Surface runoff (mm a^{-1})	78	80	82
Groundwater flow (mm a^{-1})	67	94	83
Subsurface lateral flow (mm a^{-1})	2	2	10
Shallow aquifer recharge (mm a^{-1})	82	85	94
Deep aquifer recharge (mm a^{-1})	9	12	14
Actual evapotranspiration (mm a^{-1})	911	876	863
Potential evapotranspiration (mm a^{-1})	2081	2081	2081
Change in soil water storage (mm a^{-1})	0	0	0
Total sediment yield (ton ha^{-1} a^{-1})	9	5	3

High disparities in spatial patterns of surface runoff and sediment yield within the research area are displayed in Fig. 6.9. The patterns simulated by SWAT are different according to the soil database used in the simulation and reveal impacts of changing HRU patterns (with changing physical properties) as affected by different soil mapping approaches as well as the aggregation of the soil parameters within the mapping units in each sub-catchment.

When analyzing the ranges of the annual spatial patterns according to the different databases (Fig. 6.9), the combined effects of the coarser SOTER map unit and the aggregated soil layers (by aggregating soil properties) are most visible for the surface runoff (varying from 0 to 150 mm/y for SM_VP against 0 to 310 mm/y for OM_RP and SM_RP).

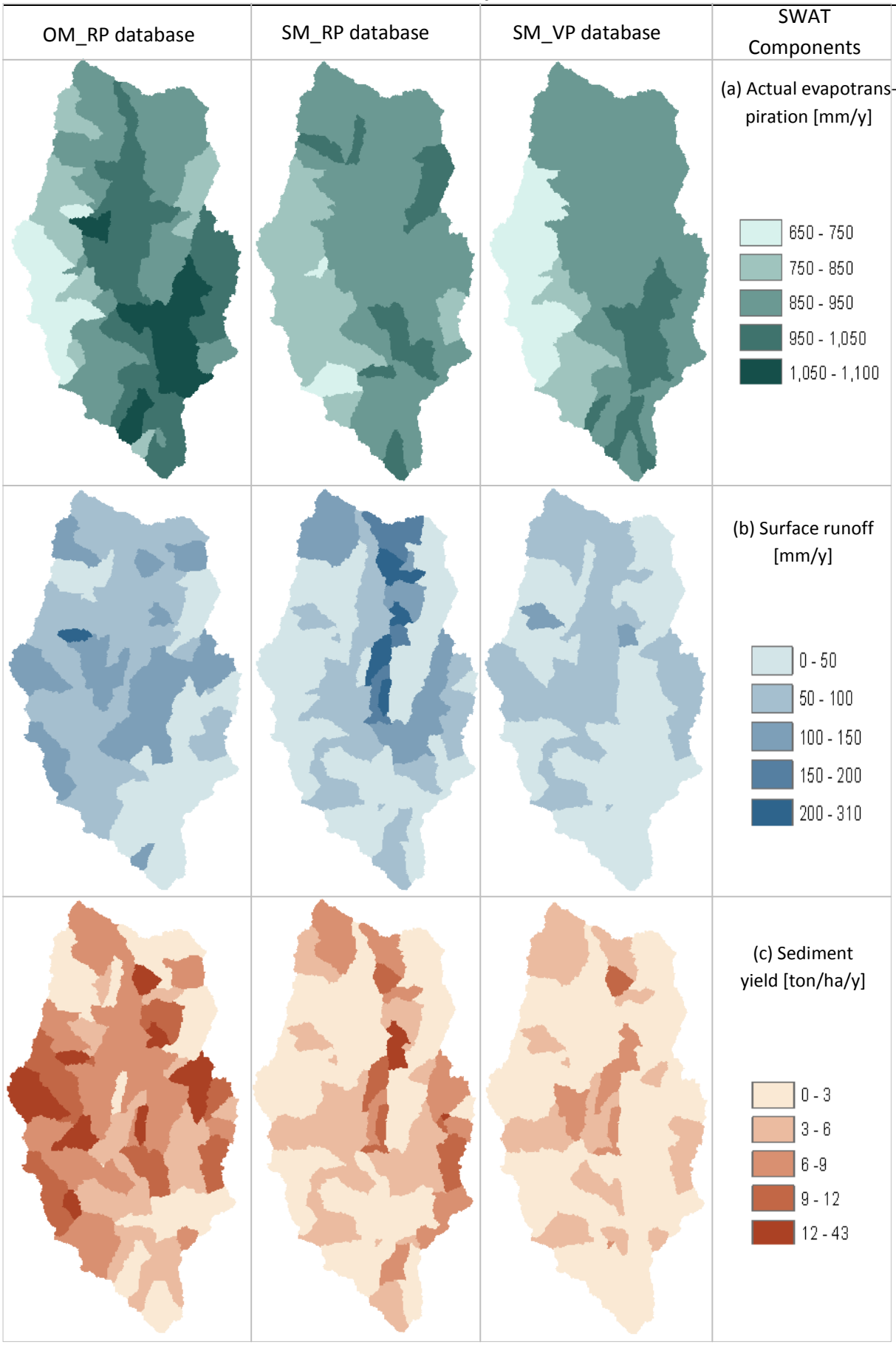

Fig. 6.9. Mean annual values for (a) actual evapotranspiration, (b) surface runoff, and (c) sediment yield for the soil databases OM_RP, SM_RP and SM_VP used in this study. Values are shown for the sub-catchments used in the simulation.

6.3.4. Parameter sensitivities and fitted values

High sensitivities are computed for the curve numbers (CN2) that clearly discriminate the ORSTOM database (OM_RP) from the SOTER database (SM_RP and SM_VP), while all other parameters show a relatively low sensitivity. Tab. 6.6 shows the sensitivity index for the mean squared error of the discharge at the investigated sub-catchment outlet.

Table 6.7 shows the fitted model parameter values for the different soil databases. Important conclusions can be drawn from this table which are primarily related to the values of the curve number (CN2), the soil-available water capacity (SOL_AWC), the saturated soil conductivity (SOL_K), and the soil evaporation compensator factor (ESCO):

(1) Compared to the initial parameterization, the curve number (CN2) decreases for all soil databases in very clear ranges (-13 for the OM_RP, -16 for SM_VP and -8 for the SM_RP). This difference of more than 4 units occurring in the CN2 values for both, the OM_RP and SM_RP database, has no influence on the catchment's annual surface runoff, but significantly changes its patterns. This clearly shows the effects of changes in CN2 value patterns caused by the mapping approach as discussed in the chapter 3.5.

(2) An important difference of more than 7 units is found in the CN2 values when comparing the SM_RP and SM_VP databases. Again, this has no influence on the catchment's annual surface runoff, but has significantly changed its spatial patterns. This is attributed to the combined effects of the soil mapping unit aggregation and the soil parameter aggregation, which cannot clearly be separated at this level.

(3) Contrary to the CN2 values, the soil-available water capacity (SOL_AWC) increases when comparing the SM_RP database with the OM_RP database. This difference is indirectly caused by changes in the HRU patterns (with changed soil water conditions) due to the soil mapping approaches. No clear difference can be identified for the soil available water capacity changes between the SM_RP and SM_VP databases.

(4) In general, the saturated soil conductivity increases for the OM_RP database while it decreases for the SOTER database. This trend is comparable to the available water capacity values found when comparing the OM_RP and SM_RP database. Therefore the interpretation is similar.

(5) The soil evaporation factor ESCO increases between 0.15 (OM_RP) and 0.23 (SM_RP and SM_VP). This indicates once more the effects of modified HRU patterns (changes in soil hydrological properties and changes in soil pore distribution, crusting, and soil cracking patterns) due to the soil mapping approach.

In summary, on the one hand, the trends found in the change of the model parameters (specifically for the CN2 and the ESCO) discriminate clearly the effects of soil mapping approaches from those of mapping unit/parameter aggregation when comparing model results obtained using different databases. On the other hand, while parameters such as the soil available water capacity and the saturated soil conductivity vary similarly for the SOTER databases, the soil evaporation factor minimizes the effects of the aggregation of soil parameter within the mapping units.

Figure 6.10 shows the correlation of the model parameters available water content and soil hydraulic conductivity before and after model calibration. For the OM_RP database, a weak correlation exists within the initial parameterization that also exists after calibration. In contrast, both parameters are strongly correlated in the SM_VP and SM_RP simulations. Although SWAT could be calibrated for the three databases, differences between the soil mapping approaches could not be balanced out.

Tab. 6.6. Sensitivity index SI10 of the model parameters for the mean squared error of daily discharges. CN2: SCS Curve Number; ALPHA_BF: base flow recession constant; GW_DELAY: groundwater delay.

Parameter	Spatial influence	OM_RP		SM_RP		SM_VP	
CN2	HRU scale	0.56	Hi.	0.43	Hi.	0.11	Med.
ALPHA_BF	Catchment scale	0.01	Lo.	0.00	Lo.	0.02	Lo.
GW_DELAY	Catchment scale	0.00	Lo.	0.00	Lo.	0.02	Lo.

Lo. = Low sensitivity (SI < 0.05); Med. = Medium sensitivity (0.05≤ SI < 0.2); Hi. = High sensitivity = (0.2 ≤ SI < 1); Very high sensitivity = (SI ≥ 1).

Tab. 6. 7. Fitted model input parameter values. Shown are the calibrated values, their ranges and the Changing Method (CM); a: initial values were modified by an absolute change (± x units); v: initial values were replaced by a new estimate; r: initial values were modified by a relative change (in %).CN2: SCS Curve Number; SOL_AWC: soil available water capacity, ALPHA_BF: base flow recession constant; SOL_K: soil hydraulic conductivity, RCHRG_DP: aquifer percolation coefficient, GWQMN: minimum water level for base flow generation, GW_REVAP: groundwater re-evaporation rate, REVAPMN: threshold water level in a shallow aquifer for capillary rise, ESCO: Soil evaporation compensation factor, GW_DELAY: groundwater delay. For more details see text.

Parameter	CM (initial range)	OM_RP	SM_RP	SM_VP
		Value (final range)	Value (final range)	Value (final range)
CN2 [-]	a (-10 ..+10)	-12.97 (-14.10..-11.01)	- 8.33 (-9..-7)	-15.89 (-18..-14)
ALPHA_BF [d]	v (+0.03 ..+0.17)	0.16 (+0.158..+0.16)	0.11 (+0.1..+0.12)	0.12 (+0.11..+0.14)
SOL_AWC1 [vol. %]	r (-0.3 ..+0.3)	- 0.18 (-0.29..-0.11)	0.28 (+0.23..+0.3)	0.17 (+0.12..+0.21)
SOL_AWC2 [vol. %]	r (-0.3 ..+0.3)	- 0.33 (-0.42..-0.23)	0.36 (+0.35..+0.47)	- 0.01 (-0.02..0.09)
SOL_AWC3 [vol. %]	r (-0.3 ..+0.3)	- 0.18 (-0.26..-0.10)	0.39 (+0.33..+0.4)	-
SOL_AWC4 [vol. %]	r (-0.3 ..+0.3)	- 0.09 (-0.24..-0.10)	0.39 (+0.34..+0.44)	-
SOL_AWC5 [vol. %]	r (-0.3 ..+0.3)	-	0.34 (+0.33..+0.4)	-
SOL_AWC6 [vol. %]	r (-0.3 ..+0.3)	-	0.31 (+0.3..+0.4)	-
SOL_K1 [mm/h]	r (-0.5 ..+0.5)	0.18 (+0.07..+0.49)	0.31 (+0.29..+0.36)	-0.24 (-0.36..-0.11)
SOL_K2 [mm/h]	r (-0.5 ..+0.5)	0.73 (+0.10..+0.78)	-0.25 (-0.27..-0.2)	-0.24 (-0.32..-0.14)
SOL_K3 [mm/h]	r (-0.5 ..+0.5)	0.30 (+0.22..+0.52)	-0.44 (-0.44..-0.34)	-
SOL_K4 [mm/h]	r (-0.5 ..+0.5)	0.55 (+0.16..+0.6)	-0.04 (-0.12..-0.04)	-
SOL_K5 [mm/h]	r (-0.5 ..+0.5)	-	-0.02 (-0.02..+0.03)	-
SOL_K6 [mm/h]	r (-0.5 ..+0.5)	-	-0.12 (-0.13..-0.04)	-
RCHRG_DP [-]	v (+0.05 ..+0.07)	0.06 (+0.53..+0.067)	0.06 (+0.056..+0.06)	0.06 (+0.05..+0.07)
GWQMN [mm]	v (+10 ..+30)	28.91 (+25..+31.41)	22.84 (+20.5..+25.7)	19.70 (+18.3..+22.3)
GW_REVAP [-]	v (+0.01 ..+0.2)	0.11 (+0.1..+0.13)	0.11 (+0.08..+0.11)	0.15 (+0.1..+0.16)
REVAPMN [mm]	v (+0.01 ..+10)	7.66 (+4.12..+8)	0.96 (+0.32..+2.89)	6.53 (0.18..+0.26)
ESCO [-]	v (+0.01 ..+0.9)	0.15 (+0.062..+0.345)	0.23 (+0.19..+0.26)	0.23 (0.18..+0.26)
GW_DELAY [d]	v (+25 ..+35)	28.99 (28.11..+29.81)	30.87 (30.5..+31.7)	30.14 (+30.6..+31.3)

Many studies demonstrate a strong influence of spatial input data on modeling results (Chaplot, 2005; Zhao et al., 2006; Romanowicz et al., 2005; Chaubey et al., 2005; Thieken et al., 1999; Bormann, 2006). The scale of the database influences spatial variation in the modeling parameters over the sub-catchments and HRUs (Heuvelmans et al., 2004). As previously discussed, threshold concepts are used for determining the number of sub-catchments and HRUs. Therefore, both the scale of the database and the chosen threshold controls how the database is considered in the modeling exercise. For example, Chaplot (2005) analyzed the effect of the DEM and the scale of the soil map on water, nitrogen, and sediment dynamics in a small catchment. He confirmed that with increasingly accurate information, simulation quality increases. Nevertheless, Chaplot (2005) states that changing the spatial patterns of HRUs would probably have changed the results of his study due to the non-linear effect of thresholds on the model's results. To avoid this effect, the same thresholds were considered in this study, when using the different soil databases. Therefore, the changes occurring in the modeling issues (when applying the different databases) are directly related to differences in soil mapping approaches which affect considerably and directly the HRU patterns and indirectly the physical HRU parameters with high impacts on runoff and sediment yield patterns. This proves that not only the database scale affects the modeling issue, but also the mapping approach behind the database.

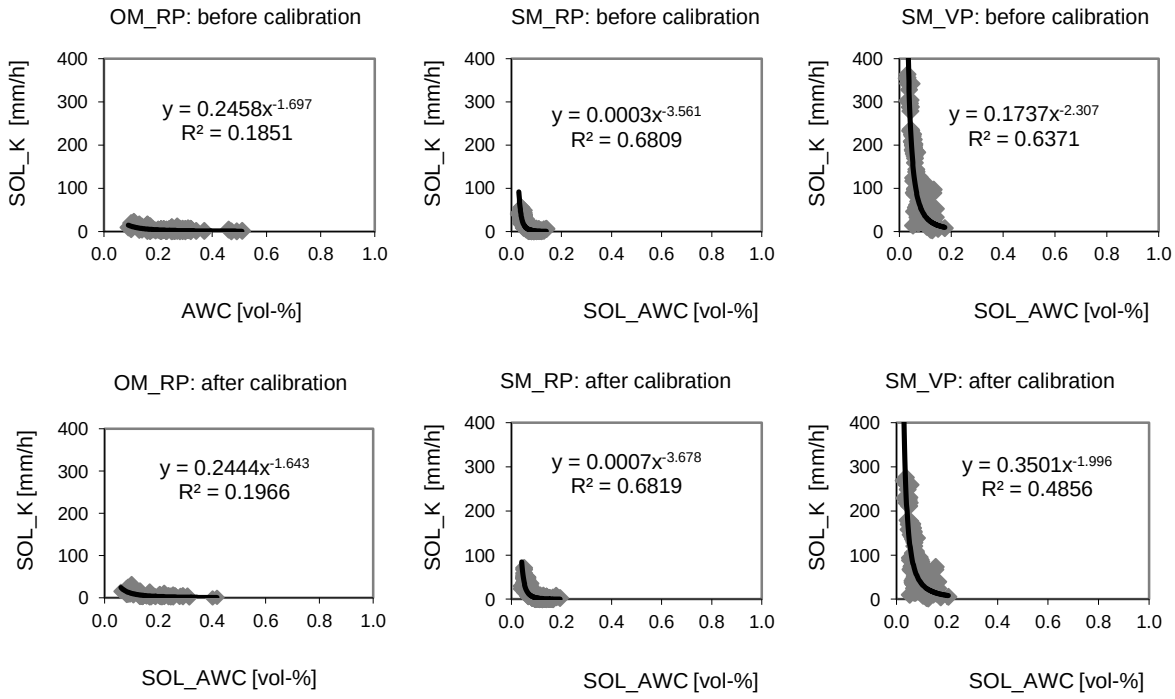

Fig. 6.10. Correlation between soil available water capacity (SOL_AWC) and soil hydraulic conductivity (SOL_K) before and after calibration for the investigated three soil data bases.

6.4. Conclusion

It is well known that the quality of any application of environmental models depends on the underlying database (Bormann et al., 1999). Often, the calibration of model parameters is used to fill data gaps and to reduce the uncertainty of available information. In this study, it was shown that not only the soil parameters themselves are uncertain and produce uncertain model outputs, but also the concept used to develop the soil map. This uncertainty is well known concerning soil maps of different scales (Bormann et al., 1999) but is rarely investigated for the same scale. One of the reasons of the scale dependency of the impact of the soil map on modeling results is that coarsening the soil map usually does not consider their application in environmental modeling, which would require that the aggregation rules depend on the problem to be solved.

In this study, a comprehensive database of physical and hydraulic soil properties was developed for the study region using two different approaches for the soil maps, one of them having been further divided into two differing concepts. Although, from a scientific point of view, the SOTER approach may be more appropriate, this is not necessarily true for its application in environmental modeling. In this study, soil data were used to simulate water fluxes and sediment yield at the regional scale (6980 km^2).

The simulations result in statistical indicators (coefficient of determination, model efficiency, and index of agreement) with an acceptable quality (about 0.70 for discharge) but with a slight underestimation of the total water yield computed for the coarser old SOTER map. With respect to discharge, the calibration balanced out the differences in the databases, and has resulted in significant changes in the model parameters. The validation identified the less coarse new SOTER map as the best (with respect to discharge modeling) used in our study (showing higher model efficiency (0.59), higher coefficient of determination (0.61), and higher index of agreement (0.87)).

Besides the changes in the model parameters, combined effects of the coarser old SOTER map units vs. aggregated soil layers have shown a distinct influence on the simulated lateral subsurface flow and

the spatial pattern of sediment yield within the study area. This leads to the conclusion that the old SOTER map that consists of coarser mapping units and aggregated soil layers cannot be adequately used for the simulation of sediment yield. Model calibration reduces the drawbacks of this approach but does not generally solve the problem. Although the CPCS soil map produces lateral flows comparable to the best approach in this study (less coarse new SOTER), the quality measures are weak. Furthermore, mean annual sediment yield is significantly higher compared to the use of the other two mapping approaches. High disparities in surface runoff, evapotranspiration and sediment yield patterns within the research area were found and reveal impacts of changing hydrology response unit patterns (due to changes in mapping unit patterns) originating from soil mapping approaches as well as the aggregation of the soil parameters within the mapping units. These have shown that SWAT could be calibrated successfully for the three databases regarding the total discharge dynamics, but the spatial patterns of the differences persist. Depending on the modeling issue this may cause a significant bias in the model results.

The study has shown how the soil mapping concepts affect the hydrological modeling. For modeling future development of the Ouémé catchment, this must be taken into account in the uncertainty quantification and focus should be laid on how the concept interacts with the model structural errors. As alternative, the e-SOTER project (Regional pilot platform as European Union contribution to a Global Soil Observing System) was suggested and is tested since 2008. This approach considers new methodologies that combine remote sensing (soil pattern recognition) with the standardization of available soil attributes collected by earlier surveys and high resolution digital elevation models. This is a quite promising perspective for future updating SOTER maps used for modeling studies in the Ouémé catchment.

7. Modeling the effects of crop patterns and management scenarios on N and P loads to surface and groundwater[2]

Abstract

Assessment studies of N and P loads to water systems have developed from simple descriptions based on monitoring and sampling into the analysis of multiple scenarios using simulation models. In this study, water, sediment, and nutrient delivery to the stream flow at the Donga-Pont river catchment outlet (586 km², cf. Fig. 2.5) in the Republic of Benin, West Africa were simulated incorporating local management practices including detailed crop systems, fertilization and manure deposition, using the Soil and Water Assessment Tool (SWAT).
At the study scale (586 km²), cropping systems are not mapped. Therefore, a land use map was refined for the study area, enabling the evaluation of four management scenarios: detailed crop systems with fertilizer supplied only to cotton, rice and maize, as is common in Benin (Sc0); detailed crop systems without the use of fertilizer (Sc0a); the original land use map with similar fertilizer inputs to all cropping systems (Sc1); and the original land use map without fertilizer inputs (Sc1a). Compared to the first scenario, the latter two scenarios, commonly used in regional scale modeling, exhibited distinct biases in plant growth parameters (e.g., water and nitrogen stress days), crop yields, water yield, sediment yield and nitrogen load.
Finally, it was apparent that at the catchment scale, decreases in water yield and nutrient loading were induced by reductions in rainfall (as the result of climate change scenarios), but the effects of the decline in precipitation were counteracted by the effects of changes in land use (land use scenarios). This indicates the strength of the relationship between agriculture and water quality (sediment and nutrient transport) within the Donga-Pont catchment. It was clear that management practices such as fertilizer inputs are among the principal factors controlling this dynamic. Moreover, high spatial variation in the groundwater nitrate concentration, reaching 42 mg/l, was observed.

Keywords: SWAT, management scenarios, land degradation, water quality, climate change, land use change.

7.1. Introduction

Catchment hydrology is affected by vegetation types, soil properties, geology, topography, land use practices, and the spatio-temporal patterns of interactions among these factors (Tomer and Schilling, 2009). Land use practices and climate variables make water erosion and nitrogen and phosphorus losses the primary threats to sustainable agricultural development and to the maintenance of water quality (Vezina and Bonn, 2006). Soil erosion (sediment and nutrient loss) affects soil properties, directly decreasing rooting depths and water storage capacity, and leads to soil compaction, crusting, water-logging and a decrease of biological activity. Harsh climatic conditions, high rainfall intensities, prolonged dry seasons, extensive drought periods, high population growth, and the excessive use of resources have made tropical ecosystems particularly vulnerable to soil erosion and erosion-induced soil degradation (Hiepe, 2008).
Compared to temperate regions, the decline in food productivity is often more drastic in the tropics due to the harsh climate, low soil fertility, and the poor quality of the subsoil or unstable soil properties (Lal, 1990; Steiner, 1994; Hiepe, 2008). For instance, in the center of Benin, the average crop yield for maize has decreased to 550 kg ha^{-1} (compared to approximately 10 tons ha^{-1} in Europe

[2] Published as: Bossa, A.Y., Diekkrüger, B., Giertz, S., Steup, G., Sintondji, L.O., Agbossou, E.K., Hiepe, C., 2012. Modeling the effects of changing crop patterns and management practices on N and P loads to surface water and groundwater in a semi-humid catchment (West Africa). Agricultural Water Management 115, 20-37.

and the USA) despite the residual effects of cotton fertilizer (Igué, 2000). In many tropical soils, fertility is restricted to the organic matter in the topsoil, which declines about five times faster than in temperate regions because the dominant clay mineral, kaolinite, has a very low potential cation exchange capacity (Ahn 1970; Steiner, 1994; Hiepe, 2008). The farming systems have shifted in response, from maize/yam-based systems to maize/cassava-based systems and then to groundnut or beans when the soils become poorer. Fallowing (the primary management practice used to restore soil fertility in the region) periods are becoming shorter, there is more pressure on marginal lands, and agriculture is becoming progressively more intensive. Fertilizer use is increasing because experiments in Benin have demonstrated that an application of mineral N, P, K (90, 39, 75 kg ha^{-1} a^{-1}) outyielded all other soil fertility maintenance strategies on Acrisols and Luvisols (widespread soils) by approximately 1 ton ha^{-1} (Akondé, 1995; Agbo, 1999; Igué, 2000). Additionally, high yielding crop varieties are often introduced to reach a stable yield of 2 tons ha^{-1}, regardless of the degree of degradation at a specific site or the sustainability of the management practices. According to the Regional Center for Agriculture Promotion (CeRPA) in the north of Benin, an average of 100 to 250 kg ha^{-1} of fertilizer (NPK + Urea) is applied for cotton, rice and maize, primarily on Acrisols, Lixisols and Luvisols. In contrast, according to the online World Bank database, total fertilizer consumptions of 103 kg ha^{-1} a^{-1} for the USA, 160 kg ha^{-1} a^{-1} for Germany and 468 kg ha^{-1} for China were recorded for the year 2008.

High fertilizer inputs (without any associated structural or organic technologies), monoculture cultivation, uncontrolled agricultural land expansion and the traditional bush fire practices common in Benin are likely to be indirectly damaging water resources and ecosystems in the region by influencing the intensity of pollutant particle loads. The Natural Resources Management and Environment Department of the Food and Agriculture Organization (FAO, 1996) stated that pollution by sediments has two major dimensions: (1) the physical dimension—topsoil loss and land degradation due to gully and sheet erosion, which leads to high levels of turbidity in receiving waters and to off-site ecological and physical impacts from deposition into river and lake beds and (2) the chemical dimension—the silt and clay fraction (<63 µm fraction) is a primary carrier of adsorbed chemicals, especially nitrogen, phosphorus, chlorinated pesticides and most metals, which are transported by the sediment into the aquatic system, where they may cause damage.

Reducing water and soil degradation requires knowledge of the processes and sources of diffuse pollution at the local and regional scales, as well as an assessment of the long-term potential environmental impacts. Fohrer et al. (2005) stated that the application of hydrological models can clarify the processes involved and support well-balanced management decisions. This has helped several European countries to develop environmental regulations and new agricultural policies to mitigate the negative impacts of diffuse source pollution and protect stream habitats from eutrophication (Lam et al., 2010).

Previous investigations and integrated modeling studies in West Africa, including those of the IMPETUS Project (Speth et al., 2010) in Benin (in the upper Ouémé catchment), have contributed to improving knowledge of the degradation processes at the local to regional scales. Sediment load rates greater than 3 ton ha^{-1} in agricultural lands were measured and simulated. Land use and climate change impacts (Thamm et al. 2005; Judex, 2008; Paeth et al., 2005) have been estimated to contribute in the range of -4 to 25% to the observed sediment yield (Hiepe, 2008). Future investigations, including the current work, are expected to take into account the chemical dimension of erosion-related degradation.

Numerous ecohydrological simulation models have been developed within recent decades to develop the best management scenarios, which is essential for decision support. The Soil and Water Assessment Tool (SWAT) (Arnold et al., 1998) is a conceptual, continuous time model that was developed in the early 1990s to assist water resource managers in assessing the impacts of management and climate on water supplies and non-point source pollution in catchments and large river systems (Arnold and Fohrer, 2005). SWAT was found to meet the requirements of the European Union Water Framework Directive, as reported by Pohlert et al. (2005).

The SWAT model is applied in the current work to simulate the physical and chemical degradation of land and water at the field scale in a meso-scale catchment (Donga-Pont catchment—586 km²; cf. Fig. 1). As has been established, one prerequisite for making full use of distributed physical-based models is the existence and easy accessibility of a large amount of data, including detailed spatial information on natural parameters such as geology, soil, vegetation and man-made impacts such as water abstractions, agricultural practices and discharges of pollutants (Sintondji, 2005). Many studies demonstrate the strong influence of the scale of available input data on modeling results (Zhao et al., 2006; Romanowicz et al., 2005; Chaubey et al., 2005; Thieken et al., 1999; Bormann, 2006). The scale of the available data influences the spatial variation in the modeling parameters among the sub-catchments (Heuvelmans et al., 2004). For example, Chaplot (2005) analyzed the effects of DEM and the soil map scale on sediment and nitrogen dynamics in a small catchment and confirmed that with increasingly accurate information, the simulation quality increases. The resolution of land use data was also shown to greatly affect the modeled sediment and nitrogen dynamics. For example, Brown et al. (1993) indicated that predictions using the ANSWERS model exhibited drift anomalies at land use map resolutions greater than 120 m. In this study, agricultural lands in the available land use map were refined into different cropping systems to more accurately assess sediment and nutrient dynamics at the scale of the Donga-Pont catchment.
This current research specifically aims to (1) assess the impacts of crop and fertilizer patterns on simulated plant growth; (2) provide insight into the physical and chemical pollution of surface water and groundwater in relation to management practices, including fertilizer use; and (3) quantify the effects of future global change on soil and water degradation. These types of information are required for supporting well-balanced management decisions to preserve the long-term fertility of the soil and the health of the population and the environment.

7.2. Materials and methods

The location of the Donga-Pont sub-catchment is shown in the Fig. 2.5 in the chapter 2. Detailed descriptions of SWAT model components including soil loss, nutrient transport as well as water quality components are provided in the chapter 4. Input data such as soil, land use, and climate are described in the chapter 2. Calibration and validation data such as discharge and sediment- nutrient concentrations are described in the chapter 5.
At the considered catchment scale, cropping systems are not reflected in the available land use map derived from LANDSAT ETM+ satellite images from 2003. Within SWAT, the term "Agricultural Land Generic (AGRL)“ is used to refer to all crops with similar physical and physiological characteristics without considering individual characteristics or fertilizer demand. Although often used for simulating a mean behavior of all crops, strong differences in the crop calendar and fertilizer demand between the crop types are ignored. This may lead to simplifications in the application of the model, which risks causing a bias in the results. To quantify the bias in the modeling results, the available land use map has been refined, allowing the evaluation of four modeling scenarios (Tab. 3):

1) **Sc0** - agricultural lands (AGRL) were refined into 12 cropping systems with mineral fertilizer supply only to cotton, rice and maize, as is common in Benin. Grazing (manure deposition) is considered;
2) **Sc1** - agricultural lands (AGRL) were not refined, but it was assumed that all crops receive fertilizer inputs similar to the total fertilizer amount applied in Sc0 divided by the total agricultural area. Grazing (manure deposition) is also considered;
3) **Sc0a** - considers Sc0 without fertilization and grazing operations; and
4) **Sc1a** - considers Sc1 without fertilization and grazing operations.

As they are common in Benin, the fertilizers (Tab. 7.2) NPKSB, Urea, and P_2O_5 were specified in this study. Many other variables were specified: (1) the N and P element fractions of the total fertilizer applied to the soil surface, (2) the heat unit fraction for management operations, (3) tillage depth, (4) the mixing efficiency, (5) the burning fraction of biomass, (6) the number of grazing days, (7) the

biomass eaten and manure deposited, etc. Heat unit may be defined as the accumulated number of daily temperature degrees above a certain threshold base temperature (needed to reach plant maturity), which varies among crop species. The mixing efficiency of the tillage implement defines the fraction of the residue, nutrients, and bacteria pool in each soil layer that is redistributed through the depth of soil that is mixed by the implement.

Tab. 7.1. Descriptions of modeling scenarios Sc0 and Sc1. Crop system scale: whereas Sc0 includes a set fertilizer amount for only cotton, maize and rice, Sc1 divides the total amount applied in Sc0 over the total agricultural area. Catchment scale: the total amount of fertilizer applied at the crop scale is extrapolated to the whole catchment area. AGRL means agricultural lands, a common term with no distinction among crop systems.

				At the crop system scale		At the catchment scale	
Scenario	Crop	Cropland (ha)	Cropland (%)	N (kg/ha)	P (kg/ha)	N (kg/ha)	P (kg/ha)
Sc0	Peanut	3185	11			10	3
	Cotton	1448	5	51	20		
	Cowpeas	2027	7				
	Yam	6080	21				
	Maize	6659	23	60	18		
	Cassava	2027	7				
	Sweet potato	290	1				
	Pear Millet	1158	4				
	Rice	1158	4	106	18		
	Sorgho	4053	14				
	Tomato	290	1				
	Bambara Groundnut	579	2				
Sc1	AGRL	28952	100	21	6	10	3

Tab. 7.2. Management operations scheduled for cotton, maize and rice. T1, T2 and T3: tillage operations; F1, F2 and F3: fertilization; PlB: beginning of plant growth; Hk: harvest; E: end of the growing season; Bu: burning. NPKSB: nitrogen-phosphorus-potassium-sulfur-boron

Parameter (Cotton)	T1	PlB	F1	T2	T3	F2	HK	Bu
Heat unit fraction	0.00	0.15	0.16	0.20	0.35	0.36	1.2	1.36
NPKSB (14%N-10%P) (kg ha^{-1})			200 (28-20)					
Urea (46%N) (kg ha^{-1})						50 (23)		
Tillage depth (cm)	25			10	10			
Mixing efficiency	0.5			0.25	0.25			
Burning fraction of residual biomass								0.7

Parameter (Maize)	T1	PlB	T2	T3	F1	F2	F3	HK	Bu
Heat unit fraction	0.00	0.15	0.18	0.34	0.35	0.35	0.66	1.2	1.5
P_2O_5 (44%P) (kg ha^{-1})						40 (18)			
Urea (46%N) (kg ha^{-1})					65 (30)		65 (30)		
Tillage depth (cm)	25		10	10					
Mixing efficiency	0.5		0.25	0.25					
Burning fraction of residual biomass									0.6

Parameter (Rice)	T1	PlB	T2	F1	T3	F2	F3	HK	Bu
Heat unit fraction	0.00	0.15	0.18	0.19	0.43	0.44	0.75	1.2	1.5
P_2O_5 (44%P) (kg ha^{-1})						40 (18)			
Urea (46%N) (kg ha^{-1})				130 (60)			100 (46)		
Tillage depth (cm)	25		10		10				
Mixing efficiency	0.5		0.25		0.25				
Burning fraction of residual biomass									0.8

Parameter (Pasture)	PlB	Grazing	E	Bu
Heat unit fraction	0.15	0.2 --	1.2	1.6
Grazing days		300		
Biomass eaten: beef/dairy - sheep - goat (kg ha^{-1} d^{-1})		76 - 24 - 28		
Biomass trampled: beef/dairy - sheep - goat (kg ha^{-1} d^{-1})		15 - 5 - 6		
Cattle manure (1%N-0.4%P-3%ORGN-0.7%ORGP-95%NH3N) (kg ha^{-1} d^{-1})		38		
Sheep manure (1%N-0.4%P-3%ORGN-0.7%ORGP-95%NH3N) (kg ha^{-1} d^{-1})		12		
Goat manure (1%N-0.4%P-3%ORGN-0.7%ORGP-95%NH3N) (kg ha^{-1} d^{-1})		64		
Burning fraction of biomass				0.1

7.3. Results and discussion

7.3.1. Water dynamics and water balance

Fig. 7.1 shows the simulated daily discharges for the model calibration (2006 – 2008) and validation (2001 – 2005) periods at the Donga-Pont catchment outlet. The measures of the quality of model fit to the daily measured discharges show satisfactory values. The model efficiency (ME) and the coefficient of determination (R^2) are 0.68 and 0.67, respectively, for the calibration period and 0.58 and 0.51, respectively, for the validation period. This relatively low quality measure for the fit of the model to the daily measurements was partly caused by the auto-calibration, which considered sediments and nutrients together simultaneously with discharge. Separate calibration significantly improved ME and R^2 up to 0.75, but did not produce in an appropriate result for the nutrient processes.

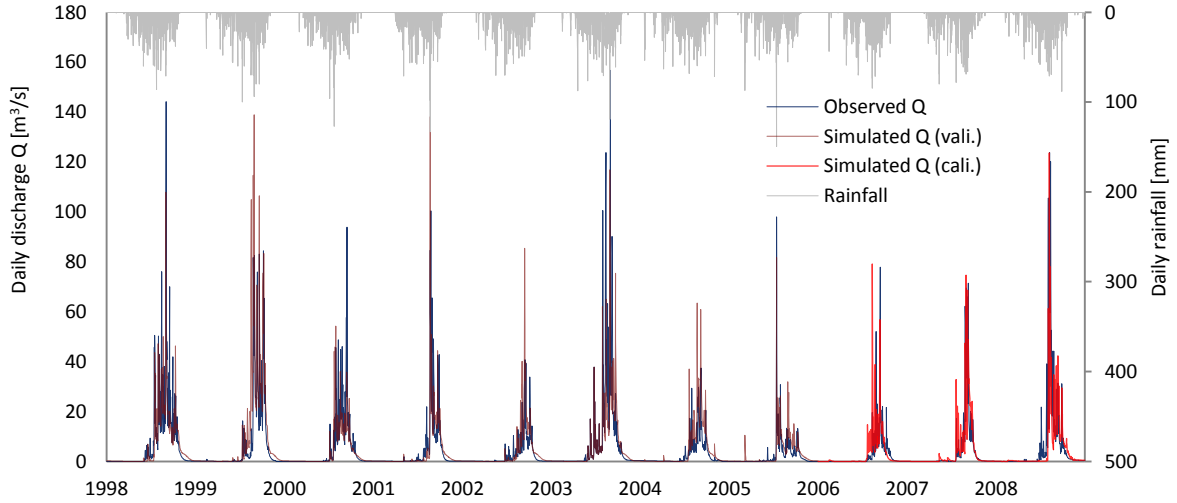

Fig. 7.1. Simulated vs. observed discharge at the catchment outlet: calibration period 2006 – 2008, validation period 2001 – 2005; modeling scenario Sc0. The model efficiency (ME) and the coefficient of determination (R^2) are 0.68 and 0.67, respectively for the calibration period and 0.58 and 0.51, respectively for the validation period.

Less accurate predictions of single peaks are also shown over the validation period, partly due to the measurement errors during periods of exceptional flooding in the years 1999 and 2003, in which full discharge over the bank was observed at the gauging station. Differences are also caused by the SWAT structure because it is a continuous time model with a daily time step, and subscale processes such as single-event flood routing cannot be efficiently predicted. In addition, the daily measured precipitation for 24 h starts at 6:00 am and may not match well to the daily average discharge values, which were measured for 24 h beginning at midnight (Lam et al., 2010).
Stream flow recessions were reproduced satisfactorily, demonstrating the model's ability to effectively reproduce the catchment's groundwater flow. Tab. 5 shows the simulated water balance components for the scenario Sc0 over the calibrated period (2006 - 2008).

Tab. 7.3. Simulated water balance components for the scenario Sc0 over the calibrated period (2006 - 2008).

Water balance components	Scenario Sc0 (mean values from 2006 to 2008)
Precipitation (mm a^{-1})	1211.3
Surface runoff (mm a^{-1})	147.2
Groundwater flow (mm a^{-1})	96.1
Groundwater uptake (to soil/plants) (mm a^{-1})	61.6
Deep aquifer recharge (mm a^{-1})	29.6
Total water yield (mm a^{-1})	245.6
Actual evapotranspiration (mm a^{-1})	874.3

7.3.2. Sediment dynamics

Sediment load dynamics are presented in Fig. 7.2 at a daily time scale, where the simulated results were compared with measurements at the catchment outlet for both the calibration and the validation period. Good agreements concerning quality assessment were obtained with a model efficiency (and a coefficient of determination) of 0.67 (0.69) for the calibration period (2008) and 0.55 (0.58) for the validation period (2005).

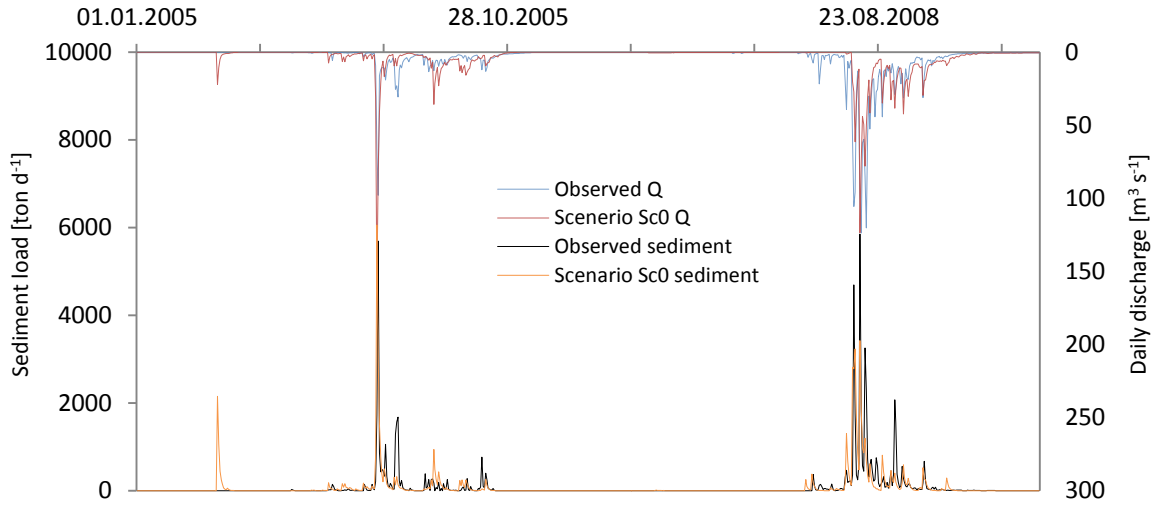

Fig. 7.2. Simulated vs. observed sediment yields at the catchment outlet for modeling scenario Sc0: calibration period 2008, validation period 2005. Model efficiency (and a coefficient of determination) of 0.67 (0.69) for the calibration period (2008) and 0.55 (0.58) for the validation period (2005). Data for 2005 were collected by Hiepe (2008).

Measured and simulated sediment peaks accompany runoff peaks and reach a daily maximum of 6,000 tons at the catchment outlet compared to the annual total of approximately 40,000 tons. This indicates the important role of single runoff events for sediment delivery to the catchment outlet and leads to the conclusion that poor simulations of runoff peaks will result in a significant bias in the annual sediment yield. This was particularly difficult to balance in the calibration, as discharge, sediment and nitrate were simultaneously calibrated with an underestimation of the calibration year (2008) and an overestimation of the validation year (2005). Overall, good agreements of the model fit to the measurements were obtained, although mean deviations of ±14% were observed for both the calibration and validation periods compared to the measurements.

7.3.3. Nitrate dynamics

The nitrate dynamics for single days of the calibration and validation periods are presented in Fig. 7.3. Disturbances of the measurements at the catchment gauging station in the year 2009 due to construction activity inhibited further validation. Therefore, validation was performed by comparing the model results with measurements at the Bétérou gauging station downstream (cf. Fig. 2.5, catchment size 10,072 km^2). Good agreements concerning the model fit to the measurements were obtained, with a model efficiency (and a coefficient of determination) of 0.99 (0.99) for the calibration period (2008) and 0.78 (0.95) for the validation period (2008 - 2009).
Tab. 6 presents the correspondence between measurements in mg/l and estimated loads in kg. As can be seen from this table, the minimum and the mean observed values of the nitrate concentration are close, but significantly different for the corresponding load values. This is caused by the difference in the daily water volume that transports the nitrate, which indicates once more the important role of daily runoff events in nitrate loss processes.

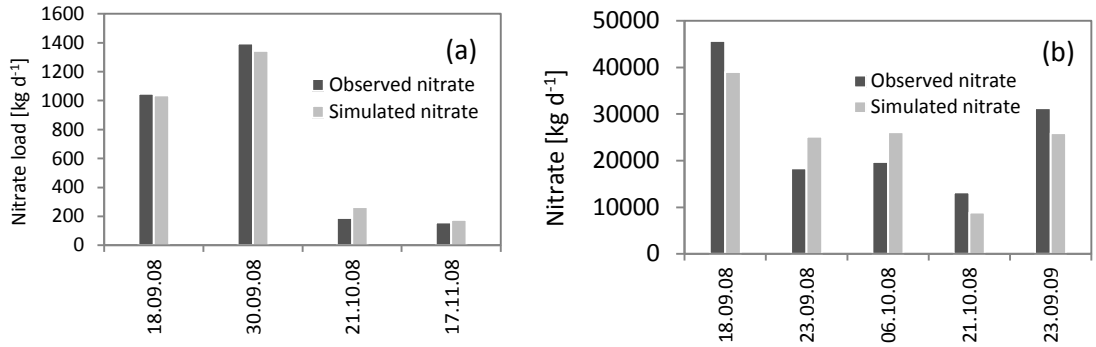

Fig. 7.3. Simulated vs. observed nitrate yields at the catchment outlet for modeling scenario Sc0: (a) calibration period 2008, (b) spatial validation period 2008 – 2009 (at Bétérou outlet, cf. Fig. 2.5). Model efficiency (and a coefficient of determination) of 0.99 (0.99) for the calibration period (2008) and 0.78 (0.95) for the validation period (2008 - 2009).

Tab. 7.4. Correspondence between daily nitrate concentrations and nitrate loads (observed and simulated) at the Donga-Pont gauging station.

	Observed nitrate		Simulated nitrate	
	Concentration [mg/l]	Load [kg]	Concentration [mg/l]	Load [kg]
Mean	1.95	698	1.97	705
Maximum	3.02	1396	2.91	1344
Minimum	1.28	159	1.41	175

7.3.4. Organic N and P load

As explained above, pollution by sediment has two major dimensions: (1) the physical dimension—top soil loss and land degradation by erosion, which leads both to excessive levels of turbidity in receiving waters and to off-site ecological and physical impacts from deposition in river and lake beds, and (2) the chemical dimension—the silt and clay fraction, the primary carrier of adsorbed chemicals such as nitrogen and phosphorus, which are transported by sediment into the aquatic system. Fig. 7.4 and 7.5 show the weekly simulated versus observed sediment and associated organic N and P deliveries at the catchment gauging station. Organic N and P are not calibrated. Because it was assumed that a good adjustment of the soil nutrient pools would be reflected in their simulations, only a validation was performed.

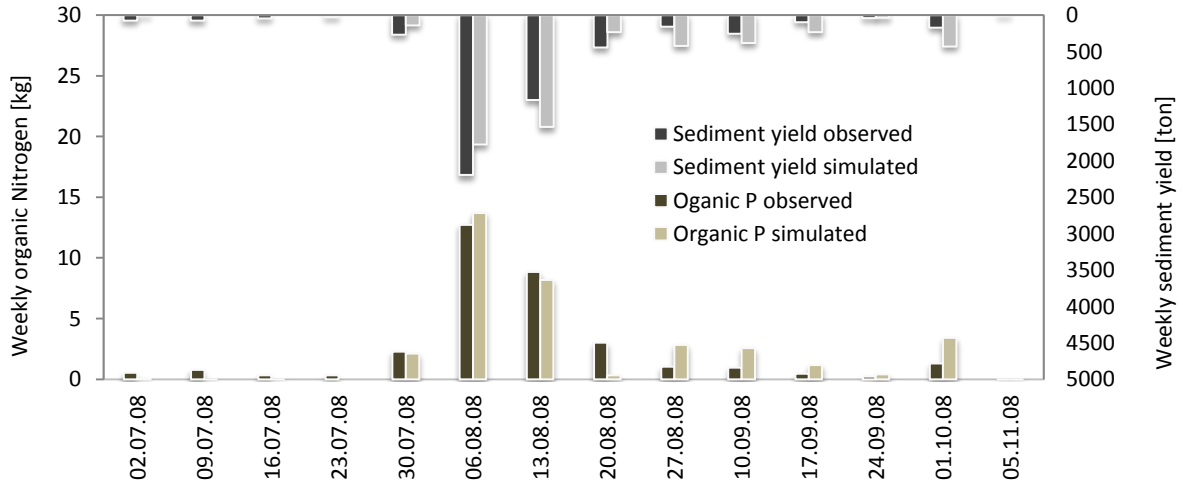

Fig. 7.4. Simulated vs. observed organic phosphorus and sediment yield at the Donga-Pont sub-catchment outlet for modeling scenario Sc0 (validation); model efficiency (and coefficient of determination) of 0.99 (0.89) for the organic P and 0.89 (0.88) for the sediment yield.

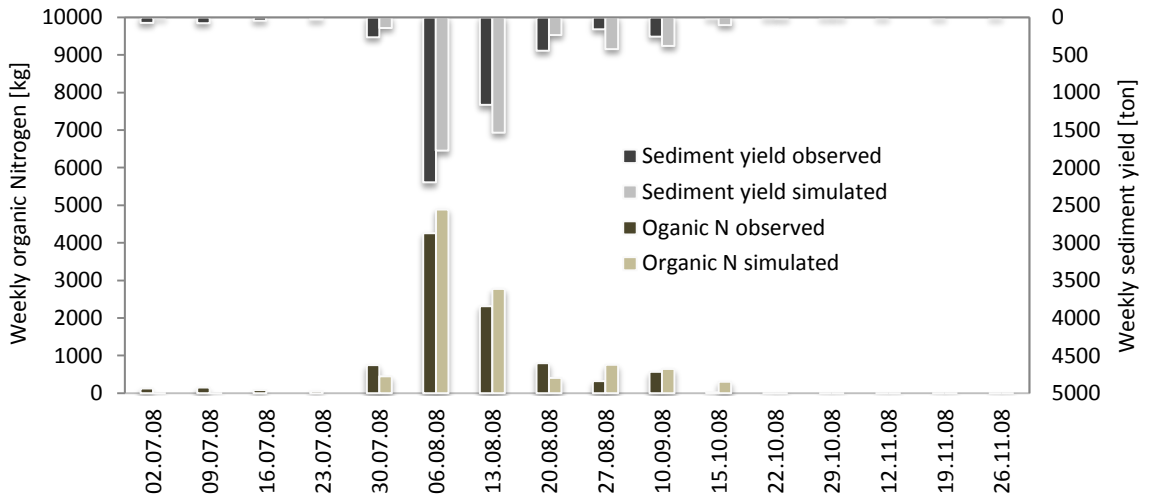

Fig. 7.5. Simulated vs. observed organic nitrogen and sediment yields at the Donga-Pont sub-catchment outlet for the modeling scenario Sc0 (validation). Model efficiency (and coefficient of determination) of 0.95 (0.97) for organic N and 0.91 (0.91) for the sediment yield.

As concluded for the delivery of sediment to the catchment outlet, a poor simulation of runoff peaks will result in a significant bias in the annual nutrient yield. The dynamics of organic nitrogen loss from the soil are important, with a maximum weekly loss of more than 4 tons, in contrast with the relatively insignificant loss of organic phosphorus, which exhibited a maximum weekly loss of 13 kg for the entire catchment.

7.3.5. Effects of management scenarios

Calibration was performed only for scenario Sc0, and the calibrated parameters were directly used for scenarios Sc0a, Sc1 and Sc1a. As can be seen from Tab. 7.5, the water yield, sediment yield and N dynamics are well simulated considering the reference scenario Sc0. The common simplification scenarios (scenarios Sc1 and Sc1a) lead to a distinct bias in the water, sediment and nutrient yields as well as the biomass production, crop yield and related measures such as the days with water and nitrogen stress (Fig. 7.6 and 7.7). This must be considered when SWAT is calibrated at the catchment scale, ignoring local-scale differences in land use and fertilizer application.
For reference scenario Sc0 with a fertilization rate (mineral N) of 10 kg ha^{-1} a^{-1}, nitrate loads to surface and ground-water were simulated as 0.6 kg ha^{-1} a^{-1} (35 ton a^{-1} for the whole catchment) and 7 kg ha^{-1} a^{-1} (410 ton a^{-1}), respectively. The silt and clay particle load totaled 0.5 ton ha^{-1} a^{-1} (29,300 ton a^{-1}) with an associated organic nitrogen load of 0.8 kg ha^{-1} a^{-1} (88 ton a^{-1}). These values clearly indicate that the study area is impacted by land and water degradation processes, defined as human-induced or natural processes that negatively affect terrestrial ecosystem services such as the taking up, storing and recycling of water, energy, and nutrients. The direct effects of such degradation are threats to food security and social development and damage to biodiversity and ecosystems.

Tab. 7.5. Effects of crop patterns and management on the simulations for the period 2006 to 2008.

Water balance components and sediment loading	Sc0	Sc0a	Sc1	Sc1a
Precipitation (mm a^{-1})	1211.3	1211.3	1211.3	1211.3
Surface runoff (mm a^{-1})	147.2	156.8	142.42	139.7
Groundwater flow (mm a^{-1})	96.1	86.7	98.82	73.7
Groundwater uptake (to soil/plants) (mm a^{-1})	61.6	144.9	38.51	70.4
Deep aquifer recharge (mm a^{-1})	29.6	43.2	25.18	26.7
Total water yield (mm a^{-1})	245.6	245.3	243.3	215.3
Actual evapotranspiration (mm a^{-1})	874.3	774	898.3	898.7
Total sediment loading (ton ha^{-1} a^{-1})	0.5	0.6	0.4	0.8

Nutrient transport rates	Sc0	Sc0a	Sc1	Sc1a
Organic N loading (kg ha^{-1} a^{-1})	0.8	1	0.7	1.1
NO_3 yield in surface flow (kg ha^{-1} a^{-1})	0.6	0.4	0.2	0.2
NO_3 leached to shallow aquifer (kg ha^{-1} a^{-1})	7	4	4.1	3.6
NO_3 yield in baseflow (kg ha^{-1} a^{-1})	2.8	1	1.9	1.4
Soluble P yield in surface flow (kg ha^{-1} a^{-1})	0.2	0.1	0.2	0
Soluble P yield leached (kg ha^{-1} a^{-1})	1.8	0.5	1.5	0.5
Organic P loading (kg ha^{-1} a^{-1})	0	0	0	0

Plant growth output parameters	Sc0	Sc0a	Sc1	Sc1a
Final N fertilizer (kg ha^{-1} a^{-1})	10.4	0	10.6	0
Final P fertilizer (kg ha^{-1} a^{-1})	3	0	3	0
Biomass (ton ha^{-1} a^{-1})	6.7	5	3.9	2.1
Yield (ton ha^{-1} a^{-1})	1	0.5	0.7	0.1
Nitrogen stress (d a^{-1})	42	50	49	58
Water stress (d a^{-1})	38	43	31	30
Temperature stress (d a^{-1})	12	12	4	4

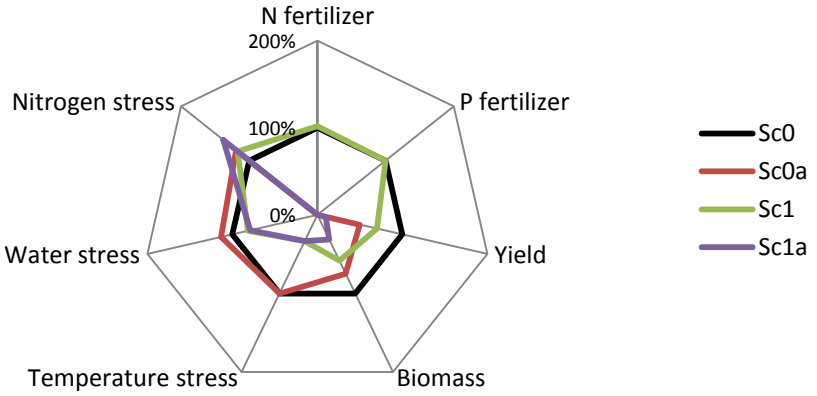

Fig. 7.6. Comparison of plant growth characteristics for the modeling scenarios

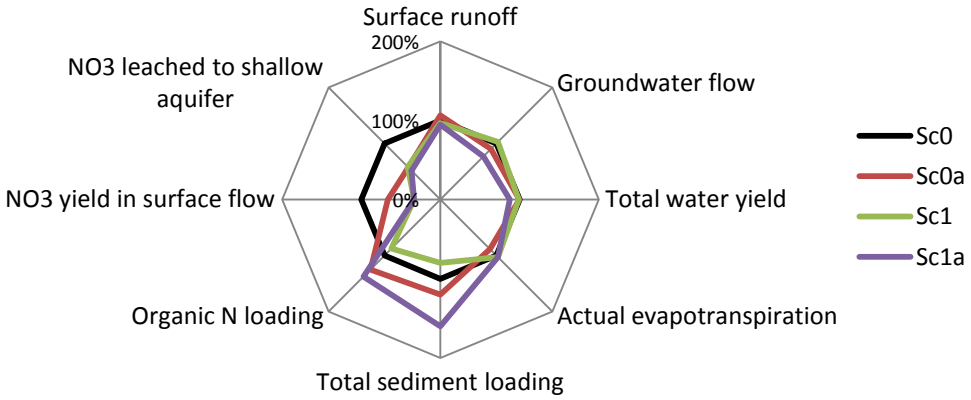

Fig. 7.7. Water balance and nutrient load water systems according to the modeling scenarios.

Groundwater supplies the majority of the water used in households in the Donga-Pont catchment area as well as the municipal drinking water (Kamagaté, 2006). It is important not only for these beneficial uses but also because it provides recharge water to streams, rivers, lakes and wetlands, and any degradation in a given area will automatically affect the area ecosystems.

The simulation results (Sc0, 2006–2008) show that nitrate was contributed to the groundwater via percolation (an annual average of 7 kg ha^{-1}). The daily concentration of nitrate in base flow (from the shallow aquifers) averages 1.4 mg/l compared to a maximum of 9.1 mg/l for the catchment as a whole. This is likely to result in high spatial variation (cf. Tab. 7.6 and Fig. 7.8) within the catchment aquifer systems, which may involve risks for the population, primarily those using private wells without periodic quality tests. Tab. 7.6 and Fig. 7.8 show the results of the groundwater quality investigation conducted within the research area from 2002 to 2010 (available from the Integrated Data Bank of the General Directorate of Water of Benin), comprising 49 drillings. An average of 6.99 mg/l, a maximum of 42.24 mg/l and a minimum of 0.44 mg/l were recorded for the nitrate concentration. Although the mean value is comparable to those simulated in this study, the high spatial variation of the nitrate load of ground water is confirmed. Obviously, agricultural land management is the primary driver of this issue, which should lead to strict regulation policies. The lack of regulation policies, as observed today, will simply lead to limitations to resource accessibility and even the closing of many already-used drillings in the future. The U.S. Environmental Protection Agency (USEPA) has established a federal drinking water standard MCL (maximum contaminant level) of 10 mg/l for nitrate-nitrogen (an equivalent of 45 mg/l of nitrate) because it was proven that exposure to nitrate in concentrations over the MCL is associated with a condition called methemoglobenemia or "blue-baby syndrome" in infants six months of age and younger (USEPA, 1990). However, the maximum contamination level for nitrates in drinking water recommended by the World Health Organization (WHO, 2008) and relayed by the Food and Agriculture Organization (FAO, 2011) is 50 mg/l, which is higher than the US federal drinking water standard.

Tab. 7.6. Observed water quality parameters of 49 drillings within the study area (2002-2010). Data available from the Integrated Data Bank of the General Directorate of Water of Benin.

	Mean value	Maximum	Mean deviation
Nitrate NO_3- [mg/l]	6.99	42.24	4.63
Ammonium NH_4^+ [mg/l]	0.07	2.3	0.05
Phosphate PO_4 [mg/l]	0.7	3.1	0.3
pH	7.16	8.5	0.6
Conductivity [µs/cm]	305	1079	104

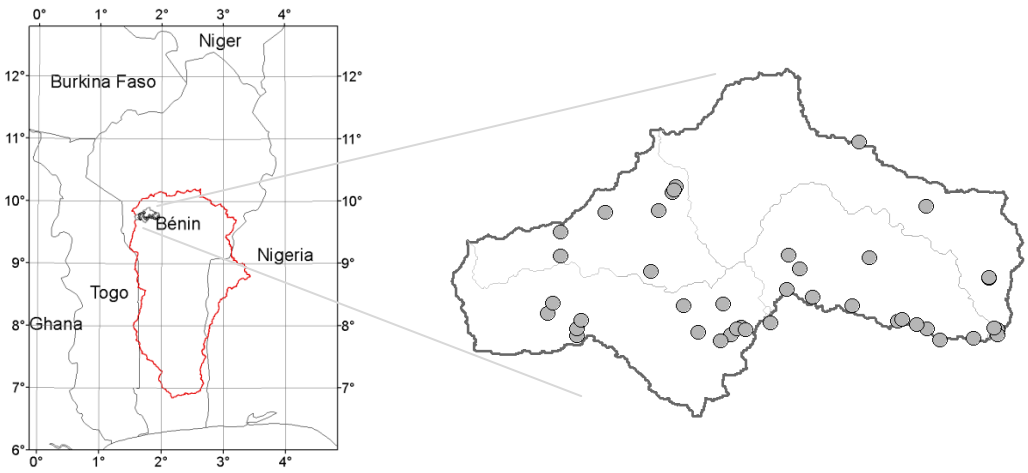

Fig. 7.8. Drilling locations (49) within the Donga-Pont sub-catchment. Information available from the Integrated Data Bank of the General Directorate of Water of Benin.

7.3.6. Effects of climate and land use change

To clarify the relationship between agricultural practices, primarily fertilizer use, and land and water degradation within the catchment, the climate change scenarios (A1B and B1) and the land use change scenarios (La and Lb) described in the chapter 5 were used to evaluate potential changes in renewable water resources as well as sediment and nutrient transport to the catchment gauging station.
Potential changes in the model results in accordance with the climate and land use change scenarios were calculated in reference to modeling scenario Sc1, considered a baseline, given the fact that the land use scenario maps do not consider future changes in cropping systems.

Climate scenarios
The effects of the climate change scenarios (from 2010 to 2029), are summarized in Tab. 7.7. Similar to the trend observed for the climate change scenarios, a reduction in rainfall will cause reductions in surface runoff, sediment and related organic nitrogen losses, and nitrate loads to the surface and groundwater at the watershed outlet. Especially for the period 2010-2014, the water balance components and sediment, nitrate, and organic N loads to surface runoff increased by up to 50%. Notably, severe flooding events that involve material and financial damages to the population, as occurred in the year 2010, remain relevant for this period.

Tab. 7.7. Changes in water balance, sediment yield, nutrient yield, and plant growth parameters according to climate scenarios A1B and B1 and management scenario Sc1. Deviations from the reference scenario (2000-2009) are shown in brackets.

		A1B		B1		A1B		B1	
	Reference	[2010-2014]		[2010-2014]		[2025-2029]		[2025-2029]	
Rainfall (mm a^{-1})	1233.4	1296	(5.1)	1177	(-4.6)	1116	(-9.5)	1138	(-7.7)
Water yield (mm a^{-1})	242.7	358.7	(47.8)	261	(7.5)	206	(-15.3)	225	(-7.2)
Groundwater flow (mm a^{-1})	106	146.5	(38.2)	110	(4.0)	91.6	(-13.6)	101	(-5.2)
Surface runoff (mm a^{-1})	135.7	210.8	(55.3)	149	(10.0)	113	(-17.0)	123	(-9.1)
Evapotranspiration (mm a^{-1})	927.3	842.6	(-9.1)	848	(-8.6)	864	(-6.9)	854	(-7.9)
Sediment yield (ton ha^{-1} a^{-1})	0.4	0.6	(50.0)	0.5	(25.0)	0.4	(0.0)	0.4	(0)
Organic N load (kg ha^{-1} a^{-1})	0.7	1	(42.9)	0.8	(14.3)	0.6	(-14.3)	0.7	(0)
NO_3 in surface runoff (kg ha^{-1} a^{-1})	0.2	0.3	(50.0)	0.2	(0.0)	0.2	(0.0)	0.2	(0)
NO_3 in groundwater flow (kg ha^{-1} a^{-1})	1.6	1.6	(0.0)	1.5	(-6.3)	1.2	(-25.0)	1.2	(-25)
Leached nitrate (kg ha^{-1} a^{-1})	3.3	3.3	(0.0)	3.2	(-3.0)	2.6	(-21.2)	2.6	(-21)
Nitrogen stress (d a^{-1})	41.6	47.2	(13.5)	44.1	(6.0)	44.6	(7.2)	46.7	(12.3)
Temperature stress (d a^{-1})	3.2	4	(25.0)	4.9	(53.1)	5.4	(68.8)	5	(56.3)
Water stress (d a^{-1})	45.1	41.7	(-7.5)	41.8	(-7.3)	41.9	(-7.1)	40.5	(-10)
Biomass (ton ha^{-1} a^{-1})	3.3	3.3	(0.0)	3.3	(0.0)	3.2	(-3.0)	3.2	(-3)

Land use scenarios
The effects of the land use change scenarios (from 2010 to 2029) are shown in Tab. 7.8 for the annual rate of applied fertilizer (mineral N), surface runoff, sediment losses, organic nitrogen losses, nitrate loads to surface runoff and N leached to the shallow aquifer. The increase in agricultural land area results in increases in the different simulated components for both scenarios La and Lb. Surface runoff, sediment and organic nutrient losses increase at a relatively high rate (50%), inducing high levels of pollution of surface water and groundwater of up to 50% in response to the combination of increasing agricultural lands and management practices, which were kept similar to those implemented in modeling scenario Sc1. This was primarily the case for land use scenario Lb, where large areas of savannahs (up to 40%) were converted to cropland.

Tab. 7.8. Changes in the water balance, sediment yield, nutrient yield, and plant growth parameters according to climate scenarios A1B and B1 and management scenario Sc1. Deviations from the reference scenario (2000-2009) are shown in brackets.

		La		Lb		La		Lb	
	Reference	[2010-2014]		[2010-2014]		[2025-2029]		[2025-2029]	
Rainfall (mm a^{-1})	1233.4	1233	(0.0)	1233	(0.0)	1233	(0.0)	1233	(0.0)
Water yield (mm a^{-1})	242.7	246.8	(1.7)	267.5	(10.2)	267	(10.0)	263	(8.5)
Groundwater flow (mm a^{-1})	106	100.7	(-5.0)	112.9	(6.5)	114	(7.2)	88.8	(-16.2)
Surface runoff (mm a^{-1})	135.7	145.1	(6.9)	153.8	(13.3)	152	(12.3)	174	(28.4)
Evapotranspiration (mm a^{-1})	927.3	915.4	(-1.3)	910.5	(-1.8)	915	(-1.3)	919	(-0.9)
Sediment yield (ton ha^{-1} a^{-1})	0.4	0.4	(0.0)	0.5	(25.0)	0.5	(25.0)	0.7	(75.0)
Organic N load (kg ha^{-1} a^{-1})	0.7	0.7	(0.0)	0.8	(14.3)	0.8	(14.3)	1	(42.9)
NO3 in surface runoff (kg ha^{-1} a^{-1})	0.2	0.3	(50.0)	0.3	(50.0)	0.3	(50.0)	0.3	(50.0)
NO3 in groundwater flow (kg ha^{-1} a^{-1})	1.6	1.6	(0.0)	1.9	(18.8)	2.3	(43.8)	2.3	(43.8)
Leached nitrate (kg ha^{-1} a^{-1})	3.3	3.7	(12.1)	3.8	(15.2)	4.5	(36.4)	4.8	(45.5)
Nitrogen stress (d a^{-1})	41.6	44.2	(6.3)	40.6	(-2.4)	41	(-1.4)	32.9	(-20.9)
Water stress (d a^{-1})	45.1	47.6	(5.5)	48.2	(6.9)	47	(4.2)	44	(-2.4)
Biomass (ton ha^{-1} a^{-1})	3.3	4.6	(39.4)	4.5	(36.4)	4.5	(36.4)	3.9	(18.2)

Combined scenarios

The combined scenarios were evaluated as shown in Tab. 7.9 as well as in Fig. 7.9. The 2010-2014 simulation period shows an increase in rainfall of up to 10%; an increase in the water balance components (water yield, groundwater flow, surface runoff) of up to 75%; a decrease in evapotranspiration of up to 5%; a decrease in sediment yield and organic N load of up to 80%; increases in nitrate in surface runoff, nitrate leached to the shallow aquifer and biomass of up to 150%; increases in water stress of up to 50%; and increases in nitrogen and temperature stress of up to 10%. Globally, for the period 2010 – 2014, climate changes had the dominant impact on the model results. The simulation period 2025-2029 shows a decrease in rainfall of up to 10%; a decrease in water yield and groundwater flow of up to 50%; an increase in surface runoff of up to 50%; a decrease in evapotranspiration of up to 10%; an increase in sediment yield and organic N load of up to 100%; an increase in leached nitrate and nitrate in surface runoff of up to 40%; an increase in biomass of up to 20%; and increases in temperature, water and N stresses of up to 50%. Clearly, the simulation period 2025 – 2029 is also dominated by climate change effects regardless of the land use scenarios; however, land use scenario Lb exhibited larger effects compared to scenario La. This may be explained by the contrast between "stronger economic development, controlled urbanization, large-scale irrigation schemes, and a 3.2% population growth per year (scenario La)" and "a weak national economy, uncontrolled settlement and farmland development, and a 3.5% population growth per year (scenario Lb)".

Tab. 7.9. Water balance and soil degradation rate according to the combined climate and land use scenarios and modeling scenario Sc1.

	2000-2009	2010-2014				2025-2029			
	Reference	LaA1B	LaB1	LbA1B	LbB1	LaA1B	LaB1	LbA1B	LbB1
Rainfall (mm a^{-1})	1233.4	1296.4	1177	1296.4	1177	1116	1138	1116	1138
Water yield (mm a^{-1})	242.7	375.4	270.7	395.1	285.8	221.9	244.9	221.8	246.7
Groundwater flow (mm a^{-1})	106	153.7	112.3	163.6	120	95.5	107	75	87.4
Surface runoff (mm a^{-1})	135.7	220.3	157	230.4	164.6	125.1	136.5	145.9	158.4
Evapotranspiration (mm a^{-1})	927.3	835.2	840.7	830.1	835.5	857.4	847.3	854.7	845.2
Sediment yield (ton ha^{-1} a^{-1})	0.4	0.6	0.5	0.7	0.5	0.4	0.5	0.6	0.6
Organic N load (kg ha^{-1} a^{-1})	0.7	1	0.8	1.1	0.9	0.7	0.8	1	1
NO_3 in surface runoff (kg ha^{-1} a^{-1})	0.2	0.4	0.3	0.4	0.3	0.2	0.2	0.2	0.3
NO_3 in groundwater flow (kg ha^{-1} a^{-1})	1.6	1.9	1.7	2.2	2	2.1	2	2	2
Leached nitrate (kg ha^{-1} a^{-1})	3.3	3.9	3.8	3.9	3.8	4.1	4	4.3	4.1
Nitrogen stress (d a^{-1})	41.6	50.3	46.2	47.1	43	46	49	34.9	37.1
Temperature stress (d a^{-1})	3.2	4.2	5.5	3.7	4.8	5	4.7	2.7	2.7
Water stress (d a^{-1})	45.1	43.9	44.3	44.8	45.3	44.5	43.2	42	40.8
Biomass (ton ha^{-1} a^{-1})	3.3	4.4	4.4	4.3	4.3	3.8	3.9	3.8	3.8

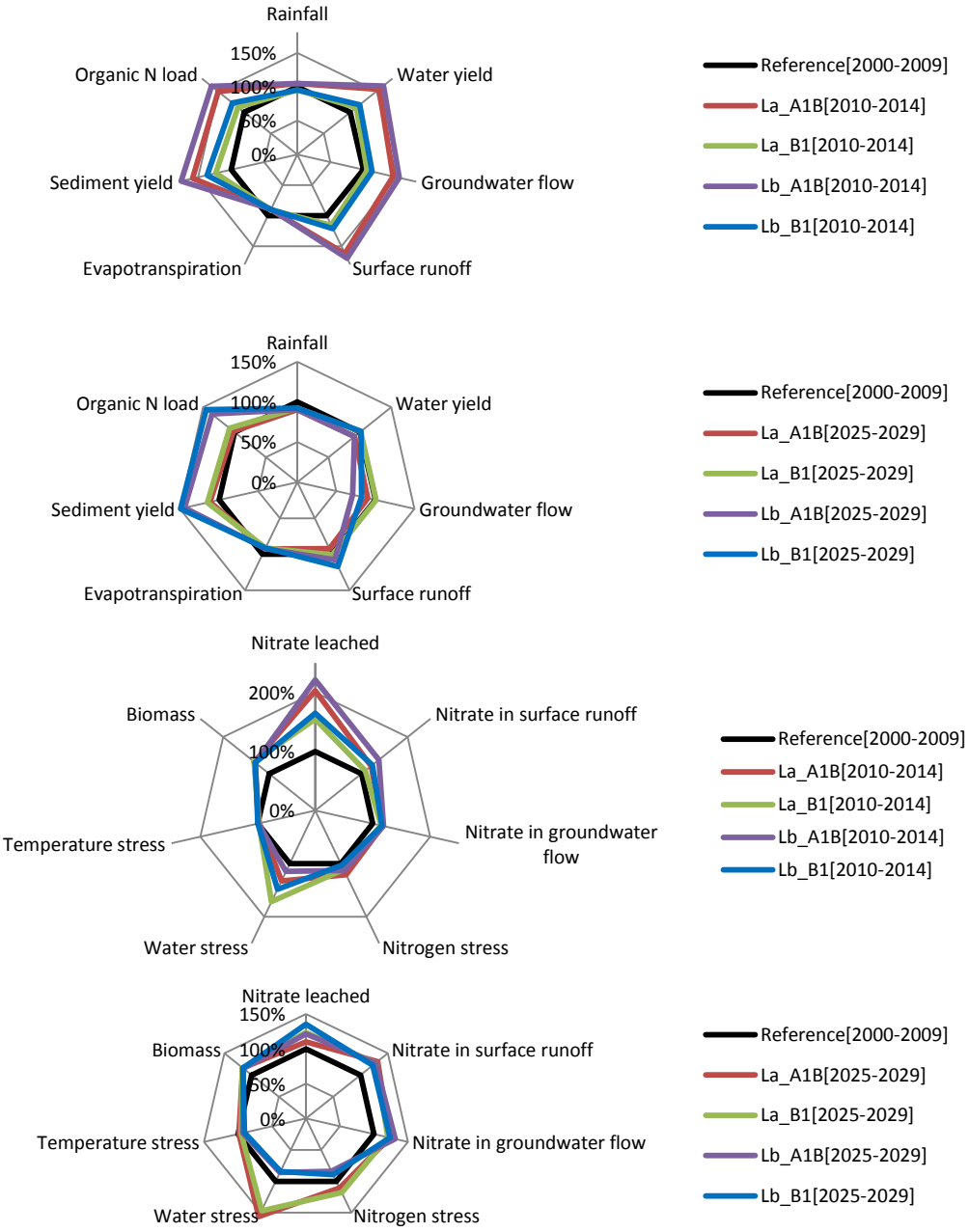

Fig. 7.9. Predicted changes according to the combined climate and land use scenarios and modeling scenario Sc1.

One may infer from these results that an increase in rainfall resulted in increases in the water yield, groundwater recharge, surface runoff, and the nutrient loads to surface runoff and groundwater systems. The combined effects of a decrease in rainfall and an increase in the daily temperature resulted in decreases in the water yield, groundwater recharge and the pollution rate of surface water and groundwater. However, due to land use change (increasing croplands), the surface runoff, yield of sediment and associated organic nutrients and groundwater pollution increased. Finally, it appears that the induced decreases in water yield and land degradation rate (due to the reduced rainfall) may be counteracted by the effects of land use change. This indicates the strength of the relationship between agriculture and water quality (sediment and nutrient transport) within the Donga-Pont catchment.

3.7. Parameter sensitivity and uncertainty issue

The sensitivities (lt-Statl) of the model input parameters (cf. details in the chapter 4) to the measurements (discharge, sediment and nitrate data) and the final calibrated values are presented in Tab. 7.10. As described in the chapter 4, these lt-Statl sensitivities are calculated using the sequential uncertainty fitting algorithm with the sum of squared error (SS) set as a three degree objective function, taking into account the discharge and the sediment and nitrate loads simultaneously. The sensitivity significance P-values (obtained with a t-test) are also provided (a value close to zero has a high significance) (cf. details in the chapter 4). The soil erodibility factor (USLE_K) is identified as the most sensitive parameter, followed by the nitrogen percolation factor (NPERCO), effective channel hydraulic conductivity (Ch_K2), soil depth (SOL_Z) and the threshold depth for groundwater flow to occur (GWQMN).
The SUFI-2 procedure uses a sequence of steps in which the initial (large) uncertainties in the model parameters are progressively reduced until a certain calibration requirement based on the prediction uncertainty is reached (Abbaspour et al., 2004). Tab. 6 summarized the final optimized uncertainties for discharge and sediment transport obtained through the model calibration.
In the final calibrated parameter set, more than 50% of the measurements (P-factor) were captured by the 95% prediction uncertainty, and the ratio of the average distance between the 2.5^{th} and 97.5^{th} percentiles of the cumulative distribution of the simulated variable and the standard deviation of the corresponding measured variable (R-factor) was less than 0.5. However, an unexpected R-factor value (1.83) is obtained for the nitrate load as a consequence of the discontinuous time-scale of the data.

Tab. 7.10. Input parameter sensitivity and calibrated values (SUFI-2, Abbaspour, 2008). lt-Statl is the sensitivity (high value means high sensitivity). P-values are the significance of the sensitivity (values close to zero indicate high sensitivity).

Parameter	Description	Fitted values	lt-Statl	P-values
ESCO	Soil evaporation compensation factor [-]	0.38	0.84	0.41
SOL_Z	Soil depth [mm]	0.27	1.20	0.24
CN2	Curve number [-]	6.65	0.30	0.77
GWQMN	Threshold depth for ground water flow to occur [mm]	38.75	1.17	0.26
REVAPMN	Threshold water level in shallow aquifer for revap [mm]	15.25	0.11	0.91
Ch_K2	Effective channel hydraulic conductivity [mm/hr]	3.95	1.39	0.18
Sol_K	Saturated hydraulic conductivity [mm/hr]	-0.78	0.29	0.77
GW_DELAY	Ground water delay [day]	15.08	0.16	0.87
USLE_P	Practice factor [-]	0.13	0.26	0.80
USLE_K	Soil erodibility factor [0.013 t m^2h/(m^3 t cm)]	0.03	1.89	0.07
SPEXP	Exponent for calculating max sediment retrained [-]	1.35	0.25	0.81
SURLAG	Surface runoff lag coefficient [-]	0.19	0.16	0.88
ALPHA_BF	Base flow recession factor [day]	0.06	0.50	0.62
NPERCO	Nitrate percolation coefficient [-]	0.49	1.58	0.13
RCHRG_DP	Fraction of deep aquifer percolation [-]	0.25	0.24	0.81

Tab. 7.11. Uncertainty quality measures for the calibration of discharge, sediment and nitrate load. The P-factor is the percentage of measured data bracketed by the 95% prediction uncertainty. The R-factor is the ratio between the average distance between the 2.5th and 97.5th percentiles of the cumulative distribution of the simulated variable and the standard deviation of the corresponding measured variable.

	Discharge	Sediment	Nitrate
Calibration period	2006-2008	2008	2008
p-factor	0.57	0.61	0.75
R-factor	0.24	0.08	1.83

7.4. Conclusion

Currently, many factors alter the relationship between agriculture and the environment. Agriculture's direct and indirect impacts on water resources and human well-being are recognized all over the world. In this study, the SWAT agro-hydrological model was used to simulate the current and future status of land and water degradation in the Donga-Pont catchment. The model was able to accurately simulate the daily dynamics of water and sediment as well as nitrate and organic nutrient transportation.

The quality of the spatial information, primarily the accuracy of diffuse-source agricultural pollution, is crucial for modeling soil nutrient dynamics, biomass and crop yield with an acceptable uncertainty level. The predictions based on a simple aggregation of the cropping systems (in the land use maps) are associated with high uncertainties.

Water yield and all water balance components increased over the period 2010-2014 and decreased from 2025-2029 as a result of the changing climate. High risks of severe flooding events remain pertinent for the period 2010-2014.

The model results showed the susceptibility of nutrients to removal from soils to the detriment of surface water and groundwater quality, driven by climate change, which emerges as a challenging factor for agricultural nutrient management in the Donga-Pont catchment.

The expansion of croplands increased the amount of nutrient loss from soils (water quality deterioration) at the catchment scale, in spite of the decreases of water balance components over the period 2025-2029. It is clear that management practices such as fertilizer inputs remain a principal driver of this dynamic. Furthermore, groundwater investigations within the catchment have shown nitrate concentrations close to the World Health Organization and US federal drinking water standards for the maximum nitrate contamination level.

In addition to the regulation of agricultural inputs to cotton, rice and maize fields suggested by this work, special attention should be paid to potentially vulnerable areas such as inland valleys, which were not adequately parameterized in our work due to the technical limitations of the model.

8. Estimating scale effects of catchment properties on modeling soil and water degradation[3]

Abstract

Distributed physically-based models require large amount of data, including detailed spatial information (e.g. geology, soil, vegetation). The relevance of spatial information highly depends on the modeling scale and may control the modeling issue, mainly model parameters, which already depend on model assumptions and target processes. In this study, scale dependent catchment properties were used to derive SWAT model parameters (for ungauged basins) using uncertainty thresholds and statistical approaches. Six individual sub-basins of the Ouémé River (Benin) ranging from 586 to 10,072 km^2 in size were investigated, leading to the multi-scale modeling of discharge, sediment and nutrient dynamic. The Sequential Uncertainty Fitting approach was applied for calibration and an uncertainty analysis. Calibrated parameters set were considered only when more than 50% of the measurements were captured by the 95% prediction uncertainty, and when the ratio of the average distance between 2.5 and 97.5 percentiles of the cumulative distribution of the simulated variable and the standard deviation of the corresponding measured variable was less than 0.5. Regression models between the calibrated model parameter sets and linearly independent catchment property sets were established. Following a confidence threshold of 5%, nine predicted model parameters (e.g. soil depth) may fall within the confidence interval with 95 to 99% of chance, and six model parameters (e.g. Curve Number) may be predicted with 83 to 93% of chance. Globally, geology appeared to be a major driver of the regional hydrological response, correlating significantly with eleven out of fifteen model parameters. Validation was performed by applying the derived model parameters at different scales (1,200 and 25,000 km^2) with goodness-of-fit (to daily measurements) around 0.7 for Nash-Sutcliffe model efficiency and R^2. This study revealed that runoff-sediment-nutrient dynamic (soil and water degradation) may be simulated for ungauged large scale catchments in Benin with reasonable degree of accuracy.

Keywords: SWAT; Uncertainty; Catchment properties; Modeling scale; Soil and water degradation.

8.1. Introduction

The complexity of hydrological processes depends on the environmental heterogeneity (e.g. soil distribution, topography, geology, vegetation, anthropogenic impacts) and has to be analyzed in connection with the spatial scale.

Earlier works (von Bandat, 1962; Strahler, 1964; Beven, 1981; Germann, 1986, 1990; Kneale and White, 1984; Jones, 1987; Chappell and Ternan, 1992; Dunne, 1978, Jenny, 1980; Blöschl and Sivapalan, 1995) have for instance illustrated catchment subsurface spatial heterogeneity in connexion to the scale (Fig. 8.1): (1) at the local scale, soils often exhibit macropores such as cracks, root holes or wormholes, which can transport the bulk of the flow with a minimum contribution of the soil matrix (macropore flows become operative with a certain thresholds in precipitation intensity and antecedent moisture); (2) at the hillslope scale, preferential flow may occur through

[3] Published as: Bossa, A.Y. and Diekkrüger, B., 2012. Estimating scale effects of catchment properties on modeling soil and water degradation. In : R. Seppelt, A.A. Voinov, S. Lange, D. Bankamp (Eds.), Managing Resources of a Limited Planet. Proceedings of the Sixth Biennial International Congress on Environmental Modeling and Software (iEMSs), Leipzig, Germany (in press).

high conductivity layers and pipes and water may exfiltrate to the surface as return flow; (3) heterogeneity at the catchment scale may relate to different soil types and properties, valley floors show different soils as hillslopes and ridges; and (4) at the regional scale, geology is often dominant through soil formation (parent material) and controls on the stream network density.

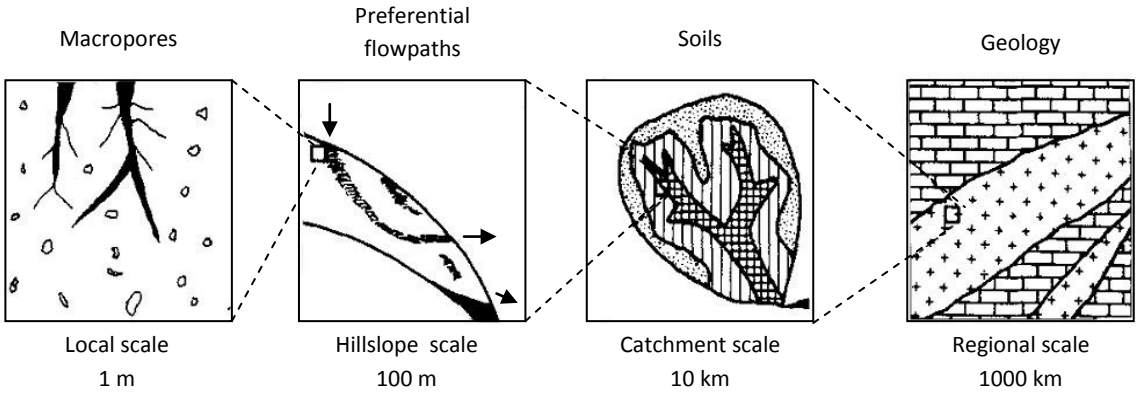

Fig. 8.1. Heterogeneity (variability) of catchments and hydrological processes at a range of spatial scale (Source: after Blöschl and Sivapalan, 1995)

This understanding has led to the development of several conceptual, distributed or physical-based (e.g. SWAT, WASIM, UHP-HRU, SIMULAT-H, etc.), attempting to quantify the hydrological variability occuring at a range of scales by subdividing the catchment into a number of sub-areas: sub-catchments, hillslopes, hydrological response units, contour-based elements, and square grid elements (Abbott et al., 1986; Sivapalan and Viney, 1994a, 1994b; Diekkrüger and Arning, 1995; Arnold et al., 1998; Giertz et al., 2006). It was a great successful step for hydrological modeling, but which nevertheless opened discussions on the model structural errors, including the scale-effects in the internal aggregation (FitzHugh and Mackay, 2000) that complicate the parameter uncertainty issues for large scale applications. In addition, the lack and the non-accurate boundary condition data (e.g. stream water-sediment-nutrient measurements) at large scale may affect the magnitude of model parameters which may have finally no physical meaningfulness, carrying too bad information. These still are a severe limitation raising once more the traditional hydrology concern of large-scale catchment modeling (regionalization), which is crucial for long-term climate and land use impact assessment in a data-poor environment like in Benin and the whole West Africa region.
Multi-scale applications of the Soil and Water Assessment Tool (SWAT) model [Arnold et al., 1998] in the Ouémé-Bonou catchment (49,256 km²) in Benin have shown a strong spatial scale dependent variations in the model parameters [Lawal et al., 2004; Sintondji, 2005; Busche et al., 2005; Hiepe, 2008; Bossa et al., 2012]. Although the model parameters highly depend on the model assumptions and the target processes, they vary significantly under physical catchment property influences especially when moving between different catchment scales. For instance when comparing two sub-catchments within the Ouémé catchment (upstream - Donga-Pont (586 km²) and downstream – Bétérou (10,072 km²), cf. Fig. 2.5), investigated physical catchment properties (e.g. slopes, soil distribution, land cover) differ significantly, causing different behavior, and in consequence completely different model parameters [Hiepe, 2008]. Bárdossy [2007] stated that in principle, if the models are based on the basic principles of physics (mass and energy conservation), the estimation of model parameters should be a straightforward task. Nevertheless, the extreme heterogeneity of the influencing parameters, such as soil properties or the unresolved spatial and temporal variability of meteorological variables (mainly rainfall) limits the applicability of physically-based models to process studies even on small well observed experimental catchments.
Furthermore, an increase in the size of the investigated catchment is often related to a decrease in data availability and to the scale of the underlying information [Bormann et al., 1999]. At the field scale for instance, a soil map or a land use map of 1:5,000 are commonly available, which may

decrease to the scale of 1:200,000 or less in regional studies. This is often called parameter crisis [e.g., Stoorvogel & Smaling, 1998], which is felt at almost any scale that is related to initial conditions, boundary conditions and model parameters.
For environmental modeling it is important to know (1) how knowledge of different small-scale processes may efficiently contribute to the simulation of large-scale behavior and (2) how and with which uncertainties model parameters are transferable to ungauged catchments. Several study [Andersen et al., 2001; Wooldridge and Kalma, 2001; Heuvelmans et al., 2004] discussed the significance of the spatial variability in parameter optima for a large-scale model applications and found that the spatially-distributed parameterization obtained by a multi-site calibration leads to a better model fit than the single-site calibration that treat model parameters as spatially invariant. Wale et al. [2009] as well as Gitau and Chaubey [2010] concluded that regression-based parameter sets can be obtained and used for simulating hydrologic responses satisfactorily.
The SWAT model is applied in the current work to simulate the physical and chemical degradation of land and water for six individual sub-catchments of the Ouémé River in Benin. For that, an advanced regionalization methodology has been applied to develop scale dependent regression-based parameter models for accurately simulating water-sediment-nutrient fluxes at ungauged and large scale basins. The methodology considers physical catchment properties depending on spatial scale (ranging from 586 to 10,072 km^2 in size) as explanatory variables for estimating SWAT model parameters. Such an approach avoids the limitations caused by model internal aggregation that often leads to increased uncertainties in the model parameters, and solves at the same time the problem of lack and non-accurate data (e.g. stream water-sediment-nutrient measurements) at the Ouémé-Bonou gauging station (49,256 km^2).

8.2. Methods

8.2.1. Modeling approach

The location of the Donga-Pont sub-catchment is shown in the Fig. 2.5 in the chapter 2. Detailed descriptions of SWAT model components including soil loss, nutrient transport as well as water quality components are provided in the chapter 4. Input data such as soil, land use, and climate are described in the chapter 2. Calibration and validation data such as discharge and sediment- nutrient concentrations are also described in the chapter 5.
The modeling approach is summarized in Fig. 8.2. General input data such as digital elevation model, soil data and land use data are used to compute selected physical catchment attributes presented in Tab. 8.1. They are also used as input for SWAT, which was run for six individual Ouémé sub-catchments. Auto-calibration and uncertainty analysis were performed applying the SUFI-2 procedure (Sequential Uncertainty Fitting version 2), using the SWAT-CUP interface [Abbaspour, 2008], based on SWAT outputs and various measurements from the sub-catchment gauging stations (cf. chapter 5). SPSS and Minitab software were used for statistical analysis, based on a correlation analysis performed to identify physical catchment properties meaningful for each model parameter.
Calibrated parameter sets were considered only when more than 50% of the measurements were captured by the 95% prediction uncertainty, and when the ratio of average distance between 2.5 and 97.5 percentiles of the cumulative distribution of the simulated variable and the standard deviation of the corresponding measured variable was less than 0.5.

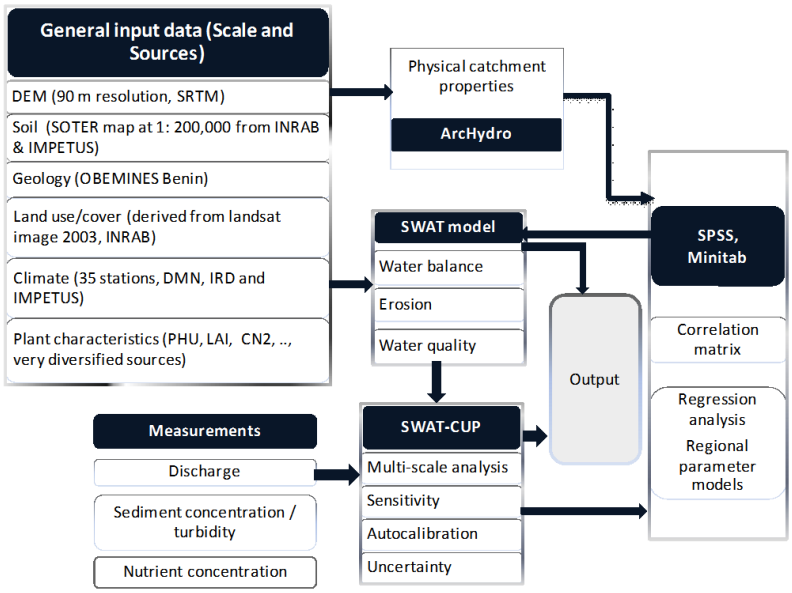

Fig. 8.2. Schematization of the modeling approach. Soil and land use data are from IMPETUS (Christoph et al., 2008) and INRAB (Institut National de la Recherche Agricole du Bénin; Igue, 2005), Climate data are from IMPETUS, IRD (Institut de Recherche pour le Développement), and DMN (Direction de la Météorologie Nationale), Geology data is from OBEMINES (Office Béninoise des MINES).

Tab. 8.1. Selected physical catchment properties.

Catchment properties	Description
Catchment area	Reflects volume of water that can be generated from rainfall
Length of longest flow path	Distance from the catchment's outlet to the most distant source on the catchment boundary
Hypsometric integral	Describes the distribution of elevation across the catchment area.
Average altitude	Average elevation of the catchment from SRTM DEM
Average slope of catchment	Calculated from digital elevation model SRTM DEM pixel by pixel
Drainage density	Total stream length for the basin divided by catchment area
Basin shape	Circularity index: the ratio of perimeter square to the area of the catchment. Elongation ratio: the ratio of length of longest drainage to diameter of a circle which has the same area as the basin
Land cover (%)	Forest, grassland, cropland, savannah, ..
Soil (%)	Lixisols, leptosols, vertisols, ..
Geology (%)	Migmatite, granite, alterite, ..

8.2.2. Multiple linear regression analysis

Due to various limitations, which are mainly data availability problems, only 6 sub-catchments are used in the statistical analysis step. A total of 26 catchment characteristics have been initially used to perform a Variable Inflation Factor (VIF) analysis to avoid collinearity problems (Eq. 8.1). Only one characteristic was considered if a computed VIF between two characteristics exceeded a threshold value of 10. This has resulted in a final use of 16 catchment characteristics to compute a correlation matrix with the calibrated model parameters. Higher correlations than 0.7 for a given model parameter have indicated which catchment characteristics may explain this model parameter.
Scale dependent parameter models have been computed (in a multiple linear regression form, using the statistical tool SPSS), where each model input parameter is explained by one or many catchment properties. Coefficients of determination and Fisher probabilities were the criteria used to select the best parameter models.

$$VIF = 1/\left(1 - r_{ij}^2\right) \quad \text{(Eq. 8.1)}$$

$$Y' = \beta_0 + \beta_1 X_1 + \beta_2 X_2 + \beta_3 X_3 + ... + \beta_n X_n \quad \text{(Eq. 8.2)}$$

where r_{ij}^2 is the collinearity coefficient, $\beta_1, \beta_2, \ldots., \beta_n$ are regression coefficients, $X_1, X_2, X_3, \ldots, X_n$ are independent variables (catchment characteristics), Y' is the dependant variable (model parameter) and β_0 is an intercept of the regression line.

8.3. Results and discussion

8.3.1. Multi sub-catchment scale calibration

Accordingly to the investigated Ouémé sub-catchments, model goodness-of-fit to the daily discharge, sediment and nutrient measurements are listed in Tab. 8.2 Regarding discharge simulations, poor model efficiency were obtained for validation in Vossa and Kaboua sub-catchments (0.34 and 0.40 respectively) due mainly to peak overestimation caused partly by land use map derived from 2003 Landsat images, which considered more agricultural areas than the reality of the validation period (1995 – 1998).
Critical model performances were obtained for sediment simulation in the Bétérou sub-catchments, where the model efficiency decreased even to 0.14. This may be mainly caused by strong hysteresis effects observed at this station, which was not equipped of turbidity probe as used at the Donga-Pont and Atchérigbé gauging stations to minimize this effect.
Nitrate load was in general well represented in the model with coefficients of determination ranging from 0.62 to 0.99 and model efficiencies ranging from 0.54 to 0.99. Higher performances were observed for smaller sub-catchments.

Tab. 8.2. Model goodness of fit to measurements for the different sub-catchments involved in the multiple regression analysis, for model calibration. Information concerning validation are provided in brackets.

		Donga	Vossa	Térou	Atchérigbé	Kaboua	Bétérou
Discharge	Period	2006-2008 (1998- 2005)	1998-2000 (1995)	2002-2005 (1998-2001, 2006)	2007- 2008 (2001-2006, 2009)	2004- 2006 (1995-1998)	2006-2009 (1998-2005)
	R^2	0.72 (0.58)	0.75 (0.63)	0.75 (0.61)	0.89 (0.71)	0.73 (0.55)	0.75 (0.64)
	NS	0.72 (0.51)	0.75 (0.34)	0.74 (0.51)	0.82 (0.62)	0.67 (0.40)	0.60 (0.59)
Sediment	Period	2008 (2005)	- -	2004-2005 (2006)	2008 (2009)	- -	2008-2009 (2004-2005)
	R^2	0.69 (0.58)	-	0.44 (0.33)	0.66 (0.67)	-	0.43 (0.27)
	NS	0.67 (0.55)	-	0.41 (0.32)	0.64 (0.67)	-	0.30 (0.14)
Nitrate	Period	2008 (2008-2009)	- -	- -	2008 (2009)	- -	2008-2009 (2008)
	R^2	0.99 (0.95)	-	-	0.86 (0.62)	-	0.73 (0.52)
	NS	0.99 (0.78)	-	-	0.81 (0.54)	-	0.70 (0.46)

Simulated versus observed daily water discharge and sediment yield are shown in Fig. 8.3 and 8.4 for the Atchérigbé sub-catchment (cf. Fig. 2.5). Recession periods were generally well represented. Less accurately predictions of single peaks are also shown in some years, partly due to the measurement errors during exceptional flooding years (2003 and 2007) in which over bank full discharge was observed at the gauging station. As already indicated in the chapter 6, differences are also usually caused by the SWAT structure, since it is a continuous time model with a daily time step and subscale processes such as single-event flood routing cannot be efficiently predicted. In addition, the daily measured precipitation for 24 h starts at 6:00 am and may not well match to the daily average discharge values, which were measured for 24 h from midnight on (Lam et al., 2010). As it can be

seen from the figures in the year 2008, discharge measurement gaps of even more than 10 days can happen due mainly to technical problems.

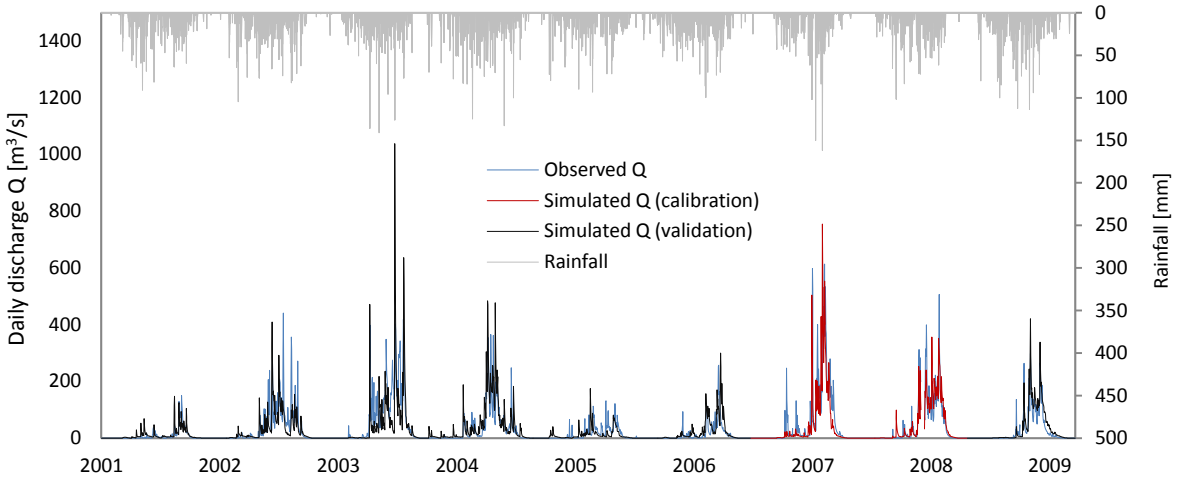

Fig. 8.3. Simulated vs. observed daily discharge for the Atchérigbé sub-catchment (6978 km^2). Calibration period was 2007 to 2008 (R^2=0.89 and ME=0.83), validation period was 2001-2006, and 2009 (R^2=0.71 and ME=0.62).

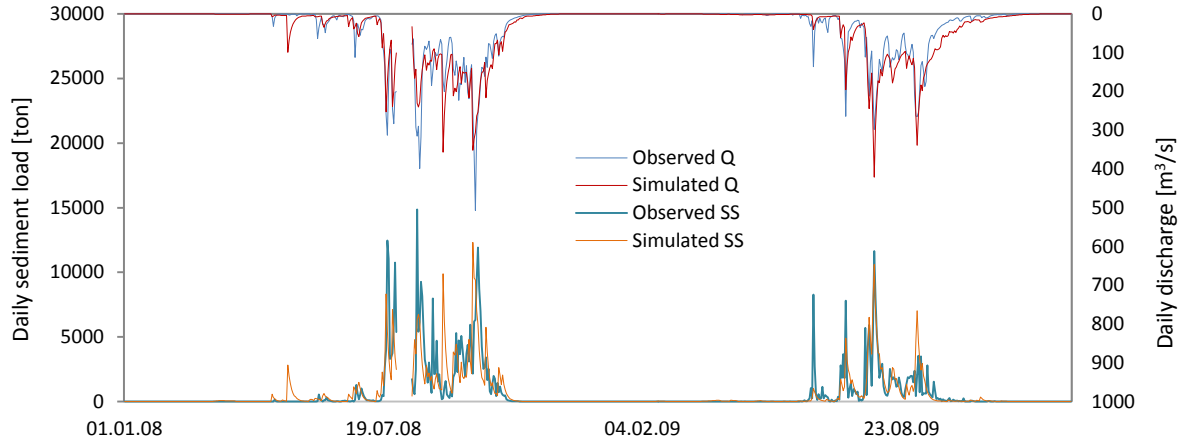

Fig. 8.4. Simulated vs. Observed daily sediment yield for Atchérigbé sub-catchment (6978 km^2). Calibration period was 2008 (R^2=0.66 and ME=0.64), validation period was 2009 (R^2=0.67 and ME=0.67). SSC = suspended sediment.

Simulated versus observed daily stream water nitrate load are shown in Fig. 8.5 for the same Atchérigbé sub-catchment. Similarly to the sediment yield, nitrate peaks accompanied discharge peaks mainly caused by combined effects of increase nitrate loading and increase in water volume. Due to the sampling time scale (one time a week) several peaks were missed, but did not affect the model calibration.

According to FAO (1996), water degradation by sediment has a chemical dimension - the silt and clay fraction, primary carrier of adsorbed chemicals, like nitrogen and phosphorus, which are transported by sediment into the aquatic system. Fig. 7.6 shows weekly simulated versus observed organic N and P delivery at the Atchérigbé gauging station. Organic N and P were not calibrated. Since it was assumed that a good adjustment of soil nutrient pools would be reflected in their simulations, only a validation was performed. Model goodness-of-fit were acceptable: 0.58 (R^2) and 0.78 (NS) for organic Nitrogen and 0.89 (R^2) and 0.96 (NS) for organic Phosphorus.

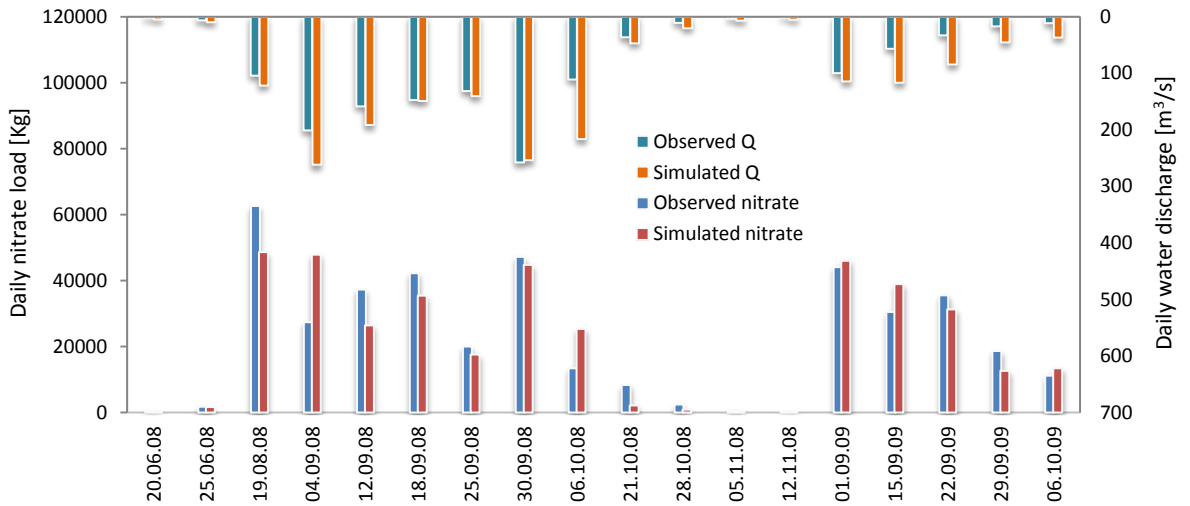

Fig. 8.5. Simulated vs. observed daily nitrate load for Atchérigbé sub-catchment (6978 km^2). Calibration period was 2008 (R^2=0.86 and ME=0.81), validation period was 2009 (R^2=0.62 and ME=0.54).

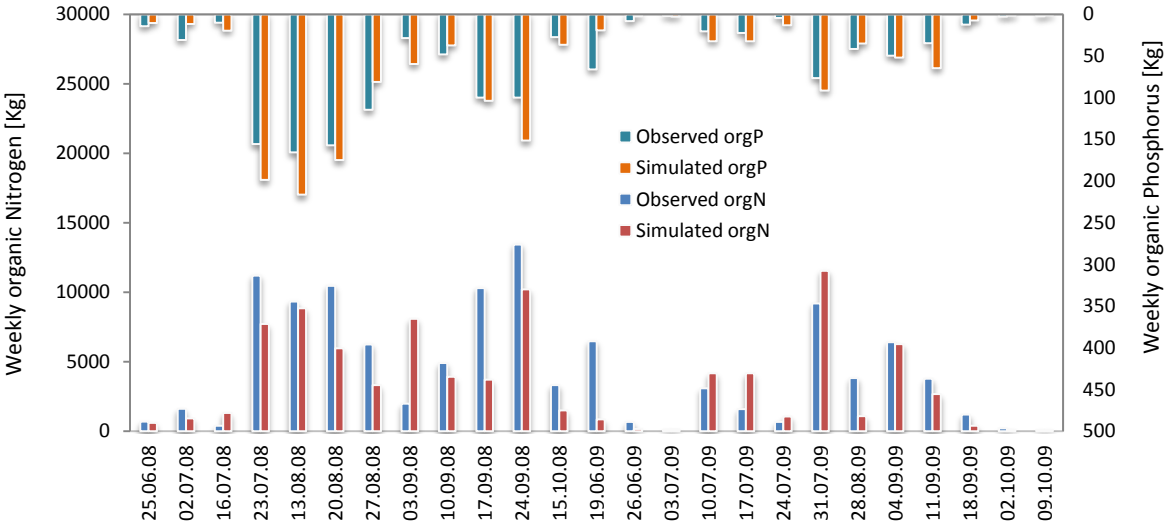

Fig. 8.6. Simulated vs. observed weekly organic N and P load for the Atchérigbé sub-catchment (6978 km^2). Only validation was performed from 2008 to 2009 with R^2=0.58 and ME=0.78 for organic Nitrogen and R^2=0.89 and ME=0.96 for organic Phosphorus.

8.3.2. Calibrated model parameters

Calibrated model parameters as obtained for the six sub-catchments involved in the multiple regression analysis are listed in the Tab. 8.3. Fifteen sensitive parameters were found sufficient to represent the simulated processes. The parameters have a fairly homogeneous overview with some particular distinctions. That is for example the case of the practice factor (USLE_P) which is almost zero for the Bétérou sub-catchment. It is also the case of the soil erodibility factor (USLE_K) which has harshly relatively and negatively changed (-0.57) for the same sub-catchment. This may be partly explained by the combined effects of high percentage of savannahs (54%) and higher percentage of lateritic consolidated soil layers (8% against a maximum of 4% for the others, cf. Tab. 8.4), known to be resistant to erosion.

To have more confidence on the calibrated values, the base flow recession factors (ALPHA_BF) for example were computed directly from discharge measurements and were found completely consistent with the calibrated values.

Tab. 8.3. Calibrated model parameter involved in the multiple regression analysis.

Parameter	Description	Donga	Vossa	Térou	Atchérigbé	Kaboua	Bétérou
ESCO	Soil evaporation compensation factor [-]	0.38	0.28	0.49	0.35	0.28	0.43
SOL_Z	Soil depth [mm]	0.27	0.01	0.37	0.16	0.06	0.03
CN2	Curve Number [-]	6.65	3.86	5.55	6.24	3.97	2.51
GWQMN	Threshold depth for ground water flow to occur [mm]	38.75	7.50	47.50	28.50	30.50	43.50
REVAPMN	Threshold water level in shallow aquifer for revap [mm]	15.25	6.50	45.50	18.50	26.50	26.50
Ch_K2	Effective channel hydraulic conductivity [mm/hr]	3.95	1.00	12.77	10.65	1.00	12.52
Sol_K	Saturated hydraulic conductivity [mm/hr]	-0.78	-0.65	-0.73	-0.35	-0.82	-0.66
GW_DELAY	Ground water delay [day]	15.08	17.12	23.25	10.87	16.04	24.80
USLE_P	Practice factor [-]	0.13	0.10	0.07	0.15	0.18	0.00
USLE_K	Soil erodibility factor [0.013 t m^2h/(m^3 t cm)]	0.03	0.16	0.08	0.14	0.25	-0.57
SPEXP	Exponent for calculating max sediment retrained [-]	1.35	1.07	1.21	1.20	1.28	1.38
SURLAG	Surface runoff lag coefficient [-]	0.19	0.35	0.24	0.25	0.17	0.10
ALPHA_BF	Base flow recession factor [day]	0.06	0.17	0.07	0.12	0.11	0.15
NPERCO	Nitrate percolation coefficient [-]	0.49	0.88	0.74	0.71	0.32	0.67
RCHRG_DP	Fraction of deep aquifer percolation [-]	0.25	0.20	0.17	0.22	0.15	0.29

8.3.3. Catchment properties and parameter models

The computed catchment properties are presented in Tab. 8.4. The lowest variations were found for average slope of the catchment, the percentage of level, the circularity index and the elongation ratio. The highest variation was found for the geological components percentage of alterites and lateritic consolidated soil layers.

Tab. 8.4. Catchment physical attributes as computed for the sub-catchments. CV means coefficient of variation.

Catchment Attributes	Donga	Affon	Vossa	Térou	Atchérigbé	Kaboua	Bétérou	Savè	Ouémé	CV
Area (km^2)	586.4	1178.8	1934.7	2344.3	6978.4	9458.7	10072.1	23487.9	49256.0	1.35
Length longest flow path (km)	64.4	102.54	94.0	108.7	174.2	294.0	220.2	415.0	622.4	0.79
Drainage density (km/ km^2)	2.09	2.10	2.04	2.11	2.17	1.99	2.20	2.16	3.8	0.25
Hypsometric integral	0.4	0.38	0.3	0.3	0.3	0.5	0.4	0.5	0.4	0.20
Average slope of catchment	2.6	2.51	3.1	2.6	2.7	2.9	2.5	2.8	2.7	0.07
Percentage of level	99.9	99.86	99.2	99.4	98.3	99.8	99.6	99.2	99.8	0.01
Circularity Index	51.8	69.54	48.0	48.2	50.0	77.1	47.6	58.7	64.2	0.19
Elongation ratio	2.4	2.65	1.9	2.0	1.8	2.7	1.9	2.4	2.5	0.16
Average altitude (m)	395.9	392.72	273.8	392.9	191.0	350.5	355.0	327.9	270.7	0.21
Crop land (%)	47.8	32.26	30.0	17.0	45.2	31.7	25.6	21.8	37.6	0.32
Savannah (%)	48.8	61.78	30.1	65.1	23.7	34.2	54.4	52.1	43.3	0.31
Lixisol (%)	32.4	23.00	90.6	58.0	39.1	43.8	42.7	52.1	57.3	0.40
Alterites (%)	12.23	1.52	0.0	34.48	0.0	2.00	3.35	5.0	2.7	1.62
Granites (%)	20.16	27.27	12.08	0.0	4.3	18.00	9.55	5.8	4.7	0.79
Migmatites (%)	45.78	42.50	82.43	50.25	65.05	70.00	68.76	73.6	68.0	0.22
Lateritic consolidated soil layers (%)	0.13	2.81	0.24	0.32	0.0	1.50	8.16	4.8	4.1	1.14

Tables 8.5 and 8.6 show respectively the correlation matrix (calibrated parameters versus catchment properties in a non-colineality condition) and the performed regression-based parameter models. As explained before, higher correlations than 0.7 for given model parameters have indicated which catchment properties may explain these model parameters. For instance, the parameter soil evaporation compensation factor (ESCO) is correlated with average slope of the catchment, percentage of savannah and alterites. This has led to two parameter models: (1) a simple linear regression (ESCO = 0.177 + 0.005 (% savannah)) with a Fisher probability of 0.022 and a R^2 of 0.75, (2) a multiple linear regression (ESCO = 0.935 - 0.217 (Average slope of catchment) + 0.00327 (% Alterites)) with a Fisher probability of 0.022 and a R^2 of 0.92. The second parameter model was finally retained because of higher R^2 given the same value obtained for the Fisher probability. But

the real raised problem is the physical and hydrological meaningful of the performed equations. In general, all the computed parameter models are meaningful and completely consistent with the theoretical fundament of the model parameters.

For instance, theoretically, the soil evaporation compensation factor (ESCO) adjusts the depth distribution for evaporation from the soil to account for the effect of capillary action, crusting, and cracks. This parameter is negatively proportional to the maximum evaporation in a nonlinear fashion. Therefore, larger values result in less evaporation, and thus a larger water yield. On the one hand this gives sense to the positive correlation found between ESCO and percentage of savannahs and should be strengthen by a negative correlation between ESCO and percentage of croplands which is unfortunately found equal to -0.43 (insufficient). On the other hand it gives also sense to the negative correlation (-0.79) between ESCO and the average slope of the catchment and the positive correlation (0.80) between ESCO and the percentage of alterites. Because terrain slopes (average slope of the catchment) and geology (alterites) are factors that highly affect soil depths and soil layer distribution (indirectly pore distribution and crusting).

Another example is the correlation between soil depth and percentage of migmatites, which makes sense given the soil formation processes. Indeed, apart from water induced relocation processes (erosion), occurring at the soil surface and visible at local and hillslope scale (Diekkrüger, 2010), at the lower boundary of the soil, rocks are weathered and incorporated into the soil. This is part of processes called soil formation that may not exclude scale dependent relationships between soil depth and the intensity of bedrock (migmatites in this study). Thus, migmatite is very prominent in the basin (Tab. 8.4) and its spatial pattern may affect soil formation as well as dominant hydrological processes at regional scale.

Globally, with respect to process representation in SWAT model, one can read from the performed equations that in the Ouémé catchment, geology appears to be a major driver of hydrological response, correlating significantly with eleven out of fifteen model parameters. This is consistent with Blöschl and Sivapalan (1995), stating that at the regional scale, geology is often dominant through soil formation (parent material) and controls the main hydrological processes. Slope appears to be powerful to control the channel conductivity, groundwater threshold for base flow generation and soil evaporation compensation (accounting for capillary, crusting and cracking actions). Soil type lixisol (a dominant soil type within the Ouémé catchment) partly explained the surface runoff lag and the maximum retrained sediment. Lateritic consolidated soil layer explained the soil susceptibility to erosion (sediment loading) and drainage density explains the fraction of aquifer percolation.

Following a confidence threshold alpha of 5%, 9 predicted parameters (e.g. soil depth, soil evaporation compensation factor, saturated hydraulic conductivity, threshold depth for ground water flow to occur, effective channel hydraulic conductivity, nitrate percolation coefficient) may fall within the confidence interval with 95 to 99% of chance, and 6 parameters (e.g. Curve Number, USLE practice factor, exponent for calculating max sediment retrained, surface runoff lag coefficient) may be predicted with 83 to 93% of chance (cf. Tab. 8.6).

Figure 8.7 shows correlations between calibrated and predicted model parameters with associated 95% confidence interval. Weak coefficients of determination were obtained for the curve number (0.49), the Fraction of deep aquifer percolation (0.55), Threshold water level in shallow aquifer for revap (0.60), the USLE practice factor (0.51). This may be caused by the fact that the catchment properties used to explain these parameters are perhaps insufficient to completely capture the processes behind.

Tab. 8.5. Correlation matrix (calibrated parameters vs. Catchment attributes) with respect to a non-collinearity condition.

Physical Attributes	ESCO	SOL_Z	CN2	GWQMN	REVAPMN	Ch_K2	ALPHA_BF	USLE_K	NPERCO	SPEXP	SURLAG	USLE_P	GW_DELAY	SOL_K	RCHRG_DP
Area (km^2)	-0.15	-0.56	-0.60	0.16	0.18	0.22	0.44	-0.38	-0.36	0.38	-0.62	-0.04	0.12	0.17	0.07
Length longest flow path (km)	-0.29	-0.52	-0.55	0.10	0.22	-0.01	0.31	-0.12	-0.54	0.31	-0.54	0.18	0.05	-0.04	-0.22
Drainage density (m/ km^2)	0.63	0.14	0.01	0.48	0.19	0.87	0.09	-0.73	0.39	0.36	-0.36	-0.63	0.26	0.57	0.74
Hypsometric integral	-0.39	-0.15	-0.04	0.15	0.04	-0.49	-0.29	0.24	-0.98	0.50	-0.52	0.58	-0.25	-0.51	-0.29
Average slope of catchment	-0.79	-0.49	-0.21	-0.91	-0.53	-0.77	0.47	0.61	0.19	-0.78	0.73	0.43	-0.33	-0.06	-0.58
Percentage of level	0.11	0.06	-0.25	0.33	0.15	-0.35	-0.29	-0.20	-0.55	0.54	-0.47	-0.16	0.45	-0.96	0.07
Circularity Index	-0.53	-0.25	-0.14	-0.06	0.08	-0.55	-0.13	0.44	-0.83	0.18	-0.27	0.66	-0.26	-0.44	-0.59
Elongation ratio	-0.34	0.00	0.04	0.14	0.07	-0.59	-0.42	0.34	-0.94	0.42	-0.39	0.56	-0.18	-0.70	-0.38
Average altitude (m)	0.49	0.41	-0.08	0.62	0.49	0.00	-0.51	-0.25	-0.41	0.55	-0.48	-0.32	0.62	-0.89	0.05
Crop land (%)	-0.43	-0.04	0.57	-0.24	-0.65	-0.33	-0.23	0.24	-0.30	0.16	0.02	0.58	-0.84	0.34	0.29
Savannah (%)	0.88	0.58	-0.05	0.80	0.72	0.52	-0.43	-0.48	0.00	0.46	-0.43	-0.66	0.82	-0.53	0.22
Lixisol (%)	-0.28	-0.29	-0.35	-0.68	-0.25	-0.31	0.55	0.24	0.67	-0.83	0.77	-0.17	0.18	-0.02	-0.34
Alterites (%)	0.80	0.88	-0.66	0.64	0.78	0.45	-0.67	0.06	0.10	-0.82	0.00	-0.28	0.49	0.06	-0.22
Granites (%)	-0.58	-0.36	0.66	-0.25	-0.56	-0.79	-0.06	0.11	-0.64	0.57	-0.23	0.39	-0.30	0.49	0.11
Migmatites (%)	-0.68	-0.90	0.76	-0.76	-0.49	-0.37	0.94	0.01	0.30	0.95	0.32	0.01	-0.06	-0.14	-0.15
Lateritic consolidated soil layers (%)	0.28	-0.46	-0.51	0.37	0.16	0.40	0.47	-0.92	-0.04	0.29	-0.72	-0.71	0.66	-0.30	0.61

Tab. 8.6. Best parameter model (multiple regression analysis) and resulting values for three independent catchments (Affon, Savè and Ouémé).

parameters	Equations	R^2	Fisher p	Affon	Savè	Ouémé
ESCO	= 0.935 - 0.217 (Average slope of catchment) + 0.00327 (% Alterites)	0.92	0.022	0.39	0.34	0.37
SOL_Z	= 0.758 - 0.01 (% Migmatites)	0.81	0.015	0.33	0.02	0.08
SOL_K	= 26.991 -0.278 (% Percentage of level)	0.92	0.023	-0.77	-0.58	-0.76
CN2	= 10.0 - 0.0824 Migmatites (%)	0.49	0.12	6.50	3.94	4.40
GWQMN	= 185 - 49.2 (Average slope of catchment) - 0.255 (% Migmatites)	0.85	0.05	50.49	26.89	37.28
REVAPMN	= 16.5 + 0.769 (% Alterites)	0.60	0.07	37.47	20.37	18.56
Ch_K2	= 56.1 - 16.0 (Average slope of the catchment) - 0.461 (% Granites)	0.98	0.033	3.31	8.12	11.53
ALPHA_BF	= - 0.0794 + 0.00300 (% Migmatites)	0.87	0.01	0.05	0.14	0.12
GW_DELAY	= 19.0 - 0.248 (% Crop land) + 0.165 (% Savannah)	0.98	0.042	21.19	22.17	16.82
USLE_P	= 0.129 - 0.0143 (% Lateritic consolidated soil layer)	0.51	0.1	0.09	0.06	0.07
USLE_K	= 0.162 - 0.0848 (% Lateritic consolidated soil lay)	0.85	0.01	-0.08	-0.24	-0.18
NPERCO	= 1.72 - 3.80 (% Hypsometric integral) + 0.00779 (% Circularity Index) - 0.033 (% Elongation ratio)	0.85	0.05	0.74	0.08	0.47
RCHRG_DP	= - 0.758 + 0.462 (Drainage density (km/ km^2))	0.55	0.09	0.21	0.24	0.99
SPEXP	= 1.47 - 0.00454 Lixisol (%) + 0.00011 Migmatites (%)	0.70	0.169	1.24	1.22	1.47
SURLAG	= 0.109 + 0.003 Lixisol (%) - 0.016 Lateritic consolidated soil layers (%)	0.93	0.104	0.07	0.19	0.22

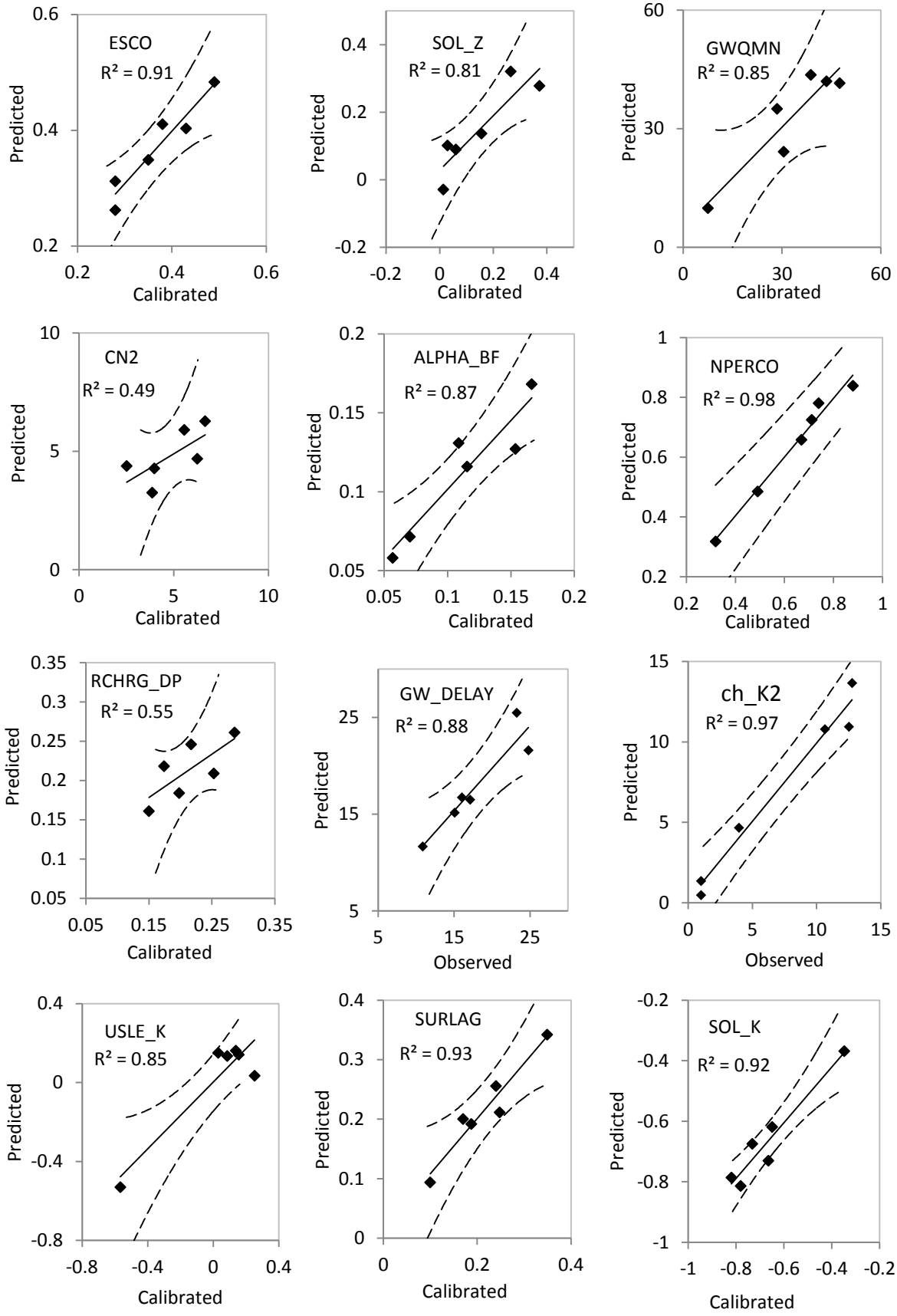

Fig. 8.7. Predicted vs. Calibrated model parameter with associated 95% confidence interval. Parameter definitions are provided in the Tab. 8.3.

8.3.4. Validation at different scales

Scale dependent parameter sets (Tab. 8.6) were calculated from the performed parameter models for independent and different sub-catchment scales (Affon, 1179 km^2 and Savè 23488 km^2), and were used for validation. Satisfactorily model goodness-of-fit to the daily total discharge were obtained (Affon: 0.70 for R^2 and 0.61 for model efficiency; Savè: 0.71 for R^2 and 0.67 for model efficiency). Recession periods were generally well represented (Fig. 8.8). As mentioned for the calibration results, less accurately predictions of single peaks occurred in some years, usually caused by the SWAT structure, since it is a continuous time model with a daily time step and subscale processes such as single-event flood routing cannot be efficiently predicted.

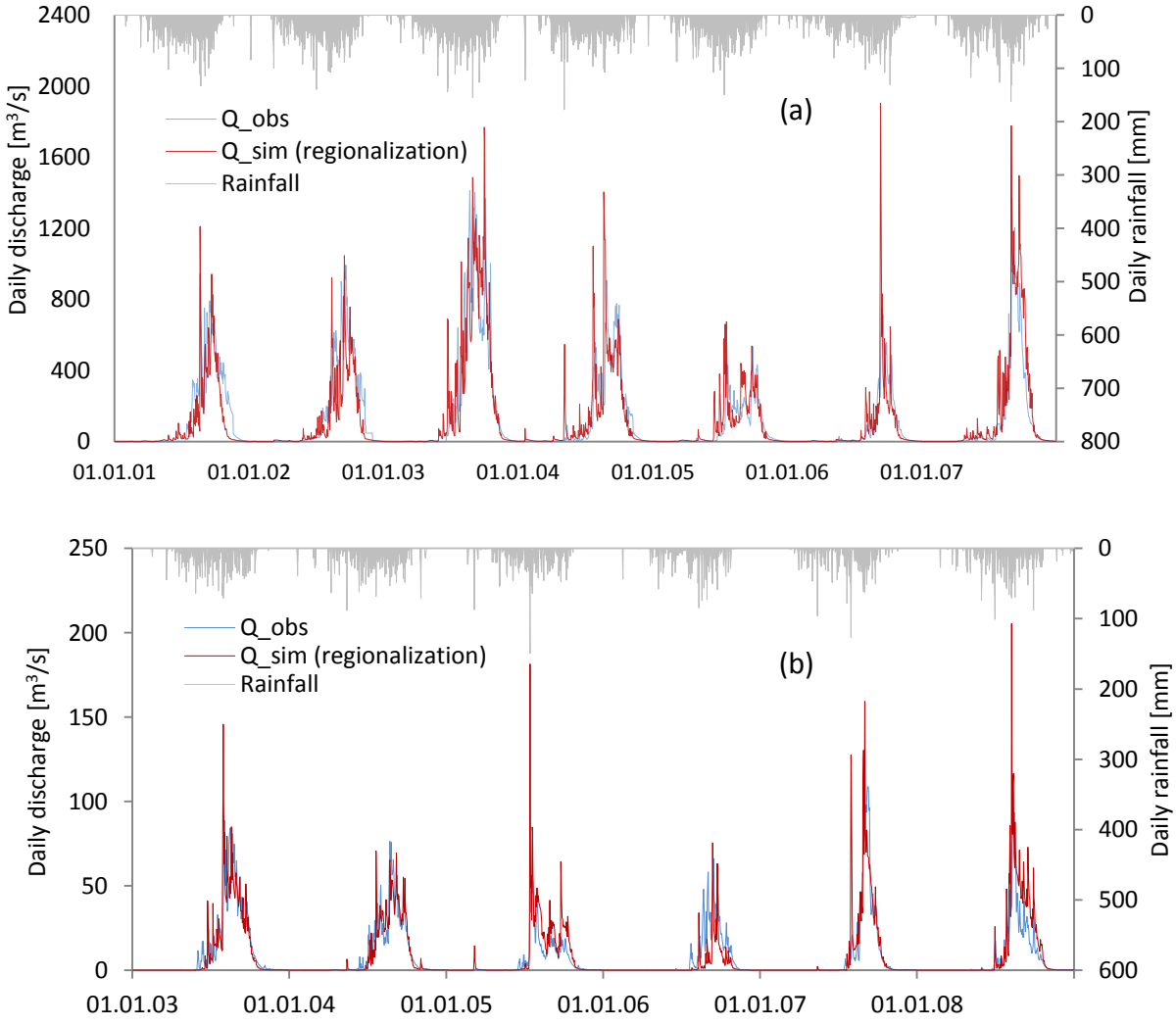

Fig. 8.8. Observed vs. simulated total discharge using the regression-based parameters for: (a) the Savè sub-catchment (23,488 km^2), with 0.71 for R^2 and 0.67 for model efficiency (ME); and (b) the Affon sub-catchment (1179 km²), with 0.70 for R^2 and 0.61 for model efficiency (ME).

8.3.5. Hotspots of soil degradation

At the whole Ouémé-Bonou catchment scale (about 49,256 km^2, cf. Fig. 2.1), surface runoff was simulate to 77 mm a^{-1} (hiding a spatial pattern ranging from 0 to 350 mm a^{-1}), sediment yield was

evaluated to 0.3 ton ha^{-1} a^{-1} (with a range from 0 to 10 ton ha^{-1} a^{-1}) and lost soil organic nitrogen was evaluated to 1.2 kg ha^{-1} a^{-1} (hiding a spatial pattern ranging from 0 to 20 kg ha^{-1} a^{-1}) for the period 2000 to 2009 (Tab. 8.7 and Fig. 8.9). These results open the perspective of predicting more accurately water, sediment and nutrient transport of ungauged catchment and allow assessing climate and land use impacts at large catchment scale in a data-poor environment in Benin.

Tab. 8.7. Mean annual water components and total sediment and organic nitrogen yield for the Ouémé-Bonou catchment (period 2000 – 2009).

Rainfall (mm a^{-1})	1138.90
Water yield (mm a^{-1})	224.62
Surface runoff (mm a^{-1})	76.99
Groundwater flow (mm a^{-1})	147.63
Evapotranspiration (mm a^{-1})	794.80
Sediment yield (ton ha^{-1} a^{-1})	0.32
Organic N load (kg ha^{-1} a^{-1})	1.18

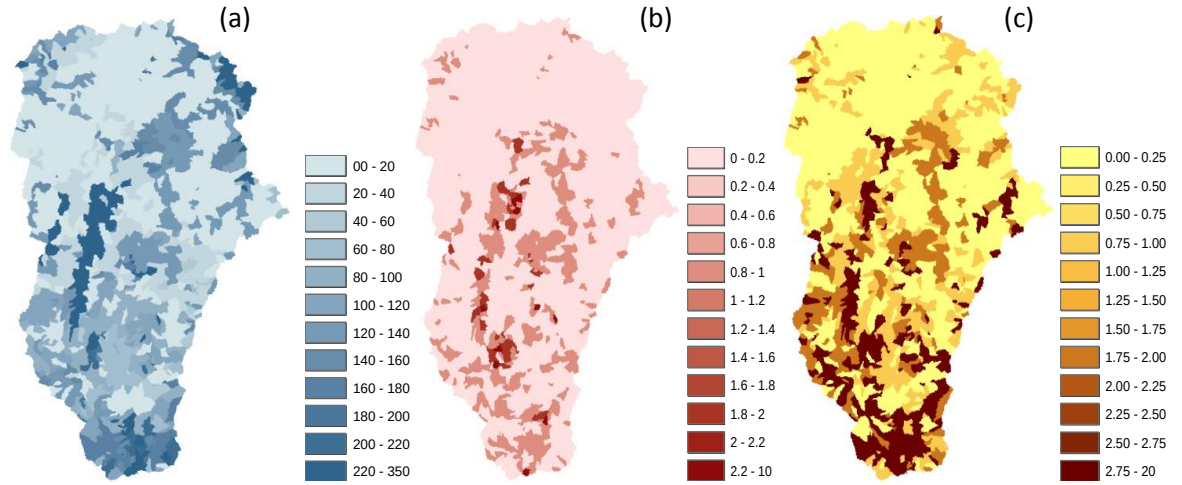

Fig. 8.9. Simulated results in the Ouémé-Bonou catchment. (a) : Surface runoff pattern (mm a^{-1}) ; (b): Sediment yield pattern (ton ha^{-1} a^{-1}); (c): Organic Nitrogen yield pattern (kg ha^{-1} a^{-1}) (period 2000 – 2009).

8.3.6. Uncertainty analysis

The SUFI-2 procedure uses a sequence of steps in which the initial (large) uncertainties in the model parameters are progressively reduced until a certain calibration requirement based on the prediction uncertainty is reached (Abbaspour et al., 2004). In this study, as explained before, calibrated parameter set were considered only when more than 50% of the measurements (P-factor) were captured by the 95% prediction uncertainty, and when the ratio of average distance between 2.5 and 97.5 percentiles of the cumulative distribution of the simulated variable and the standard deviation of the corresponding measured variable (r-factor) were less than 0.5. Table 7.8 summarized the final optimized uncertainties for discharge and sediment transport through the multi scale calibration and validation, while Fig. 7.10 presents the final optimized 95% prediction uncertainty band for both discharge and sediment transport for the Atchérigbé sub-catchment from 2008 to 2009. In general, the final r-factor values met the quality requirements for all simulated variables, while the p-factor values were poor for sediment transport in some sub-catcments (0.31, 0.34, and 0.40 respectively for Térou, Bétérou and Atchérigbé sub-catchments). According to Abbaspour et al (2004) this indicates that the calibrated parameter ranges produced several relatively poor simulations, and that a higher degree of multi-objective formulation is needed in the objective function to limit the number of bad simulations. But in this specific case, it may be caused

partly by the hysteresis problems encountered in some sub-catchments (e.g Bétérou), since an objective function of degree 3 (sum of square error of discharge, sediment and nitrate) was used.

Tab. 8.8. Uncertainty quality measures for the different sub-catchments involved in the multiple regression analysis.

		donga	vossa	terou	zou	kaboua	beterou
Discharge	Period	1998-2008	1995-2000	2002-2007	2001- 2009	1995- 2006	1998-2009
	p-factor	0.57	0.63	0.62	0.53	0.5	0.52
	r-factor	0.24	0.36	0.5	0.33	0.49	0.59
Sediment	Period	2005, 2008		2004 - 2005	2008-2009		2008 - 2009
	p-factor	0.57		0.31	0.4		0.34
	r-factor	0.08		0.48	0.27		0.64

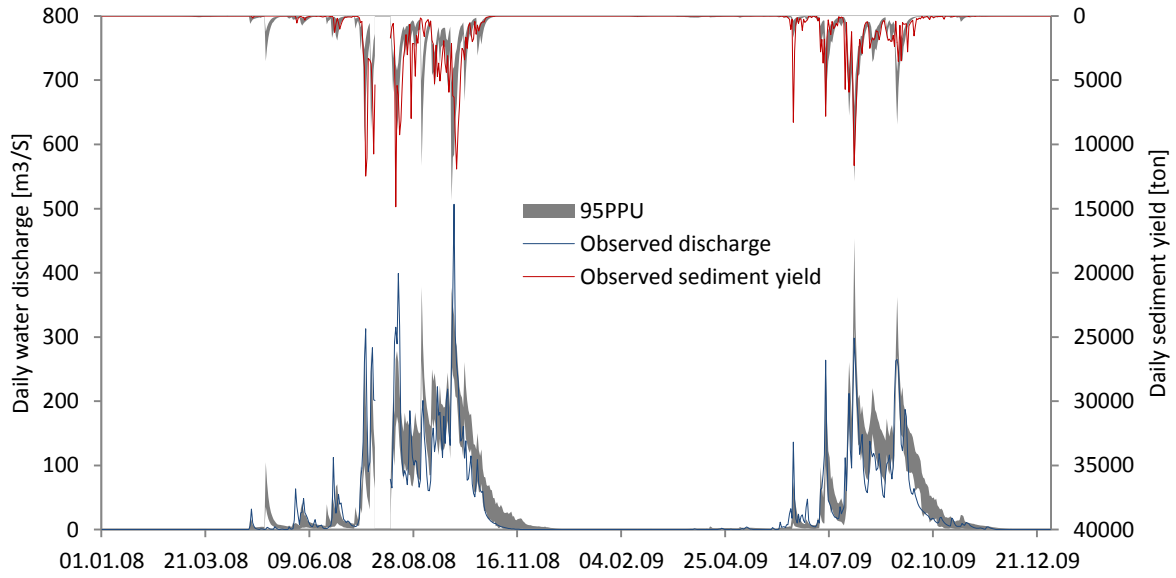

Fig. 8.10. Uncertainty in the model predictions for Atchérigbé sub-catchment: Observed daily discharge and sediment yield bracketed by the 95 percent prediction uncertainties. 95PPU is defined as 95 percent prediction uncertainties.

Other source of uncertainties was the decrease of constraint level in the calibration of the Vossa and Kaboua sub-catchments, where boundary condition data such as sediment and nutrient measurements were not used. Consequently, the objective function was reduced only to discharge variable. This would have certainly affected the parameters, by increasing the level of bad information (Abbaspour et al., 2004) that would not be beneficial in the statistical analysis.
In general the model parameter uncertainty issues were acceptable, since a clear coherency appeared in the final parameter matrix, which was successfully correlated with the scale dependent catchment physical properties. This is possible because of the robustness of the Sequential Uncertainty Fitting approach. Better results may be obtained if the algorithm used could consider many objective functions (e.g. sum of square error, model efficiency of Nash and Sutcliffe, coefficient of determination, etc.) simultaneously.

8.4. Conclusion

Facing the contemporary environmental challenges (impacts of global change) and the uncertainties (induced by the lack of data) for land and water management in Benin, the development of advanced regionalization methods is crucial. In this study, an advanced regionalization methodology has been applied to develop scale dependent regression-based parameter models for accurately simulating water-sediment-nutrient fluxes at ungauged and large scale catchments in Benin.

In this study, scale dependent physical catchment properties are used to explain (statistically) and derive SWAT model parameters for ungauged catchments. With respect to process representation in SWAT model, geology appears to be a major driver of hydrological response, correlating significantly with eleven out of fifteen model parameters. Slope appears to be powerful to control the channel conductivity, groundwater threshold for base flow generation and soil evaporation compensation (accounting for capillary, crusting and cracking actions). Soil type lixisol (a dominant soil type within the Ouémé catchment) partly explains the surface runoff lag and the maximum retrained sediment. Lateritic consolidated soil layer explained the soil susceptibility to erosion (sediment loading) and drainage density explains the fraction of aquifer percolation.

Although the computed regression-based parameter models are physically meaningful and consistent with the theoretical fundament of the model parameters, they contain uncertainty due to the non-uniqueness of the considered calibrated parameter set, which is caused by limited available information. For improving the data base, a new data collection policy must be developed. However the model parameter uncertainty issues were acceptable, since a clear coherency appeared in the final parameter matrix, which was successfully correlated with the scale dependent catchment physical properties. This is partly due to the robustness of the Sequential Uncertainty Fitting approach. Repetitive applications of the here-tested regionalization approach (using different simulation models) should lead to further understanding of scale dependent physical controls on the hydrological response in order to improve the physical meaning of the developed statistical relationships.

9. Simulating land and water degradation under land use and climate change scenarios: from meso (586 km²) to regional scale (49,256 km²)

Abstract

Among factors that contribute to the impacts of the current climate and land use change in West Africa countries including Benin are: lack of information, low management capabilities, overexploitation of land resources including forests, increases in population, uncontrolled settlement, etc.. In order to support well-balanced management decisions, number of these factors is often used as drivers for calculating land use and climate change scenarios for the impact quantification, using distributed physical-based models.

In this chapter, scale dependent parameter models developed in the chapter 8 were used to simulate the impacts of climate and land use scenarios on water yield, sediment and nutrient transport at the Ouémé-Bonou catchment scale (49,256 km²). This methodology solved two difficulties in model setup in the Ouémé catchment: the scale-effects on the model parameters and the associated uncertainty issues for large scale model application and the lack and non-accurateness of boundary condition data (e.g. stream water-sediment-nutrient measurements). The results were discussed in comparison to the simulation results obtained for a meso-scale catchment (Donga-Pont catchment, 586 km^2, cf. Fig. 2.5), based on the management scenario Sc1 developed in the chapter 7.

Regardless the simulation scale, it appeared that surface runoff, groundwater flow, sediment and organic nitrogen load were dominantly affected by land use change by -8 to +50%, while water yield and evapotranspiration were dominantly affected by climate change by -31 to +2%. Comparison made for both simulation scales, have shown that variables such as surface runoff, groundwater flow, sediment and nutrient transport, mainly sensitive to land use change were significantly affected by increasing scale, while variables such as water yield and evapotranspiration, mainly sensitive to climate change, have changed almost similarly for the both scales.

Sediment yield was more important at the meso catchment scale (ranging from 0.4 to 0.6 ton ha^{-1} a^{-1} against 0.32 to 0.45 ton ha^{-1} a^{-1} at the larger catchment scale), due to less retrained sediment at large scale. However, organic nitrogen yield simulated at the large catchment scale was more important (roughly 1.2 to 1.7 ton ha^{-1} a^{-1} against 0.5 to 1 ton ha^{-1} a^{-1} at the meso scale catchment), as consequences of high rate of very fine particle load from abundant threatened areas as shown by the spatial pattern.

9.1. Introduction

Erosion and soil degradation have evolved in very considerable proportions in Africa, especially in tropical Africa. Moreover, to achieve the Millennium Development Goals (UNDP, 2005), it is crucial to take serious measures against erosion and soil degradation, which are primarily sheet and gully erosion that scours the humus horizon in one generation (Roose et al., 2004).

Many researches have been conducted in parts of Africa to understand the processes as for the determinant and promoting causes, related to the specific climatological, meteorological and soil condition (Giertz et al., 2006, Bormann et al. 2005; Laouina et al., 2004, Roose et al., 2004, Speth et al., 2010). Many studies in Benin (Gbessemehlan, 1988; Biaou, 1995; Dissou, 1992; Sintondji, 2005; Bormann et al., 2005; Hiepe, 2008; Speth et al., 2010) showed a fast degradation of natural resources including the loss of agricultural soils of up to 40 ton ha^{-1} a^{-1} compared to 3.9 ton ha^{-1} a^{-1} in the savannahs.

Vulnerability to change, whether climate-induced or related to changes in land use/land cover, is a major threat, consisting at the same time of a water dimension (lower level of the water table), an agrarian dimension (falling yields) and an environmental dimension (weakening of the soil and

increasing erosion) (Laouina et al., 2004). Several investigations on the global change processes and its impact on the hydrological cycle (Bormann et al., 2005; Speth et al., 2010) have shown that global climate change has a significant influence on the regional water resources.
Any interaction to solve the problem must consist to a prior investigation of the involved processes from local to regional scales, and an assessment of long-term potential environmental impacts, since solutions could be only given at local scale.
In this chapter the degradation trends between two different scale catchments were compared. One meso-scale catchment (Donga-Pont; 586 km²) for which more data were available and where farming practices were more easily investigated and provided in the model (cf. chapter 7). The other catchment is very large (Ouémé-Bonou; 49,256 km², Benin) with less available data, where evaluations were based on a preliminary regionalization methodology developed in chapter 8, which considers scale dependent regression-based parameter models as alternative for accurately simulating water-sediment-nutrient fluxes at large scale basins in Benin. This methodology has considered physical properties of catchments, depending on spatial scale (ranging from 586 to 10,072 km^2 in size) as explanatory variables for SWAT model parameters. Such an approach may limit the effects of model internal aggregation that often increase uncertainties in the model parameter, and solve at the same time the problem of the lack and non-accuracy of data (e.g. stream water-sediment-nutrient measurements) at the Ouémé-Bonou gauging station.
Based on these readily made models, and as for the objectives of this study, order of magnitude of impacts of climate and land use scenarios were compared for the studied catchments. Land use and climate change impacts were then evaluated, using two land use scenarios (La, stronger economic development, controlled urbanization, 3.2% population growth per year; and Lb, weak national economy, uncontrolled settlement and farmland development, 3.5% population growth per year (RIVERTWIN, 2007)) and two climate change scenarios (computed using the regional climate model REMO, nested in the global circulation model ECHAM5/MPI-OM and driven by the IPCC SRES scenarios A1B and B1 (Paeth et al., 2008)).

9.2. Materials and method

For the model calibration, local management operations as well as calibrated model parameters described in the chapter 7 for the management scenario Sc1 were considered for the Donga-Pont catchment. As explained in chapter 7, SWAT model was applied to simulate the dynamic of soil nutrient pools from the field scale considering interactions with various inputs like fertilization and grazing. Therefore, water, sediment, and nutrient delivery to the stream flow at the Donga-Pont river catchment outlet (586 km²) are simulated considering local management practices. As for the Ouémé-Bonou catchment (49,256 km²), the regionalization methodology developed in the chapter 8 is used for simulating water-sediment-nutrient fluxes.

9.3. Results and discussion

9.3.1. Impacts of climate scenarios

As shown in Tab. 9.1, scaling effects were directly reflected by the simulated surface runoff, which ranges from 100 to 140 mm per year for the Donga-Pont catchment (586 km²), while varying from 60 to 80 mm per year for the Ouémé-Bonou catchment (49,256 km²). In the both scales, annual sediment yield and actual evapotranspiration have significantly decreased (of up to 20%) over the simulated years (2000 to 2029) with a small resumption (of up to 5%) for the period 2025 to 2029. Groundwater flow decreased significantly from 15 to 22% for the Donga-Pont catchment and from 4 to 17% for the Ouémé-Bonou catchment. Sediment yield was more important at the Donga-Pont catchment scale, ranging from 0.3 to 0.4 ton ha^{-1} a^{-1} against 0.3 ton ha^{-1} a^{-1} for the Ouémé-Bonou

catchment. This may be explained by less retrained sediment at large scale, due for instance to deposit in the inland valleys, which become important at large scales (Speth et al., 2010). Conversely, the simulated organic nitrogen yields for the Ouémé-Bonou catchment (roughly 1.2 ton ha^{-1} a^{-1}) were two times the computed amount for the Donga-Pont catchment (0.6 to 0.7 ton ha^{-1} a^{-1}). This may be simply due to the distribution of hotspots which may be important at large scales. It may also be the consequence of high rate of very fine particle load from given threatened areas. Fig. 9.1 shows a decreasing trend for all the simulated components (of up to 20%), regardless the different scenarios, but more pronounced for the Donga-Pont catchment.

Tab. 9.1. Simulated SWAT components under climate scenarios (with unchanged land use map derived from 2003 landsat image). Deviation (in %) from the reference scenario (2000-2009) are shown in brackets.

Donga-Pont (586 km²)	Reference [2000-2009]	A1B [2015-2019]	B1 [2015-2019]	A1B [2025-2029]	B1 [2025-2029]
Rainfall (mm a^{-1})	1233.4	1096.7 (-11)	1113.9 (-10)	1116.0 (-10)	1138.0 (-8)
Water yield (mm a^{-1})	254.7	206.9 (-19)	215.5 (-15)	205.6 (-19)	225.3 (-12)
Groundwater flow (mm a^{-1})	117.6	98.9 (-16)	100.3 (-15)	91.6 (-22)	100.5 (-15)
Surface runoff (mm a^{-1})	137.2	106.7 (-22)	113.7 (-17)	112.6 (-18)	123.4 (-10)
Evapotranspiration (mm a^{-1})	923.7	839.1 (-9)	849.2 (-8)	863.6 (-7)	854.1 (-8)
Sediment yield (ton ha^{-1} a^{-1})	0.4	0.3 (-25)	0.3 (-25)	0.4 (0)	0.4 (0)
Organic N load (kg ha^{-1} a^{-1})	0.7	0.6 (-14)	0.6 (-14)	0.6 (-14)	0.7 (0)

Ouémé-Bonou (49,256 km²)	Reference [2000-2009]	A1B [2015-2019]	B1 [2015-2019]	A1B [2025-2029]	B1 [2025-2029]
Rainfall (mm a^{-1})	1138.9	1035.2 (-9)	1045.2 (-8)	1041.5 (-9)	1074.9 (-6)
Water yield (mm a^{-1})	224.6	191.4 (-15)	189.0 (-16)	186.2 (-17)	218.0 (-3)
Groundwater flow (mm a^{-1})	147.6	127.5 (-14)	123.7 (-16)	122.8 (-17)	142.2 (-4)
Surface runoff (mm a^{-1})	77.0	63.9 (-17)	65.3 (-15)	63.4 (-18)	75.8 (-2)
Evapotranspiration (mm a^{-1})	794.8	734.3 (-8)	747.5 (-6)	745.8 (-6)	740.2 (-7)
Sediment yield (ton ha^{-1} a^{-1})	0.3	0.3 (0)	0.3 (0)	0.3 (0)	0.3 (0)
Organic N load (kg ha^{-1} a^{-1})	1.2	1.1 (-8)	1.1 (-8)	1.1 (-8)	1.2 (0)

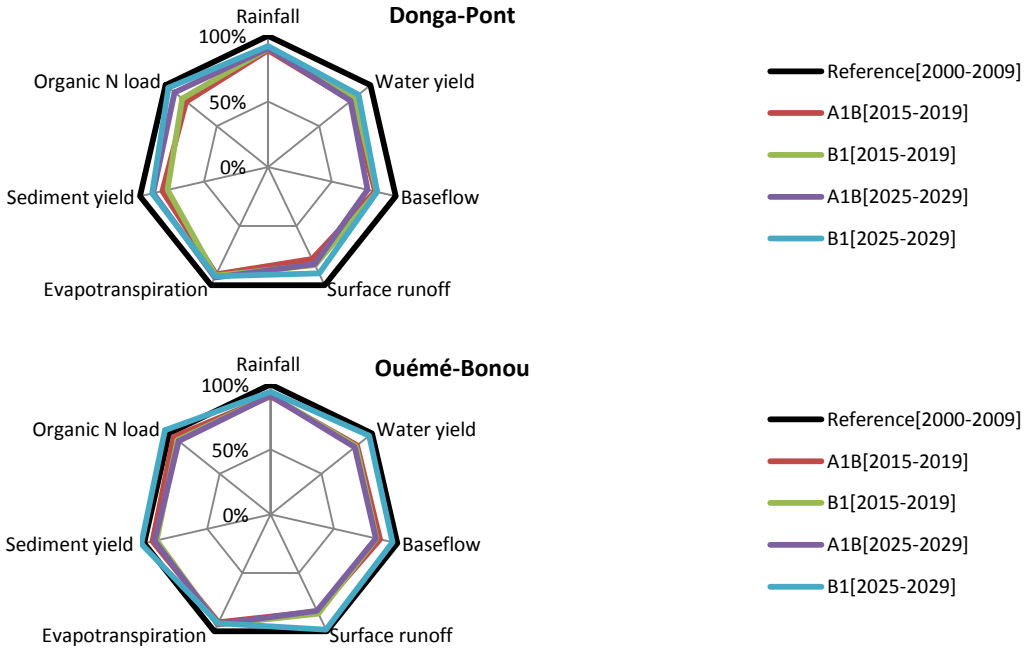

Fig. 9.1. Simulated trends under climate scenarios (with unchanged 2003 land use).

One can conclude that the large scale simulations may have decreased SWAT component (surface runoff, groundwater flow, sediment yield, organic nitrogen load) sensitivity to climate change.

Similar results were found by (Hiepe, 2008; Giertz et al., 2010) in the upper Ouémé catchment using SWAT model and the same IPCC (Intergovernmental Panel on Climate Change) SRES scenarios A1B and B1.

9.3.2. Impacts of land use scenarios

As indicated in the chapter 5, changes in the Ouémé land use according to the scenarios La and Lb are mainly expressed by the conversion of the savannah into croplands and pastures in a range of 10 to 20% of the agricultural lands for the scenario La (stronger economic development, controlled urbanization, 3.2% population growth per year) and 20 to 40% for the scenario Lb (weak national economy, uncontrolled settlement and farmland development, 3.5% population growth per year).
Accordingly, an increasing surface runoff was simulated (from 2000 to 2029) for the both scenarios La and Lb, but in a pronounced way for the scenario Lb (Tab 9.2 and Fig. 9.2). This increase ranges from 9 to 27% for the Donga-Pont catchment and between 22 and 57% for the Ouémé-Bonou catchment. In spite of this simulated increase for the surface runoff, water yield has change in a very small rate (roughly ±5%), forcing a decrease of the groundwater flow (between -9 and -27% for the Donga-Pont catchment and between -22 and -57% for the Ouémé-Bonou). This is manifestly the proof of decrease of the infiltration rate over the study area, and a severe threat to its groundwater systems. Sediment yield has increased from 25 - 75% for the Donga-Pont catchment and from 33 – 66% for the Ouémé-Bonou catchment. Organic nitrogen load has increased from 14 – 43% for the Donga-Pont catchment and from 17 – 58% for the Ouémé-Bonou.
Evapotranspiration has decreased from 0.5 to 1.1% for the Donga-Pont catchment and 0.8 to 2% for the Ouémé-Bonou catchment. For this trend the land use scenario Lb differs from the other by showing the highest underlying simulated rates, as already discussed above for the other components.
In summary (combining the sections 9.3.1 and 9.3.2), surface runoff was found more sensitive to land use change (+22 to +75% of changes) than climate change (-5 to -20% of changes), evapotranspiration was more sensitive to climate change (-8 to -12% of changes) than land use change (-0.5 to -2% of changes) and groundwater flow was less sensitive to climate change (-4 to -22%) than land use change (-9 to -57%). Sediment yield was more sensitive to land use (+25 to +75%) than climate change (-25 to 0%). Organic nitrogen load was more sensitive to land use change (+14 to +58%) than climate change (-8 to -14%).
At the large catchment scale (Ouémé-Bonou), sediment yield has decreased (-25% for the climate scenarios and -57% for the land use scenarios) and organic nitrogen load has increased (100% for the climate scenarios and 175% for the land use scenarios) in reference to the meso scale catchment (Donga-Pont).

Tab. 9.2. Simulated SWAT components under land use scenarios (with unchanged climate condition of the period 2000 to 2009). Deviation (in %) from the reference scenario (2000-2009) are shown in brackets.

Donga-Pont	Reference [2000-2009]	La [2015-2019]	Lb [2015-2019]	La [2025-2029]	Lb [2025-2029]
Rainfall (mm a^{-1})	1233.4	1233.4 (0)	1233.4 (0)	1233.4 (0)	1233.4 (0)
Water yield (mm a^{-1})	254.7	228.7 (-10)	236.7 (-7)	267.0 (5)	263.4 (3)
Groundwater flow (mm a^{-1})	117.6	78.8 (-33)	79.0 (-33)	113.6 (-3)	88.8 (-24)
Surface runoff (mm a^{-1})	137.2	149.1 (9)	157.0 (14)	152.4 (11)	174.3 (27)
Evapotranspiration (mm a^{-1})	923.7	913.7 (-1)	918.0 (-1)	915.3 (-1)	919.1 (0)
Sediment yield (ton ha^{-1} a^{-1})	0.4	0.5 (25)	0.6 (50)	0.5 (25)	0.7 (75)
Organic N load (kg ha^{-1} a^{-1})	0.7	0.8 (14)	0.9 (29)	0.8 (14)	1.0 (43)

Ouémé-Bonou	Reference [2000-2009]	La [2015-2019]	Lb [2015-2019]	La [2025-2029]	Lb [2025-2029]
Rainfall (mm a^{-1})	1138.9	1138.9 (0)	1138.9 (0)	1102.0 (-3)	1138.9 (0)
Water yield (mm a^{-1})	224.6	231.5 (3)	238.8 (6)	233.6 (4)	243.0 (8)
Groundwater flow (mm a^{-1})	147.6	137.9 (-7)	128.8 (-13)	133.9 (-9)	121.7 (-18)
Surface runoff (mm a^{-1})	77.0	93.7 (22)	110.0 (43)	99.7 (29)	121.3 (58)
Evapotranspiration (mm a^{-1})	794.8	788.9 (-1)	782.1 (-2)	787.4 (-1)	778.8 (-2)
Sediment yield (ton ha^{-1} a^{-1})	0.3	0.4 (33)	0.4 (33)	0.4 (33)	0.5 (67)
Organic N load (kg ha^{-1} a^{-1})	1.2	1.4 (17)	1.7 (42)	1.5 (25)	1.9 (58)

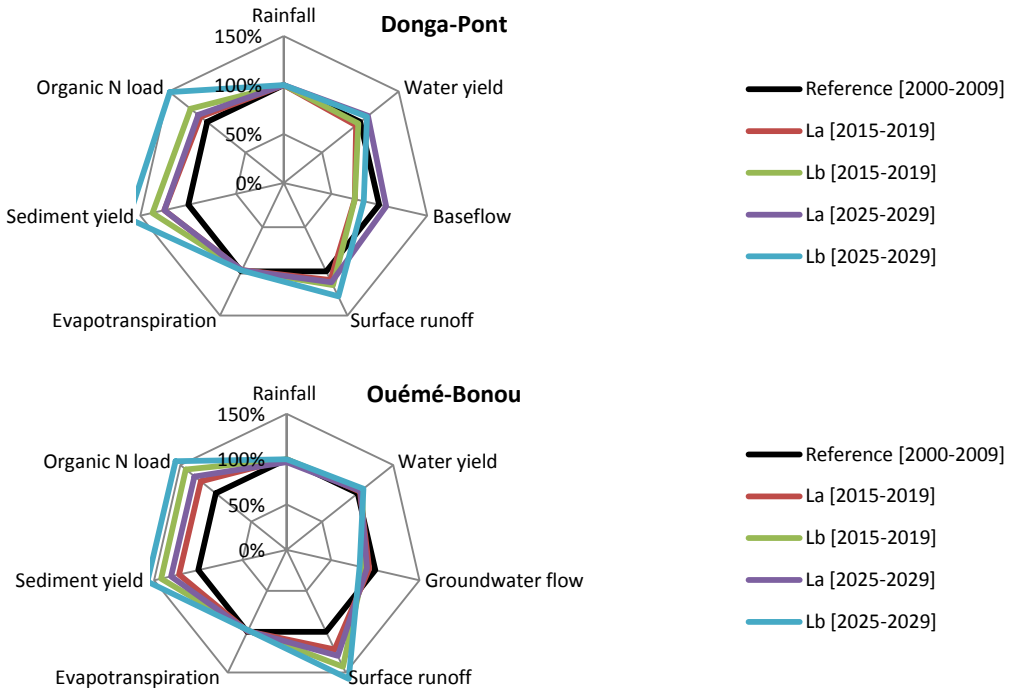

Fig. 9.2. Simulated trends under land use scenarios (with unchanged climate: 2000-2009)

9.3.3. Impacts of combined climate and land use scenarios

In reference to the results discussed in the sections 9.3.1 and 9.3.2, an overview of combined land use and climate change scenario effects on the degradation trend presented in Tab. 9.3 and Fig. 9.3 identified climate change as the major driver of the changes in water yield and evapotranspiration. At the meantime, land use changes raises as the major driver affecting surface runoff, groundwater flow, sediment yield and organic nitrogen load. Stronger effects of climate change were computed for the time period 2015 to 2019 in the Donga-Pont catchment scale, which have been significantly compensated (not completely) by the land use change effects over the time period 2025 - 2029.

Tab. 9.3. Simulated SWAT components under land use and climate scenarios (2015 to 2019). Deviation (in %) from the reference scenario (2000-2009) are shown in brackets.

Donga-Pont	Reference [2000-2009]	La & A1B [2015-2019]	La & B1 [2015-2019]	Lb & A1B [2015-2019]	Lb & B1 [2015-2019]
Rainfall (mm a^{-1})	1233.4	1096.7 (-11)	1113.9 (-10)	1096.7 (-11)	1113.9 (-10)
Water yield (mm a^{-1})	242.7	191.7 (-21)	201.1 (-17)	199.1 (-18)	206.8 (-15)
Groundwater flow (mm a^{-1})	135.7	116.4 (-14)	123.1 (-9)	123.5 (-9)	130.4 (-4)
Surface runoff (mm a^{-1})	106.0	74.1 (-30)	76.6 (-28)	74.5 (-30)	75.1 (-29)
Evapotranspiration (mm a^{-1})	927.3	831.7 (-10)	841.5 (-9)	833.6 (-10)	843.7 (-9)
Sediment yield (ton ha^{-1} a^{-1})	0.4	0.5 (20)	0.4 (-8)	0.5 (15)	0.4 (7)
Organic N load (kg ha^{-1} a^{-1})	0.7	0.5 (-29)	0.6 (-10)	0.7 (0)	0.7 (3)

Ouémé-Bonou	Reference [2000-2009]	La & A1B [2015-2019]	La & B1 [2015-2019]	Lb & A1B [2015-2019]	Lb & B1 [2015-2019]
Rainfall (mm a^{-1})	1138.9	1035.2 (-9)	1045.2 (-8)	1035.2 (-9)	1045.2 (-8)
Water yield (mm a^{-1})	224.6	195.9 (-13)	194.1 (-14)	201.1 (-10)	200.1 (-11)
Groundwater flow (mm a^{-1})	77.0	75.7 (-2)	78.1 (1)	87.3 (13)	90.6 (18)
Surface runoff (mm a^{-1})	147.6	120.2 (-19)	116.0 (-21)	113.9 (-23)	109.5 (-26)
Evapotranspiration (mm a^{-1})	794.8	730.8 (-8)	743.4 (-6)	726.2 (-9)	738.1 (-7)
Sediment yield (ton ha^{-1} a^{-1})	0.3	0.4 (9)	0.3 (6)	0.4 (25)	0.4 (22)
Organic N load (kg ha^{-1} a^{-1})	1.2	1.3 (13)	1.3 (9)	1.5 (29)	1.5 (26)

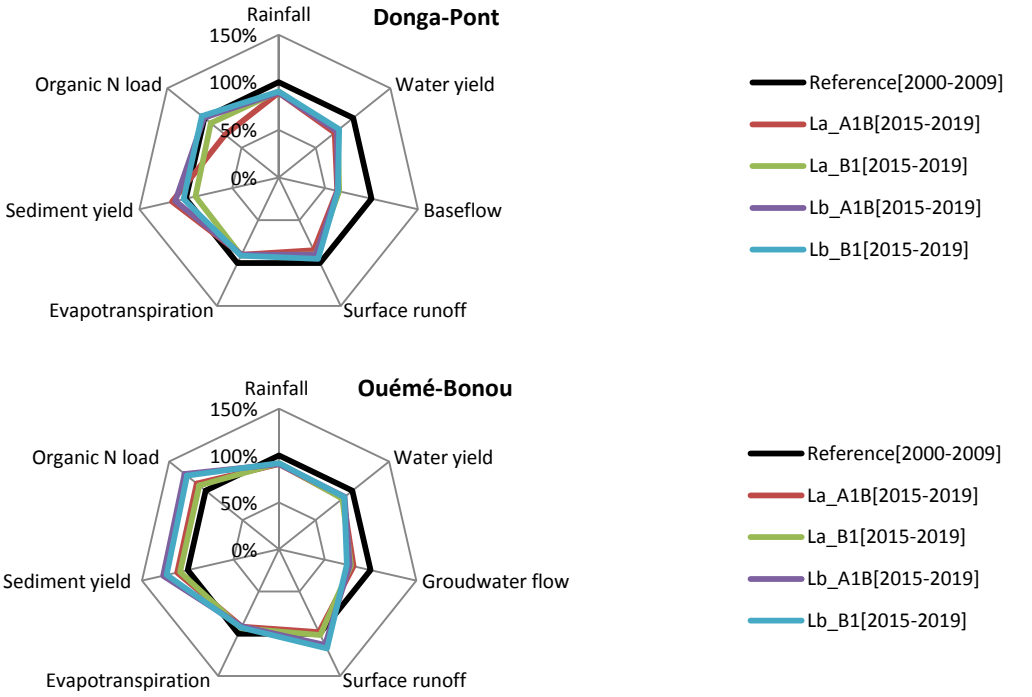

Fig. 9.3. Simulated trends under land use and climate scenarios (2015 to 2019).

At the Donga-Pont scale (Tab. 9.3 and Fig. 9.3, time period 2025 – 2029), annual surface runoff may change from -8 to +17%. The decrease (-8%) (scenarios La + A1B) was mainly drive by climate change, while land use change effects have mainly resulted in an increase (+17%) (scenarios La + B1, Lb + A1B and Lb + B1). Sediment yield increased for all the scenarios from 12.5 to 50%, and organic nitrogen load also has increased from 1.4 to 46% (driving by land use changes). Under climate change effects, water yield has changed from -9 to +1.6%, groundwater flow from -29 to 1% and evapotranspiration from -9 to -7.5%.

At the Ouémé-Bonou scale (Tab. 9.3 and Fig. 9.3, time period 2025 – 2029), annual surface runoff may change from +5.7 to +42% for all the scenarios, driving by land use change. Sediment yield increased for all the scenarios from 15.6 to 41%, and organic nitrogen load also has increased from 15 to 47% (driving by land use changes). Under climate change effects, water yield has changed from -14 to +0.6%, groundwater flow from -30.5 to -16% and evapotranspiration from -8.4 to -7%.

Regardless the modeling scale, the simulated impacts for the land use and climate change scenarios, over the simulated period 2000 to 2029 (30 years) may be summarized as follow: (1) surface runoff, groundwater flow, sediment and organic nitrogen load are found mainly sensitive to land use change with roughly -8 to 50% of changes; and (2) water yield and evapotranspiration are found more sensitive to climate change with roughly -31 to +2% of changes as consequence of rainfall reduction and temperature increase (cf. chapter 5).

In addition the results suggest that variables such as surface runoff, groundwater flow, sediment and transported nutrients, mainly sensitive to land use change were significantly affected by the increasing scale, while variables such as water yield and evapotranspiration, mainly sensitive to climate change, have changed almost similarly for the both scales. An application of the conceptual semi-distributed model UHP-HRU (Universal Hydrological Program – Hydrological Response Unit) in the same study area, using the physical-based model SIMULAT-H as benchmark (Giertz et al., 2010), has led to a similar conclusion that water yield is more influenced by climate than land used, which more affects runoff components (surface runoff vs. interflow and base flow). Results of scenario analysis from the same work (Giertz et al., 2010) revealed that the amount of renewable water decreases during the period 2001 – 2049 in both climate IPCC (Intergovernmental Panel on Climate

Change) SRES (Special Report on Emission Scenarios) scenarios A1B and B1, which were also used in the present study.

Sediment yield were more important at the Donga-Pont catchment scale, ranging from 0.4 to 0.6 ton ha^{-1} a^{-1} against 0.32 to 0.45 ton ha^{-1} a^{-1} at the Ouémé-Bonou catchment scale. This may be explained by less retrained eroded particles at large scale, due to sequestration in the inland valleys, which become important at large scales (Speth et al., 2010). According to Diekkrüger (2010), high erosion rates are often observed at the local scale, but sediment yield, which is the net transport out of the catchment, decreases with increasing size of the catchment. This is consistent with the results obtained.

In the meantime, the simulated organic nitrogen yield for the Ouémé-Bonou catchment (roughly 1.2 to 1.7 ton ha^{-1} a^{-1}) were almost two time the computed amount for the Donga-Pont catchment (roughly 0.5 to 1 ton ha^{-1} a^{-1}). This may be the consequences of high rate of very fine particle load from given threatened areas, which may become important at large scale.

Tab. 9.4. Simulated SWAT components under land use and climate scenarios (2025 to 2029). Deviation (in %) from the reference scenario (2000-2009) are shown in brackets.

Donga-Pont	Reference [2000-2009]	La & A1B [2025-2029]		La & B1 [2025-2029]		Lb & A1B [2025-2029]		Lb & B1 [2025-2029]	
Rainfall (mm a^{-1})	1233.4	1116.0	(-10)	1138.0	(-8)	1116.0	(-10)	1138.0	(-8)
Water yield (mm a^{-1})	242.7	221.9	(-9)	244.9	(1)	221.8	(-9)	246.7	(2)
Groundwater flow (mm a^{-1})	135.7	125.1	(-8)	136.5	(1)	145.9	(7)	158.4	(17)
Surface runoff (mm a^{-1})	106.0	95.5	(-10)	107.0	(1)	75.0	(-29)	87.4	(-18)
Evapotranspiration (mm a^{-1})	927.3	857.4	(-8)	847.3	(-9)	854.7	(-8)	845.2	(-9)
Sediment yield (ton ha^{-1} a^{-1})	0.4	0.5	(13)	0.5	(15)	0.6	(45)	0.6	(50)
Organic N load (kg ha^{-1} a^{-1})	0.7	0.7	(1)	0.8	(9)	1.0	(36)	1.0	(46)

Ouémé-Bonou	Reference [2000-2009]	La & A1B [2025-2029]		La & B1 [2025-2029]		Lb & A1B [2025-2029]		Lb & B1 [2025-2029]	
Rainfall (mm a^{-1})	1138.9	1041.5	(-9)	1060.9	(-7)	1041.5	(-9)	1060.9	(-7)
Water yield (mm a^{-1})	224.6	193.3	(-14)	215.8	(-4)	201.6	(-10)	223.3	(-1)
Groundwater flow (mm a^{-1})	77.0	81.4	(6)	91.7	(19)	99.0	(29)	109.6	(42)
Surface runoff (mm a^{-1})	147.6	111.9	(-24)	124.1	(-16)	102.6	(-30)	113.8	(-23)
Evapotranspiration (mm a^{-1})	794.8	740.4	(-7)	734.6	(-8)	733.0	(-8)	728.3	(-8)
Sediment yield (ton ha^{-1} a^{-1})	0.3	0.4	(16)	0.4	(22)	0.4	(34)	0.5	(41)
Organic N load (kg ha^{-1} a^{-1})	1.2	1.4	(15)	1.5	(25)	1.6	(37)	1.7	(47)

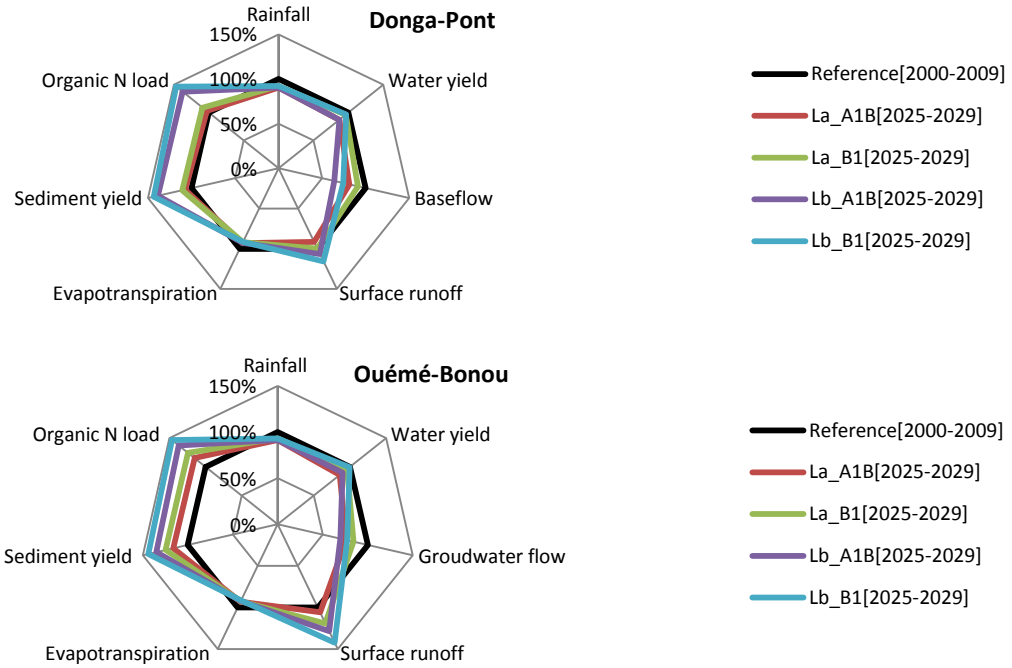

Fig. 9.4. Simulated trends under land use and climate scenarios (2025 to 2029).

Fig. 9.5, 9.6 and 8.7 show respectively surface runoff, sediment yield and organic nitrogen load pattern for the combined scenarios (La & A1B), (La & B1), (Lb & A1B) and (Lb & B1) from 2000 to 2030 within the Ouémé-Bonou catchment. Accordingly to the land use dynamic, the simulated pattern reflected higher and increasing degradation in the agricultural land. Surface runoff varies from 0 to 350 mm a^{-1}, sediment yield varies from 0 to 10 ton ha^{-1} a^{-1} and lost soil organic nitrogen varies from 0 to 20 kg ha^{-1} a^{-1}. Lost soil organic nitrogen shows higher dynamic and more threatened areas compared to sediment yield. This is completely consistent with the findings in section 9.3.3. As land use change was identified as the major driver of the ongoing land degradation, the scenario Lb (pessimistic, weak national economy, uncontrolled settlement and farmland development, 3.5% population growth per year) must be avoided in order to exclude the combinations (Lb & A1B) and (Lb & B1) for which larger threatened areas are shown in the figures.

SWAT model was applied in the upper Ouémé catchment to evaluate the effects of climate change and land use change on soil erosion (Hiepe, 2008; Giertz et al., 2010; Speth et al., 2010). In the combined land use and climate scenarios, the soil erosion increases with a large variability within the study area, which shows the high impact of land use change. The study has concluded that area with a high potential of cropland expansion, future sediment yield will be driven by land use change and may therefore strongly increase. Conversely, in the areas with a low potential for cropland expansion and strong reductions in rainfall, future sediment yield may decrease.

These findings are consistent with the results presented in this study, which furthermore suggest an extension to soil organic nutrients.

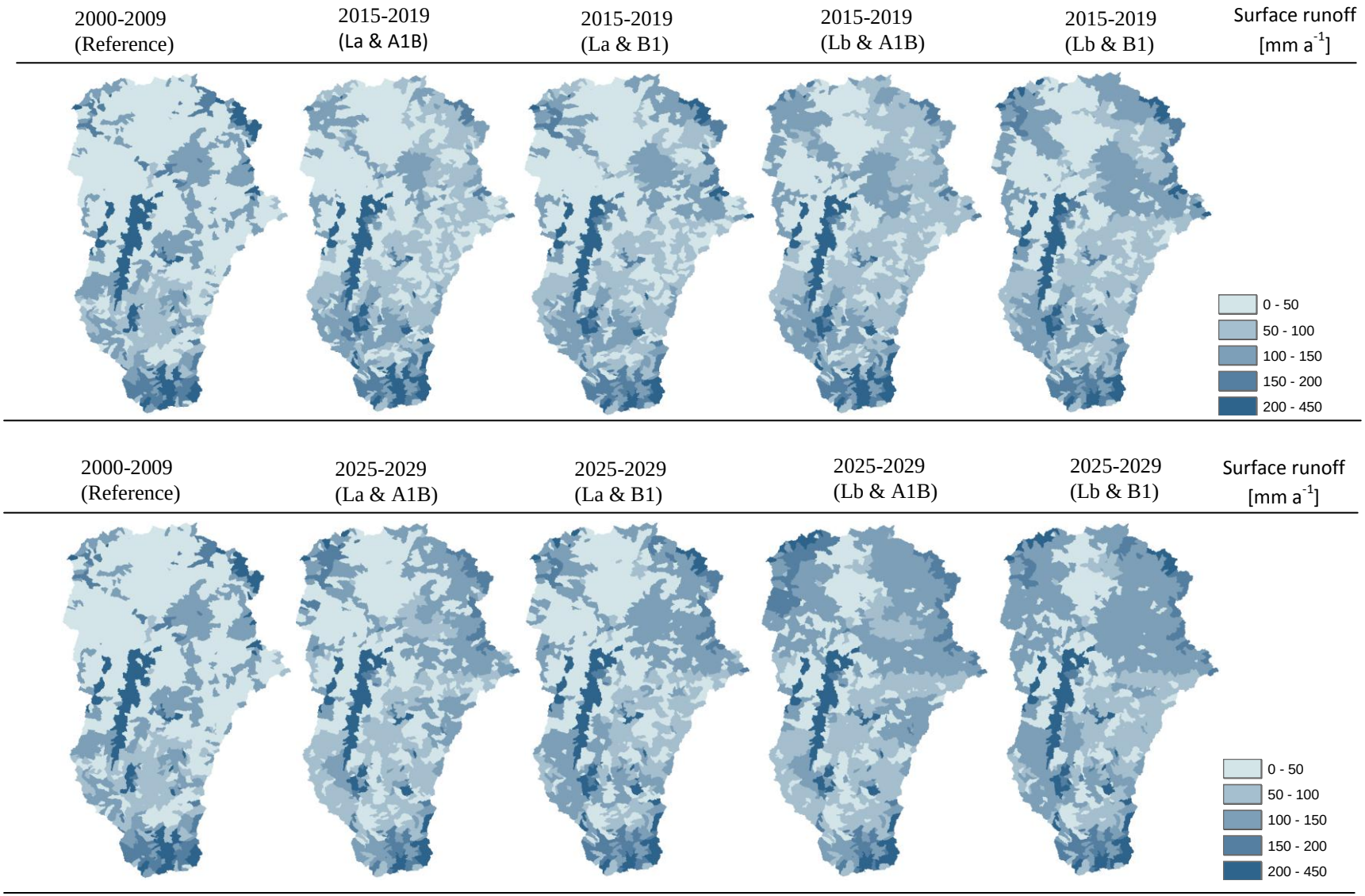

Fig. 9.5. Impacts of land use and climate change on surface runoff patterns in the Ouémé-Bonou catchment.

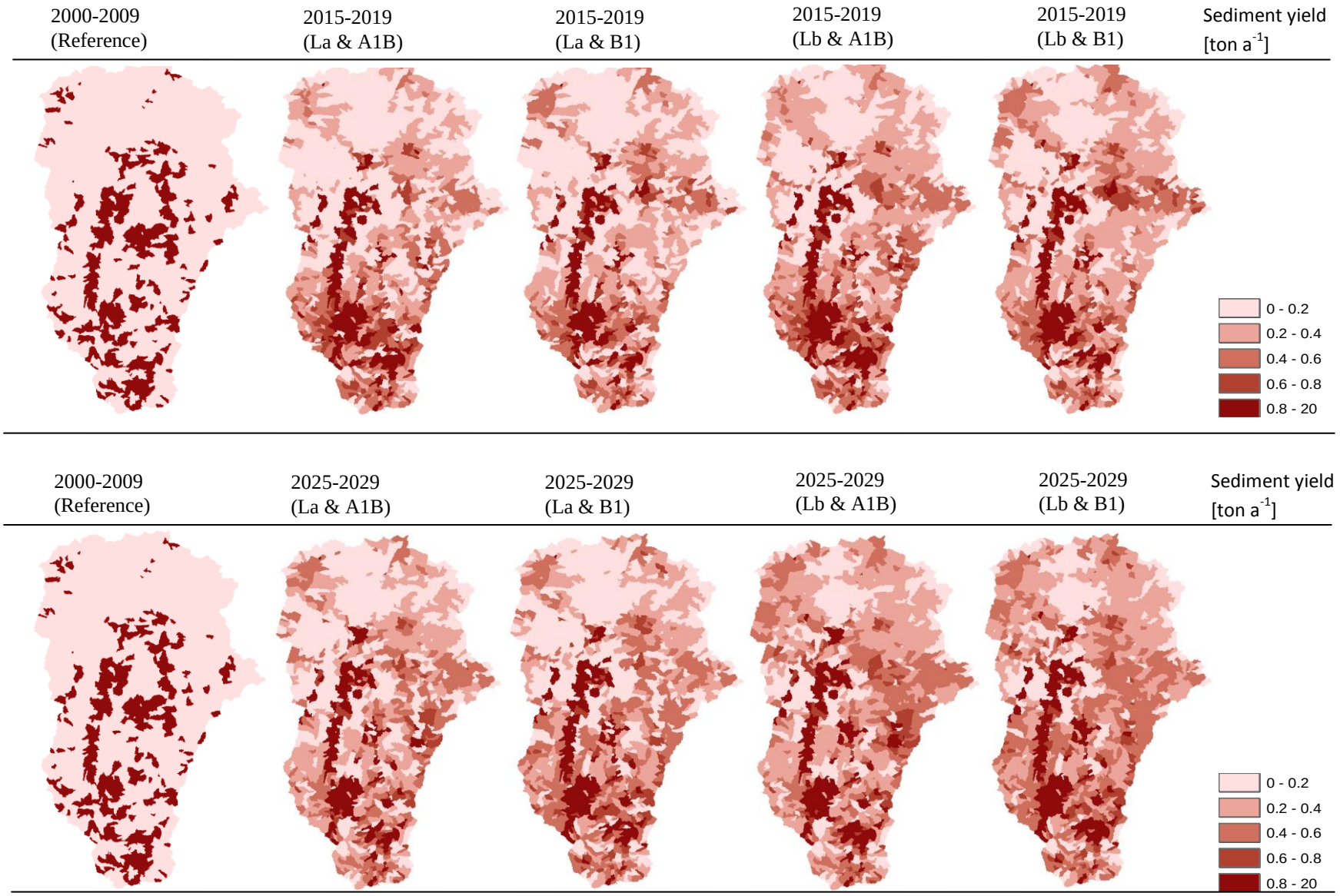

Fig. 9.6. Impacts of land use and climate change on sediment yield patterns in the Ouémé-Bonou catchment.

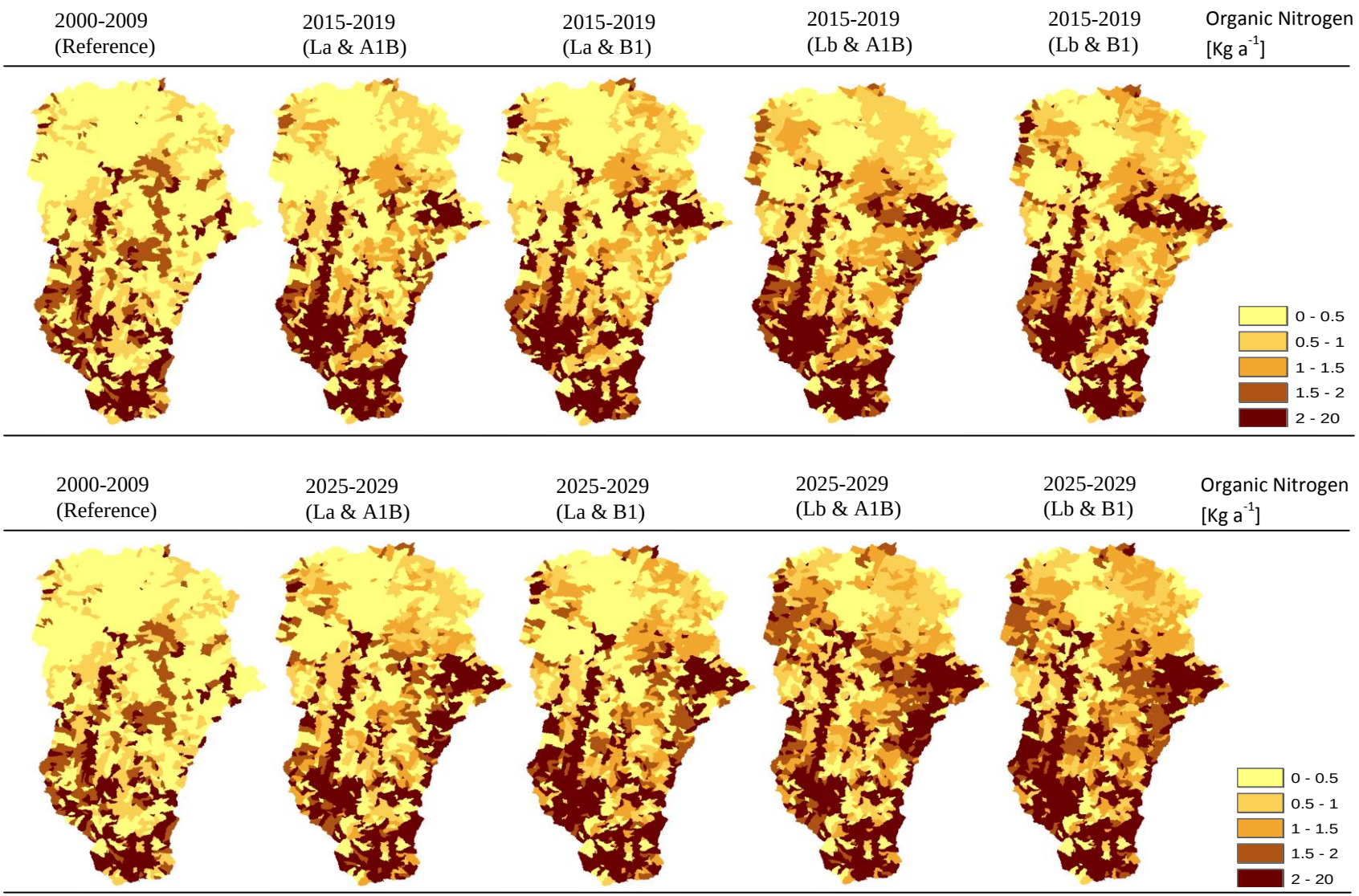

Fig. 9.7. Impacts of land use and climate change on Organic Nitrogen patterns in the Ouémé-Bonou catchment.

9.4. Conclusion

Soil and water are essential natural resources, available in limited quantities, but are nowadays dangerously exposed to the vagaries of climate and land use change. Balancing the future degradation requires a sufficient understanding of processes behind at different scales, a task that may not be possible without an overriding of difficulties related to data availability in a data-poor environment such as Benin.

In this chapter the lack and non-accurate boundary condition data (e.g. stream water-sediment-nutrient measurements), have been overridden, and simulated climate and land use change impacts on the ongoing soil and water degradation at the Ouémé-Bonou catchment scale (50,000 km^2) were compared to a meso scale (586 km^2) results.

Results revealed significant and increasing impacts over years. Surface runoff, groundwater flow, sediment and organic nitrogen load were affected by land use change (as dominant effects) of -8 to +50%, while water yield and evapotranspiration were affected by climate change (as dominant effects) of -31 to +2%. These rates may be reached gradually over years and according to the scenario development,

It was found that variables such as sediment and soil nutrients, mainly sensitive to land use change were significantly affected by the increasing catchment scale. Furthermore, while sediment yield decreases with increasing size of the catchment, lost soil organic nitrogen increases with the size of the catchment.

These works is a significant contribution for supporting sustainable management strategies to drive stronger economic development that considers controlled settlements, controlled farmland extension, less pressures on natural vegetations, and sustainable farming system managements.

This study reveals the relevancy and the efficiency of the modeling strategy used for bridging the data gap, since the results are consistent with previous findings within the study area. Future works should focus on the interaction between uncertainties associated with the scenarios data and the model structural errors. This will help to clearly quantify the uncertainties in the simulated impacts which are not investigated in this work.

10. General Conclusion and perspectives

Among the many challenges facing the sub-Sahara African countries, is the well-balanced and sustainable management of natural resources, which begins with their quantitative and qualitative assessment, while specifying the gross uncertainties that are often associated. The present work perfectly fits in with this logic. It focuses on three types of uncertainty: (1) uncertainty due to the to soil mapping approach, (2) uncertainty due to the aggregation of land use types at the regional and uncertainty due to the model simplifications. This work allowed (1) to report on the validity of SOil and TERrain (SOTER) maps for hydrologic simulations in Benin, (2) to test a regionalization methodology using multi-scale investigations, (3) to give an extensive insight of relationships between agriculture and the dynamics of nutrient and sediment loading, and (4) finally the quantification of potential impacts of climate change and land use on water resources and soil degradation.

It is well known that the quality of any application of environmental models depends on the underlying database (Bormann et al., 1999). Often, the calibration of model parameters is used to fill data gaps and to reduce the uncertainty of available information, but may not be sufficient to balance local impacts of differences in the available information (database). The importance of these local impacts may be seen as quality measure for selecting adequately the data to be involved in a modeling work.

In this study, a comprehensive database of physical and hydraulic soil properties was developed for the study region using two different approaches for the soil maps, one of them having been further divided into two differing concepts. Although, from a scientific point of view, the SOil and TERrain (SOTER) approach may be more appropriate, this is not necessarily true for its application in environmental modeling. Thus, the SOTER maps have been evaluated and found valid for simulating hydrological processes. Beyond this aspect, it was shown that not only the soil parameters themselves are uncertain and produce uncertain model outputs, but also the concept used to develop the soil map. This uncertainty is well known concerning soil maps of different scales (Bormann et al., 1999) but is rarely investigated for the same scale. It was then proved that SWAT could be calibrated successfully for different soil databases regarding the total discharge dynamics, but the spatial patterns of the differences persist. Depending on the modeling issue this may cause a significant bias in the model results.

For modeling future development of the Ouémé catchment, this must be taken into account in the uncertainty quantification and focus should be laid on how the concept interacts with the model structural errors. As alternative, the e-SOTER project (Regional pilot platform as European Union contribution to a Global Soil Observing System) was suggested and is tested since 2008. This approach considers new methodologies that combine remote sensing (soil pattern recognition) with the standardization of available soil attributes collected by earlier surveys and high resolution digital elevation models. This is a quite promising perspective for future updating SOTER maps used for modeling studies in the Ouémé catchment.

Many problems alter the relationship between agriculture and the environment. Its direct and indirect impacts on water resources and human well-being are known all over the world. In this study, the SWAT model has been used to simulate the current and future vulnerability of surface water and groundwater quality. The model was able to accurately simulate the daily dynamic of water and sediment as well as nitrate and organic N and P transport. High spatial variations in groundwater nitrate partly explained the simulated dynamic and indicated that agricultural land management controls mainly this issue and should lead to strict regulation policies. Future scenario developments have shown clearly an increasing contamination rate in response to increasing conversion of savannahs to croplands. No regulation policies as observed today may simply lead to limitations in the water resources accessibility and the closing of many already used drillings.

The quality of the spatial information, mainly the accuracy of agricultural diffuse source pollution is crucial for modeling the soil nutrient dynamic, biomass and crop yield, with an acceptable uncertainty level. This may be critical at regional scale, where cropping systems are rarely mapped,

leading to simplifications in the model application with the risk to cause a bias in the results. In this work, predictions based on simple aggregation of the cropping systems are associated with high uncertainties for the soil nutrient dynamic, biomass, crop yield as well as water and nitrogen stress. These forms of uncertainties are often neglected and should be considered in the scenario elaborations for supporting well-balanced management decisions.

To bridge the data gap (water discharge, sediment and nutrient concentration, required for the model calibration) and estimate the impacts of climate and land use change at the whole Ouémé-Bonou catchment level, scale dependent physical catchment properties were used to explain (statistically) and derive SWAT model parameters. Although the computed regression-based parameter models are physically meaningful and consistent with the theoretical fundament of the model parameters, they contain uncertainty due to the non-uniqueness of the considered calibrated parameter set, which is caused by limited available information. For improving the data base, a new data collection policy must be developed. However the model parameter uncertainty issues were acceptable, since a clear coherency appeared in the final parameter matrix, which was successfully correlated with the scale dependent catchment physical properties. Repetitive applications of the tested regionalization approach (using different simulation models) should lead to further understanding of scale dependent physical controls on the hydrological response in order to improve the physical meaning of the developed statistical relationships.

The results revealed significant and increasing impacts of climate and land use change over years according to the evaluated scenarios. Surface runoff, groundwater flow, sediment and organic nitrogen load were dominantly affected by land use change, while water yield and evapotranspiration were dominantly affected by climate change. It was shown the susceptibility of nutrients to be lost from soils, driven by the climate change, which emerges as a factor that is challenging agricultural nutrient managements in the study area.

These works is a significant contribution for supporting sustainable management strategies to drive stronger economic development that considers controlled settlements, controlled farmland extension, less pressures on natural vegetations, and sustainable farming system managements. This study reveals the relevance and the efficiency of the modeling strategy used for bridging the data gap, since the results are consistent with previous findings within the study area. Future works should focus on the interaction between uncertainties associated with the scenarios data and the model structural errors. This will help to clearly quantify the uncertainties in the simulated impacts which are not investigated in this work.

References

Abbaspour, K.C., 2008. SWAT Calibration and Uncertainty Programs - A User Manual. Department of Systems Analysis, Integrated Assessment and Modeling (SIAM), Eawag, Swiss Federal Institute of Aquatic Science and Technology, Duebendorf, Switzerland, 95pp. http://www.eawag.ch/organisation/abteilungen/siam/software/swat/index_EN.

Abbaspour, K.C., Johnson, A., Van Genuchten, M. Th., 2004. Estimating uncertain flow and transport parameters using a sequential uncertainty fitting procedure. Vadose Zone Journal. 3, 1340-1352.

Abbott, M.B., Bathurst, J.C., Cunge, J.A., O'Connell, P.E., Rasmussen, J. 1986. An introduction to the European Hydrological System - Systeme Hydrologique Europeen, "SHE", 2: structure of a physically-based, distributed modeling system, J. Hydrol., 87, 61-77.

Acutis, M., Donatelli, M., 2003. SOILPAR 2.00: software to estimate soil hydrological parameters and functions, Eur. J. Agron. 18 (2003), pp. 373–377.

Agbo, P. B., 1999. Restoring crop productivity in West Africa: the potential of agroforestry. Long-term mulching and fertilizer effects on maize and cassava intercropping in the West Africa subhumid zone. PHD thesis. Hohenheim Tropical Agricultural Series n° 7 Margraf Verlag Germany.

Ahn, P., 1970. West African Soils. Oxford (UK), Oxford University Press. 332pp.

Akondé, T. P., 1995. Potential of Alley Cropping with Leucaena leucocephala (Lam.) de Wit and Cajanus cajan (L.) Millsp. For maize (Zea mays L.) and Cassava (Manihot esculenta Crantz) production on an Acrisols in Benin Republic (West Africa) Hohenheimer Bodenkundliche Hefte 25. Inst. für Bodenkunde Uni. Hohenheim. 166 pp.

Ali, M.H. (2010) Fundamentals of Irrigation and On-Farm Water Management. Volume 1. Springer Publisher. 583 p.. ISBN 978-1-4419-6334-5.

Allen, R.G., Jensen, M.E., Wright, J.L., Burman, R.D., 1989. Operational estimates of evapotranspiration. Agronomy Journal 81: 650-662.

Ambroise, B., 1999. La dynamique du cycle de l'eau dans un basin versant. Bucarest : Editions H.G.A., pp. 200.

Andersen, J., Refsgaard, J. C., Jensen K. H., 2001. Distributed hydrological modeling of the Senegal River Basin – model construction and validation. J. Hydrol., 247, 200-214.

Anderson, M.G., Bates, P.D., (Eds.) 2001. Model validation – perspectives in hydrological sciences. Wiley, 500 p.

Arnold, J. G., Allen, P. M., Muttiah, R., Bernhardt., G., 1995. Automated base flow separation and recession analysis techniques. Ground Water 33(6), 1010-1018.

Arnold, J.G., Alllen, P.M., 1999. Validation of automated methods for estimating baseflow and groundwater recharge from stream flow records. Journal of the American Water Resources Association 35 (2), 411-424.

Arnold, J.G., Fohrer, N., 2005. SWAT2000: current capabilities and research opportunities in applied watershed modeling. Hydrol. Process 19, 563–572.

Arnold, J.G., Srinivasan, R., Muttiah, R.S., Allen, P.M., 1999. Continental scale simulation of hydrologic balance. J. Am. Wat. Res. Assoc. 35(5), p. 1037 - 1051

Arnold, J.G., Srinivasan, R., Muttiah, R.S., Williams, J.R., 1998. Large area hydrologic modeling and assessment part I: model development. Journal of the American Water Resources Association 34(1): 73-89.

Bárdossy, A., 2007. Calibration of hydrological model parameters for ungauged catchments, Hydrol. Earth Syst. Sci., 11, 703–710, available at: http://www.hydrol-earth-syst-sci.net/11/703/2007/.

Baumer, O.W., 1990. Prediction of soil hydraulic parameters. Proceedings of International Workshop in Indirect Methods for Estimating the Hydraulic Properties of Unsaturated Soils. USDA-ARS/University of California, Riverside, CA.

Becker, A., Braun, P., 1999. Disaggregation, aggregation and spatial scaling in hydrological modelling. J. Hydrol. 217, 239–252.

Beven, K., 1981. Kinematic subsurface stormflow, Wat. Resour. Res., 17, 1419-1424.

Beven, K.J., 2001. Rainfall-runoff modeling. The Primer. John Wiley and sons, pp. 360.

Beven, K., Binlley, A., 1992. The future of distributed models: model calibration and uncertainty prediction. Hydrological Processes, 6(3), 279–298.

Biaou, G., 1995. Agriculture durable: que recouvre-t-elle? Discussions de quelques points de vue contradictoires. Communication au symposium général du RESPAO; IITA, Cotonou, Bénin.

Blöschl, G., Sivapalan, M., 1995. Scale issues in hydrological modeling: A review. Hydrological Processes, 9, 251-290

Bocquier, G., 1971. Génèse et 'evolution de deux toposéquenses de sols tropicaux du Tchad. Interprétation biogodynamique. Thèse Sci. Strasbourg et Mém. ORSTOM. n°62., 1973. 350p.

Bollinne, A., Rosseau, P., 1978. Erodibilité des sols de moyenne et haute Belgique. Utilisation d'une méthode de calcul du facteur K de l'équation universelle de perte en terre. – Bull. Soc. Géogr. de Liège 14, 127-140.

Bormann, H., 2006. Impact of spatial data resolution on simulated catchment water balances and model performance of the multi-scale TOPLATS model, Hydrol. Earth Syst. Sci., 10, 165–179.

Bormann, H., Diekkrüger, B., Richter, O., 1999. Effects of spatial data resolution on the calculation of regional water balances. In: Diekkrüger, B., Kirkby, M. & U. Schröder (Eds.): Regionalization in Hydrology, IAHS-Publication 254:193-202.

Bormann, H., Giertz, S. Diekkrüger, B., 2005. Hydrological catchment models: process representation, data availability and applicability for water management—case study for Benin. Regional Hydrological Impacts of Climatic Change - Impact Assessment and Decision Making (Proceedings of symposium S6 held during the Seventh IAHS Scientific Assembly at Foz do Iguaçu, Brazil, April 2005). IAHS Publ. 295, p. 86 – 93.

Bossa, A.Y., 2007. Modélisation du bilan hydrologique dans le bassin du Zou à l'exutoire d'Atchérigbé: contribution à l'utilisation durable des ressources en eau. Master thesis. Faculty of Agricultural Sciences, University of Abomey-Calavi, Benin.

Bossa, A.Y., Diekkrüger, B., Igué, A.M., Gaiser, T., 2012. Analyzing the effects of different soil databases on modeling of hydrological processes and sediment yield. Geoderma, 173-174, 61–74.

Boulet, R., 1974. Toposéquences de sols tropicaux en Haute-Volta. Equilibre et déséquilbre pédobioclimatiques. Thèse sci. Strasbourg et Mém. ORSTOM n° 85, 1978, 272p.

Bouraoui, F., Galbiati, L.., Bidoglio, G., 2002. Climate change impacts on nutrient loads in the Yorkshire Ouse catchment (UK). Hydrology and Earth System Sciences, 6(2), 197 – 209.

Brown, D.G., Bian, L., Walsh, S.J., 1993. Response of a distributed watershed erosion model to variations in input data aggregation levels. Comput. Geosci. 19 (4), 499–509.

Brown, J.D., Heuvelink, G.B.M., 2005. Assessing uncertainty propagation through physically based models of soil water flow and solute transport In: M.G. Anderson and J.J. McDonnell (Editors), Encyclopaedia of Hydrological Sciences. John Willey & Sons Lds., Chichester, 1181 - 1195.

Busche, H., Hiepe, C., Diekkrüger, B., 2005. Modeling the Effects and Land Use and Climate Change on Hydrology and Soil Erosion in a Sub-humid African Catchment. 3rd International SWAT Conference Proceedings, Zurich. http://www.brc.tamus.edu/swat/3rdswatconf/Bookofabstracts-3rdswatconf1.pdf (consulted on 10.03.2011).

C.P.C.S., 1967. Classification des sols. E.N.S.A. Grignon, 87 p. multigr.

Castany, G., 1961. Méthodes d'études des nappes aquifères, AISH/IAHS publication n°56, 55-67.

Chaplot, V., 2005. Impact of DEM mesh size and soil map scale on SWAT runoff, sediment, and NO3–N loads predictions. J. Hydrolo., 312, 207–222.

Chappell, N., Ternan, L., 1992. Flow path dimensionality and hydrological modeling, Hydrological Processes, 6, 327-345.

Chaubey, I., Cotter, A.S., Costello, T.A., Soerens, T.S., 2005. Effect of DEM data resolution on SWAT output uncertainty. Hydrological Processes, 19, 621–628.

Christiaens, K., Feyen, J., 2002. Use of sensitivity and uncertainty measures in distributed hydrological modeling with an application to the MIKE SHE model. Water Resources Research, 38(9), doi:10.1029/2001WR000478.

Christoph, M., Fink, A. Diekkrüger, B. Giertz, S. Reichert, B., Speth, P., 2008. IMPETUS: Implementing HELP in the Upper Ouémé Basin. Water SA (online). Volume 34, No. 4, Special HELP edition, page 481-490.

Clarke RT. 1973. A review of some mathematical models used in hydrology, with observations on their calibration and use. J. Hydrol., 19, 1–20.

Cochemé, J., and P. Franquin, 1967: An agroclimatology survey of a semi-arid area in Africa south of the Sahara. WMO Tech. Note, 86. Geneva, Switzerland, 136pp.

Cochrane, T.T., de Castro, N.F., Netto, J.M., 1981. An explanatory manual for CIAT´s computerized land resource study of tropical America. CIAT, Cali, Columbia.

Coffey, M.E., Workman, S.R., Taraba, J.L., Fogle, A.W., 2004. Statistical procedures for evaluating daily and monthly hydrologic model predicitions. Transactians of the ASAE 47(1): 59-68.

De Marsily, G., 1994. Hydrogéologie : comprendre et estimer les écoulements souterrains et le transport des polluants, Ecole Nationale Supérieure des Mines de Paris, 243 pp.

De Marsily, G., 1995. L'eau. Flammarion, Coll. Dominos, Paris, 126 pp.

De Roo, A.D.J., 1993. Modelling surface runoff and soil erosion in catchments using Geographical Information System. Validity and applicability of the ANSWERS model in two catchments in the loess area of Limburg (the Nederlands) and one in Devon (UK), Netherlands Geographical Studies (1993), p. 157.

Diederich, M., Simmer, C., 2010. Weather and climate monitoring in Benin. In: Speth, P., Christoph, M., Diekkrüger, B., (Eds.) Impacts of Global Change on the Hydrological Cycle in West and Northwest Africa. Springer, Heidelberg, Germany. p. 114-121.

Diekkrüger, B., 2003. Upscaling of Hydrological Models by Means of Parameter aggregation techniques. In: H. Neugebauer H. and C. Simmer (Eds.). Dynamics of Multiscale Earth Systems. Lecture Notes in Earth Sciences. Springer-Verlag, Berlin. p.145-165.

Diekkrüger, B., 2010. Continental hydrosphere. In: Speth, P., M. Christoph & B. Diekkrüger (Eds.) Impacts of Global Change on the Hydrological Cycle in West and Northwest Africa. Springer, Heidelberg, Germany. p. 166-167.

Diekkrüger, B., Arning, M., 1995. Simulation of water fluxes using different methods for estimating soil parameters. Ecological Modeling 81(1-3), 83-95.

Diekkrüger, B., Busche, H., Giertz, S., Steup, G., 2010. Hydrology. In: Speth, P., Christoph, M., Diekkrüger, B., (Eds.) Impacts of Global Change on the Hydrological Cycle in West and Northwest Africa. Springer, Heidelberg, Germany. p 60-64.

Dissou, M., 1992. Evaluation comparative et multidimensionnelle des modes de détention et de gestion de ressources naturelles au Bénin. FAO / Bénin.

Doevenspeck, M., 2005. Migration im ländlichen Benin. Sozialgeographische Untersuchungen an einer afrikanischen Frontier. Fakultät für Biologie, Chemie und Geowissenschaften. Bayreuth, Universität Bayreuth. Dissertation.

Dubrouecq, D., 1967. Etude des sols de la région ouest Dassa-Zoumé. Etude no. 98, CENAP, Bénin. 96p.

Duchaufour, P., 1988. Pedologie. 2nd ed. Masson. Paris. 224p.

Dunne, T., 1978. 'Field studies of hillslope flow processes' in Kirkby, M. J. (Ed.), Hillslope Hydrology. Wiley, Chichester. pp. 227-293.

Durbroeucq, D., 1977. Carte pédologique de reconnaissance du Dahomey au 1/200 000: feuille Bante. ORSTOM, Cotonou, 122p. Multigr.

El Fahem, T., 2007. Hydrogeology in the Upper Ouémé catchment (Benin). Institute of Geology. Bonn, University of Bonn. Dissertation.

Falkenmark, M, and C Widstrand. Population and Water Resources: A Delicate Balance. Population Bulletin, Population Reference Bureau, 1992.

FAO, 1996. Control of water pollution from agriculture. ISSN: 0254-5284. Available at: http://www.fao.org/docrep/W2598E/W2598E00.htm (consulted on 10.05. 2012).

FAO, 2011. Agricultural Drainage Water Management in Arid and Semi-Arid Areas. ISSN 0254–5284. ftp://ftp.fao.org/docrep/fao/005/y4263e/y4263e00.pdf (consulted on 10.05. 2012).

Faure, P., Volkoff, B., 1998. Some factors affecting regional differentiation of the soils in the Republic of Benin (West Africa). Catena 32: 281-306.

Fink, A. H., Christhoph, M., Born, K., Brücher, T., Piecha, K., Pohle, S., Schulz, O., Ermert, V., 2010. Climate. In: Speth, P., Christoph, M., Diekkrüger, B., (Eds) Impacts of Global Change on the Hydrological Cycle in West and Northwest Africa. Springer, Heidelberg, Germany.

Fink, A. H., Christhoph, M., Born, K., Brücher, T., Piecha, K., Pohle, S., Schulz, O., Ermert, V., 2010a. Climate. In: Speth, P., Christoph, M., Diekkrüger, B., (Eds.) Impacts of Global Change on the Hydrological Cycle in West and Northwest Africa. Springer, Heidelberg, Germany.

Fink, A. H., Paeth, H., Ermert, V., Pohle, S., Diederich, M., 2010b. Meteorological processes influencing the weather and climate of Benin. In: Speth, P., Christoph, M., Diekkrüger, B., (Eds) Impacts of Global Change on the Hydrological Cycle in West and Northwest Africa. Springer, Heidelberg, Germany.

Fitts, C.R., 2002. Groundwater Science. San Diego, Academic Press.

FitzHugh, T. W., Mackay, D. S., 2000. Impacts of input parameter spatial aggregation on an agricultural nonpoint source pollution model. J. Hydrol., 236(1-2), 35-53.

Fohrer, N., Haverkamp, S., Frede, H.-G., 2005. Assessment of the effects of land-use patterns on hydrologic landscape functions: development of sustainable land-use concepts for low mountain range areas. Hydrological Processes, 19, 659–672.

Fritz, C., 1996. Boden- und Standortsmuster in geomorphen Einheiten Süd-Bénins (Westafrika). Hohenheimer Bodenkundliche Hefte 29. Hohenheim University, Stuttgart, Germany. 143 p.

Gaiser, T., Goldbach, H., Giertz, S., Hiepe, C., Klose, A., 2010. Soils. In: Speth, P., Christoph, M., Diekkrüger, B., (Eds.) Impacts of Global Change on the Hydrological Cycle in West and Northwest Africa. Springer, Heidelberg, Germany.

Gaiser, T., Graef, F., Cordeiro, J.C., 2000. Water retention characteristics of sandy soils with contrasting clay mineral composition in semi-arid tropical regions. Australian Journal of Soil Research 38, 523-536.

Gaiser, T., Judex, M., Igué, A., M., Paeth, H., Hiepe, C., 2011. Future productivity of fallow systems in Sub-Saharan Africa: Is the effect of demographic pressure and fallow reduction more significant than climate change? Agricultural and Forest Meteorology, 151, 1120–1130.

Gbessemehlan, V.Y., 1988. Crise agraire et stratégies paysannes dans le Sud-Est du Bénin : Etude de cas des districts ruraux d´Avrankou, d´Adjarra et d´Akpro-Missérété : province de l´Ouémé. Thèse d´Ingénieur Agronome. FSA / UNB. Abomey-Calavi ; Bénin.

Germann, P. F., 1990. 'Macropores and hydrologic hillslope processes' in Anderson, M. G. and Burt, T. P. (Eds.), Process Studies in Hillslope Hydrology. Wiley, Chichester. pp. 327-367.

Giertz, S., Diekkrüger, B., Steup, G., 2006. Physically-based modeling of hydrological processes in a tropical headwater catchment in Benin (West Africa) - process representation and multi-criteria validation. Hydrol. Earth Syst. Sci., 10, Pages 829-847. Available at: www.hydrol-earth-syst-sci.net/10/829/2006/.

Giertz, S., Hiepe, C., Steup, G., Sintondji, L., Diekkrüger, B., 2010. Hydrological processes and soil degradation in Benin. In: Speth, P., M. Christoph & B. Diekkrüger (Eds.): Impacts of Global Change on the Hydrological Cycle in West and Northwest Africa. Springer, Heidelberg, Germany. p. 168-197.

Götzinger, J., 2007. Distributed Conceptual Hydrological Modeling-Simulation of Climate, Land Use Change Impact and Uncertainty Analysis. Doctoral thesis, University of Stuttgart, Germany. http://elib.uni-stuttgart.de/opus/volltexte/2007/3349/pdf/Diss_Goetzinger_ub.pdf (consulted on 10.05.2010).

Gunn, R.H., Beattie, J.A., Reid, R.E., van de Graff, R.H.M., 1990. Australian soil and land survey handbook. Inkata Press, Melbourne. 300p.

Haase, G., Neumeister, H., Aurada, K.D., 1984. Natural conditions and problems of their complex utilisation in the Germany Democratic Republic. Geo Journal 8. 1, 053-065.

Haase, G., Schmidt, R., 1971. Bodenregionen in der DDR. Arch. Acker- u. Pflanzenbau u. Bodenkd. Bd. 15 H. 11 S. 885-895. Berlin.

Hargreaves, G.L., Hargreaves, G.H., Riley, J.P., 1985. Agricultural benefits for Senegal River Basin. Journal of Irrigation and Drainage Engineering. 111(2), 113-124.

Heldmann, M., Bollig, M., Hadjer, K., Kirscht, H., Mulindabigwi, V., 2010. Population, ethnicity, and religion. In: Speth, P., Christoph, M., Diekkrüger, B., (Eds.) Impacts of Global Change on the Hydrological Cycle in West and Northwest Africa. Springer, Heidelberg, Germany.

Heuvelmans, G., Muys, B., Feyen, J., 2004. Analysis of the spatial variation in the parameters of the SWAT model with application in Flanders, Northern Belgium. Hydrology and Earth System Sciences. 8(5), p. 931-939, http://hal.archivesouvertes.fr/ docs/00/30/49/73/PDF/hess-8-931-2004.pdf (consulted on 10.05.2010).

Hiepe, C., 2008. Soil degradation by water erosion in a sub-humid West-African catchment, a modelling approach considering land use and climate change in Benin. Doctoral thesis University of Bonn, Germany. http://hss.ulb.uni-bonn.de/diss_online/math_nat_fak/2008/ hiepe_claudia (consulted on 05.04.2011).

Igue, A., M., Houndagba, C., J., Gaiser, T., Stahr, K., 2006. Land Use/Cover Map and its Accuracy in the Oueme Basin of Benin (West Africa). Conference on International Agricultural Research for Development. Tropentag 2006. University of Bonn.

Igué, A.M., 1985. Analyse structurale et représentation cartographique d´une couverture ferrallitique dún bassin versant sur formations schiteuses á Lokpasso en Côte-d'Ivoire. Mémoire 2e année ORSTOM. Abidjan-Paris.

Igué, A.M., 1991. Etude pédologique de la ferme de Samiondji S/préfecture de Zagnanado. Etude n° 292 CENAP Cotonou.

Igué, A.M., 1996. Etude pédologique du bas-fond de Gankpétin (Dassa). CBF/UCN-Bénin, rapport annuel, CENATEL Cotonou Bénin.

Igué, A.M., 1997. Land description and land evaluation in savanna of Central-Benin: Example Dassa-Lèma. Tropentag 1997, University of Hohenheim, Stuttgart, Germany.

Igué, A.M., 2000. The Use of Soil and Terrain Digital Database for Land Evaluation Procedures- Case study of Central Benin. Hohenheimer Bodenkundliche Hefte. Heft N° 58 pp.235. University of Hohenheim, Stuttgart, Gemany. ISSN 0942-0754.

Igué, A.M., 2005. Soil information system for the Oueme basin. http://www.rivertwin.de/ assets/publications/D15_ SLISYS_Oueme basin2.pdf (consulted on 05.08.2009).

Igué, A.M., A. Floquet and K. Stahr, K., 2000. Land use and farming systems in Benin. In: Graef, F., P. Lawrence and M. von Oppen (Eds.): Adapted farming in West Africa: Issues, potentials and perspectives. Verlag Ulrich E. Grauer, Stuttgart, Germany. Stuttgart, S. 227–238.

IMPETUS, 2002. Zweiter Zwischenbericht. Integratives Management-Projekt für einen effizienten und tragfähigen Umgang mit Süßwasser in Westafrika: Fallstudien für ausgewählte Flußeinzugsgebiete in unterschiedlichen Klimazonen. Available at: http://www.impetus.uni-koeln.de/fileadmin/content/veroeffentlichungen/projektberichte/zwischenbericht2002.pdf.

INSAE, 2003. Recensement général de la population et de l'habitation de février 2002. Résultats Provisoires. Institut National de la Statistique et de l'Analyse Economique Benin, Unpublished.

Jenny, H., 1980. The Soil Resource. Springer, New York. 377 pp.

Jones, J. A. A., 1987. 'The effect of soil piping on contributing areas and erosion patterns', Earth Surf. Process. Landforms, 12,229-248.

Judex, M., 2008. Modellierung der Landnutzungsdynamik in Zentralbenin mit dem XULU-Framework. PhD-thesis, University of Bonn. http://hss.ulb.uni-bonn.de/2008/1419/1419.pdf (consulted on 05.06.2012).

Junge, B., 2004. Die Böden des oberen Ouémé-Einzugsgebietes in Benin/Westafrika - Pedologie, Klassifizierung, Nutzung und Degradierung. Dissertation. Institut für Bodenkunde. Bonn, Universität Bonn.

Kamagaté, B., 2006. Fonctionnement hydrologique et origine des écoulements sur un bassin versant en milieu tropical de socle au Bénin : bassin versant de la Donga (haute vallée de l'Ouémé). Thèse de doctorat, Université Montpellier II, France, 319p.

Kuczeraa, G., Parent, E., 1998. Monte Carlo assessment of parameter uncertainty in conceptual catchment models: the Metropolis algorithm. J. Hydrol. 211(1–4), 69–85.

Kneale, W. R., and White, R. E. 1984. The movement of water through cores of a dry (cracked) clay-loam grassland topsoil. J. Hydrol., 67, 361-365.

Krause, P., Boyle, D.P., Bäse, P., 2005. Comparison of different efficiency criteria for hydrological model assessment. Advances in Geoscience 5, 89-97.

Kros, J., de Vries, W., Janssen, P., Bak, C., 1993. The uncertainty in forecasting regional trends of forest soil acidification. Water, Air and Soil Poll. 66: 29-58.

Lal, R., 1990. Soil erosion in the tropics. Principles & Management. New York, McGraw-Hill,Inc. 580pp.

Lam, Q. D., Schmalz, B., Fohrer, N., 2010. Modeling point and diffuse source pollution of nitrate in a rural lowland catchment using the SWAT model. Agricultural Water Management 97, 317-325.

Laouina, A., Coelho, C., Ritsema, C., Chaker, M., Nafaa, R., Fenjiro, I., Antari, M., Ferreira, A., Van Dijck, S., 2004. Dynamique de l'eau et gestion des terres dans le contexte du changement global, analyse agro-hydrologique dans le bassin du Bouregreg (Maroc), Sécheresse 15(1), 66-77.

Lawal, O., Gaiser, T., Stahr, K., 2004. Effect of land use changes on sediment load in the Zagbo River Catchment in Southern Benin. Deutscher Tropentag 2004. Berlin/Germany, Institute for Soil Science and Land Evaluation, University of Hohenheim, D-70599 Stuttgart/Germany.

Le Barbe, L., Lebel, T., Tapsoba, D., 2002. Rainfall variability in West Africa during the years 1950–90. Journal of Climate 15, 187–202.

Le Lay, M., 2006. Modélisation hydrologique dans un contexte de variabilité hydro-climatique. Une approche comparative pour l'étude du cycle hydrologique à méso-échelle au Bénin, Thèse de doctorat, Université Joseph Fourrier, INPG, LTHE.

Leduc C., Favreau G. et Schroeter P., 2001. Long-term rise in a Sahelian water-table: the Continental Terminal in South-West Niger. J. Hydrol., 243, 43-54.

Loague, K., VanderKwaak, J.E., 2004. Physics-based hydrologic response simulation: platinum bridge, 1958 Edsel, or useful tool. Hydrological Processes, 18, 2949–2956.

Maeir, R., 2004. Standortseignung für Baumwolle in einer Kleinlandschaft in Zentralbenin. Studienarbeit der Agrarwissenschaften (B.Sc.). pp43. Universität Hohenheim, Stuttgart Germany. Available at: http://www.rivertwin.de/assets/BSc_maier.pdf.

Mahé, G., Paturel, J.E., Servat, E., Conway, D., Dezetter, A., 2005. The impact of land use change on soil water holding capacity and river modeling in the Nakambe river, Burkina Faso. J. Hydrol., 300(1-4), 33-43.

Maidment, D.R., 1992. Handbook of Hydrology, McGraw-Hill, 1400pp

Margaret, W. G., Chaubey, I., 2010. Regionalization of SWAT Model Parameters for Use in Ungauged Watersheds. Water 2010, 2, 849-871; doi:10.3390/w2040849.

McElroy, A. D., Chiu, S. Y., Nebgen, J.W., and others, 1976. Loading functions for assessment of water pollution from nonpoint sources. EPA document EPA 600/2-76-151. USEPA, Athens, GA.

McKay, M.D., Beckman, R.J., Conover, W.J., 1979. A comparison of three methods for selecting values of input variables in the analysis of output from a computer code. Technometrics 21, p. 239 – 245.

Menz, G., 2010. Topography and natural regions. In: Speth, P., Christoph, M., Diekkrüger, B., (Eds.) Impacts of Global Change on the Hydrological Cycle in West and Northwest Africa. Springer, Heidelberg, Germany. p 40-44.

Monteith, J.L., 1965. Evaporation and the environment. In: The state and movement of water in living organisms. XIXth Symposium of the Society of Experimental Biology. Swansea, Cambridge University Press: 205-234.

Morgan, R.P.C., 1979. Soil erosion. Longman Group limited, London. Published in the United States of America by Longman Inc., New york.

Morgan, R.P.C., 1986. Soil erosion and conservation. Longman Scientific & Technical, Longman Group UK limited Essex CM20 2JE, England and associated Companies throughout the world. Copublished in the United States with John Wiley & Sons, Inc., 605 Third Avenue, New York, NY 10158.

Morris, M.D., 1991. Factorial sampling plans for preliminary computational experiments. Technometrics, 33(2), p. 161-174.

Murdoch, P.S., Baron, J.S. and Miller, T.L., 2000. Potential effects of climate change on surface-water quality in North America. J. Amer. Water Resour. Assoc., 36, 347–366.

Musy, A., Soutter, M., 1991. Physique du sol, Presses Polytechniques et Universitaires Romandes, Lausanne, 335 pp.

Nash, J. E., Sutcliffe, J. V., 1970. River flow forecasting through conceptual models - Part I - A discussion ofprinciples. J. Hydrol., 10(3), 282-290.

Neitsch, S.L., Arnold J.G., Kiniry, J.R., Williams, J.R, 2001. Soil and Water Assessment Tool Theoretical Documentation Version 2000. Agricultural Research Service. Tempel, Texas.

Ngo-Duc, T., 2005. Modélisation des bilans hydrologiques continentaux : variabilité interannuelle et tendances. Comparaison aux observations, thèse de doctorat de l'université Paris 6, 160p. Available at: http://tel.archives-ouvertes.fr/docs/00/05/51/84/PDF/these_Thanh_Sep2005.pdf

Novotny, V., Olem, H., 1994. Water Quality: Prevention, Identification, and Management of Diffuse Pollution, Van Nostrand Reinhold, New York, 1054 p.

OBEMINES, 1989. Notice explicative de la carte geologique a 1 : 200.000. Republique populaire du Benin. Min. de l'Industrie.

Oeurng, C., Sauvage, S., Sánchez-Pérez, J., 2010. Dynamics of suspended sediment transport and yield in a large agricultural catchment, southwest France. Earth Surface Processes and Landforms, DOI: 10.1002/esp.1971.

Paeth, H., 2004. Key factors in African climate change evaluated by a regional climate model. Erdkunde 58, 290-315.

Paeth, H., Born, K., Podzun, R., Jacob, D., 2005. Regional dynamic downscaling over West Africa: Model evaluation and comparison of wet and dry years. Meteorol. Zeit., 14, 349–367.

Paeth, H., Born, K., Girmes, R., Podzun, R. and Jacob, D., 2009. Regional climate change in tropical Africa under greenhouse forcing and land-use changes. Climate, 22, 114-132.

Paeth, H., Diederich, M., 2010. Postprocessing of simulated precipitation for impact research in West Africa. Part II: a weather generator for daily data. Climate Dynamics, 1–12.

Pappenberger, F., Beven, K.J., 2006. Ignorance is bliss: Or seven reasons not to use uncertainty analysis, Water resour. Res., 42, WO5302, doi: 10.1029/2005WR004820.

Paturel, J., E., Ouedraogo, M., Servat, E., Mahé, G., Dezetter, A., Boyer, J., F., 2003. The concept of rainfall and stream flow normals in West and Central Africa in a context of climatic variability. Hydrological Sciences Journal, 48(1), 125-136.

Penman, H.L., 1956. Evaporation: An introductory survey. Netherlands Journal of Agricultural Science 4:7-29.

Pohle, S., Fink, A., H., Giertz, S., Diekkrüger, B., 2010. Hydr-meteorological measurements in Benin. In: Speth, P., Christoph, M., Diekkrüger, B., (Eds.) Impacts of Global Change on the Hydrological Cycle in West and Northwest Africa. Springer, Heidelberg, Germany.

Pohlert, T., Huisman, J. A., Breuer, L., Frede, H. –G., 2005. Modeling of point and non-source pollution of nitrate with SWAT in the river Dill, Germany. Advances in Geosciences, 5, 7-12.

Porembski, S., Finckh, M., Orthmann, B., 2010. Flora and Vegetation. In: Speth, P., Christoph, M., Diekkrüger, B., (Eds.) Impacts of Global Change on the Hydrological Cycle in West and Northwest Africa. Springer, Heidelberg, Germany.

Priestley, C.H.B., Taylor, R.J., 1972. On the assessment of surface heat flux and evaporation using large scale parameters. Monthly Weather Review 100: 82 – 92.

Rawls, W. J., Brakensiek, D.L., 1982. Estimating soil water retention from soil properties. Amer. Soc. of Civil Engin., J. of Irrig. and Drain. 108: 166-171.

Rawls, W.J., Brakensiek, D.L., 1985. Prediction of soil water properties for hydrologic modelling. In E.E. Jones and T.J. Ward (Eds.). Watershed Management in the Eighties. Proc. of Symp. sponsored by Comm. on Watershed Management, I & D Division, ASCE. ASCE Convention, Denver, CO, April 30-May 1, pp. 293-299.

Reeuwijk, L.P., 1995. Procedures for Soil Analysis. Fifth edition. ISRIC Technical Paper 9. Wageningen, The Netherlands. 105pp.

Refsgaard, J.Ch., Storm, B., 1996. Construction, calibration and validation of hydrological models. In: Abbot, B.M., Refsgaard, J.Ch. (Eds.), Distributed Hydrological Modeling. Kluwer Academic Publishers, p. 321.

Reichert, B., Klose, S., Kocher, A., 2010. Geology. In: Speth, P., Christoph, M., Diekkrüger, B., (Eds.) Impacts of Global Change on the Hydrological Cycle in West and Northwest Africa. Springer, Heidelberg, Germany.

Ritchie, J.T., 1972. A model for predicting evaporation from a row crop with incomplete cover. Water Resour. Res. 8:1204-1213.

RIVERTWIN, 2007. Adapted and integrated model for the Ouémé River basin. Project co-funded by the European Commission within the Sixth Framework programme, GOCE-CT-2003-505401. Final report. University of Stuttgart, Institute for Landscape Planning and Ecology.

Romanawicz, A.A., Vanclooster, M., Rounsevell, M., La Junesse, I., 2005. Sensitivity of the SWAT model to the soil and land use data parameterisation: a case study in the Thyle catchment, Belgium. Ecological Modeling 187 (2005) 27–39.

Roose, E., De Noni, G., 2004. Recherches sur l'érosion hydrique en Afrique : revue et perspectives, Science et changements planétaires / Sécheresse. Volume 15, Numéro 1, 121-9.

Schuol, J., Abbaspour, K.C., Srinivasan, R., Yang, H., 2008. Estimation of freshwater availability in the West African sub-continent using the SWAT hydrologic model. J. Hydrol., 352, 30-49.

Séguis, L., Cappelaere, B., Milési, G., Peugeot, C., Massuel, S., Favreau, G., 2004. Simulated impacts of climate change and land-clearing on runoff from a small Sahelian catchment. Hydrological Processes, 18, 3401–3413.

Sharpley, A.N., Williams, J.R., eds. 1990. EPIC-Erosion Productivity Impact Calculator, 1. model documentation. U.S. Department of Agriculture, Agricultural Research Service, Tech. Bull. 1768.

Shelton, M., 2009. Hydroclimatology: perspectives and applications, Cambridge University Press, New York.

Singer, U. (2005). Entwicklungsprojekte im ländlichen Benin im Kontext von Migration und Ressourcenverknappung. Eine sozialgeographische Analyse. Fakultät für Biologie, Chemie und Geowissenschaften. Bayreuth, Universität Bayreuth. Dissertation: 256p. Available at: http://opus.ub.uni-bayreuth.de/volltexte/2006/209/pdf/Singer.pdf.

Sintondji, L.O., Agbossou, K.E., Ahamide, B., Bossa, A.Y., Konnon, D., Igue, A.M., 2009. Modélisation du bilan hydrique dans le bassin du Zou à l'exutoire d'Atchérigbé : Contribution à l'utilisation durable des ressources en eau dans le département des collines, centre-Bénin. Annales de l'Université de Ouagadougou, 7(C), 137-169.

Sintondji, L., 2005. Modeling the rainfall-runoff process in the Upper Ouémé catchment (Térou in Benin Republic) in a context of global change: extrapolation from the local to the regional scale. PhD Thesis in Hydrology and Environmental Management of the Mathematics and the Natural Sciences Faculty of the University of Bonn. Shaker Verlag GmbH., Aachen Germany.

Sivapalan, M., Viney, N. R. 1994a. Large scale catchment modeling to predict the effects of land use and climate, Water, J. Aust. Wat. Wasfewat. Assoc., 21, 33-37.

Sivapalan, M., Viney, N. R. 1994b. 'Application of a nested catchment model for predicting the effects of changes in forest cover'. In: Ohta, T. (Ed.) Proc. Int. Symp. Forest Hydrology, Univ. Tokyo, Tokyo. IUFRO, pp. 315-322.

Sloan, P.G., Moore., I.D., 1984. Modeling subsurface stormflow on steeply sloping forested watersheds. Water Resources Research. 20(12), 1815-1822.

Smith, K.A., Mullins., C.E., 2000. Soil and environmental analysis: physical methods. 2nd Ed. New York Basel. Marcel Dekker, Inc.

Soil Conservation Service Engineering Division, 1986. Urban hydrology for small watersheds. U.S. Department of Agriculture, Technical Release 55.

Soil Conservation Service, 1972. Chapter 4: Hydrology In National Engineering Handbook.

Speth, P., Christoph, M., Diekkrüger, B., (Eds.) 2010. Impacts of Global Change on the Hydrological Cycle in West and Northwest Africa. Springer Publisher. 675 p.ISBN: 978-3-642-12956-8.

Sporer, K., 1999. Nutzungspotentiale und Nutzungsbewertung von Böden des kristallinen Sockels in Südbenin. Diplomarbeit Geographisches Institut der Eberhard-Karl-University. Tübingen Germany.

Srinivasan, R., Zhang, X., Arnold, J., 2010. SWAT ungauged: hydrological budget and crop yield predictions in the upper mississippi river basin. American Society of Agricultural and Biological Engineers ISSN 2151-0032, 53(5), 1533-1546.

Stahr, K., Bleich, K.E., Graef, F., 1995. A geomorphological approach using satellite images for land use planning in the Ct3 and Liptako (SW-Niger). In Universität Hohenheim (Ed.): Standortgemäße Landwirtschaft in Westafrica. Arbeits- und Ergebnisbericht 1994-1996, SFB 308, Stuttgart

Steiner, K., 1994. Ursachen der Bodendegradation und Ansätze für eine Förderung der nachhaltigen Bodennutzung im Rahmen der Entwicklungszusammenarbeit. Eschborn, GTZ: 148 Seiten.

Stoorvogel, J. J., Smaling, E. M. A., 1998. Research on soil fertility decline in tropical environments: Integration of spatial scales. Nutrient cycling in Aroecosystems 50: 151 – 158.

Strahler, A. N. 1964. 'Quantitative geomorphology of drainage basins and channel networks' in Chow, V. T. (Ed.), Handbook of Applied Hydrology. McGraw-Hill, New York. pp. 4.39-4.76.

Stricker, J. N. M., Kim, C. P., Feddes, R. A. et al. (1993). The terrestrial hydrological cycle. In Energy and Water Cycles in the Climate System, ed. E. Raschke and D. Jacob. NATIO ASI Series, I 5. Berlin: Springer-Verlag, pp. 419–44.

Takle, E.S., Jha, M., Anderson, C.J., 2005. Hydrological cycle in the upper Mississippi River basin: 20th century simulations by multiple GCMs. Geophysical Research Letters 32(18).

Thamm, H.-P., Judex, M., Menz, G., 2005. Modeling of Land-Use and Land-Cover Change (LUCC) in Western Africa using Remote Sensing. Photogrammetrie, Fernerkundung, Geoinformation, 3, 191–199.

Thieken, A.H., Lücke, A., Diekkrüger, B., Richter, O., 1999. Scaling input data by GIS for hydrological modeling. Hydrological Processes, 13, 611–630.

Tomasella J., Hodnett, MG., 1998. Estimating soil water retention characteristics from limited data in. Brazilian. Soil Science 163, 190–202.

Tomer, M.D., Schilling, K.E., 2009. A simple approach to distinguish land-use and climate-change effects on watershed hydrology. J. Hydrol., 376:24-33.

UN, 2005. The Millennium Development Goals Report. New York: United Nations. Available at: http://unstats.un.org/unsd/mi/pdf/mdg%20book.pdf.

UNDP, 2003. Human Development Report 2003: Millennium Development Goals: A Compact Among Nations to End Human Poverty. New York: United Nations Development Program.

UNESCO, 1992. Glossaire International d'Hydrologie. Available at: www.cig.ensmp.fr/~hubert/glu/HINDFRT.HTM.

USEPA. 1990. The Lake and Reservoir Restoration and Guidance Manual, Second Edition. (OWRS, EPA 440/4-90-006). United States Environmental Protection Agency, Office of Water, Washington, DC.

van Engelen, V., Ting-tiang, W., (Eds.) 1995. Global and National Soils and Terrain Digital Databases (SOTER). World Resource Report 74. Available at: http://www.isric.org/isric/webdocs/Docs/Soterep.PDF.

Van Genuchten, M.T., 1980. A closed-form equation for predicting the hydraulic conductivity of unsaturated soils. Soil Science Society of America Journal, 44(5), 892–898.

Van Griensven, A., Meixner, T., 2007. A global and efficient multi-objective auto-calibration and uncertainty estimation method for water quality catchment models. J Hydroinform 9(4):277–291.

Van Noordwijk, M., Van Roode, M. McCallie, E.L., Lusiana, B., 1998. Erosion and Sedimentation as Multiscale, Fractal Processes: Implications for Models, Experiments and the Real World. In: Soil erosion at multiple scales. Principles and methods for assessing causes and impacts. Edited by F. W. T. PENNING DE VRIES, F. AGUS and J. KERR. Wallingford, UK, CABI Publishing: 223-254.

Vezina, K., Bonn, F., 2006. Modélisation et analyse de la dynamique spatio-temporelle des relations société-érosion et pollution diffuse en milieu agricole : études de cas au Viêtnam et au Québec. Centre d'applications et de recherches en télédétection (CARTEL), 2500 boulevard de l'Université, Université de Sherbrooke, Canada. http://geolittomer.univnantes.fr/StockageUMR/COLLOQUE/pdf/C2_0305_VEZINA.pdf (consulted on 05.06. 2012).

Volkoff, B., 1966. Les sols de la région Ouest Savalou à 1:100 000. Etude no. 91, CENAP, Bénin. 62p.

Volkoff, B., 1969. Carte pédologique de reconnaissance du Dahomey au 1/200 000: feuille Dassa-Zoumè (Socle cristallin). ORSTOM, Cotonou, 66p. Multigr.

von Bandat, H. F., 1962. Aerogeology. Gulf Publishing, Houston. 350 pp.

Vrugt, J.A., Gupta, H.V., Bouten, W., Sorooshian, S., 2003. A shuffled complex evolution metropolis algorithm for estimating posterior distribution of watershed model parameters. In: Duan Q, Sorooshian S, Gupta HV, Rousseau AN, Turcotte R (Eds.) Calibration of watershed models. AGU, Washington, DC. doi:10.1029/006WS07.

Vrugt, J.A., ter Braak, C.J. F., Clark, M.P., Hyman, J.M., Robinson, B.A., 2008. Treatment of Input Uncertainty in Hydrologic Modeling: Doing Hydrology Backwards with Markov Chain Monte Carlo Simulation. Water Resources Research, vol. 44, W00B09, 15 pp.

Wale, A., Rientjes, T. H., Gieske, A. S. M., Getachew, H. A., 2009. Ungauged catchment contributions to Lake Tana's water balance. Hydrological Processes, 23, 3682-3693.

Ward, R. C. and Robinson, M. (2000). Principles of Hydrology. 4th edn. London: McGraw-Hill.

Weischet, W., Endlicher, W., 2000. Regionale Klimatologie – 2. Die Alte Welt: Europa, Afrika, Asien. Stuttgart, Teubner.

Weller, U., 2002. Land Evaluation and Land Use Planning for Southern Benin (West Africa). Hohenheimer Bodenkundliche Hefte. Heft N° 67. University of Hohenheim, Stuttgart, Gemany. ISSN 0942-0754, 166 p.

WHO, 2008. Guidelines for drinking-water quality. ISBN 97892 41547611. http://www.who.int/water_sanitation_health/dwq/fulltext.pdf (consulted on 05.06. 2012).

Williams, J. R., Hann, R.W., 1978. Optimal operation of large agricultural watersheds with water quality constraints. Texas Water Resources Institute, Texas A&M Univ., Tech. Rep. No. 96.

Williams, J.R., 1975. Sediment-yield prediction with universal equation using runoff energy factor. p. 244-252. In Present and prospective technology for predicting sediment yield and sources: Proceedings of the sediment yield workshop, USDA Sedimentation Lab., Oxford, MS, November 28-30, 1972. ARS-S-40.

Williams, J.R., Hann, R.W., 1978. Optimal operation of large agricultural watersheds with water quality constraints. Texas Water Resources Institute, Texas A&M Univ., Tech. Rep. No. 96.

Willmott, C.J., 1981. On the validation of models. Physical Geography 2: 184pp.

Wooldridge, S. A., Kalma, J., 2001. Regional scale hydrological modeling using multiple-parameter landscape zones and a quasi-distributed water balance model. Hydrol. Earth Syst. Sci., 5, 59-74.

Wright, E. P., Burgess, W., 1992. The hydrogeology of crystalline basement in Africa. Geol Soc Spec Pap 66: 264

Yerima, B.P.K., van Ranst, E., 2005. Major Soil Classification Systems Used in the Tropics: Soils of Cameroon. Trafford Publishing. p. 277. ISBN 1412057892.

Youssouf, I., 1982. Reconnaissance pédologique dans les forêts de Ketou et de Dogo. Etude no. 252, CENAP, Bénin. 76 p.

Zhao, Y., Shi, X.,Weindorf, D.C., Yu, D., Sun,W.,Wang, H., 2006. Map scale effects on soil organic carbon stock estimation in North China. Soil Science Society of America Journal 70, 1377–1386.

Zannou, A., 2006. Détermination des termes du bilan hydrologique sur le bassin de l'Ouémé supérieur : approche annuelle et mensuelle avec calcul d'incertitudes associées. Master Recherche Eau et Environnement, University of Montpellier II, 81p.